Stability and Finite Element Analysis of Fractionally Damped Mechanical Systems

Von der Fakultät Konstruktions-, Produktions- und Fahrzeugtechnik
der Universität Stuttgart
zur Erlangung der Würde eines Doktor-Ingenieurs (Dr.-Ing.) genehmigte
Abhandlung

Vorgelegt von

Matthias Hinze
aus Blankenburg (Harz)

Hauptberichter:	Prof. Dr. ir. habil. Remco I. Leine
Mitberichter:	Prof. Dr. rer. nat. habil. Kai Diethelm
	Apl. Prof. Dr. rer. pol. Dr. rer. nat. Rudolf Hilfer
Tag der mündlichen Prüfung:	27.09.2021

Institut für Nichtlineare Mechanik der Universität Stuttgart

2021

Sorgen Sie dafür, dass Sie Schätze sammeln,
nicht Flittergold und unechte Perlen,
nicht eine tote Last eingelernten Gedächtnisstoffes
und gelehrten Wissenskrames, sondern nur reinstes Gold:
Gedanken und die Fähigkeit, ruhig und klar
und leidenschaftslos zu denken, stark und gesund zu fühlen,
aber nicht nur in dem, was Sie selbst
und Ihre kleinen persönlichen Interessen betrifft,
sondern in dem, was ans Tiefste der Menschheit rührt.
Zersplittern Sie nicht Ihre Zeit durch törichte
und geistlose Vergnügungen, vergessen Sie nicht,
wie unendlich kurz die Ihnen zugemessene Spanne ist.
Hinter Ihnen liegt die Unendlichkeit, vor Ihnen das Leben,
das nicht immer leicht ist zu leben,
und dahinter das Unendliche und Unbekannte.

Gösta Magnus Mittag-Leffler

Zum Andenken an Gerhard Hinze

Preface

The work presented in this thesis results from my time at the Institute for Nonlinear Mechanics at the University of Stuttgart. I want to thank my doctoral advisor Prof. Dr. Remco I. Leine for his support throughout my research activities. Our discussions, his intuition and constructive ideas influenced this work a lot. Furthermore, I would like to thank Dr. André Schmidt for laying the foundations of my engagement at the institute and sharing his knowledge in engineering and fractional calculus.

I am grateful to Prof. Dr. Kai Diethelm for the instructive collaboration during the last years and to Prof. Dr. Rudolf Hilfer for his interest in my work and his advice. I thank both for agreeing to be the co-referees for my thesis.

Special thanks go to Dr. Nina Müller-Hoeppe and Christian Lerch from the BGE Technology GmbH. They introduced the topic of applied fractional calculus in viscoelasticity to me and provided the basis for this thesis and my future work.

I want to thank all my colleagues at the Institute for Nonlinear Mechanics for sharing good times and teaching me the foundations of mechanics. I am especially grateful to Giuseppe Capobianco, Simon Sailer, Dr. André Schmidt and Dr. Simon R. Eugster for the review of my manuscript. Further thanks go to the students who wrote a thesis under my supervision, in particular to Markus Hahn who constructed my test bench.

Finally, I would like to thank my friends, family and particularly my dearest Momo for their love and support.

I gratefully acknowledge the funding of my research by the Federal Ministry of Education and Research (Grant No. 01IS17096B).

Stuttgart, June 2021 Matthias Hinze

Contents

Abstract

This dissertation is concerned with the stability of mechanical systems with fractional damping and the numerical treatment of fractional constitutive laws in the finite element method. It provides a reformulation of the infinite state representation of fractional derivatives, which leads to a numerical scheme for the solution of quite general fractional-order problems and contributes to the formulation of a Lyapunov stability framework for fractionally damped systems. The approach is motivated by the advantages of using fractional calculus to describe viscoelastic material behavior over large timescales.

The mathematical foundations of fractional calculus are presented and particularly formulated on unbounded intervals. This leads to a correct initialization of fractional-order problems and the consideration of the full material history in the applied context of viscoelasticity. Furthermore, several numerical methods for the solution of fractional-order differential equations are studied and compared to the novel scheme based on the reformulated infinite state representation, which is implemented, analyzed and tested.

An introduction to the theory of linear viscoelasticity is given and the use of fractional calculus in this respect is motivated. The functional character of fractional-order operators requires some generalizations of the mechanical theory and computational methods. In the field of stability theory, a generalization of the direct method of Lyapunov for the case of fractional damping is provided and embedded in the theory of functional differential equations. Particularly, Lyapunov functionals are formulated in terms of the (reformulated) infinite state representation and the method is applied to linear mechanical and a class of controlled nonlinear dynamical systems. In the field of structural mechanics, a formulation of the finite element method for the case of fractional constitutive behavior is introduced. The novel numerical scheme is implemented and some initial benchmark problems are studied.

Zusammenfassung

Diese Dissertation befasst sich mit der Stabilität von mechanischen Systemen mit fraktionaler Dämpfung und der numerischen Behandlung fraktionaler Stoffgesetze in der Methode der finiten Elemente. Es wird eine neue Formulierung der infinite-state-Darstellung fraktionaler Ableitungen vorgestellt, die einerseits zu einem numerischen Verfahren zur Lösung relativ allgemeiner Probleme fraktionaler Ordnung führt und andererseits zur Formulierung eines Stabilitätskonzepts im Sinne von Lyapunov für fraktional gedämpfte Systeme beiträgt. Der gewählte Ansatz ist motiviert durch die Vorteile von fraktionaler Analysis zur Beschreibung von viskoelastischem Materialverhalten über lange Zeiträume.

Die mathematischen Grundlagen der fraktionalen Analysis werden eingeführt und insbesondere auf unbeschränkten Intervallen formuliert. Dies führt zu einer korrekten Initialisierung von Problemen fraktionaler Ordnung und ermöglicht die Berücksichtigung der kompletten Materialhistorie im Kontext von Viskoelastizität. Des Weiteren werden einige numerische Methoden zur Lösung fraktionaler Differentialgleichungen betrachtet und mit dem neuen Verfahren basierend auf der umformulierten infinite-state-Darstellung verglichen.

Die klassische Theorie der linearen Viskoelastizität wird vorgestellt und die Verwendung fraktionaler Analysis in diesem Kontext wird motiviert. Der funktionale Charakter fraktionaler Operatoren erfordert einige Verallgemeinerungen von mechanischer Theorie und Rechenmethoden. Auf dem Gebiet der Stabilitätstheorie wird eine Verallgemeinerung der direkten Methode von Lyapunov für den Fall fraktionaler Dämpfung eingeführt und eingebettet in die Theorie von Funktionaldifferentialgleichungen. Insbesondere werden dabei Lyapunov-Funktionale im Sinne der (umformulierten) infinite-state-Darstellung genutzt. Die Methode wird auf lineare mechanische Systeme sowie eine Klasse nichtlinearer dynamischer Regelsysteme angewendet. Als Beitrag auf dem Gebiet der Strukturmechanik wird eine Formulierung der Methode der finiten Elemente für fraktional viskoelastische Stoffgesetze eingeführt. Die Implementierung des neuen numerischen Verfahrens wird vorgestellt und dessen Anwendbarkeit anhand von ersten Beispielen nachgewiesen.

Notation

General

a, B	scalars
$\mathbf{a}$, $\mathbf{B}$	vector or matrix
i, j, k, l, m, n	integer numbers and indices
t	time
x, q, f, V	real-valued functions
$\mathbf{x}$, $\mathbf{q}$, $\mathbf{f}$	vector-valued functions
lim	limit
min, max	minimum, maximum
inf, sup	infimum, supremum
Re, Im	real and imaginary part of a complex number
$s_n^{(\beta,\gamma)}$, $w_n^{(\beta,\gamma)}$	nodes and weights of Gauss-Jacobi quadrature
$\operatorname{dist}(x, M)$	distance between a point x and a set M

Sets and spaces

E, M, Q	sets
$\bar{Q}$	closure of the set Q
$\in$	member of
$\subset$, $\supset$	subset or superset of
$\mathbb{N}$, $\mathbb{N}_0$	positive or nonnegative integers
$\mathbb{R}$, $\mathbb{C}$	real or complex numbers
$\mathbb{R}^n$	n-dimensional space of real-valued vectors
$\|\cdot\|_2$	Euclidean norm on $\mathbb{R}^n$
$L_1[t_0, T]$	integrable functions on $[t_0, T]$
$A^n[t_0, T]$	functions with $(n-1)$th-order absolutely continuous derivative
$C_0(-\infty, T]$	continuous functions vanishing at $-\infty$
$BV[0, \infty)$	functions of bounded variation on compact subintervals
$CB((-\infty, 0]; \mathbb{R}^n)$	$\mathbb{R}^n$-valued bounded continuous functions
$BU((-\infty, 0]; \mathbb{R}^n)$	$\mathbb{R}^n$-valued bounded uniformly continuous functions
$\|\cdot\|_\infty$	uniform norm on function spaces

Operators

I_{t_0}, $\mathrm{I}_{t_0}^n$	integral and n-fold iterated integral with initial time t_0
D, $(\cdot)'$, D^n, $(\cdot)^{(n)}$	first-order and nth-order derivative
$\frac{\mathrm{d}}{\mathrm{d}t}$, $\dot{(\cdot)}$	time derivative
$\mathrm{I}_{t_0}^{\alpha}$	fractional Riemann-Liouville integral
${}^{\mathrm{RL}}\mathrm{D}_{t_0}^{\alpha}$, ${}^{\mathrm{C}}\mathrm{D}_{t_0}^{\alpha}$	fractional Riemann-Liouville or Caputo derivative
${}^{\mathrm{C}}\mathrm{D}^{\alpha}$	Liouville-Weyl type of Caputo derivative
$\mathcal{O}$	Landau notation
$\mathcal{L}$, $\mathcal{L}^{-1}$	(inverse) Laplace transform
$\mathbf{A}^{\mathrm{T}}$	matrix transpose
$\mathrm{Ker}(\mathbf{A})$	kernel of a matrix $\mathbf{A}$
$\mathrm{Res}(\cdot, s)$	residual at the pole s

Special functions

$\Gamma(\alpha)$	Euler Gamma function
$B(\alpha, \beta)$	Euler Beta function
$\mathrm{E}_{\alpha}(\cdot)$	one-parameter Mittag-Leffler function
$Z(\eta, \cdot)$, $z(\eta, \cdot)$	infinite states
μ_{α}	kernel of infinite state representation
$\mathrm{K}_{\omega}(\alpha, \cdot)$	kernel of reformulated infinite state representation
Θ, δ	Heaviside step function and Dirac distribution

Mechanics

$\boldsymbol{\sigma}$, $\boldsymbol{\varepsilon}$	Cauchy stress and linear strain tensors
σ_{ij}, σ_{yz}, ε_{ij}, ε_{yz}	components of stress and strain
$\tilde{\boldsymbol{\sigma}}$, $\tilde{\boldsymbol{\varepsilon}}$	Voigt notation of stress and strain
$\mathbf{u}(\mathbf{x}, t)$	displacement field
G_{ijkl}, G, G_h, G_d	relaxation function
J_{ijkl}, J, J_h, J_d	creep function
τ_{σ}, τ_{ε}	relaxation or retardation time
R_{σ}, R_{ε}, S_{σ}, S_{ε}	relaxation or retardation spectra
E^*, J^*	complex modulus or complex compliance

Abbreviations

ODE, FODE	(fractional-order) ordinary differential equation
DAE	differential algebraic equation
FDE	functional differential equation
PC	predictor-corrector scheme
ISS, RISS	(reformulated) infinite state scheme

CHAPTER 1

Introduction

This thesis deals with two different aspects in modeling viscoelastic material behavior described by fractional derivatives, namely the stability of mechanical systems with fractional damping and the numerical treatment of fractional constitutive laws in the finite element method. Both topics involve challenging tasks as the associated mechanical models include the entire material history, leading to functional equations. The following introductory chapter serves as a motivation and outline for this thesis. An overview of the relevant literature is given and the objective, aims and contributions of the thesis are presented.

1.1 Motivation for fractional calculus in mechanics

Most materials in nature and technical applications cannot exclusively be identified as *solid* or *fluid*. Their actual behavior is something in between these two theoretical concepts related to *elasticity* and *viscosity*. This means particularly that a material sample under constant loading does not only show an instantaneous elastic deformation but an additional time-dependent strain, called *creep* and that an imposed constant deformation of a specimen results in a stress that is decreasing from its initial value, known as *relaxation*. More generally, the current material response possibly depends on the history of stress and strain inputs. Such phenomena are summarized under the term *viscoelasticity* and are typically observed for polymers, rubber, concrete, soils, tissues and many other materials. It is a natural question in mechanics, how this behavior can be modeled, quantified and predicted. When the time-dependent material response occurs on a small time range, the viscoelastic behavior is well represented by exponential functions. However, if long-term creep or relaxation (over years) is observed, the exponential approach is not suitable any more and a much slower power law behavior yields a better representation, see Figure 1.1. The latter case links viscoelasticity to the mathematical theory of *fractional calculus*, which is the theoretical foundation and main theme of this thesis.

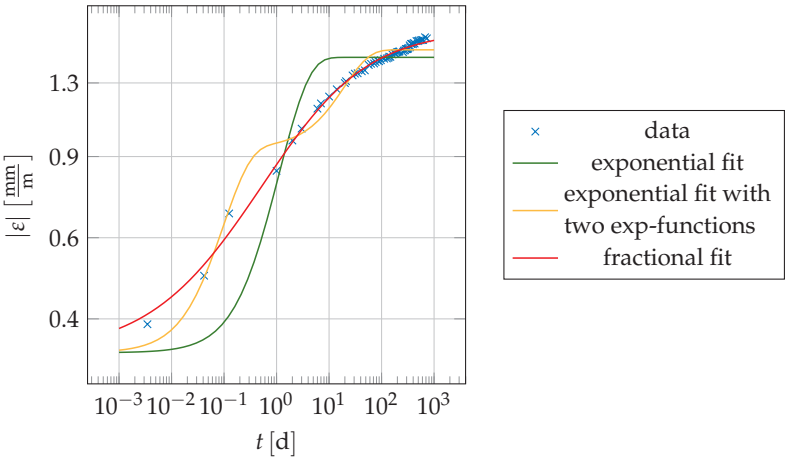

Figure 1.1: Fitting of concrete creep data over two years using exponential and fractional models.

Fractional calculus[1] deals with integrals and derivatives of non-integer order which can be described by convolution integrals with weakly singular (power law) kernels. Accordingly, fractional-order operators take account of the history of a function, which directly represents the inherent memory property in viscoelasticity. This functional character, combined with the weak singularity of the kernel, leads to several difficulties in numerical computation and requires theoretical generalizations in applications. Two such application areas are considered subsequently.

Many problems in industrial applications result from a loss of *stability* in dynamical systems, i.e., a desired equilibrium or steady-state behavior of a system can be lost under small perturbations and is substituted by unwanted (possibly destructive) vibrations. These problems can be solved through improved design, vibration absorbers or feedback control, which require methods to prove stability of the augmented systems. Particularly for the nonlinear case, the *direct method of Lyapunov* is a powerful tool in this respect. The method, which was originally developed for ordinary differential equations (ODEs), yields a stability statement by using certain storage and comparison functions, for which no explicit knowledge of the system solution is required. In order to apply this method to viscoelastic

[1]The mathematical theory dates back to a conversation of Leibniz and l'Hospital in 1695 and its foundation has been developed in the 19th century. Since the 1970s, fractional calculus has regained much interest in the scientific community leading to many advances in theory and applications, see Mainardi (2010, Sec. 1.5).

materials described by fractional constitutive laws, it has to be generalized in the context of *functional differential equations (FDEs)* and new storage functionals have to be developed.

Another problem in fractional viscoelasticity is the structural analysis in terms of the *finite element method (FEM)*. The FEM is a numerical method for the solution of boundary value problems. In structural analysis, it is used to approximate the deformation of arbitrary continuous bodies under special loading conditions by discretization in small spatial elements. The implementation of a viscoelastic constitutive law in the FEM requires a suitable formulation, which can be even more challenging in the fractional case. An effective numerical solution of fractional-order differential equations in the FEM context is an ongoing research problem.

1.2 Literature overview

Basic theory and numerical approaches

The modern era of fractional calculus is based on several books, starting with Oldham and Spanier (1974), and followed (among others) by Samko et al. (1993); Miller and Ross (1993); Podlubny (1999); Hilfer (2000); Diethelm (2010). Therein, many major problems in theory and applications of fractional calculus are (implicitly) formulated and (partly) solved, including existence, uniqueness and continuity results as well as numerical approaches for certain fractional-order differential equations. Especially, these books have raised the discourse about different definitions of fractional derivatives, among which the *Grünwald-Letnikov*, *Riemann-Liouville* and *Caputo* approach are the most popular. Connected to the choice of definition is the question how associated differential equations are initialized. Particularly, the idea of initializing a fractional differential equation by a single initial datum, as it is known from ordinary differential equations, has generated a lot of interest for the fractional Caputo derivative. Yet, it has been argued by Kempfle and Schäfer (2000); Lorenzo and Hartley (2008); Trigeassou et al. (2011a); Hartley et al. (2013) that the entire history of a function has to be known and used for a correct initialization of fractional differential equations, leading to a fractional calculus on unbounded intervals. This insight, however, appears to be mostly ignored in the applied literature. Formal contributions to fractional calculus on unbounded intervals are among others given by Miller and Ross (1993, Chap. VII); Samko et al. (1993, Chap. 2) and recently by Kleiner and Hilfer (2019a,b) with an application to dielectric relaxation, see Kleiner and Hilfer (2021).

Another important issue in fractional calculus is the numerical solution of fractional-order differential equations. This problem is particularly delicate due to the non-local character of integral operators in combination with weakly singu-

lar kernels. The classical numerical methods can be divided mainly into *product integration rules* and *fractional linear multistep methods*, which both act on Volterra integral equations, see Diethelm et al. (2020). A popular and well-examined representative of the first class is the predictor-corrector scheme by Diethelm et al. (2002, 2004). The second class of methods is based on the approach by Lubich (1986), which particularly includes the frequently-used Grünwald-Letnikov scheme, see Podlubny (1999, Chaps. 7, 8). Both types of methods lead to computationally expensive algorithms with large memory requirements as the entire function history is considered for the approximation of fractional derivatives or integrals. There is, however, a third class of methods which circumvents the above problems by approximating fractional-order through high-dimensional integer-order differential equations, i.e., the non-local problem is replaced by a system of local problems which can be solved by standard integrators. Such methods are in the following referred to as *infinite state schemes*[2], being based on the infinite state representation of fractional derivatives, see Trigeassou et al. (2012a,b). There are various possibilities to formulate such methods and several technical issues. The pioneering work by Yuan and Agrawal (2002); Chatterjee (2005) shows certain drawbacks mentioned by Schmidt and Gaul (2006) and was improved by Diethelm (2008). Further improvements or variations are given by Birk and Song (2010); Li (2010); Jiang et al. (2017); Baffet (2019). Another branch of fractional-order numerical analysis deals with the computation of the *Mittag-Leffler function*, see Gorenflo et al. (2014), which represents the eigenfunction of certain fractional-order differential operators. Numerical methods in this respect were given by Gorenflo et al. (2002); Hilfer and Seybold (2006); Seybold and Hilfer (2009) and later by Garrappa (2014, 2015).

Fractional viscoelasticity and FEM

For the application of fractional calculus to the description of viscoelastic materials, the kernel of fractional derivatives and integrals is used to model long-term creep and relaxation processes. Early contributions identify a power-law behavior of viscoelastic media, see Gemant (1936); Scott Blair (1947); Gerasimov (1948); Rabotnov (1948); Nolle (1950). Later, the empirical method has been connected directly to the theory of fractional calculus, see Caputo and Mainardi (1971); Koeller (1984); Bagley and Torvik (1985) and the physical consistency of fractional viscoelastic models has been discussed by Bagley and Torvik (1986); Lion (2001). In most applications of fractional viscoelasticity, the mechanical behavior of rubber

[2]The infinite states are approximated by a finite number of states, each satisfying an ordinary differential equation. There is no standard notation for this class of schemes in the literature. Alternative names are *nonclassical methods*, see Diethelm (2008) or *kernel compression schemes*, see Baffet (2019) and Diethelm et al. (2020).

and polymers is investigated, see e.g. Schmidt and Gaul (2002). Recently, fractional viscoelastic models have been used to model asphalt and concrete creep, see Celauro et al. (2012) and di Paola and Granata (2016), respectively.

In order to simulate the mechanical behavior of viscoelastic structures, a finite element formulation of fractional constitutive laws is required, which has to be combined with a suitable solver of fractional-order differential equations. A first formulation is given by Bagley and Torvik (1983) in the Laplace domain. This approach has been generalized for the time domain by Bagley and Calico (1991); Fenander (1996). Therefore, the equations of motion are transformed to order $2 + \alpha$ and solved in terms of a fractional-order state space vector. Enelund and Josefson (1997) derive the three-dimensional generalization of a fractional viscoelastic constitutive law for the isotropic case and introduce a finite element approach solving fractional-order equations of order 2 using the Grünwald-Letnikov scheme. The formulation is generalized for the anisotropic case by Enelund et al. (1999). Both methods use an internal variable approach, given in general form by Simo and Hughes (1998). Another formulation by Padovan (1987) incorporates the constitutive law in a slightly different way, using the Grünwald-Letnikov scheme as well. The method is adapted and improved by Schmidt and Gaul (2002). All authors mentioned so far consider the geometrically linear case. Formulations in the context of large deformations are given by Adolfsson and Enelund (2003) and, recently Zopf et al. (2015); Zhang et al. (2020). Both of the latter contributions use an infinite state scheme similar as Birk and Song (2010) for the time integration. Zhang et al. (2020) include an additional accuracy optimization.

Lyapunov theory for systems with fractional damping

The introduction of fractional damping in (controlled) nonlinear systems asks for a generalization of the Lyapunov stability framework, which is well-known for ODEs. The stability of linear fractional-order systems is determined by the spectral condition of Matignon (1996). Furthermore, there exist results e.g. on generalized linear matrix inequalities by Sabatier et al. (2010) and fractional-order control, see Monje et al. (2010). The direct method of Lyapunov for the fractional-order case is examined by several authors, see Lakshmikantham et al. (2009); Li et al. (2010); Duarte-Mermoud et al. (2015); Agarwal et al. (2015); Burton (2011). Thereby, typically a fractional-order derivative of Lyapunov functions is studied in order to obtain a stability statement. A different approach connected to the infinite state representation of fractional derivatives is considered by Trigeassou et al. (2011b, 2016a,b); Trigeassou and Maamri (2019). The method uses Lyapunov functionals given in terms of infinite states and examines their evolution in time. The approach is particularly useful for mechanical systems with additional fractional damping.

1.3 Objective, aims and contributions

The objective of the thesis is to improve and contribute to the mathematical foundation, nonlinear analysis and numerical simulation of fractionally damped mechanical systems. In the following section, certain open problems in the literary canon are seized and the corresponding aims of the thesis are derived. The particular contributions of subsequent chapters in order to tackle and solve some of these problems are summarized.

Fractional calculus on unbounded intervals

An overall aim, that is linked to the correct initialization of fractional derivatives, is a consistent description of fractional calculus on unbounded intervals. The topic is not only rarely studied in theoretical contributions on fractional calculus but even less in applied contexts due to technical difficulties and the simplicity of the classical bounded approach connected to simple initial data. It is, however, important for a consistent description of fractional viscoelasticity and the stability theory for fractionally damped systems. Accordingly, this aim, which contributes to strengthen the mathematical foundation of fractionally damped mechanical systems, is pursued in all chapters of the thesis. Section 2.2 provides a classification of fractional-order differential equations on unbounded intervals and relates them to other well-known types of differential and integral equations. Further, in Section 2.3, it is shown how fractional derivatives and integrals on unbounded intervals can be understood in the context of the infinite state representation. This insight is used in Chapters 3 and 6 for the formulation of associated numerical schemes. The fractional Zener model in Section 4.2 is also given on unbounded intervals[3]. In Chapter 5, the stability of fractionally damped systems (with infinite memory) is studied, which naturally leads to an embedding in the theory of *FDEs with infinite delay*. In summary, the thesis provides a consistent formulation of fractional calculus considering infinite memory in theory, numerical analysis and applications.

Numerical solution of fractional-order problems

A second aim of the thesis is the development of an efficient numerical scheme for fractional-order systems based on the infinite state representation, thereby circumventing some of the drawbacks of the classical approaches mentioned above. The advantages of such methods are accompanied by the issue to find an ap-

[3]Including the entire history of stress and strain is actually a natural approach in viscoelasticity. However, the initialization time instant is typically set to zero (instead of $-\infty$) without cause, when fractional operators come into play, see Mainardi (2010, Sec. 3.1.1).

propriate quadrature rule to approximate the occurring integral of infinite states. The major difficulty is thereby to handle the weak singularity of the integrand. A new strategy to tackle this problem is given in Chapter 3 by introducing a *reformulated infinite state representation*, see Hinze et al. (2019). This approach leads to an integral of infinite states with a new kernel which is integrable and vanishes asymptotically. An associated algorithm, called *reformulated infinite state scheme (RISS)*, is derived and a full error analysis is given. The results of RISS for several benchmark problems are shown and compared to the predictor-corrector method by Diethelm et al. (2002, 2004) and a classical infinite state scheme. Moreover, the new method is used to solve the problems in the examples of Chapters 5 and 6.

Fractional constitutive laws and FEM

The reformulated infinite state representation leads to another contribution in a field of applied fractional calculus, namely the formulation of fractional constitutive laws within the finite element method. As finite element schemes are inherently computationally expensive, it is even more important to provide fast and accurate time-stepping schemes when fractional viscoelastic constitutive laws are considered. In this respect, it is the aim to implement RISS in the finite element method. In Chapter 6, a fractional Zener model is given in terms of the reformulated infinite state representation. This formulation is generalized for a three-dimensional, homogeneous, isotropic and viscoelastic continuum and introduced in the principle of virtual work in order to obtain a scheme to solve the discretized structural dynamic equations. The procedure is tested for a one- and a two-dimensional example and the results are compared to the associated closed form solutions.

Lyapunov stability framework for fractionally damped systems

A large part of the thesis deals with a generalization of the Lyapunov stability framework for systems of ODEs with additional fractional damping. As this concept leads to FDEs, the classical stability definition has to be adapted together with the known methods to obtain stability statements including the *direct method of Lyapunov*. In view of this setting, it is the aim to introduce a theoretical foundation for the direct method of Lyapunov and to formulate Lyapunov functionals in the context of fractionally damped systems. To tackle this problem, the Lyapunov stability theory for FDEs with infinite delay is elaborated in Section 5.2 and applied to Lyapunov functionals in infinite state representation adapted from Trigeassou et al. (2011b, 2016a,b) in Sections 5.3 and 5.4. It is a particular contribution to use and refine the mentioned Lyapunov functionals in the theoretical context of FDE stability. Moreover, the stability framework is established in the following

steps in Sections 5.3 and 5.4, see Hinze et al. (2020a,b). The basic construction of Lyapunov functionals is performed for the single degree-of-freedom fractionally damped oscillator. Considering additional non-negative viscous damping, it is shown that the potential energy of a springpot derived in Section 4.4 is the key to formulate Lyapunov functionals for the proof of asymptotic stability. For the case of additional negative viscous damping, a detailed spectral analysis is performed to obtain stability criteria. Furthermore, it is shown that the reformulated infinite state representation leads to a stability proof with the help of a Lyapunov functional. The method is generalized at first for linear finite-dimensional mechanical systems with fractional damping and, secondly, for a class of controlled nonlinear dynamical systems. The latter application requires a generalized theory of convergent dynamics as well as the use of an invariance principle for asymptotically autonomous FDEs.

1.4 Outline

The introductory chapter is followed by some theoretical foundations of fractional calculus in Chapter 2. Section 2.1 provides the definitions of fractional integrals and derivatives and explains the correspondence between the Riemann-Liouville and the Caputo derivative as well as the associated Liouville-Weyl generalizations. Moreover, the Laplace transform of the Caputo derivative and the Mittag-Leffler functions as eigenfunctions of the Caputo operator are introduced. A classification of different types of *fractional-order ordinary differential equations (FODEs)* is given in Section 2.2. The equations are particularly related to Volterra integral and more general functional differential equations, which are frequently met throughout the thesis. The infinite state representation of fractional integrals and derivatives is given in Section 2.3. This representation forms the basis for numerical schemes to solve FODEs, provides a mechanical interpretation of fractional derivatives and is the starting point for the formulation of Lyapunov functionals. Numerical schemes based on the infinite state representation together with the classical predictor-corrector scheme are presented in Section 2.4.

The reformulated infinite state scheme introduced in Chapter 3 is a modification of numerical schemes based on the infinite state representation. The novel formulation of fractional derivatives is given in Section 3.1 and the associated scheme RISS is illustrated in Section 3.2. A full error analysis of the method is given in Section 3.3 and the performance is studied on the basis of several benchmark problems in Section 3.4. Particularly, the results of RISS are compared to a usual infinite state scheme and the predictor-corrector scheme.

The rest of the thesis deals with different (but connected) applications of the (reformulated) infinite state representation and associated numerical schemes.

Chapter 4 provides a motivation for the use of fractional calculus in mechanics as it introduces fractional viscoelasticity. In Section 4.1, the basic properties of classical linear viscoelastic constitutive laws are given in terms of exponential relaxation and creep functions, which correspond to discrete relaxation and retardation spectra. Moreover, the dynamic properties of viscoelastic models are expressed by complex modulus and complex compliance functions. The fundamental component of fractional viscoelastic models known as *springpot* is introduced in Section 4.2. It is shown that a springpot yields a continuous relaxation spectrum and the correspondence of its complex modulus and the reformulated infinite state representation is explicated. Additionally, the *fractional Zener model* representing a viscoelastic solid is given by Mittag-Leffler creep and relaxation functions. An application of the fractional Zener model to describe the creep of salt concrete is provided in Section 4.3. The model parameters are identified from the experimental data of a compression test. The advantages of fractional over classical viscoelastic models are discussed. Finally, Section 4.4 contains a mechanical interpretation of a springpot by an infinite number of springs and dashpots. The approach emphasizes that a springpot leads to a continuous relaxation spectrum and it yields a useful potential energy expression for the springpot.

The use of fractional calculus in material modeling requires a generalization of mathematical methods in mechanics. In this respect, two different fields, namely stability theory and the finite element method are addressed in Chapters 5 and 6, respectively. The classical theory of stability in the sense of Lyapunov for ODEs is given in Section 5.1. Particularly, the direct method of Lyapunov is introduced including the basic Lyapunov theorem as well as the invariance principle for (asymptotically) autonomous systems. The approach is generalized in Section 5.2 for the less-standard case of FDEs with infinite delay and it is shown that mechanical systems with additional fractional damping belong to this class. Several examples of such systems are considered in Section 5.3 and Lyapunov functionals based on the (reformulated) infinite state representation are examined in order to prove stability statements. The approach is generalized in Section 5.4 for certain controlled nonlinear systems with fractional damping. Thereby, a tracking control problem is solved with the help of an incremental Lyapunov function.

In Chapter 6, an implementation of the fractional Zener model in the finite element method is presented. The formulation of the constitutive law for a 3D continuum is introduced in Section 6.1 using an internal variable model and the reformulated infinite state representation. An associated finite element formulation is given in Section 6.2. The numerical implementation using RISS is described in Section 6.3. Two examples are given as initial benchmarks.

The results of the thesis are concluded in Chapter 7. Some remarks and an outlook on further questions and future work are given.

1.5 Embedding of the thesis in the project ProVerB

The research presented in this thesis is part of the project *ProVerB: Prognosewerkzeuge für das mechanische Verhalten von Beton über lange Zeiträume zur Sicherheitsanalyse von Verschlusssystemen für Endlagerstätten*, which is financed by the program *KMU-innovativ* of the German Federal Ministry of Education and Research (Grant No. 01IS17096B). It is a joint project of the Institute for Nonlinear Mechanics and the Materials Testing Institute (MPA) of the University of Stuttgart together with the Gesellschaft für numerische Simulation (GNS) in Brunswick.

The objective of this program is the development of tools for the prediction of the mechanical behavior of salt concrete over long time spans in order to use this material in structures for sealing final disposal sites. The outstanding operational lifetime and security aspects for these structures lead to special requirements for the material models used and it is the aim to analyze, whether a fractional constitutive law is capable of representing the long-term creep and relaxation processes of salt concrete. Moreover, the project goal is to develop fast algorithms for the implementation of fractional viscoelastic constitutive laws in a user subroutine for the commercial FEM software *Abaqus*. The results of this project are particularly reported in Chapters 3, 4 and 6 of this thesis. The parameters of a fractional Zener model are calibrated in Section 4.3 using experimental data of creep tests with salt concrete. These tests were performed at MPA as part of ProVerB. Furthermore, the finite element formulation in Chapter 6 forms the basis for the Abaqus user subroutine written at GNS.

CHAPTER 2

Fractional calculus

The present chapter deals with fractional calculus - the mathematical theory of differentiation and integration to an arbitrary (non-integer) order. The basic terms and properties regarding fractional derivatives and integrals as well as the related differential and integral equations mentioned here, can be found in the classical textbooks by Oldham and Spanier (1974); Samko et al. (1993); Podlubny (1999); Diethelm (2010) in similar notation but much more detail. Additionally, an interpretation of certain fractional-order differential and integral equations as Volterra functional equations or functional differential equations, see Burton (1985, 2005); Hale (1977); Volterra (1959), is provided. Special consideration is given to the infinite state representation of fractional derivatives and integrals as introduced by Matignon (1998); Montseny (1998) and elaborated by Trigeassou et al. (2011a, 2012a,b). An associated numerical scheme together with a classical method to solve certain fractional-order differential equations is presented according to the explanations by Hinze et al. (2019).

2.1 Definitions and properties

Fractional integral and derivatives

Consider a real-valued function $x : [t_0, T] \to \mathbb{R},\ t \mapsto x(t)$, where the argument t is referred to as time. For an integrable function $x \in L_1[t_0, T]$, denote by

$$\mathrm{I}_{t_0} x(t) := \int_{t_0}^{t} x(\tau)\mathrm{d}\tau, \quad t \in [t_0, T] \tag{2.1}$$

the (first-order) integral of x in $[t_0, t]$ and for a differentiable function x, identify

$$\mathrm{D}x(t) = \dot{x}(t) := \frac{\mathrm{d}x}{\mathrm{d}t}(t), \quad t \in [t_0, T] \tag{2.2}$$

as the (first-order) derivative[1] of x at time t. The basic idea of fractional calculus is the generalization of (2.1) and (2.2) to integrals and derivatives of arbitrary order. Classically, the n-fold iterates of the operators I and D for $n \in \mathbb{N}$ are defined recursively as

$$\begin{aligned} \mathrm{I}_{t_0}^1 &:= \mathrm{I}_{t_0}, \quad \mathrm{I}_{t_0}^n := \mathrm{I}_{t_0}\mathrm{I}_{t_0}^{n-1}, \quad n \geq 2, \\ \mathrm{D}^1 &:= \mathrm{D}, \quad \mathrm{D}^n = \mathrm{D}\mathrm{D}^{n-1}, \quad n \geq 2 \end{aligned}$$

and are called nth-order integral and derivative, respectively. For brevity, the common notation

$$\mathrm{D}^n x(t) = x^{(n)}(t), \quad n \in \mathbb{N}$$

is used for the nth-order derivative of x. Moreover, the nth-order integral is given by the explicit formula

$$\mathrm{I}_{t_0}^n x(t) = \int_{t_0}^t \frac{(t-\tau)^{n-1}}{(n-1)!} x(\tau)\mathrm{d}\tau, \quad n \in \mathbb{N}, \tag{2.3}$$

which can be shown by induction. In order to deduce an arbitrary-order integral from (2.3), a generalization of the factorial function is needed, which is given by the so-called *Euler Gamma function*

$$\Gamma(\alpha) = \int_0^\infty u^{\alpha-1}\mathrm{e}^{-u}\mathrm{d}u, \quad \alpha > 0, \tag{2.4}$$

see Erdélyi (1953, Chap. 1) for a vast collection of properties of Γ. Indeed, the Gamma function fulfills

$$\Gamma(1) = \int_0^\infty \mathrm{e}^{-u}\mathrm{d}u = \lim_{b\to\infty} \left[-\mathrm{e}^{-u}\right]_0^b = \lim_{b\to\infty} (1-\mathrm{e}^{-b}) = 1,$$

and

$$\Gamma(1+\alpha) = \int_0^\infty u^\alpha \mathrm{e}^{-u}\mathrm{d}u = \lim_{\substack{a\to 0+ \\ b\to\infty}} \left[-u^\alpha \mathrm{e}^{-u}\right]_a^b + \int_0^\infty \alpha u^{\alpha-1}\mathrm{e}^{-u}\mathrm{d}u = \alpha\Gamma(\alpha)$$

such that

$$\Gamma(n) = (n-1)!, \quad n \in \mathbb{N} \tag{2.5}$$

holds. Two other properties of the Gamma function are utilized within this thesis, namely the reflection formula

$$\Gamma(\alpha)\Gamma(1-\alpha) = \frac{\pi}{\sin(\alpha\pi)}, \quad \alpha \in (0,1), \tag{2.6}$$

[1] For the derivative of a function with respect to its argument which is different from t, the usual notation $(\cdot)'$ is used instead of $(\dot{\cdot})$.

see Erdélyi (1953, Eq. 1.2(6)) and the identity

$$B(\alpha,\beta) := \int_0^1 s^{\alpha-1}(1-s)^{\beta-1}\mathrm{d}s = \frac{\Gamma(\alpha)\Gamma(\beta)}{\Gamma(\alpha+\beta)}, \quad \alpha,\beta > 0, \tag{2.7}$$

known as the *Euler Beta function* $B(\alpha,\beta)$, see Erdélyi (1953, Sec. 1.5). The use of (2.5) in (2.3) justifies the following definition.

Definition 2.1. Let $x \in L_1[t_0,T]$ and $\alpha > 0$. Define

$$\mathrm{I}_{t_0}^{\alpha} x(t) = \int_{t_0}^{t} \frac{(t-\tau)^{\alpha-1}}{\Gamma(\alpha)} x(\tau)\mathrm{d}\tau \tag{2.8}$$

for $t \in [t_0,T]$ as the *fractional Riemann-Liouville integral* of order α of x at time t. For $\alpha = 0$, set $\mathrm{I}_{t_0}^{0} x := x$.

The integral in (2.8) exists for almost all $t \in [t_0,T]$ according to Tonelli's theorem, as it is a convolution of integrable functions, see Diethelm (2010, Thm. 2.1). Moreover, in view of (2.5), (2.8) coincides with the classical definition (2.3) for integer orders $\alpha \in \mathbb{N}$. To define an associated generalized derivative operator, consider the fundamental theorem of classical calculus in the form

$$\mathrm{D}\mathrm{I}_{t_0} x = x \text{ almost everywhere in } [t_0,T]$$

for $x \in L_1[t_0,T]$. Moreover, if $x \in A^n[t_0,T]$ for $n \in \mathbb{N}$, i.e., x has an absolutely continuous $(n-1)$th-order derivative and $\mathrm{D}^n x \in L_1[t_0,T]$ exists almost everywhere in $[t_0,T]$, it follows for some $m \in \mathbb{N}$, $m > n$

$$\mathrm{D}^n x = \mathrm{D}^m \mathrm{I}_{t_0}^{m-n} x.$$

This idea may be generalized as follows.

Definition 2.2. Let $\alpha \geq 0$, $m \in \mathbb{N}$ such that $m-1 \leq \alpha < m$ and $x \in A^m[t_0,T]$. Define

$${}^{\mathrm{RL}}\mathrm{D}_{t_0}^{\alpha} x(t) = \mathrm{D}^m \mathrm{I}_{t_0}^{m-\alpha} x(t) = \frac{\mathrm{d}^m}{\mathrm{d}t^m} \int_{t_0}^{t} \frac{(t-\tau)^{m-\alpha-1}}{\Gamma(m-\alpha)} x(\tau)\mathrm{d}\tau$$

for $t \in [t_0,T]$ as the *fractional Riemann-Liouville derivative* of order α of x at time t.

Remark 2.3. The assumptions on x given in Definition 2.2 are sufficient but not necessary for the existence of the fractional Riemann-Liouville derivative. However, these conditions allow for the representation in the subsequent proposition.

To get across Remark 2.3, consider the function

$$x(t) = (t-t_0)^{\beta}, \quad -1 < \beta < 0,$$

which does not have a derivative that is integrable in $[t_0, T]$ for some $T > t_0$ but for $\alpha \in (0, 1+\beta)$, the fractional Riemann-Liouville derivative results in

$$\begin{aligned}
{}^{\mathrm{RL}}\mathrm{D}^{\alpha}_{t_0} x(t) &= \frac{\mathrm{d}}{\mathrm{d}t} \int_{t_0}^{t} \frac{(t-\tau)^{-\alpha}}{\Gamma(1-\alpha)} (\tau - t_0)^{\beta} \mathrm{d}\tau \\
&= \frac{1}{\Gamma(1-\alpha)} \int_0^1 (1-s)^{-\alpha} s^{\beta} \mathrm{d}s \frac{\mathrm{d}}{\mathrm{d}t} (t-t_0)^{1+\beta-\alpha}, \\
&= \frac{1}{\Gamma(1-\alpha)} \frac{\Gamma(1-\alpha)\Gamma(1+\beta)}{\Gamma(2+\beta-\alpha)} (1+\beta-\alpha)(t-t_0)^{\beta-\alpha} \\
&= \frac{\Gamma(1+\beta)}{\Gamma(1+\beta-\alpha)} (t-t_0)^{\beta-\alpha},
\end{aligned}$$

where the substitution $s = \frac{\tau - t_0}{t - t_0}$ and (2.7) are used.

Proposition 2.4. *Consider the assumptions in Definition 2.2 and $m-1 < \alpha < m$. Then, ${}^{\mathrm{RL}}\mathrm{D}^{\alpha}_{t_0} x$ exists almost everywhere in $[t_0, T]$ and*

$$ {}^{\mathrm{RL}}\mathrm{D}^{\alpha}_{t_0} x(t) = \sum_{k=0}^{m-1} \frac{(t-t_0)^{k-\alpha}}{\Gamma(k-\alpha+1)} x^{(k)}(t_0) + \int_{t_0}^{t} \frac{(t-\tau)^{m-\alpha-1}}{\Gamma(m-\alpha)} x^{(m)}(\tau) \mathrm{d}\tau. $$

Proof. For abbreviation, introduce the function

$$ w(t) := \frac{t^{m-\alpha-1}}{\Gamma(m-\alpha)} $$

with antiderivative W (for which $W(0)$ exists) and prove the equation

$$ \frac{\mathrm{d}^m}{\mathrm{d}t^m} \int_{t_0}^{t} w(t-\tau) x(\tau) \mathrm{d}\tau = \sum_{k=0}^{m-1} w^{(m-k-1)}(t-t_0) x^{(k)}(t_0) + \int_{t_0}^{t} w(t-\tau) x^{(m)}(\tau) \mathrm{d}\tau \tag{2.9} $$

by induction over m. Confine to the initial step

$$\begin{aligned}
\frac{\mathrm{d}}{\mathrm{d}t} \int_{t_0}^{t} w(t-\tau) x(\tau) \mathrm{d}\tau &= \frac{\mathrm{d}}{\mathrm{d}t} \left(\left[-W(t-\tau) x(\tau) \right]_{t_0}^{t} + \int_{t_0}^{t} W(t-\tau) x'(\tau) \mathrm{d}\tau \right) \\
&= \frac{\mathrm{d}}{\mathrm{d}t} \left(W(t-t_0) x(t_0) - W(0) x(t) + \int_{t_0}^{t} W(t-\tau) x'(\tau) \mathrm{d}\tau \right) \\
&= w(t-t_0) x(t_0) + \int_{t_0}^{t} w(t-\tau) x'(\tau) \mathrm{d}\tau,
\end{aligned}$$

where partial integration is used. The induction step is straightforward. The property

$$ w^{(m-k-1)}(t) = \frac{t^{k-\alpha}}{\Gamma(k-\alpha+1)} $$

together with (2.9) complete the proof. □

The claim in Proposition 2.4 relates the fractional Riemann-Liouville derivative to another possible definition of a fractional derivative.

Definition 2.5. Let $\alpha > 0$, $m \in \mathbb{N}$ such that $m - 1 < \alpha \leq m$ and $x \in A^m[t_0, T]$. Define

$$ {}^{\mathrm{C}}\mathrm{D}^{\alpha}_{t_0} x(t) = \mathrm{I}^{m-\alpha}_{t_0} \mathrm{D}^m x(t) = \int_{t_0}^{t} \frac{(t-\tau)^{m-\alpha-1}}{\Gamma(m-\alpha)} x^{(m)}(\tau) \mathrm{d}\tau \tag{2.10} $$

for $t \in [t_0, T]$ as the *fractional Caputo derivative* of order α of x at time t and for $\alpha = 0$, set ${}^{\mathrm{C}}\mathrm{D}^0_{t_0} x := x$.

The use of Definition 2.5 in Proposition 2.4 yields the relation

$$ {}^{\mathrm{RL}}\mathrm{D}^{\alpha}_{t_0} x(t) = \sum_{k=0}^{m-1} \frac{(t-t_0)^{k-\alpha}}{\Gamma(k-\alpha+1)} x^{(k)}(t_0) + {}^{\mathrm{C}}\mathrm{D}^{\alpha}_{t_0} x(t), \quad \alpha \notin \mathbb{N}_0. \tag{2.11} $$

For the integer-order case $\alpha \in \mathbb{N}_0$, both fractional derivatives coincide with the classical definition. In the general case $\alpha \notin \mathbb{N}_0$, the difference between the Riemann-Liouville and the Caputo definition is given by (2.11). Thereby, in view of Remark 2.3, note that the fractional Riemann-Liouville operator has a wider domain than the Caputo derivative. Accordingly, (2.11) can even be considered as a more general definition of the Caputo derivative. There are two possible situations leading to coincidence of both definitions. The finite sum on the right-hand side of (2.11) vanishes either if $x^{(k)}(t_0) = 0$ for $k = 0, \ldots, m-1$ or, if an infinite lower bound, i.e., the limit case $t_0 \to -\infty$ is considered, which is sometimes referred to as *Liouville-Weyl fractional derivative*, see Mainardi (2010, Chap. 1.4). The latter case asks for an analysis on unbounded intervals and will be of major interest in this thesis. The proof of Proposition 2.4 reveals that it is sufficient for $x(t)$ to fulfill

$$ x(t) = \mathcal{O}\left(|t|^{\alpha-m-\varepsilon}\right), \quad t \to -\infty,\ \varepsilon > 0 $$

such that (2.11) is still valid for $t_0 \to -\infty$ as $W(t - t_0)x(t_0)$ remains bounded. An extensive analysis of the Liouville-Weyl case is given by Samko et al. (1993, Chap. 2).

Before restricting the further studies on a certain type of fractional derivatives, another general property related to (an aspect of) a generalized fundamental theorem is stated.

Proposition 2.6. *Let $x \in A^1[t_0, T]$ and $\alpha > 0$. It holds*

a) ${}^{\mathrm{RL}}\mathrm{D}^{\alpha}_{t_0} \mathrm{I}^{\alpha}_{t_0} x = x$ *almost everywhere and*

b) ${}^{\mathrm{C}}\mathrm{D}^{\alpha}_{t_0} \mathrm{I}^{\alpha}_{t_0} x = x$ *almost everywhere.*

Accordingly, both definitions of fractional derivatives represent a left inverse of the fractional Riemann-Liouville integral.

Proof. The integer-order case is given by the fundamental theorem. For the case $m-1 < \alpha < m$, $m \in \mathbb{N}$ the semigroup property of the fractional integral is used, see Diethelm (2010, Thm. 2.2). For *a)*, consider

$$ {}^{\mathrm{RL}}\mathrm{D}^{\alpha}_{t_0}\mathrm{I}^{\alpha}_{t_0}x = \mathrm{D}^m\mathrm{I}^{m-\alpha}_{t_0}\mathrm{I}^{\alpha}_{t_0}x = \mathrm{D}^m\mathrm{I}^{m}_{t_0}x = x. $$

For *b)*, define the function $y(t) := \mathrm{I}^{\alpha}_{t_0}x(t)$. For $k = 0, \dots, m-1$, it holds $\alpha - k > 0$ and, using Definition 2.1 leads to

$$ \mathrm{D}^k y = \mathrm{I}^{\alpha-k}_{t_0}x \;\text{ and }\; y^{(k)}(t_0) = \mathrm{I}^{\alpha-k}_{t_0}x(t_0) = 0. $$

In view of (2.11) and *a)*, one obtains

$$ {}^{\mathrm{C}}\mathrm{D}^{\alpha}_{t_0}\mathrm{I}^{\alpha}_{t_0}x = {}^{\mathrm{C}}\mathrm{D}^{\alpha}_{t_0}y = {}^{\mathrm{RL}}\mathrm{D}^{\alpha}_{t_0}y = {}^{\mathrm{RL}}\mathrm{D}^{\alpha}_{t_0}\mathrm{I}^{\alpha}_{t_0}x = x. $$ □

In the following, (almost exclusively) fractional Riemann-Liouville integrals and Caputo derivatives of order $\alpha \in (0,1)$ and with initial time $t_0 = 0$ or $t_0 \to -\infty$ are studied. As the latter case is the most important one, the simplified notation

$$ \mathrm{I}^{\alpha} := \mathrm{I}^{\alpha}_{-\infty}, \quad {}^{\mathrm{C}}\mathrm{D}^{\alpha} := {}^{\mathrm{C}}\mathrm{D}^{\alpha}_{-\infty}. $$

for the Liouville-Weyl integral and derivative (of Caputo type) is introduced. For this case and $\alpha \in (0,1)$, the fractional derivatives of some elementary functions are studied in the following example. Apparently, the results are related to the integer-order case.

Example 2.7.

a) $x(t) = \text{const.} \quad \Rightarrow \quad {}^{\mathrm{C}}\mathrm{D}^{\alpha}x \equiv 0.$

b) $x(t) = \begin{cases} (t-t_0)^{\beta}, & t > t_0, \\ 0, & t \le t_0 \end{cases}$ for some $t_0 \in \mathbb{R}$, $\beta > 0$

$$ \begin{aligned} \Rightarrow \quad {}^{\mathrm{C}}\mathrm{D}^{\alpha}x(t) &= {}^{\mathrm{C}}\mathrm{D}^{\alpha}_{t_0}x(t) = \int_{t_0}^{t} \frac{(t-\tau)^{-\alpha}}{\Gamma(1-\alpha)}\beta(\tau-t_0)^{\beta-1}\mathrm{d}\tau \\ &= (t-t_0)^{\beta-\alpha}\frac{\beta}{\Gamma(1-\alpha)}\int_0^1 (1-s)^{-\alpha}s^{\beta-1}\mathrm{d}s \\ &\overset{(2.7)}{=} \frac{\Gamma(1+\beta)}{\Gamma(1-\alpha+\beta)}(t-t_0)^{\beta-\alpha}. \end{aligned} $$

c) $x(t) = \mathrm{e}^{\lambda t}$, $\lambda \in \mathbb{C}$, $\mathrm{Re}(\lambda) \ge 0$

$$ \begin{aligned} \Rightarrow \quad {}^{\mathrm{C}}\mathrm{D}^{\alpha}x(t) &= \int_{-\infty}^{t} \frac{(t-\tau)^{-\alpha}}{\Gamma(1-\alpha)}\lambda\mathrm{e}^{\lambda\tau}\mathrm{d}\tau = \lambda^{\alpha}\mathrm{e}^{\lambda t}\frac{1}{\Gamma(1-\alpha)}\int_0^{\infty} s^{-\alpha}\mathrm{e}^{-s}\mathrm{d}s \\ &\overset{(2.4)}{=} \lambda^{\alpha}\mathrm{e}^{\lambda t}. \end{aligned} $$

d) The case c) with $\lambda = \mathrm{i}\omega$, $\omega > 0$ yields

$$\begin{aligned} {}^{\mathrm{C}}\mathrm{D}^{\alpha}\left\{\mathrm{e}^{\mathrm{i}\omega t}\right\} &= {}^{\mathrm{C}}\mathrm{D}^{\alpha}\left\{\cos(\omega t)\right\} + \mathrm{i}\,{}^{\mathrm{C}}\mathrm{D}^{\alpha}\left\{\sin(\omega t)\right\} \\ &\overset{\text{c)}}{=} (\mathrm{i}\omega)^{\alpha}\mathrm{e}^{\mathrm{i}\omega t} = \omega^{\alpha}\mathrm{e}^{\mathrm{i}(\omega t + \alpha\frac{\pi}{2})} \\ &= \omega^{\alpha}\left(\cos\left(\omega t + \alpha\frac{\pi}{2}\right) + \mathrm{i}\sin\left(\omega t + \alpha\frac{\pi}{2}\right)\right) \end{aligned}$$

$$\begin{aligned} \Rightarrow \quad {}^{\mathrm{C}}\mathrm{D}^{\alpha}\left\{\cos(\omega t)\right\} &= \omega^{\alpha}\cos\left(\omega t + \alpha\frac{\pi}{2}\right), \\ {}^{\mathrm{C}}\mathrm{D}^{\alpha}\left\{\sin(\omega t)\right\} &= \omega^{\alpha}\sin\left(\omega t + \alpha\frac{\pi}{2}\right). \end{aligned}$$

Note that the Liouville-Weyl operator ${}^{\mathrm{C}}\mathrm{D}^{\alpha}$, when applied to a function, considers its entire history. Hence, in order to solve an associated differential equation, an initial function instead of initial values are required. This approach emphasizes the nonlocal character of fractional operators. Different formulations and the advantages over an initial-value approach are discussed by Kempfle and Schäfer (2000); Lorenzo and Hartley (2008); Trigeassou et al. (2011a). The latter formulation is used in this thesis, beginning in Section 2.3. It turns out in Section 2.2 and Chapter 5 that initial functions are a natural condition in the context of functional differential equations.

Laplace transform

In subsequent chapters, several types of differential equations containing fractional Caputo derivatives of system states are studied. As for the integer-order case, the Laplace transform represents a valuable method to solve linear fractional-order differential equations. Therefore, the Laplace transform of fractional Caputo derivatives (with $t_0 = 0$) of functions is determined, which requires some general properties of the Laplace transform, see Doetsch and Nader (1974).

Definition 2.8. Let $x : [0, \infty) \to \mathbb{R}$. Define the function

$$X(s) = \mathcal{L}\left\{x(t)\right\}(s) := \int_0^{\infty} x(t)\mathrm{e}^{-st}\mathrm{d}t, \quad s \in \mathbb{C} \tag{2.12}$$

as the *Laplace transform* of x whenever the integral exists.

Proposition 2.9. *Let $x, x_1, x_2 : [0, \infty) \to \mathbb{R}$ be such that x is differentiable and the Laplace transforms of all functions exist for all s, $\mathrm{Re}(s) > \delta$ for some $\delta > 0$. Further, let $a_1, a_2 \in \mathbb{R}$ and $\beta > -1$.*

a) The Laplace transform is linear,

$$\mathcal{L}\left\{a_1x_1 + a_2x_2\right\}(s) = a_1\mathcal{L}\left\{x_1\right\}(s) + a_2\mathcal{L}\left\{x_2\right\}(s).$$

b) Power functions transform as

$$\mathcal{L}\left\{t^{\beta}\right\}(s) = \frac{\Gamma(1+\beta)}{s^{1+\beta}}.$$

c) The convolution $(x_1 * x_2)(t) := \int_0^t x_1(t-\tau)x_2(\tau)\mathrm{d}\tau$ *of* x_1 *and* x_2 *is transformed to the product of* $\mathcal{L}\{x_1\}(s)$ *and* $\mathcal{L}\{x_2\}(s)$*, i.e.,*

$$\mathcal{L}\{x_1 * x_2\}(s) = \mathcal{L}\{x_1\}(s) \cdot \mathcal{L}\{x_2\}(s).$$

d) The derivative of a function transforms as

$$\mathcal{L}\{\dot{x}\}(s) = s\mathcal{L}\{x\}(s) - x(0).$$

e) The Laplace transform of sine and cosine is given by

$$\mathcal{L}\{\sin(\omega t)\}(s) = \frac{\omega}{s^2+\omega^2}, \quad \mathcal{L}\{\cos(\omega t)\}(s) = \frac{s}{s^2+\omega^2}.$$

Using properties from Proposition 2.9, the Laplace transform of the fractional Caputo derivative with zero lower bound can be deduced as

$$\begin{aligned}\mathcal{L}\left\{{}^{\mathrm{C}}\mathrm{D}_0^{\alpha}x(t)\right\}(s) &= \mathcal{L}\left\{\frac{t^{-\alpha}}{\Gamma(1-\alpha)} * \dot{x}(t)\right\}(s) = s^{\alpha-1}\left(s\mathcal{L}\{x(t)\}(s) - x(0)\right)\\ \Rightarrow \mathcal{L}\left\{{}^{\mathrm{C}}\mathrm{D}_0^{\alpha}x\right\}(s) &= s^{\alpha}\mathcal{L}\{x\}(s) - s^{\alpha-1}x(0). \qquad (2.13)\end{aligned}$$

Definition 2.10. The *inverse Laplace transform* is given by the complex integral

$$\mathcal{L}^{-1}\{X(s)\}(t) = \frac{1}{2\pi\mathrm{i}}\int_{\delta-\mathrm{i}\infty}^{\delta+\mathrm{i}\infty} X(s)\mathrm{e}^{st}\mathrm{d}s, \quad t \geq 0,$$

where $\delta \in \mathbb{R}$ is greater than the largest real part of any singularity of X.

Mittag-Leffler functions

The solutions of linear integer-order ordinary differential equations are determined by the exponential function, which is the eigenfunction of the (first-order) derivative operator. An analogue function for fractional differential operators and a generalization of the exponential function is given in the following definition.

Definition 2.11. Let $\alpha > 0$. The function

$$\mathrm{E}_{\alpha}(t) := \sum_{k=0}^{\infty} \frac{t^k}{\Gamma(\alpha k+1)}$$

is called the *one-parameter Mittag-Leffler function* with parameter α, whenever the series converges.

Proposition 2.12. *Let $\alpha > 0$ and $\gamma, s \in \mathbb{C}$ such that $\mathrm{Re}(s) > |\gamma|^{\frac{1}{\alpha}}$. It holds the formula*

$$\mathcal{L}\left\{\mathrm{E}_\alpha(\gamma t^\alpha)\right\}(s) = \frac{s^{\alpha-1}}{s^\alpha - \gamma}\,.$$

Proof. Consider for $k \in \mathbb{N}$ the integral

$$\begin{aligned}\int_0^\infty \mathrm{e}^{-st}\frac{(\gamma t^\alpha)^k}{\Gamma(\alpha k+1)}\mathrm{d}t &= \frac{\gamma^k}{\Gamma(\alpha k+1)}\int_0^\infty \mathrm{e}^{-st}t^{\alpha k}\mathrm{d}t \\ &= \frac{\gamma^k}{\Gamma(\alpha k+1)}s^{-\alpha k-1}\int_0^\infty \mathrm{e}^{-\tau}\tau^{\alpha k}\mathrm{d}\tau = s^{-1}\left(\frac{\gamma}{s^\alpha}\right)^k,\end{aligned}$$

where (2.4) is used. An infinite sum over k leads to a geometric series that converges for $\mathrm{Re}(s) > |\gamma|^{\frac{1}{\alpha}}$ as

$$s^{-1}\sum_{k=0}^{\infty}\left(\frac{\gamma}{s^\alpha}\right)^k = s^{-1}\frac{1}{1-\frac{\gamma}{s^\alpha}} = \frac{s^{\alpha-1}}{s^\alpha-\gamma}\,.$$

As both limits (of integration and summation) exist, they can be interchanged, which, in view of Definition 2.11 completes the proof. □

The Laplace transform in (2.13) together with Proposition 2.12 finally lead to the eigenfunctions of the fractional Caputo derivative with zero lower bound, i.e., for $\gamma \in \mathbb{C}$

$$\begin{aligned}&{}^{\mathrm{C}}\mathrm{D}_0^\alpha x(t) = \gamma x(t) \quad \overset{\mathcal{L}}{\Longrightarrow} \quad s^\alpha\mathcal{L}\left\{x\right\}(s) - s^{\alpha-1}x(0) = \gamma\mathcal{L}\left\{x\right\}(s) \\ &\Rightarrow \mathcal{L}\left\{x\right\}(s) = x(0)\frac{s^{\alpha-1}}{s^\alpha-\gamma} \quad \overset{\mathcal{L}^{-1}}{\Longrightarrow} \quad x(t) = x(0)\mathrm{E}_\alpha(\gamma t^\alpha)\,.\end{aligned} \tag{2.14}$$

The section is concluded with another property of Mittag-Leffler functions, which turns out to be important in Section 4.2.

Definition 2.13. A function $x : (0,\infty) \to \mathbb{R}$ is called *completely monotonic* if it is differentiable of any order $n \in \mathbb{N}_0$ and the derivatives are alternating in sign, i.e.,

$$(-1)^n x^{(n)}(t) \geq 0, \quad t > 0.$$

The complete monotonicity property holds for the Mittag-Leffler function with negative argument as shown by Pollard (1948).

Proposition 2.14. *The Mittag-Leffler function with negative argument $\mathrm{E}_\alpha(-t)$ is completely monotonic for $\alpha \in (0,1)$.*

2.2 Fractional-order ordinary differential equations

The models considered in the subsequent chapters of this thesis are described by ordinary differential equations that additionally contain fractional Caputo derivatives of system states. In this section, such equations are introduced in a quite general form and are related to other types of functional equations that are frequently met in the literature.

An equation

$$\begin{aligned} &Aq^{(n)}(t) + B\,{}^{\mathrm{C}}\mathrm{D}^{\alpha_{n-1}} q^{(n-1)}(t) \\ &\qquad = F\left(t, q(t), {}^{\mathrm{C}}\mathrm{D}^{\alpha_0} q(t), \dot{q}(t), \ldots, {}^{\mathrm{C}}\mathrm{D}^{\alpha_{n-2}} q^{(n-2)}(t), q^{(n-1)}(t)\right) \end{aligned} \tag{2.15}$$

is denoted as an *(explicit) fractional-order ordinary differential equation (FODE)* of order $n \in \mathbb{N}$ (or $n-1+\alpha_{n-1}$ for the case $A=0$), with $A, B \in \mathbb{R}$, $A \neq 0$ or $B \neq 0$ and fractional orders $\alpha_0, \ldots, \alpha_{n-1} \in (0,1)$. In contrast to the integer-order case, an FODE is equipped with an initial function instead of initial values at one time instant, i.e., the initial condition is provided by an n-times differentiable function φ such that

$$q(s) = \varphi(s), \quad s \leq 0. \tag{2.16}$$

Accordingly, the fractional derivatives in (2.15) can as well be considered with zero initial time as

$${}^{\mathrm{C}}\mathrm{D}_0^{\alpha_i} q^{(i)}(t) = {}^{\mathrm{C}}\mathrm{D}^{\alpha_i} q^{(i)}(t) - \int_{-\infty}^{0} \frac{(t-\tau)^{-\alpha_i}}{\Gamma(1-\alpha_i)} \varphi^{(i+1)}(\tau)\mathrm{d}\tau, \quad i = 0, \ldots, n-1.$$

A *solution* of the problem (2.15) together with (2.16) is an n-times differentiable function q that fulfills (2.16) for nonpositive values and (2.15) in $[0, T)$ for some $T > 0$. Depending on the parameters in (2.15), different cases of FODEs can be distinguished, each related to different theoretical fields.

If $A = 0$, (2.15) can be formulated as

$$\begin{aligned} {}^{\mathrm{C}}\mathrm{D}_0^{\alpha_{n-1}} q^{(n-1)}(t) &= \frac{1}{B} F\left(t, q(t), {}^{\mathrm{C}}\mathrm{D}^{\alpha_0} q(t), \dot{q}(t), \ldots, {}^{\mathrm{C}}\mathrm{D}^{\alpha_{n-2}} q^{(n-2)}(t), q^{(n-1)}(t)\right) \\ &\quad - \int_{-\infty}^{0} \frac{(t-\tau)^{-\alpha_{n-1}}}{\Gamma(1-\alpha_{n-1})} \varphi^{(n)}(\tau)\mathrm{d}\tau \\ &=: \tilde{F}\left(t, q(t), {}^{\mathrm{C}}\mathrm{D}_0^{\alpha_0} q(t), \dot{q}(t), \ldots, {}^{\mathrm{C}}\mathrm{D}_0^{\alpha_{n-2}} q^{(n-2)}(t), q^{(n-1)}(t)\right). \end{aligned} \tag{2.17}$$

Therein, the influence of the initial function (2.16) is included in the first argument of $\tilde{F}$. The most simple case of (2.17) is given by

$${}^{\mathrm{C}}\mathrm{D}_0^{\alpha} q(t) = f(t, q(t)), \quad t \geq 0,\ \alpha \in (0,1), \tag{2.18}$$

which is often studied in the literature and known as *fractional differential equation*, see e.g. Podlubny (1999); Diethelm (2010). The FODE (2.18) is equivalent to a *Volterra integral equation of the second kind*

$$q(t) = \varphi(0) + \mathrm{I}_0^{\alpha}\{f(\cdot, q(\cdot))\}(t) = \varphi(0) + \int_0^t \frac{(t-\tau)^{\alpha-1}}{\Gamma(\alpha)} f(\tau, q(\tau))\mathrm{d}\tau, \tag{2.19}$$

as shown by Diethelm (2010, Lem. 6.2). The representation (2.19) is the starting point to prove existence and uniqueness of a solution of (2.18) together with (2.16) via the method of successive approximations and a fixed point theorem if f is bounded and fulfills a Lipschitz condition with respect to the second argument, see Diethelm (2010, Thms. 6.1, 6.5). In an analogue fashion, (2.17) can be related to a *Volterra functional equation*. Therefore, introduce the state

$$\mathbf{x} = \begin{bmatrix} x_0 & x_1 & \dots & x_{n-1} \end{bmatrix}^{\mathrm{T}} = \begin{bmatrix} q & \dot{q} & \dots & q^{(n-1)} \end{bmatrix}^{\mathrm{T}} \tag{2.20}$$

and obtain

$$\begin{aligned}
x_0(t) &= \varphi(0) + \mathrm{I}_0 x_1(t) \\
x_1(t) &= \dot{\varphi}(0) + \mathrm{I}_0 x_2(t) \\
&\vdots \\
x_{n-2}(t) &= \varphi^{(n-2)}(0) + \mathrm{I}_0 x_{n-1}(t) \\
x_{n-1}(t) &= \varphi^{(n-1)}(0) \\
&\quad + \mathrm{I}_0^{\alpha_{n-1}} \left\{ \tilde{F}\left(\cdot, x_0(\cdot), \mathrm{I}_0^{1-\alpha_0} x_1(\cdot), x_1(\cdot), \dots, \mathrm{I}_0^{1-\alpha_{n-2}} x_{n-1}(\cdot), x_{n-1}(\cdot)\right)\right\}(t).
\end{aligned} \tag{2.21}$$

The system of equations (2.21) is of the form

$$\mathbf{x}(t) = \begin{cases} \boldsymbol{\varphi}(t), & t \le 0, \\ \boldsymbol{\varphi}(0) + \int_0^t \mathbf{F}(\tau, \mathbf{x}(\cdot))\mathrm{d}\tau, & t > 0, \end{cases} \tag{2.22}$$

where $\mathbf{x}$ is given by (2.20), $\boldsymbol{\varphi} = \begin{bmatrix} \varphi & \dot{\varphi} & \dots & \varphi^{(n-1)} \end{bmatrix}^{\mathrm{T}}$ and $\mathbf{F}(t, \mathbf{x}(\cdot))$ operates as a functional on $\mathbf{x}$ in $(0, t)$. Such equations are studied e.g. by Volterra (1959) and Burton (2005).

Similarly, if $A \neq 0$, (2.15) can be reformulated as

$$\begin{aligned}
q^{(n)}(t) &= \frac{1}{A} F\left(t, q(t), {}^{\mathrm{C}}\mathrm{D}^{\alpha_0} q(t), \dot{q}(t), \dots, {}^{\mathrm{C}}\mathrm{D}^{\alpha_{n-2}} q^{(n-2)}(t), q^{(n-1)}(t)\right) \\
&\quad - \frac{B}{A}\left(\int_{-\infty}^{0} \frac{(t-\tau)^{-\alpha_{n-1}}}{\Gamma(1-\alpha_{n-1})} \varphi^{(n)}(\tau)\mathrm{d}\tau + {}^{\mathrm{C}}\mathrm{D}_0^{\alpha_{n-1}} q^{(n-1)}(t)\right) \\
&=: \hat{F}\left(t, q(t), {}^{\mathrm{C}}\mathrm{D}_0^{\alpha_0} q(t), \dot{q}(t), \dots, {}^{\mathrm{C}}\mathrm{D}_0^{\alpha_{n-2}} q^{(n-2)}(t), q^{(n-1)}(t)\right) \\
&\quad - \frac{B}{A} {}^{\mathrm{C}}\mathrm{D}_0^{\alpha_{n-1}} q^{(n-1)}(t),
\end{aligned}$$

which can together with (2.20) be written as

$$\begin{aligned}
x_0(t) &= \varphi(0) + \mathrm{I}_0 x_1(t) \\
x_1(t) &= \dot{\varphi}(0) + \mathrm{I}_0 x_2(t) \\
&\vdots \\
x_{n-2}(t) &= \varphi^{(n-2)}(0) + \mathrm{I}_0 x_{n-1}(t) \\
x_{n-1}(t) &= \varphi^{(n-1)}(0) \\
&\quad + \mathrm{I}_0 \left\{ \hat{F}\left(\cdot, x_0(\cdot), \mathrm{I}_0^{1-\alpha_0} x_1(\cdot), x_1(\cdot), \ldots, \mathrm{I}_0^{1-\alpha_{n-2}} x_{n-1}(\cdot), x_{n-1}(\cdot)\right)\right\}(t) \\
&\quad - \frac{B}{A} \mathrm{I}_0^{1-\alpha_{n-1}} \left\{ x_{n-1}(\cdot) - \varphi^{(n-1)}(0) \right\}(t).
\end{aligned} \tag{2.23}$$

The system (2.23) is another example of a Volterra functional equation (2.22). A proof for existence and uniqueness of solutions similar as for a Volterra integral equation such as (2.19) is given by Driver (1962, Thm. 2) and Burton (1985, Thm. 8.1.3) in the context of *functional differential equations (FDEs)*. They represent a special type of functional equations of the form

$$\dot{\mathbf{x}}(t) = \mathbf{f}(t, \mathbf{x}_t), \quad t \geq 0, \tag{2.24}$$

where $\mathbf{x}_t(s) = \mathbf{x}(t+s)$ for $s \in (-\infty, 0]$ and $\mathbf{f} : [0, \infty) \times B \to \mathbb{R}^n$ is a continuous map defined in its second argument on an open subset $B \subset X$ of a certain space X of $\mathbb{R}^n$-valued functions on $(-\infty, 0]$. Integration of (2.24) directly leads to an equation of the form (2.22). However, FDEs gave rise to an independent theoretical field, see Burton (1985); Hale (1977); Kolmanovskii and Nosov (1986). As FDEs play an essential role for the description of mechanical systems with fractional damping in Chapter 5, they are explicitly mentioned here. Particularly, using (2.20), the case $B = 0$ in (2.15) leads to the FDE

$$\begin{aligned}
\dot{x}_0(t) &= x_1(t) \\
\dot{x}_1(t) &= x_2(t) \\
&\vdots \\
\dot{x}_{n-2}(t) &= x_{n-1} \\
\dot{x}_{n-1}(t) &= \frac{1}{A} F\left(t, x_0(t), {}^{\mathrm{C}}\mathrm{D}^{\alpha_0} x_0(t), x_1(t), \ldots, {}^{\mathrm{C}}\mathrm{D}^{\alpha_{n-2}} x_{n-2}(t), x_{n-1}(t)\right).
\end{aligned} \tag{2.25}$$

Thereby, each fractional derivative in (2.25) is considered as a functional acting on $\mathbf{x}_t$, as a reparametrization $s = \tau - t$ in the fractional Caputo derivative leads to

$$\begin{aligned}
{}^{\mathrm{C}}\mathrm{D}^{\alpha_i} x_i(t) &= \int_{-\infty}^{0} \frac{(-s)^{-\alpha}}{\Gamma(1-\alpha)} x_i'(t+s)\mathrm{d}s \\
&= \int_{-\infty}^{0} \frac{(-s)^{-\alpha}}{\Gamma(1-\alpha)} (x_{i+1})_t(s)\mathrm{d}s, \quad i = 0, \ldots, n-2
\end{aligned}$$

such that (2.25) matches (2.24).

2.3 Infinite state representation

An alternative description of fractional Liouville-Weyl integrals is given by the so-called *infinite state representation*

$$\begin{aligned} \mathrm{I}^{\alpha} x(t) &= \int_0^{\infty} \mu_{\alpha}(\lambda) Z(\lambda, t) \mathrm{d}\lambda, \quad t \geq 0, \\ \dot{Z}(\eta, t) &= x(t) - \eta Z(\eta, t), \quad \eta > 0,\, t \geq 0, \\ Z(\eta, 0) &= \int_{-\infty}^{0} \mathrm{e}^{\eta\tau} x(\tau) \mathrm{d}\tau, \quad \eta > 0 \end{aligned} \tag{2.26}$$

with infinite states $Z(\eta, t)$, where

$$\mu_{\alpha}(\eta) = \frac{\sin(\alpha\pi)}{\pi} \eta^{-\alpha} \tag{2.27}$$

as introduced by Matignon (1998); Montseny (1998); Trigeassou et al. (2012b). To see the correspondence between (2.8) and (2.26), use (2.27) and (2.4) to obtain

$$\frac{t^{\alpha-1}}{\Gamma(\alpha)} = \frac{1}{\Gamma(\alpha)\Gamma(1-\alpha)} \int_0^{\infty} t^{\alpha-1} u^{-\alpha} \mathrm{e}^{-u} \mathrm{d}u = \int_0^{\infty} \mu_{\alpha}(\lambda) \mathrm{e}^{-\lambda t} \mathrm{d}\lambda, \tag{2.28}$$

where $u = \lambda t$ is substituted and the property (2.6) is used. One obtains (2.26) by inserting (2.28) in (2.8), using Fubini's theorem and the solution of the initial value problem in (2.26), viz.

$$Z(\eta, t) = \int_{-\infty}^{t} \mathrm{e}^{-\eta(t-\tau)} x(\tau) \mathrm{d}\tau, \quad \eta > 0,\, t \geq 0$$

such that

$$\begin{aligned} \mathrm{I}^{\alpha} x(t) &= \int_{-\infty}^{t} \int_0^{\infty} \mu_{\alpha}(\lambda) \mathrm{e}^{-\lambda(t-\tau)} \mathrm{d}\lambda\, x(\tau) \mathrm{d}\tau \\ &= \int_0^{\infty} \mu_{\alpha}(\lambda) \int_{-\infty}^{t} \mathrm{e}^{-\lambda(t-\tau)} x(\tau) \mathrm{d}\tau\, \mathrm{d}\lambda \\ &= \int_0^{\infty} \mu_{\alpha}(\lambda) Z(\lambda, t) \mathrm{d}\lambda. \end{aligned}$$

Accordingly, an infinite state representation of the fractional derivative ${}^{\mathrm{C}}\mathrm{D}^{\alpha}$ for $\alpha \in (0, 1)$ is given by

$$\begin{aligned} {}^{\mathrm{C}}\mathrm{D}^{\alpha} x(t) &= \mathrm{I}^{1-\alpha} \dot{x}(t) = \int_0^{\infty} \mu_{1-\alpha}(\lambda) z(\lambda, t) \mathrm{d}\lambda, \quad t \geq 0, \\ \dot{z}(\eta, t) &= \dot{x}(t) - \eta z(\eta, t), \quad \eta > 0,\, t \geq 0, \\ z(\eta, 0) &= \int_{-\infty}^{0} \mathrm{e}^{\eta\tau} x'(\tau) \mathrm{d}\tau, \quad \eta > 0 \end{aligned} \tag{2.29}$$

with infinite states $z(\eta, t)$. The two kinds of infinite states are related by the following equations, which may be obtained by using the solutions of the initial value problems in (2.29), (2.26) and partial integration as

$$\begin{aligned} z(\eta,t) &= \int_{-\infty}^{t} \mathrm{e}^{-\eta(t-\tau)} x'(\tau)\mathrm{d}\tau \\ &= \lim_{a\to-\infty} \left[\mathrm{e}^{-\eta(t-\tau)} x(\tau)\right]_a^t - \eta \int_{-\infty}^{t} \mathrm{e}^{-\eta(t-\tau)} x(\tau)\mathrm{d}\tau \\ &= x(t) - \eta Z(\eta,t) = \dot{Z}(\eta,t), \quad \eta > 0,\, t \geq 0, \end{aligned} \tag{2.30}$$

whenever x is bounded.

The infinite state representation translates fractional integrals and derivatives to integer-order at the cost of a continuum of state variables. Correspondingly, the history of the function x is transferred to initial conditions of the infinite states

$$Z(\eta,0) = \int_{-\infty}^{0} \mathrm{e}^{\eta\tau} x(\tau)\mathrm{d}\tau, \quad z(\eta,0) = \int_{-\infty}^{0} \mathrm{e}^{\eta\tau} x'(\tau)\mathrm{d}\tau.$$

The approximation of the improper integrals of infinite states in (2.26) and (2.29) by sums transforms FODEs to ordinary differential equations (ODEs) or differential algebraic equations (DAEs) and indicates a possible starting point for the formulation of numerical schemes to solve FODEs.

2.4 Classical numerical schemes

The following section provides an introduction to the classical predictor-corrector scheme and some infinite state based numerical schemes to solve (special types of) FODEs. In the next chapter, these methods are compared to a novel scheme based on a reformulated infinite state representation.

Predictor-corrector scheme

A deeply examined method to solve fractional differential equations (2.18) is the *predictor-corrector scheme (PC)* proposed by Diethelm et al. (2002) and extensively analyzed by Diethelm et al. (2004). The method considers the associated Volterra integral equation (2.19) and approximates the emerging integrals by two different quadratures in a predictor and a corrector step. The scheme is formulated for the more general case $\alpha > 0$, i.e., for an initial-value problem of the form

$$\begin{aligned} {}^{\mathrm{C}}\mathrm{D}_0^{\alpha} x(t) &= f(t, x(t)), \quad m-1 < \alpha \leq m,\ m \in \mathbb{N}, \\ x^{(k)}(0) &= x_0^{(k)}, \qquad\qquad k = 0, 1, \ldots, m-1 \end{aligned}$$

Section 2.4 is based on Hinze et al. (2019, Sec. 3)

for $t \in [0, T]$ or, equivalently for the Volterra integral equation

$$x(t) = \sum_{k=0}^{m-1} x_0^{(k)} \frac{t^k}{k!} + \int_0^t \frac{(t-\tau)^{\alpha-1}}{\Gamma(\alpha)} f(\tau, x(\tau)) \mathrm{d}\tau. \tag{2.31}$$

The integral in (2.31) is approximated by a composite trapezoidal rule with fixed time-step $h = t_j - t_{j-1}$, $j = 1, \ldots, N = \lfloor \frac{T}{h} \rfloor$, which leads to

$$\tilde{x}(t_{n+1}) = \sum_{k=0}^{m-1} x_0^{(k)} \frac{t_{n+1}^k}{k!} + \frac{h^\alpha}{\Gamma(\alpha+2)} \sum_{j=0}^{n+1} a_{j,n+1} f(t_j, \tilde{x}(t_j)) \tag{2.32}$$

with coefficients

$$a_{j,n+1} = \begin{cases} n^{\alpha+1} - (n-\alpha)(n+1)^\alpha & j = 0, \\ (n-j+2)^{\alpha+1} + (n-j)^{\alpha+1} - 2(n-j+1)^{\alpha+1} & 1 \le j \le n, \\ 1 & j = n+1. \end{cases}$$

To avoid solving the nonlinear equation (2.32) for $\tilde{x}(t_{n+1})$, the solution is estimated in a predictor step with the help of the (explicit) rectangular rule as

$$\tilde{x}_\mathrm{p}(t_{n+1}) = \sum_{k=0}^{m-1} x_0^{(k)} \frac{t_{n+1}^k}{k!} + \frac{1}{\Gamma(\alpha)} \sum_{j=0}^{n} b_{j,n+1} f(t_j, \tilde{x}(t_j))$$

with coefficients

$$b_{j,n+1} = \frac{h^\alpha}{\alpha} ((n+1-j)^\alpha - (n-j)^\alpha)$$

and corrected by (2.32) as

$$\begin{aligned} \tilde{x}(t_{n+1}) = \sum_{k=0}^{m-1} x_0^{(k)} \frac{t_{n+1}^k}{k!} + \frac{h^\alpha}{\Gamma(\alpha+2)} f(t_{n+1}, \tilde{x}_\mathrm{p}(t_{n+1})) \\ + \frac{h^\alpha}{\Gamma(\alpha+2)} \sum_{j=0}^{n} a_{j,n+1} f(t_j, \tilde{x}(t_j)). \end{aligned}$$

The scheme leads to an error estimation

$$\max_{j=0,1,\ldots,N} \left| x(t_j) - \tilde{x}(t_j) \right| = \mathcal{O}(h^p), \qquad p = \min(2, 1+\alpha), \qquad (h \to 0). \tag{2.33}$$

The method may be directly applied to FODEs (2.15) with rational differentiation orders $\alpha_0, \ldots, \alpha_{n-1}$. To this end, (2.15) is transferred to a vectorial version of (2.18), where α is the greatest common divisor of $\alpha_0, \ldots, \alpha_{n-1}$. In the general case, the irrational differentiation orders in the set $\{\alpha_0, \ldots, \alpha_{n-1}\}$ have to be approximated by rational ones. The details are given by Diethelm and Ford (2004) and Diethelm et al. (2002, Sec. 4). The algorithm may be improved, e.g. by using several corrector iterations or applying a Richardson extrapolation, see Diethelm et al. (2002, Sec. 3). In Chapter 3, this algorithm is tested using the MATLAB implementation `fde12.m` by Garrappa (2012).

Infinite state schemes

Methods based on the infinite state representation of fractional integrals and derivatives usually start with a discretization of the infinite states and a related quadrature of the improper integral in (2.26) or (2.29), which leads to approximations

$$\begin{aligned} \mathrm{I}^{\alpha} x(t) &\approx \sum_{n=0}^{N} Z_n(t) w_n, \\ \dot{Z}_n(t) &= x(t) - \eta_n Z_n(t),\ n = 0, \dots, N \end{aligned} \tag{2.34}$$

with $Z_n(t) = Z(\eta_n, t)$ or

$$\begin{aligned} {}^{\mathrm{C}}\mathrm{D}^{\alpha} x(t) &\approx \sum_{n=0}^{N} z_n(t) \tilde{w}_n, \\ \dot{z}_n(t) &= \dot{x}(t) - \eta_n z_n(t),\ n = 0, \dots, N \end{aligned} \tag{2.35}$$

with $z_n(t) = z(\eta_n, t)$. Thereby, the discrete values η_n and $w_n, \tilde{w}_n$, $n = 0, \dots, N$ are the nodes and weights of the chosen quadrature, respectively, where the kernel μ_α (resp. $\mu_{1-\alpha}$) in (2.27) is incorporated in the weights w_n (resp. $\tilde{w}_n$). The approximations (2.34) and (2.35) bring forth two difficulties: The upper bound of the integral is infinite and the kernel is weakly singular at zero. Both facts have to be considered when choosing the quadrature. Furthermore, the substitution of (2.35) into an FODE (2.15) leads to a stiff ODE (while the substitution of (2.34) in a fractional integral equation leads to a stiff DAE), asking for a dedicated stiff solver. Originally, an infinite state scheme of the form (2.34) is used by Trigeassou et al. (2012a,b) together with an adapted version of Oustaloup's filter, see Oustaloup (1995), to perform the quadrature. The parameters η_n are in this case chosen to be geometrically distributed, i.e., equidistant on a logarithmic scale. In the much-debated articles by Chatterjee (2005); Yuan and Agrawal (2002), transformed representations similar to (2.35) are introduced. The quadrature used by Yuan and Agrawal (2002) is of Gauss-Laguerre type, which is adapted to the improper integral in (2.29). However, the weak singularity is not treated appropriately in this approach and the asymptotic decay of the integrand for $\lambda \to \infty$ is rather slow, which leads to slow convergence of the scheme, see Diethelm (2008). A significant improvement may be obtained using a Gauss-Jacobi quadrature for a transformed infinite state integral as proposed by Diethelm (2008); Birk and Song (2010), which considers the weak singularity at zero. Alternatively, the use of a Galerkin method was suggested by Singh and Chatterjee (2006); Diethelm (2008). Recently, several schemes using composite quadrature rules have been introduced, e.g. by Li (2010) (composite Gauss-Legendre) and Jiang et al. (2017); Baffet (2019) (composite Gauss-Jacobi). These schemes use the advantage that particular subintervals, usually distributed over many decades, may be chosen

in advance to perform the quadrature on each interval (whereas in a single Gaussian quadrature the nodes are only determined by the zeroes of certain orthogonal polynomials).

In the following, a composite Gauss-Jacobi quadrature for (2.34) similar to the quadrature of the scheme in Baffet (2019) is described in order to compare its results to the method proposed in Chapter 3. When using this scheme, it will be referred to as *infinite state scheme (ISS)*. In general, a Gauss-Jacobi quadrature is an approximation of an integral over the interval $[-1,1]$ of a continuous function f weighted by an algebraic function with (possibly) weak singularities at the boundaries of the integration interval. It has the form

$$\int_{-1}^{1}(1+x)^{\beta}(1-x)^{\gamma}f(x)\mathrm{d}x \approx \sum_{n=0}^{N} f\left(s_n^{(\beta,\gamma)}\right) w_n^{(\beta,\gamma)}$$

with $\beta,\gamma > -1$, nodes $s_n^{(\beta,\gamma)}$ and weights $w_n^{(\beta,\gamma)}$ such that polynomials of degree $2N-1$ are integrated exactly. The details on determining the nodes and weights may be found e.g. in the book of Davis and Rabinowitz (1984, Chap. 2.7). In the present case, a composite version of this idea is used, i.e., consider $\eta_0 = 0$, $\eta_1,\dots,\eta_K$ in $(0,\infty)$ and perform a Gauss-Jacobi quadrature in each interval $(\eta_0,\eta_1),\dots,(\eta_{K-1},\eta_K)$ with nodes $\eta_{k,j} \in (\eta_k,\eta_{k+1})$ and weights $w_j^{(\beta_k,\gamma_k)}$, $j=1,\dots,J$, $k=0,\dots,K-1$. One can use a substitution

$$\begin{aligned}
&\int_a^b (x-a)^{\beta}(b-x)^{\gamma}f(x)\mathrm{d}x \\
&\qquad = \left(\frac{b-a}{2}\right)^{1+\beta+\gamma}\int_{-1}^{1}(1+s)^{\beta}(1-s)^{\gamma}f\left(\frac{b-a}{2}s+\frac{a+b}{2}\right)\mathrm{d}s \\
&\qquad \approx \left(\frac{b-a}{2}\right)^{1+\beta+\gamma}\sum_{n=0}^{N} f\left(\frac{b-a}{2}s_n^{(\beta,\gamma)}+\frac{a+b}{2}\right) w_n^{(\beta,\gamma)}
\end{aligned}$$

to adapt to the integration boundaries $a < b$. Applying this procedure to the integral in (2.26) leads for the first interval (η_0,η_1) to

$$\begin{aligned}
\int_0^{\eta_1}\mu_{\alpha}(\lambda)Z(\lambda,t)\mathrm{d}\lambda &= \frac{\sin(\alpha\pi)}{\pi}\int_0^{\eta_1}\lambda^{-\alpha}\,Z(\lambda,t)\mathrm{d}\lambda \\
&= \frac{\sin(\alpha\pi)}{\pi}\left(\frac{\eta_1}{2}\right)^{1-\alpha}\int_{-1}^{1}(1+s)^{-\alpha}\,Z\left(\frac{\eta_1}{2}(1+s),t\right)\mathrm{d}s \\
&\approx \frac{\sin(\alpha\pi)}{\pi}\left(\frac{\eta_1}{2}\right)^{1-\alpha}\sum_{j=1}^{J} Z\Bigg(\underbrace{\frac{\eta_1}{2}\left(1+s_j^{(-\alpha,0)}\right)}_{=:\eta_{0,j}},t\Bigg) w_j^{(-\alpha,0)}
\end{aligned} \tag{2.36}$$

and for the other intervals, using the abbreviation $\eta_k(s) = \frac{\eta_{k+1}-\eta_k}{2}s + \frac{\eta_k+\eta_{k+1}}{2}$, to

$$\begin{aligned}\int_{\eta_k}^{\eta_{k+1}} \mu_\alpha(\lambda)Z(\lambda,t)\mathrm{d}\lambda &= \frac{\eta_{k+1}-\eta_k}{2}\int_{-1}^{1} \mu_\alpha(\eta_k(s))Z(\eta_k(s),t)\mathrm{d}s \\ &\approx \frac{\eta_{k+1}-\eta_k}{2}\sum_{j=1}^{J} \mu_\alpha\left(\eta_k\left(s_j^{(0,0)}\right)\right) Z\left(\eta_k\left(s_j^{(0,0)}\right),t\right) w_j^{(0,0)} \qquad (2.37)\\ &= \frac{\eta_{k+1}-\eta_k}{2}\sum_{j=1}^{J} \mu_\alpha(\eta_{k,j})Z(\eta_{k,j},t)w_j^{(0,0)}\end{aligned}$$

for $k = 1,\dots,K-1$, where $\eta_{k,j} = \eta_k\left(s_j^{(0,0)}\right)$. Hence, only one set of nodes and weights

$$\left(s_j^{(-\alpha,0)}, w_j^{(-\alpha,0)}\right)_{j=1,\dots,J}$$

has to be computed for the quadrature in (2.36) and another set

$$\left(s_j^{(0,0)}, w_j^{(0,0)}\right)_{j=1,\dots,J}$$

for the case (2.37), which is independent of $k \in \{1,\dots,K-1\}$. Actually, the weak singularity only has to be considered in (2.36), while more specifically (2.37) represents a Gauss-Legendre quadrature. In summary, one obtains the approximation

$$\begin{aligned}\int_0^\infty \mu_\alpha(\lambda)Z(\lambda,t)\mathrm{d}\lambda \approx{}& \frac{\sin(\alpha\pi)}{\pi}\left(\frac{\eta_1}{2}\right)^{1-\alpha}\sum_{j=1}^{J} Z(\eta_{0,j},t)w_j^{(-\alpha,0)} \\ &+ \sum_{k=1}^{K-1}\frac{\eta_{k+1}-\eta_k}{2}\sum_{j=1}^{J} \mu_\alpha(\eta_{k,j})Z(\eta_{k,j},t)w_j^{(0,0)}\end{aligned}$$

of the integral in (2.26), which may be used in (2.34), where $N = K \cdot J$. To use this approximation for solving a fractional integral equation, an appropriate DAE solver still has to be chosen. As the coefficients η_n of Z_n in the ODEs of (2.34) become huge numbers for large n, the resulting DAEs will usually be stiff such that explicit time stepping methods fail, see Diethelm (2008, Sec. 3.2). Therefore, in subsequent numerical examples, MATLAB's stiff solver `ode15s.m` is chosen, which uses an implicit (backward differentiation) method.

CHAPTER 3

Reformulated infinite state scheme

The reformulation of the infinite state representation as introduced by Hinze et al. (2019) is the fundamental instrument in this thesis. It leads to a numerical method to solve fractional-order ordinary differential equations and is applied in stability theory as well as for a finite element formulation of fractionally damped systems in the subsequent chapters. This chapter provides the formulation and the associated numerical scheme together with a detailed error analysis. The performance of the method is demonstrated for several benchmark problems and compared to the methods described in the previous chapter.

3.1 Reformulated infinite state representation

The *reformulated infinite state representation* is introduced as an expansion of the integration kernel in (2.29) by the term $\lambda^2 + \omega^2$ for a real number $\omega > 0$. The following properties will prove to be useful in the proposed reformulation.

Proposition 3.1.

$$\int_0^\infty \frac{\mu_\alpha(\lambda)}{\lambda + s} \mathrm{d}\lambda = s^{-\alpha}, \quad s \in \mathbb{C}\backslash\mathbb{R}^-,\ \alpha \in (0,1). \tag{3.1}$$

Proof. Making use of the Laplace transform of $\mathrm{e}^{-\lambda t}$

$$\begin{aligned}\mathcal{L}\left\{\mathrm{e}^{-\lambda t}\right\}(s) &= \int_0^\infty \mathrm{e}^{-\lambda t}\mathrm{e}^{-st}\mathrm{d}t = \int_0^\infty \mathrm{e}^{-(\lambda+s)t}\mathrm{d}t \\ &= \left[-\frac{1}{\lambda+s}\mathrm{e}^{-(\lambda+s)t}\right]_0^\infty = \frac{1}{\lambda+s},\end{aligned}$$

Chapter 3 is based on Hinze et al. (2019, Sec. 4).

one obtains Equation (3.1) using Fubini's theorem, (2.4) and (2.6) as

$$\begin{aligned}\int_0^\infty \frac{\mu_\alpha(\lambda)}{\lambda+s}\mathrm{d}\lambda &= \frac{\sin(\alpha\pi)}{\pi}\int_0^\infty \lambda^{-\alpha}\int_0^\infty \mathrm{e}^{-(\lambda+s)t}\mathrm{d}t\mathrm{d}\lambda\\ &= \frac{\sin(\alpha\pi)}{\pi}\int_0^\infty \mathrm{e}^{-st}\int_0^\infty \lambda^{-\alpha}\mathrm{e}^{-\lambda t}\mathrm{d}\lambda\mathrm{d}t\\ &= \frac{\sin(\alpha\pi)}{\pi}\int_0^\infty \mathrm{e}^{-st}\Gamma(1-\alpha)t^{\alpha-1}\mathrm{d}t\\ &= \frac{\sin(\alpha\pi)}{\pi}\Gamma(1-\alpha)\Gamma(\alpha)s^{-\alpha} = s^{-\alpha}.\end{aligned}$$

□

Remark 3.2. The result of Proposition 3.1 is also used by Trigeassou et al. (2012b) (without proof). A similar proof as the one given here may be found in the article of Wei et al. (2016).

Proposition 3.3. *For $\alpha \in (0,1)$ and $\omega > 0$, the identities*

$$\int_0^\infty \frac{\mu_{1-\alpha}(\lambda)}{\lambda^2+\omega^2}\mathrm{d}\lambda = \cos\left(\frac{\alpha\pi}{2}\right)\omega^{\alpha-2}, \tag{3.2}$$

$$\int_0^\infty \frac{\mu_{1-\alpha}(\lambda)\lambda}{\lambda^2+\omega^2}\mathrm{d}\lambda = \sin\left(\frac{\alpha\pi}{2}\right)\omega^{\alpha-1} \tag{3.3}$$

hold.

Proof. Substitute $\eta = \lambda^2$ and $\mathrm{d}\eta = 2\lambda\,\mathrm{d}\lambda$ in the integral and obtain

$$\begin{aligned}\int_0^\infty \frac{\mu_{1-\alpha}(\lambda)}{\lambda^2+\omega^2}\mathrm{d}\lambda &= \frac{\sin(\alpha\pi)}{\pi}\int_0^\infty \frac{\lambda^{\alpha-1}}{\lambda^2+\omega^2}\mathrm{d}\lambda = \frac{\sin(\alpha\pi)}{2\pi}\int_0^\infty \frac{\eta^{\frac{\alpha}{2}-1}}{\eta+\omega^2}\mathrm{d}\eta\\ &= \frac{\sin(\alpha\pi)}{2\sin\left(\frac{\alpha\pi}{2}\right)}\int_0^\infty \frac{\mu_{1-\frac{\alpha}{2}}(\eta)}{\eta+\omega^2}\mathrm{d}\eta.\end{aligned}$$

Using the sine-double-angle formula and (3.1) directly yields (3.2). The proof of (3.3) is analogous. □

Remark 3.4. Similar assertions as in Proposition 3.3 are proven by Trigeassou et al. (2016b).

Expansion of the integral in (2.29) by the term $\lambda^2+\omega^2$ for a fixed $\omega > 0$ leads together with the infinite states in (2.26), (2.30) and Proposition 3.3 to

$$\begin{aligned}{}^{\mathrm{C}}\mathrm{D}^\alpha x(t) &= \int_0^\infty \frac{\mu_{1-\alpha}(\lambda)\lambda}{\lambda^2+\omega^2}\lambda z(\lambda,t)\mathrm{d}\lambda + \omega^2\int_0^\infty \frac{\mu_{1-\alpha}(\lambda)}{\lambda^2+\omega^2}z(\lambda,t)\mathrm{d}\lambda\\ &= \int_0^\infty \frac{\mu_{1-\alpha}(\lambda)\lambda}{\lambda^2+\omega^2}\mathrm{d}\lambda\,\dot{x}(t) - \int_0^\infty \frac{\mu_{1-\alpha}(\lambda)\lambda}{\lambda^2+\omega^2}\dot{z}(\lambda,t)\mathrm{d}\lambda\\ &\quad + \omega^2\int_0^\infty \frac{\mu_{1-\alpha}(\lambda)}{\lambda^2+\omega^2}\mathrm{d}\lambda\,x(t) - \omega^2\int_0^\infty \frac{\mu_{1-\alpha}(\lambda)\lambda}{\lambda^2+\omega^2}Z(\lambda,t)\mathrm{d}\lambda,\end{aligned}$$

$$\begin{aligned} {}^{\mathrm{C}}\mathrm{D}^{\alpha}x(t) &= \sin\left(\frac{\alpha\pi}{2}\right)\omega^{\alpha-1}\dot{x}(t) - \int_0^{\infty}\frac{\mu_{1-\alpha}(\lambda)\lambda}{\lambda^2+\omega^2}\dot{z}(\lambda,t)\mathrm{d}\lambda \\ &\quad + \cos\left(\frac{\alpha\pi}{2}\right)\omega^{\alpha}x(t) - \omega^2\int_0^{\infty}\frac{\mu_{1-\alpha}(\lambda)\lambda}{\lambda^2+\omega^2}Z(\lambda,t)\mathrm{d}\lambda. \end{aligned} \tag{3.4}$$

The advantage of the *reformulated infinite state representation* in (3.4) is the new kernel with parameter $\omega > 0$

$$\mathrm{K}_{\omega}(\alpha,\eta) := \frac{\mu_{1-\alpha}(\eta)\eta}{\eta^2+\omega^2} = \frac{\sin(\alpha\pi)}{\pi}\frac{\eta^{\alpha}}{\eta^2+\omega^2},$$

which is integrable in $(0,\infty)$ and fulfills

$$\lim_{\eta\to 0}\mathrm{K}_{\omega}(\alpha,\eta) = \lim_{\eta\to\infty}\mathrm{K}_{\omega}(\alpha,\eta) = 0, \quad \alpha\in(0,1).$$

Furthermore, (3.4) contains only first-order derivatives of x and the infinite states $Z(\eta,\cdot)$ and $z(\eta,\cdot)$, being key to the subsequent numerical scheme, which is based on the solution of high-dimensional ODEs. Regarding (2.15), which contains several fractional orders $\alpha_i \in (0,1)$, one can generalize (3.4) to

$$\begin{aligned} {}^{\mathrm{C}}\mathrm{D}^{\alpha_i}q^{(i)}(t) &= \sin\left(\frac{\alpha_i\pi}{2}\right)\omega^{\alpha_i-1}q^{(i+1)}(t) - \int_0^{\infty}\mathrm{K}_{\omega}(\alpha_i,\lambda)\dot{Z}^{(i+1)}(\lambda,t)\mathrm{d}\lambda \\ &\quad + \cos\left(\frac{\alpha_i\pi}{2}\right)\omega^{\alpha_i}q^{(i)}(t) - \omega^2\int_0^{\infty}\mathrm{K}_{\omega}(\alpha_i,\lambda)Z^{(i)}(\lambda,t)\mathrm{d}\lambda \end{aligned} \tag{3.5}$$

for $i = 0,\ldots,n-1$ together with

$$\dot{Z}^{(i)}(\eta,t) = q^{(i)}(t) - \eta Z^{(i)}(\eta,t), \quad Z^{(i)}(\eta,0) = \int_{-\infty}^{0}\mathrm{e}^{\eta\tau}q^{(i)}(\tau)\mathrm{d}\tau, \tag{3.6}$$

$i = 0,\ldots,n$, which is related to (2.26) and (2.29).

For a fixed value of α, the function $\mathrm{K}_{\omega}(\alpha,\cdot)$ has a maximum at

$$\eta_{\max} = \sqrt{\frac{\alpha}{2-\alpha}}\omega.$$

Hence, the position of $\eta_{\max}$ may be adjusted by the magnitude of ω. The graphs of $\mathrm{K}_{\omega}(\alpha,\eta)$ for different values of $\alpha\in(0,1)$ and

$$\eta_{\max} = 1 \quad\Leftrightarrow\quad \omega := \sqrt{\frac{2-\alpha}{\alpha}} \tag{3.7}$$

are displayed in Figure 3.1. Thereby and in the following, (if not otherwise indicated) the abbreviation $\mathrm{K}(\alpha,\cdot) := \mathrm{K}_{\omega}(\alpha,\cdot)$ with ω as in (3.7) is used.

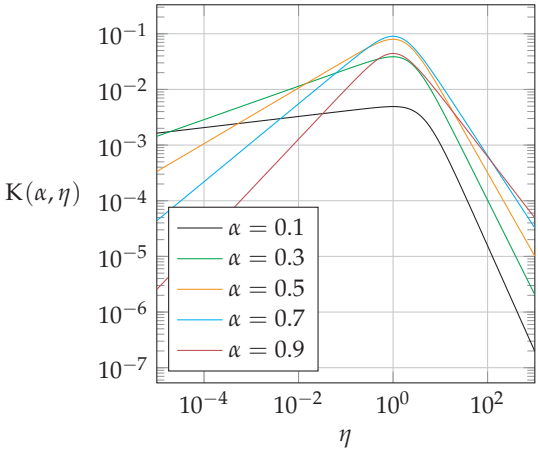

Figure 3.1: $\mathrm{K}(\alpha,\eta)$ for different values of $\alpha \in (0,1)$.

3.2 Derivation of the scheme

The key idea of the following scheme is to approximate the integrals of the infinite states $Z^{(i)}$ and their derivatives in Equation (3.5) by sums of a finite number of states

$$Z^{(i)}_{k,j}, \quad k = 0,\dots,K-1,\ j = 1,\dots,J$$

performing a composite Gaussian quadrature. The discretization of the infinite states creates two sources of error, namely the error in consequence of neglecting a part of the integration interval and the approximation error of the quadrature itself. In particular, one obtains an approximation

$$\begin{aligned}\int_0^\infty \mathrm{K}(\alpha_i,\lambda)Z^{(i)}(\lambda,t)\mathrm{d}\lambda = &\sum_{k=0}^{K-1}\sum_{j=1}^{J}\mathrm{K}(\alpha_i,\eta_{k,j})Z^{(i)}_{k,j}(t)w_{k,j}\\ &+\mathrm{Err}_1\left(Z^{(i)}(\cdot,t)\right)+\mathrm{Err}_2\left(Z^{(i)}(\cdot,t)\right)\end{aligned} \tag{3.8}$$

for the integral of infinite states as in (3.5) with errors

$$\mathrm{Err}_1\left(Z^{(i)}(\cdot,t)\right) = \int_{\eta_K}^\infty \mathrm{K}(\alpha_i,\lambda)Z^{(i)}(\lambda,t)\mathrm{d}\lambda, \tag{3.9}$$

$$\mathrm{Err}_2\left(Z^{(i)}(\cdot,t)\right) = \int_0^{\eta_K} \mathrm{K}(\alpha_i,\lambda)Z^{(i)}(\lambda,t)\mathrm{d}\lambda - \sum_{k=0}^{K-1}\sum_{j=1}^{J}\mathrm{K}(\alpha_i,\eta_{k,j})Z^{(i)}_{k,j}(t)w_{k,j}\,. \tag{3.10}$$

Thereby, similar as in Section 2.4, choose $\eta_0 = 0, \eta_1, \ldots, \eta_K$ in $(0, \infty)$ and perform a Gaussian quadrature in each interval $(\eta_0, \eta_1), \ldots, (\eta_{K-1}, \eta_K)$ with shifted Gauss-Legendre nodes

$$\eta_{k,j} = \frac{\eta_{k+1} - \eta_k}{2} s_j^{(0,0)} + \frac{\eta_k + \eta_{k+1}}{2} \in (\eta_k, \eta_{k+1}), \quad j = 1, \ldots, J,\ k = 0, \ldots, K-1$$

and weights

$$w_{k,j} = \frac{\eta_{k+1} - \eta_k}{2} w_j^{(0,0)}, \quad j = 1, \ldots, J,\ k = 0, \ldots, K-1$$

related to the standard Gauss-Legendre nodes and weights

$$s_j^{(0,0)} \text{ and } w_j^{(0,0)}, \quad j = 1, \ldots, J.$$

To abbreviate, denote

$$Z_{k,j}^{(i)}(t) := Z^{(i)}(\eta_{k,j}, t), \quad j = 1, \ldots, J,\ k = 0, \ldots, K-1.$$

Accordingly, in an arbitrary FODE (2.15), a fractional derivative ${}^{\mathrm{C}}\mathrm{D}^{\alpha_i} q^{(i)}(t)$ can be approximated with (3.5) and (3.8) as

$$\begin{aligned} {}^{\mathrm{C}}\mathrm{D}^{\alpha_i} q^{(i)}(t) = \sin\left(\frac{\alpha_i \pi}{2}\right) \omega^{\alpha_i - 1} q^{(i+1)}(t) - \sum_{k=0}^{K-1} \sum_{j=1}^{J} \mathrm{K}(\alpha_i, \eta_{k,j}) \dot{Z}_{k,j}^{(i+1)}(t) w_{k,j} \\ + \cos\left(\frac{\alpha_i \pi}{2}\right) \omega^{\alpha_i} q^{(i)}(t) - \omega^2 \sum_{k=0}^{K-1} \sum_{j=1}^{J} \mathrm{K}(\alpha_i, \eta_{k,j}) Z_{k,j}^{(i)}(t) w_{k,j}\,. \end{aligned} \tag{3.11}$$

Hence, approximate (2.15) by a system

$$\begin{aligned} &\left(A + B \sin\left(\frac{\alpha_{n-1}\pi}{2}\right) \omega^{\alpha_{n-1}-1}\right) q^{(n)}(t) - B \sum_{k=0}^{K-1} \sum_{j=1}^{J} \mathrm{K}(\alpha_{n-1}, \eta_{k,j}) \dot{Z}_{k,j}^{(n)}(t) w_{k,j} \\ &= \tilde{F}\left(t, q(t), \dot{q}(t), \ldots, q^{(n-1)}(t), \left(Z_{k,j}^{(0)}\right)_{k,j}, \ldots, \left(Z_{k,j}^{(n)}\right)_{k,j}\right) \\ &\quad - B \cos\left(\frac{\alpha_{n-1}\pi}{2}\right) \omega^{\alpha_{n-1}} q^{(n-1)} + B\omega^2 \sum_{k=0}^{K-1} \sum_{j=1}^{J} \mathrm{K}(\alpha_{n-1}, \eta_{k,j}) Z_{k,j}^{(n-1)}(t) w_{k,j} \end{aligned} \tag{3.12}$$

together with

$$\dot{Z}_{k,j}^{(i)}(t) = q^{(i)}(t) - \eta_{k,j} Z_{k,j}^{(i)}(t), \quad i = 0, \ldots, n,\ j = 1, \ldots, J,\ k = 0, \ldots, K-1, \tag{3.13}$$

related to (3.6). The system (3.12) may be transformed into a first-order ODE, which together with (3.13) can be solved by a standard ODE solver. Correspondingly, the initial function $\varphi(s)$, $s \leq 0$ of the original FODE (2.15) has to be translated to initial values $Z_{k,j}^{(i)}(0)$ for the approximating ODE through

$$Z_{k,j}^{(i)}(0) = \int_{-\infty}^{0} \mathrm{e}^{\eta_{k,j}\tau} \varphi^{(i)}(\tau) \mathrm{d}\tau, \quad i = 0, \ldots, n,\ j = 1, \ldots, J,\ k = 0, \ldots, K-1.$$

In the following, the method proposed here is referred to as *reformulated infinite state scheme (RISS)*.

Remark 3.5. The kernel $\mathrm{K}(\alpha, \eta)$ decays algebraically of order α to zero for $\eta \to 0$ such that the integrand is not differentiable at zero and the Gauss-Legendre approximation is of low order. However, the error may be controlled by choosing a small value for η_1 as shown in the next section. The advantage of a Gauss-Legendre quadrature in all subintervals (instead of a Gauss-Jacobi quadrature in $(0, \eta_1)$) is that only one set of weights and nodes can be used to discretize the infinite states $Z^{(i)}$, $i = 0, \ldots, n$. Therefore, the number of states in (3.12) does not depend on the number of fractional derivatives in (2.15). Furthermore, an explicit FODE (2.15) leads to an explicit ODE (3.12) as approximation.

3.3 Error analysis

The following analysis provides an estimation of the error resulting from the discretization of the infinite states, i.e., (3.9), (3.10). For the truncation error Err_1, estimate the infinite states $Z^{(i)}$ using the solution of (3.6) in $[\eta_K, \infty)$ as

$$\begin{aligned} \left| Z^{(i)}(\eta, t) \right| &= \left| Z^{(i)}(\eta, 0)\mathrm{e}^{-\eta t} + \int_0^t \mathrm{e}^{-\eta(t-\tau)} q^{(i)}(\tau) \mathrm{d}\tau \right| \\ &\leq C\mathrm{e}^{-\eta_K t} + \left\| q^{(i)} \right\|_\infty \int_0^t \mathrm{e}^{-\eta_K (t-\tau)} \mathrm{d}\tau = C\mathrm{e}^{-\eta_K t} + \frac{\left\| q^{(i)} \right\|_\infty}{\eta_K} \end{aligned} \tag{3.14}$$

for some constant $C > 0$ and the uniform norm $\| \cdot \|_\infty$ in $[0, t]$. Using (3.14) for fixed $t \geq 0$, one can obtain the estimation

$$\begin{aligned} \left| \mathrm{Err}_1 \left(Z^{(i)}(\cdot, t) \right) \right| &\leq \left(C\mathrm{e}^{-\eta_K t} + \frac{\left\| q^{(i)} \right\|_\infty}{\eta_K} \right) \int_{\eta_K}^{\infty} \mathrm{K}(\alpha_i, \lambda) \mathrm{d}\lambda \\ &\leq \left(C\mathrm{e}^{-\eta_K t} + \frac{\left\| q^{(i)} \right\|_\infty}{\eta_K} \right) \frac{\sin(\alpha_i \pi)}{\pi} \int_{\eta_K}^{\infty} \lambda^{\alpha_i - 2} \mathrm{d}\lambda \\ &= \left(C\mathrm{e}^{-\eta_K t} + \frac{\left\| q^{(i)} \right\|_\infty}{\eta_K} \right) \frac{\sin(\alpha_i \pi)}{\pi} \frac{\eta_K^{\alpha_i - 1}}{1 - \alpha_i} = \mathcal{O}\left(\eta_K^{\alpha_i - 2} \right), \end{aligned} \tag{3.15}$$

which shows an algebraic decay of the truncation error for growing η_K. Furthermore, because of the exponential term in (3.15), one can expect larger contributions of this term to the total error for time instants $t \ll \frac{1}{\eta_K}$.

To estimate the quadrature error, decompose

$$\mathrm{Err}_2\left(Z^{(i)}(\cdot,t)\right) = \sum_{k=0}^{K-1} \mathrm{Err}_{2,k}\left(Z^{(i)}(\cdot,t)\right)$$

with

$$\mathrm{Err}_{2,k}\left(Z^{(i)}(\cdot,t)\right) = \int_{\eta_k}^{\eta_{k+1}} \mathrm{K}(\alpha_i,\lambda) Z^{(i)}(\lambda,t)\mathrm{d}\lambda - \sum_{j=1}^{J} \mathrm{K}(\alpha_i,\eta_{k,j}) Z_{k,j}^{(i)}(t) w_{k,j}\,,$$
$$k = 0,\dots K-1$$

and introduce another estimation for $Z^{(i)}$ of the form

$$\begin{aligned}\left|Z^{(i)}(\eta,t)\right| &= \left|Z^{(i)}(\eta,0)\mathrm{e}^{-\eta t} + \int_0^t \mathrm{e}^{-\eta(t-\tau)} q^{(i)}(\tau)\mathrm{d}\tau\right| \\ &\le C + \left\|q^{(i)}\right\|_\infty \int_0^t \mathrm{d}\tau = C + \left\|q^{(i)}\right\|_\infty t,\end{aligned} \tag{3.16}$$

for some constant $C > 0$ and the uniform norm $\|\cdot\|_\infty$ in $[0,t]$. For the first interval, as the integrand is not differentiable at zero, use (3.16) to estimate for fixed $t \ge 0$

$$\begin{aligned}\left|\mathrm{Err}_{2,0}\left(Z^{(i)}(\cdot,t)\right)\right| &\le \frac{\sin(\alpha_i\pi)}{\pi}\left(C + \left\|q^{(i)}\right\|_\infty t\right) \times \\ &\qquad \left(\int_0^{\eta_1} \frac{\lambda^{\alpha_i}}{\lambda^2+\omega^2}\mathrm{d}\lambda + \sum_{j=1}^{J} \frac{\eta_{0,j}^{\alpha_i}}{\eta_{0,j}^2+\omega^2} w_{0,j}\right) \\ &\le \frac{\sin(\alpha_i\pi)}{\pi}\left(C + \left\|q^{(i)}\right\|_\infty t\right) \frac{\eta_1^{\alpha_i}}{\omega^2}\left(\int_0^{\eta_1} \mathrm{d}\lambda + \sum_{j=1}^{J} w_{0,j}\right) \\ &= 2\frac{\sin(\alpha_i\pi)}{\pi}\left(C + \left\|q^{(i)}\right\|_\infty t\right) \frac{\eta_1^{1+\alpha_i}}{\omega^2} = \mathcal{O}(\eta_1^{1+\alpha_i}),\end{aligned} \tag{3.17}$$

where the next-to-last equality holds as the quadrature is exact for constant functions. The estimation (3.17) shows an algebraic decay of $|\mathrm{Err}_{2,0}|$ for decreasing η_1 and the time-linear term in (3.17) leads to a larger contribution of this term to the total error for time instants $t \gg \frac{1}{\eta_1}$.

As the integrand is smooth in the other intervals, an approximation theorem according to Jackson can be used, see Davis and Rabinowitz (1984, Chap. 4.8) and Diethelm (2008, Thm. 9). As stated by Davis and Rabinowitz (1984), an l-times continuously differentiable function $f \in C^l[a,b]$ may be approximated by a

polynomial p_J of degree $\leq J$ as

$$\left|f(x) - p_J(x)\right| \leq C(l) \left(\frac{b-a}{J}\right)^l \left\|f^{(l)}(x)\right\|_\infty$$

for a constant $C(l) > 0$ and the uniform norm $\|\cdot\|_\infty$ in $[a,b]$. As p_J can be integrated exactly using Gauss-Legendre quadrature, one can obtain

$$\begin{aligned}\left|\mathrm{Err}_{2,k}\left(Z^{(i)}(\cdot,t)\right)\right| &\leq \int_{\eta_k}^{\eta_{k+1}} \left|\mathrm{K}(\alpha_i,\lambda)Z^{(i)}(\lambda,t) - p_J(\lambda)\right| \mathrm{d}\lambda \\ &\quad + \sum_{j=1}^{J} \left|\mathrm{K}(\alpha_i,\eta_{k,j})Z_{k,j}^{(i)}(t) - p_J(\eta_{k,j})\right| w_{k,j} \qquad (3.18) \\ &\leq 2C(l)(\eta_{k+1}-\eta_k)^{l+1} \left\|\frac{\mathrm{d}^l}{\mathrm{d}(\cdot)^l}\left(\mathrm{K}(\alpha_i,\cdot)Z^{(i)}(\cdot,t)\right)\right\|_\infty J^{-l}.\end{aligned}$$

As $\eta_1,\ldots,\eta_K$ are chosen equidistant on a logarithmic scale, the interval length is given by

$$\eta_{k+1} - \eta_k = \left(\left(\frac{\eta_K}{\eta_1}\right)^{\frac{1}{K-1}} - 1\right)\eta_k, \quad k = 1,\ldots,K-1 \qquad (3.19)$$

and it can be adjusted by the parameter K. The estimation (3.18) shows a rapid decay of the error for growing J but fixed K,η_1,η_K. However, if the ratio $\frac{\eta_K}{\eta_1}$ is increased, the parameter K has to be chosen large enough to bound the interval lengths (3.19) for large values of k.

Remark 3.6. To obtain small errors in (3.17) and (3.18), the infinite states $Z^{(i)}(\eta,\cdot)$, $i = 0,\ldots,n$ have to be sufficiently smooth with respect to $\eta \in (0,\infty)$. This requirement restricts the set of admissible initial functions. Let $\varphi^{(i)}$, $i = 0,\ldots,n$ have a support in $[-a,0]$ for some $a \in (0,\infty)$. For this case, there is no limitation for bounded initial functions as

$$\left|Z^{(i)}(\eta,0)\right| \leq \sup_{t\in[-a,0]} \left|q^{(i)}(t)\right| \int_{-a}^{0} \mathrm{e}^{\eta\tau}\mathrm{d}\tau = \sup_{t\in[-a,0]} \left|q^{(i)}(t)\right| \frac{1-\mathrm{e}^{-\eta a}}{\eta},$$

which is finite even for $\eta \to 0$. If however $\varphi^{(i)}$ is non-zero almost everywhere on the interval $(-\infty,0]$ for some $l \in \{0,\ldots,n\}$, the infinite states $Z^{(l)}(\eta,\cdot)$ can be singular. One example is a constant past $\varphi \equiv C$, which leads to $Z^{(0)}(\eta,0) = \frac{C}{\eta}$ showing a strong singularity at $\eta = 0$ such that Gauss-Legendre quadrature of $\int_0^\infty \mathrm{K}(\alpha,\lambda)Z^{(0)}(\lambda,0)\mathrm{d}\lambda$ fails.

In summary, the total error resulting from the discretization of the infinite states is given by the estimations (3.15), (3.17) and (3.18) which can be controlled by the quadrature parameters η_K, η_1 and J, K, respectively. The total error of

the reformulated infinite state scheme results from the combined error of the infinite state discretization and the time-stepping method. The latter depends on the ODE solver used, which can be chosen independently from the infinite state discretization.

3.4 Benchmark problems

In this section, a number of benchmark problems is studied, which are mainly of the form (2.15) equipped with initial functions. Most of the problems are inspired by those from Xue (2017); Xue and Bai (2017) sometimes with adapted initial conditions as the original problems do not fit the initial function approach or the fact mentioned in Remark 3.6 leads to modification of the problems. For all numerical examples, the reformulation (3.11) is applied and the quadrature parameters $K = 25$ and $J = 10$ are chosen, where $\eta_1, \dots, \eta_K$ are logarithmically spaced in $[10^{-5}, 10^5]$, i.e.,

$$\eta_1 = 10^{-5},\ \eta_K = 10^5,\ \eta_k = \eta_1 \left(\frac{\eta_K}{\eta_1}\right)^{\frac{k-1}{K-1}},\ k = 2, \dots, K.$$

The resulting ODEs are stated and solved using MATLAB's solver `ode15s.m` (absolute and relative tolerance at 10^{-8}), which uses backward differentiation formulas, see Shampine and Reichelt (1997). The results are compared to those of the methods PC and ISS mentioned in Section 2.4.

Benchmark Problem 1. Consider the simple fractional differential equation with zero initial function given by

$$\begin{aligned} {}^{\mathrm{C}}\mathrm{D}^{\alpha} q(t) &= 1 - q(t), \\ q(t) &= 0, \quad t \leq 0 \end{aligned} \tag{3.20}$$

with the closed form solution $q(t) = 1 - \mathrm{E}_{\alpha}(-t^{\alpha})$, see Figure 3.2. Using (3.12), this problem may be approximated as

$$\begin{aligned} &\sin\left(\frac{\alpha\pi}{2}\right)\omega^{\alpha-1}\dot{q}(t) - \sum_{k=0}^{K-1}\sum_{j=1}^{J} \mathrm{K}(\alpha, \eta_{k,j})\dot{Z}_{k,j}^{(1)}(t) w_{k,j} \\ &\quad = 1 - \left(1 + \cos\left(\frac{\alpha\pi}{2}\right)\omega^{\alpha}\right) q(t) + \omega^2 \sum_{k=0}^{K-1}\sum_{j=1}^{J} \mathrm{K}(\alpha, \eta_{k,j}) Z_{k,j}^{(0)}(t) w_{k,j} \end{aligned} \tag{3.21}$$

together with (3.13) and zero initial conditions in all states. The solution of (3.21) can be compared to the closed form solution of (3.20) for which the Mittag-Leffler

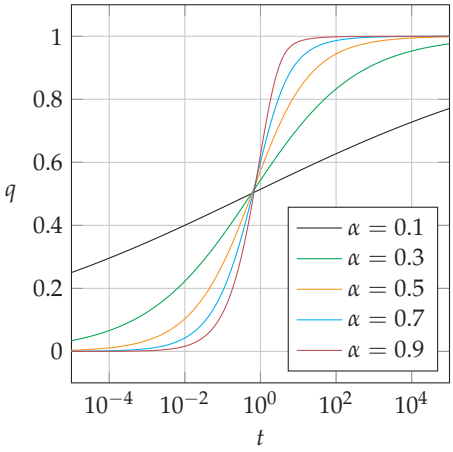

Figure 3.2: Benchmark 1: Analytical solution of (3.20) for various values of α.

function is computed with the help of the MATLAB function `ml.m` by Garrappa (2014). The absolute errors

$$\Delta^{(0)}(t) = |q(t) - \tilde{q}(t)|$$

between the exact solution $q(t)$ and its numerical approximation $\tilde{q}(t)$ are shown in Figure 3.3 for many time scales. The results are generally good but show increasing static errors for small values of α for very small and very large time scales, i.e., the method leads to a wrong approximation of the asymptotic behavior of the solution. This phenomenon is in agreement with the estimations (3.15) and (3.17), which reveal increasing errors for small and large t, respectively. In Figure 3.4, the solution of (3.21) for $\alpha = 0.1$ is compared to a scaled version of it, where the last term in (3.21) is multiplied by a factor

$$\frac{\cos\left(\frac{\alpha\pi}{2}\right)\omega^{\alpha}}{\omega^2 \sum_{k=0}^{K-1}\sum_{j=1}^{J} \mathrm{K}(\alpha, \eta_{k,j})\frac{1}{\eta_{k,j}} w_{k,j}}$$

such that the asymptotic behavior of the solution is correctly estimated. Unfortunately, the scaling leads to a larger error for smaller time scales and does not improve the approximation. It can be concluded that RISS provides a good approximation of the solution of (3.20) only in a certain time interval. However, this interval can be extended by decreasing η_1 and increasing η_K together with an appropriate choice of J and K as explained in Section 3.3.

Furthermore, for $t \in (0, 100)$ the results of RISS, ISS (applied to the fractional integral equation equivalent to (3.20)) and PC are compared in Figure 3.5.

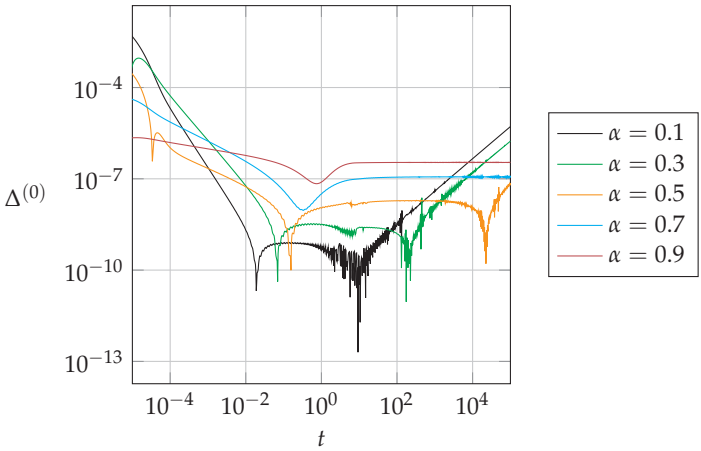

Figure 3.3: Benchmark 1: Absolute error of the numerical solution of (3.20) using RISS for various values of α.

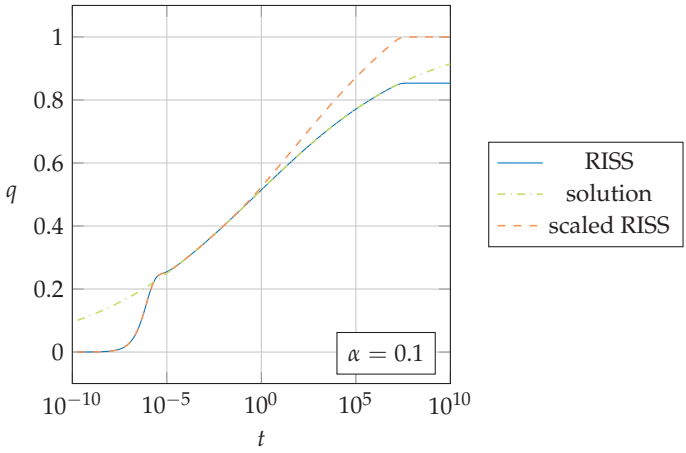

Figure 3.4: Benchmark 1: Analytical and numerical solution using RISS and a scaled version of RISS with correct approximation of the asymptotic behavior of the solution for $\alpha = 0.1$.

Thereby, the choice $J = 20$ is made for ISS such that the dimensions of the approximating ODEs in RISS and ISS are equal and, a fixed step size $h = 5 \cdot 10^{-4}$ is used for PC as this leads to a similar computation time as for RISS with the parameters specified above. Figure 3.5 shows a good performance of RISS for all chosen values of α while ISS works well only for large $\alpha \in (0,1)$ and large time scales. The main reason for that seems to be the truncation error for ISS, which can be approximated similar as in (3.15), by

$$\begin{aligned} \left| \int_{\eta_K}^{\infty} \mu_\alpha(\lambda) Z(\lambda,t) \mathrm{d}\lambda \right| &\leq C \int_{\eta_K}^{\infty} \mu_\alpha(\lambda) \mathrm{e}^{-\lambda t} \mathrm{d}\lambda + \|1-q\|_\infty \int_{\eta_K}^{\infty} \frac{\mu_\alpha(\lambda)}{\lambda} \mathrm{d}\lambda \\ &\leq C \frac{t^{\alpha-1}}{\Gamma(\alpha)} + \|1-q\|_\infty \frac{\sin(\alpha\pi)}{\alpha\pi} \eta_K^{-\alpha} \end{aligned} \tag{3.22}$$

for some constant $C > 0$ and the uniform norm $\|\cdot\|_\infty$ in $[0,t]$ while the quadrature error for ISS can be estimated similar to (3.18). The error term in (3.22) has a large influence for small time scales, especially for $\alpha \to 0$ and is of lower order in η_K than the error in (3.15). In the article of Baffet (2019), such large errors can be avoided by splitting a local part of the fractional integral (2.8) before introducing the infinite state representation. The local part is then treated by an approximation method for Volterra integrals. For PC, notice the improvement of the convergence behavior with increasing values of α corresponding to (2.33). Especially for large t, the absolute errors become smaller than for RISS. However, the computational costs for the used implementation of PC, see Garrappa (2012), behave like $\mathcal{O}\left(n \cdot \log(n)^2\right)$ with $n = \frac{T}{h}$ while RISS seems to work much more efficient. To see this, the relation between computation time and the mean absolute error $\bar{\Delta}^{(0)}$ for the three methods are presented in Figure 3.6. Therefore, the number J of quadrature nodes is increased for fixed parameters $K = 25$, $\eta_1 = 10^{-5}$ and $\eta_K = 10^5$ for RISS ($J = 1,2,3,\ldots,10$) and ISS ($\tilde{J} = 2J$) such that the dimensions of the resulting ODEs for RISS ($2KJ+1$) and ISS ($K\tilde{J}+1$) are equal. Further, the time step h for PC is decreased as $h = 10^{-\frac{J}{4}}$. For ISS, one obtains almost no reduction of the mean error for growing J. Apparently, the truncation error (3.22) is larger in magnitude than the quadrature error, which is reduced by increasing J. For RISS, a steep decay of the mean error until $J = 7$ can be observed. For larger values of J, the mean error remains almost the same as the error terms in (3.15) and (3.17) seem to predominate. For PC, a slow decay of the error with increasing computation time is visible and RISS works more efficiently in the example given.

Remark 3.7. A slight change of (3.20) leads to an FODE with a non-zero constant initial function

$$\begin{aligned} {}^{\mathrm{C}}\mathrm{D}^\alpha q(t) &= -q(t), \\ q(t) &= 1, \quad t \leq 0 \end{aligned} \tag{3.23}$$

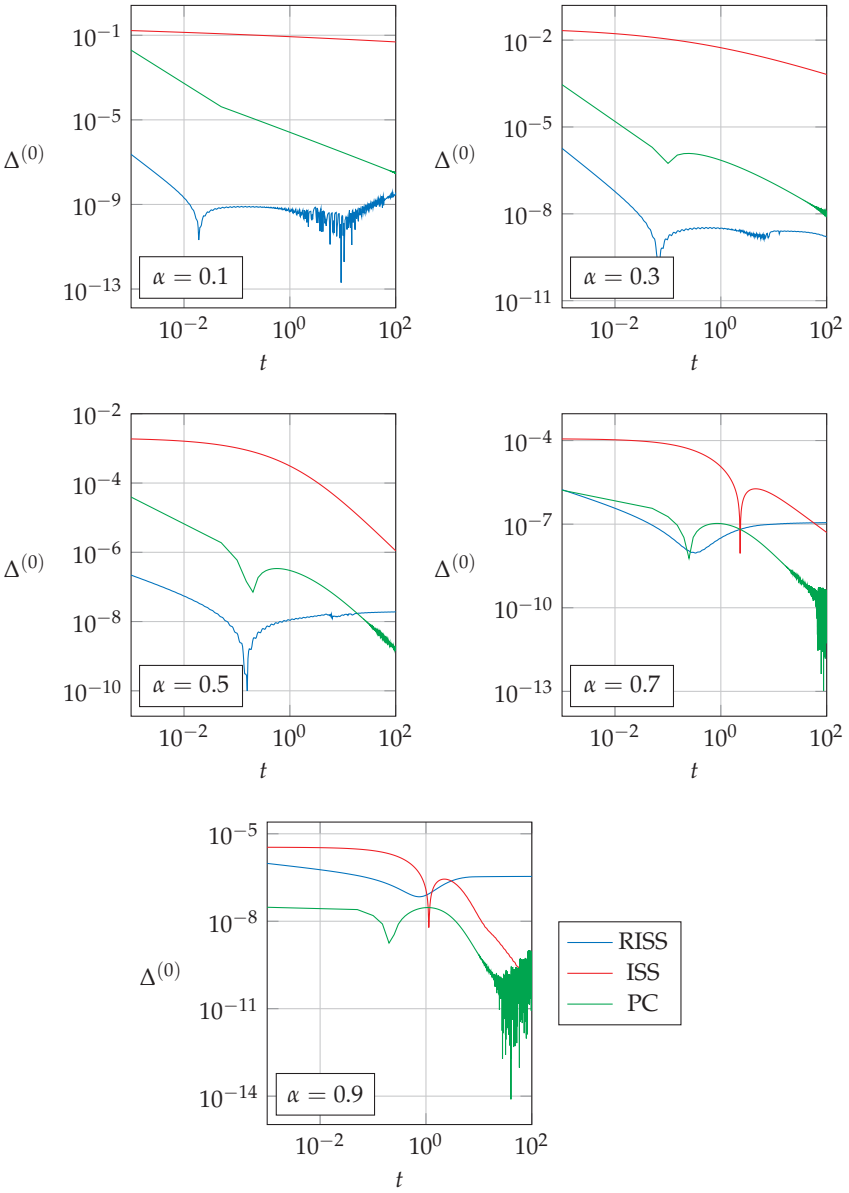

Figure 3.5: Benchmark 1: Absolute error of the numerical solution of (3.20) using RISS, ISS and PC for various values of α.

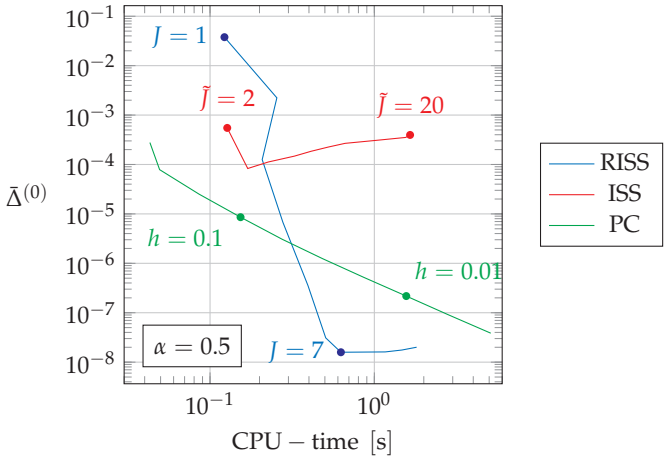

Figure 3.6: Benchmark 1: Work-precision diagram for RISS, ISS and PC for $\alpha = 0.5$.

with the closed form solution $q(t) = \mathrm{E}_\alpha(-t^\alpha)$. As $\dot{q}(t) = 0$ for $t < 0$, the fractional differential operator in (3.23) can as well be initialized at zero which leads to a classical non-zero initial condition $q(0) = 1$. As explained in Remark 3.6, RISS is not suitable for such a problem, especially for $\alpha \to 0$ (Figure 3.7). However, with the objective of modeling real systems, an infinite non-zero history seems inappropriate.

Benchmark Problem 2. Another one-term fractional differential equation with zero initial function adapted from Xue and Bai (2017) has the form

$$\begin{aligned} {}^{\mathrm{C}}\mathrm{D}^{0.7} q(t) &= f(t), \\ q(t) &= 0, \quad t \leq 0 \end{aligned} \tag{3.24}$$

with a piecewise defined right-hand side

$$f(t) = \begin{cases} \frac{1}{\Gamma(1.3)} t^{0.3}, & 0 \leq t \leq 1, \\ \frac{1}{\Gamma(1.3)} t^{0.3} - \frac{2}{\Gamma(2.3)} (t-1)^{1.3}, & t > 1. \end{cases}$$

The analytical solution of (3.24) is given by

$$q(t) = \begin{cases} t, & 0 \leq t \leq 1, \\ t - (t-1)^2, & t > 1 \end{cases}$$

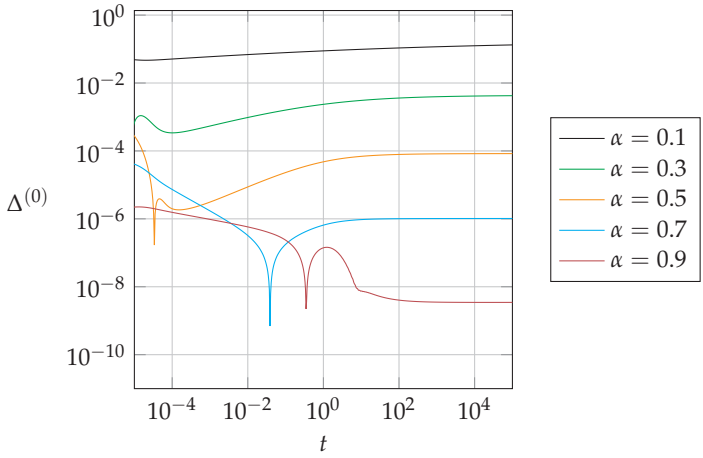

Figure 3.7: Benchmark 1: Absolute error of the numerical solution of (3.23) using RISS for various values of α.

in the interval $(0, 2)$. The approximation of (3.24) using (3.12) has the form

$$\begin{aligned}\sin\left(\frac{7\pi}{20}\right)\omega^{-0.3}\dot{q}(t) - \sum_{k=0}^{K-1}\sum_{j=1}^{J} \mathrm{K}(0.7, \eta_{k,j})\dot{Z}_{k,j}^{(1)}(t)w_{k,j} \\ = f(t) - \cos\left(\frac{7\pi}{20}\right)\omega^{0.7}q(t) + \omega^{2}\sum_{k=0}^{K-1}\sum_{j=1}^{J}\mathrm{K}(0.7, \eta_{k,j})Z_{k,j}^{(0)}(t)w_{k,j}\,.\end{aligned}$$

Again, the absolute errors using RISS, ISS and PC ($h = 5 \cdot 10^{-5}$) have been computed and the results may be found in Figure 3.8. The step size for PC is again chosen such that the computation time of PC and RISS are similar. As in Benchmark 1, the best results can be obtained using RISS.

Benchmark Problem 3. Consider a third-order FODE adapted from the second problem by Xue and Bai (2017) of the form

$$\begin{aligned}&\dddot{q}(t) + {}^{\mathrm{C}}\mathrm{D}^{0.5}\ddot{q}(t) + \ddot{q}(t) + 4\dot{q}(t) + {}^{\mathrm{C}}\mathrm{D}^{0.5}q(t) + 4q(t) = 6\cos(t), \\ &q(t) = \sqrt{2}\sin\left(t + \frac{\pi}{4}\right), \quad t \leq 0,\end{aligned} \tag{3.25}$$

which has the closed form solution $q(t) = \sqrt{2}\sin(t + \frac{\pi}{4})$ for $t > 0$. For the reformulation of (3.25), the infinite states $Z^{(i)}$, $i = 0, \ldots, 3$ that fulfill (3.6) are intro-

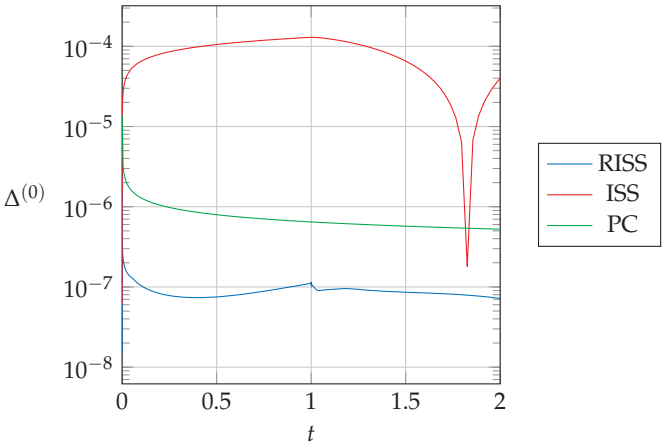

Figure 3.8: Benchmark 2: Absolute error of the numerical solution of (3.24) using RISS, ISS and PC.

duced. One can apply (3.11) in (3.25) to obtain

$$\begin{aligned}
&\left(1+\frac{1}{\sqrt{2r}}\right)\ddot{q}(t)-\sum_{k=0}^{K-1}\sum_{j=1}^{J}\mathrm{K}(0.5,\eta_{k,j})\dot{Z}_{k,j}^{(3)}(t)w_{k,j}\\
&+\left(1+\frac{\sqrt{2r}}{2}\right)\ddot{q}(t)-\omega^2\sum_{k=0}^{K-1}\sum_{j=1}^{J}\mathrm{K}(0.5,\eta_{k,j})Z_{k,j}^{(2)}(t)w_{k,j}\\
&+\left(4+\frac{1}{\sqrt{2r}}\right)\dot{q}(t)-\sum_{k=0}^{K-1}\sum_{j=1}^{J}\mathrm{K}(0.5,\eta_{k,j})\dot{Z}_{k,j}^{(1)}(t)w_{k,j}\\
&+\left(4+\frac{\sqrt{2r}}{2}\right)q(t)-\omega^2\sum_{k=0}^{K-1}\sum_{j=1}^{J}\mathrm{K}(0.5,\eta_{k,j})Z_{k,j}^{(0)}(t)w_{k,j}=6\cos(t).
\end{aligned}$$

The initial function in (3.25) may be transferred to the initial values

$$\begin{aligned}
Z^{(0)}(\eta,0)&=\int_{-\infty}^{0}\mathrm{e}^{\eta\tau}q(\tau)\mathrm{d}\tau=\frac{\eta-1}{1+\eta^2},\\
Z^{(1)}(\eta,0)&=\int_{-\infty}^{0}\mathrm{e}^{\eta\tau}q'(\tau)\mathrm{d}\tau=\frac{\eta+1}{1+\eta^2},\\
Z^{(2)}(\eta,0)&=\int_{-\infty}^{0}\mathrm{e}^{\eta\tau}q''(\tau)\mathrm{d}\tau=-\frac{\eta-1}{1+\eta^2},\\
Z^{(3)}(\eta,0)&=\int_{-\infty}^{0}\mathrm{e}^{\eta\tau}q'''(\tau)\mathrm{d}\tau=-\frac{\eta+1}{1+\eta^2}
\end{aligned}$$

of the infinite states. In Figure 3.9, the absolute error

$$\Delta^{(2)}(t) = |q(t) - \tilde{q}(t)| + |\dot{q}(t) - \dot{\tilde{q}}(t)| + |\ddot{q}(t) - \ddot{\tilde{q}}(t)|$$

is shown for $t \in (0, 1000)$, which has a maximal value $\Delta^{(2)}_{\max} \approx 10^{-6}$. Furthermore, the results of RISS and PC ($h = 10^{-4}$) on the interval $t \in (0, 100)$ are compared. Apparently, RISS works slightly better than PC in this example while the computation time for PC is by a factor 3 higher than for RISS.

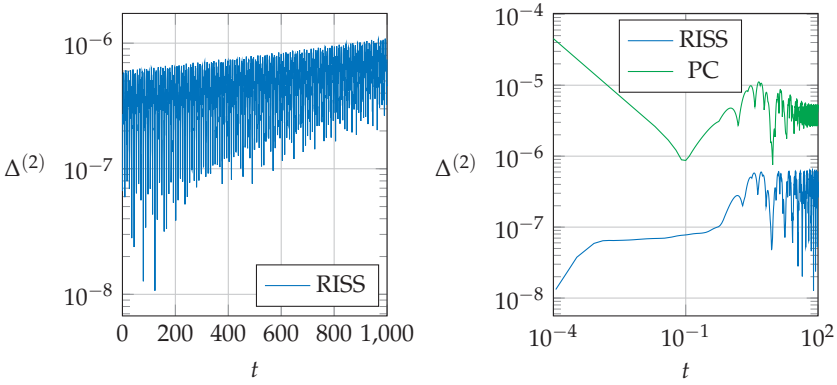

Figure 3.9: Benchmark 3: Absolute error of the numerical solution of (3.25) using RISS for $t \in (0, 1000)$ (left), $t \in (0, 100)$ (right) and PC for $t \in (0, 100)$.

Benchmark Problem 4. The nonlinear explicit FODE

$$\begin{aligned} {}^{\mathrm{C}}\mathrm{D}^{\sqrt{2}-1}\dot{q}(t) &= 2^{\sqrt{2}-0.5}\mathrm{e}^{-2t}q(t)\,{}^{\mathrm{C}}\mathrm{D}^{0.5}q(t) + 4\mathrm{e}^{4t} - \dot{q}^2(t) \\ q(t) &= \mathrm{e}^{2t}, \quad t \leq 0 \end{aligned} \tag{3.26}$$

with closed form solution $q(t) = \mathrm{e}^{2t}$ is adapted from the third problem by Xue and Bai (2017). The associated ODE of the form (3.12) and the initial conditions of the infinite states can be derived as for the previous examples. The relative error

$$\Delta^{(1)}_{\mathrm{r}}(t) = \left| \frac{q(t) - \tilde{q}(t)}{q(t)} \right| + \left| \frac{\dot{q}(t) - \dot{\tilde{q}}(t)}{\dot{q}(t)} \right| \tag{3.27}$$

using RISS is presented in Figure 3.10.

Benchmark Problem 5. The nonlinear implicit FODE

$$\begin{aligned} {}^{\mathrm{C}}\mathrm{D}^{0.2}q(t)\,{}^{\mathrm{C}}\mathrm{D}^{0.8}\dot{q}(t) + {}^{\mathrm{C}}\mathrm{D}^{0.3}q(t)\,{}^{\mathrm{C}}\mathrm{D}^{0.7}\dot{q}(t) &= 8\mathrm{e}^{4t} \\ q(t) &= \mathrm{e}^{2t}, \quad t \leq 0 \end{aligned} \tag{3.28}$$

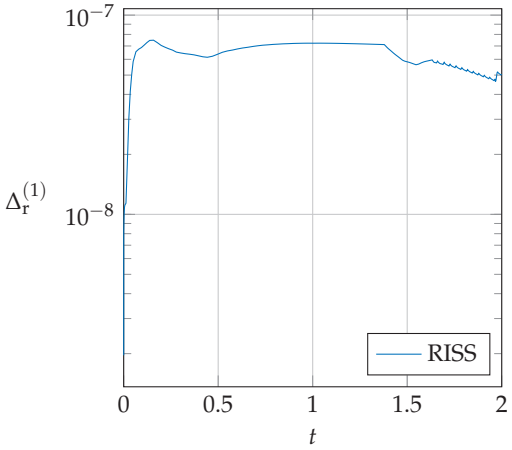

Figure 3.10: Benchmark 4: Relative error of the solution of (3.26) using RISS.

similar to the fourth problem by Xue and Bai (2017) with closed form solution $q(t) = e^{2t}$ is not of the form (2.15). Nevertheless, the reformulation (3.5) can be introduced, which leads to an implicit ODE that can be solved using MATLAB's `ode15i.m`. The relative error (3.27) is shown in Figure 3.11.

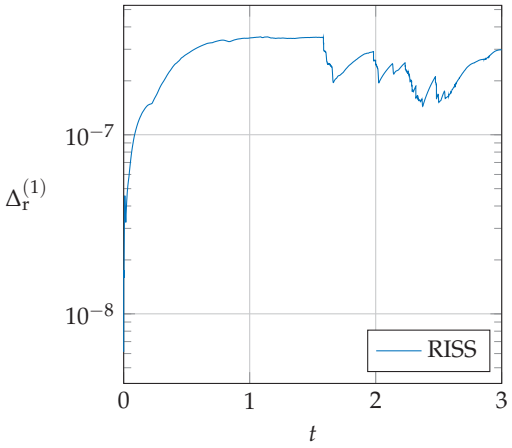

Figure 3.11: Benchmark 5: Relative error of the solution of (3.28) using RISS.

CHAPTER 4

Fractional calculus in viscoelasticity

The present chapter provides an introduction to the linear theory of viscoelasticity and reveals the role of fractional calculus in this field. The classical part mainly follows the reasoning in the books of Christensen (2013); Creus (1986); Gross (1953) and the references cited therein. The use of fractional derivatives in constitutive laws is shown to be a special case of continuous (relaxation or retardation) spectra. Moreover, a correspondence between the associated complex modulus and complex compliance function and the reformulated infinite state representation is deduced. Finally, the parameters of a fractional viscoelastic constitutive model are identified for a creep test with salt concrete and the advantages of fractional over classical models are discussed.

4.1 Classical linear viscoelasticity

Principal assumptions and integral representation

The mechanical behavior of a deformable body is, aside from the general principles of mechanics (i.e., equilibrium and compatibility equations), determined by a characteristic material behavior specified by *constitutive equations*, which relate forces and deformations. Assuming only small displacements of the body, forces and deformations can be described by the *Cauchy stress tensor* σ and the *infinitesimal strain tensor* ε as defined in any textbook on continuum mechanics, see e.g. Gurtin (1981). The characteristic property of a *viscoelastic* constitutive equation is the dependence of stress at a certain time instant on the entire history of strain and vice versa (which is different from the elastic theory where only the current stress and strain state affect each other). Besides this *memory hypothesis*, which is motivated by empirical data of materials like polymers and concrete, three further assumptions can be formulated to obtain a general viscoelastic constitutive equation. The first and self-evident property is *causality* or *non-retroactivity*, meaning that no future strain (resp. stress) state can affect the current stress (resp. strain)

state. The other two assumptions which have to be verified for a certain material in an application, are the *principle of superposition* or *linearity* and *translation-invariance* or *non-aging*. The principle of superposition implies that if two strain states ε_1 and ε_2 lead to stresses σ_1 and σ_2, respectively, then the strain $a_1\varepsilon_1 + a_2\varepsilon_2$ leads to the stress $a_1\sigma_1 + a_2\sigma_2$ for arbitrary $a_1, a_2 \in \mathbb{R}$. Translation-invariance means that for any time instant t a strain $\boldsymbol{\varepsilon}(t)$ leading to a stress $\boldsymbol{\sigma}(t)$ implies that $\boldsymbol{\varepsilon}(t-s)$ leads to $\boldsymbol{\sigma}(t-s)$ for any $s > 0$, i.e., the material behavior is independent of shifts in the time scale. Finally, the above requirements result in the formulation of the constitutive relation as

$$\sigma_{ij}(t) = \overset{\infty}{\underset{s=0}{L_{ij}}}(\varepsilon_{kl}(t-s), \varepsilon_{kl}(t)), \quad t \in (-\infty, T), \tag{4.1}$$

where L_{ij} are the components of a linear tensor functional mapping a continuous strain history

$$\varepsilon_{kl} \in C_0(-\infty, T]$$

that vanishes at the negative time limit to the corresponding stress history

$$\sigma_{ij} \in C_0(-\infty, T]$$

for some $T > 0$. The bounds of the functional correspond to the considered time range of the argument function. Particularly, the lower bound $s = 0$ and the time argument $t - s$ represent causality and translation-invariance, respectively. The Latin indices (attaining 1,2,3) indicate the usual Cartesian tensor notation and the summation convention for repeated indices. An additional continuity assumption on L_{ij} and a proposition by König and Meixner (1958, Thm. 3) lead to the representation of the linear functional in (4.1) by a *Stieltjes integral*

$$\sigma_{ij}(t) = \int_0^\infty \varepsilon_{kl}(t-s)\mathrm{d}G_{ijkl}(s), \tag{4.2}$$

where $G_{ijkl} \in BV[0, \infty)$ are functions of bounded variation on every closed subinterval in $(0, \infty)$. The proof by König and Meixner (1958) assumes the strains ε_{kl} to be continuous and defined on a bounded interval and is based on Riesz' representation theorem in its original form, see Riesz and Sz.-Nagy (1955, §§ 50-52). A generalization by Rudin (1986, Thm. 2.14) leads to the result on $C_0(-\infty, T]$. Alternative formulations of (4.2) for continuously differentiable G_{ijkl} are given by

$$\sigma_{ij}(t) = G_{ijkl}(0)\varepsilon_{kl}(t) + \int_0^\infty \varepsilon_{kl}(t-s)G'_{ijkl}(s)\mathrm{d}s \tag{4.3}$$

and for differentiable ε_{kl}, using integration by parts and the substitution $\tau = t - s$ in (4.3) by

$$\sigma_{ij}(t) = \int_{-\infty}^t G_{ijkl}(t-\tau)\varepsilon'_{kl}(\tau)\mathrm{d}\tau. \tag{4.4}$$

Another generalization for ε_{kl} vanishing in $(-\infty, 0)$ and with a step discontinuity at zero is given by

$$\sigma_{ij}(t) = \varepsilon_{kl}(0)G_{ijkl}(t) + \int_0^t G_{ijkl}(t-\tau)\varepsilon'_{kl}(\tau)\mathrm{d}\tau, \tag{4.5}$$

see Gurtin and Sternberg (1962, Thms. 3.1, 3.4), where the discontinuous strain functions are approximated by sequences of continuous functions.

The functions G_{ijkl} are known as *relaxation functions* that describe the stress relaxation of a material under unit step strain. Particularly, from (4.5) follows

$$\varepsilon_{kl}(t) = \varepsilon^0_{kl}\Theta(t) \quad \Rightarrow \quad \sigma_{ij}(t) = \varepsilon^0_{kl}G_{ijkl}(t), \tag{4.6}$$

where Θ is the *Heaviside step function*. An alternative derivation of the general form of viscoelastic constitutive laws results from reversing the roles of stress and strain in (4.1), leading especially to the analogues

$$\varepsilon_{ij}(t) = \int_{-\infty}^t J_{ijkl}(t-\tau)\sigma'_{kl}(\tau)\mathrm{d}\tau. \tag{4.7}$$

and

$$\varepsilon_{ij}(t) = \sigma_{kl}(0)J_{ijkl}(t) + \int_0^t J_{ijkl}(t-\tau)\sigma'_{kl}(\tau)\mathrm{d}\tau, \tag{4.8}$$

of (4.4) and (4.5) respectively with so-called *creep functions* $J_{ijkl} \in BV[0,\infty)$ that describe the strain answer of a material under unit step loading, i.e.,

$$\sigma_{kl}(t) = \sigma^0_{kl}\Theta(t) \quad \Rightarrow \quad \varepsilon_{ij}(t) = \sigma^0_{kl}J_{ijkl}(t), \tag{4.9}$$

which results from (4.8).

The general tensorial constitutive equations (4.4) and (4.7) can be simplified by using intrinsic and material symmetries. The intrinsic symmetries of stress and strain tensor imply

$$G_{ijkl}(t) = G_{jikl}(t) = G_{ijlk}(t),$$
$$J_{ijkl}(t) = J_{jikl}(t) = J_{ijlk}(t).$$

As material symmetry, consider the most simple case of *isotropic material behavior*, meaning that the constitutive equations remain unchanged under any time-independent rotation of the coordinate system. Let $\mathbf{R} = (R_{ij})_{i,j}$ be a rotation (i.e., $R_{ik}R_{jk} = \delta_{ij}$ and $\det(\mathbf{R}) = 1$) such that stresses $\bar{\sigma}_{mn}$ and strains $\bar{\varepsilon}_{pq}$ in the new (rotated) coordinate system may be expressed as

$$\bar{\sigma}_{mn} = R_{mi}R_{nj}\sigma_{ij}\,, \quad \varepsilon_{kl} = R_{pk}R_{ql}\bar{\varepsilon}_{pq}\,,$$

which leads together with (4.4) to

$$\bar{\sigma}_{mn}(t) = \int_{-\infty}^{t} R_{mi}R_{nj}R_{pk}R_{ql}G_{ijkl}(t-\tau)\bar{\varepsilon}'_{pq}(\tau)\mathrm{d}\tau.$$

The isotropy assumption forces the material law to remain invariant under rotation such that

$$G_{mnpq}(t) = R_{mi}R_{nj}R_{pk}R_{ql}G_{ijkl}(t), \quad t > 0$$

for arbitrary $\mathbf{R}$, meaning that the values of $\mathbf{G} = (G_{ijkl})_{i,j,k,l}$ at certain time instants are *isotropic* fourth-order tensors which are known to be determined by two independent variables, see Temple (1960). Particularly, the relaxation functions can be stated as

$$G_{ijkl}(t) = \lambda(t)\delta_{ij}\delta_{kl} + \mu(t)(\delta_{ik}\delta_{jl} + \delta_{il}\delta_{jk}), \tag{4.10}$$

where the functions λ and μ correspond to the *Lamé moduli* known from elasticity theory, see Truesdell (1973, Chap. 1.C.III.22). Finally, a decomposition of stress (resp. strain) tensor in *hydrostatic* (resp. *volumetric*)

$$\sigma_{\mathrm{h}} := \frac{1}{3}\sigma_{ii}\,, \quad \varepsilon_{\mathrm{h}} := \frac{1}{3}\varepsilon_{ii} \tag{4.11}$$

and *deviatoric* components

$$\boldsymbol{\sigma}_{\mathrm{d}} := \boldsymbol{\sigma} - \sigma_{\mathrm{h}}\mathbf{I}, \quad \varepsilon_{\mathrm{d}} := \boldsymbol{\varepsilon} - \varepsilon_{\mathrm{h}}\mathbf{I} \tag{4.12}$$

results using (4.10) in two independent constitutive equations

$$\sigma_{\mathrm{h}}(t) = \int_{-\infty}^{t} G_{\mathrm{h}}(t-\tau)\varepsilon'_{\mathrm{h}}(\tau)\mathrm{d}\tau, \quad G_{\mathrm{h}} := 3\lambda + 2\mu, \tag{4.13}$$

$$\boldsymbol{\sigma}_{\mathrm{d}}(t) = \int_{-\infty}^{t} G_{\mathrm{d}}(t-\tau)\boldsymbol{\varepsilon}'_{\mathrm{d}}(\tau)\mathrm{d}\tau, \quad G_{\mathrm{d}} := 2\mu. \tag{4.14}$$

Accordingly, the material behavior of an isotropic viscoelastic medium is completely described by the two one-dimensional integral representations (4.13) and (4.14) with relaxation functions in isotropic compression G_{h} and shear G_{d}. The brief derivation from above is given in more detail by Gurtin and Sternberg (1962, Thms. 2.3 - 2.5). An obvious alternative formulation of the creep type is given by

$$\varepsilon_{\mathrm{h}}(t) = \int_{-\infty}^{t} J_{\mathrm{h}}(t-\tau)\sigma'_{\mathrm{h}}(\tau)\mathrm{d}\tau, \tag{4.15}$$

$$\boldsymbol{\varepsilon}_{\mathrm{d}}(t) = \int_{-\infty}^{t} J_{\mathrm{d}}(t-\tau)\boldsymbol{\sigma}'_{\mathrm{d}}(\tau)\mathrm{d}\tau \tag{4.16}$$

with creep functions in isotropic compression J_{h} and shear J_{d}. The correspondence between relaxation and creep functions and further properties will be discussed in the following paragraph. For a simplified notation in one dimension, the indices of creep and relaxation functions as well as stress and strain will be omitted meanwhile. The formulation in (4.13) - (4.16) of the isotropic viscoelastic constitutive equations is revisited in Section 4.3.

Properties of relaxation and creep functions

The following derivation of further properties of relaxation functions, which is a summary of the exposition by Christensen (2013, Chap. 3), is based on the two fundamental postulates of thermodynamics, i.e., balance of energy and the entropy production inequality. The starting point for a one-dimensional isothermal constitutive law is the assumption of a non-negative *free energy function* of the form

$$\psi(t) := \frac{1}{2}\int_{-\infty}^{t}\int_{-\infty}^{t} G(2t-\tau-s)\varepsilon'(\tau)\mathrm{d}\tau\,\varepsilon'(s)\mathrm{d}s \geq 0, \tag{4.17}$$

implying

$$G(t) \geq 0, \quad t \geq 0, \tag{4.18}$$

which is in perfect agreement with experimental results. Moreover, the energy balance principle together with the assumption of a positive entropy rate leads to the *Clausius-Duhem inequality*

$$-\dot{\psi}(t) + \sigma(t)\dot{\varepsilon}(t) \geq 0.$$

Using (4.17) and a scalar version of the constitutive law (4.4), i.e.,

$$\sigma(t) = \int_{-\infty}^{t} G(t-\tau)\varepsilon'(\tau)\mathrm{d}\tau, \tag{4.19}$$

the Clausius-Duhem inequality reads as

$$-\int_{-\infty}^{t}\int_{-\infty}^{t} G'(2t-\tau-s)\varepsilon'(\tau)\mathrm{d}\tau\varepsilon'(s)\mathrm{d}s \geq 0. \tag{4.20}$$

Finally, choosing a single-step strain in (4.20) leads to

$$\dot{G}(t) \leq 0, \quad t \geq 0. \tag{4.21}$$

Similar relations for creep functions can be obtained by using the correspondence between the constitutive equation (4.19) in relaxation form and the associated relation in creep form

$$\varepsilon(t) = \int_{-\infty}^{t} J(t-\tau)\sigma'(\tau)\mathrm{d}\tau \tag{4.22}$$

according to (4.7). Substitution of the specific stress history

$$\sigma(t) = \begin{cases} 0, & t \leq 0 \\ t, & t > 0 \end{cases}$$

in (4.22) and the resulting strain rate $\dot{\varepsilon}(t) = J(t)$ in (4.19) leads to

$$\int_{0}^{t} G(t-\tau)J(\tau)\mathrm{d}\tau = t \geq 0. \tag{4.23}$$

A direct consequence of (4.23) together with (4.18) is

$$J(t) \geq 0, \quad t \geq 0. \tag{4.24}$$

Furthermore, the time-derivative of (4.23), viz.

$$G(0)J(t) + \int_0^t G'(t-\tau)J(\tau)\mathrm{d}\tau = 1 \tag{4.25}$$

results in

$$\dot{J}(t) \geq 0, \quad t \geq 0, \tag{4.26}$$

as the integral term in (4.25) is non-positive and non-increasing due to (4.21) and (4.24).

Two other factors that influence the properties of relaxation and creep functions are the *hypothesis of fading memory* and the distinction between viscoelastic fluids and solids, see Christensen (2013, Chap. 1.3). The assumption of fading memory implies that the current stress (resp. strain) is affected stronger by the more recent strain (resp. stress) history. From this point of view, the relaxation and creep representations in the form

$$\sigma(t) = G(0)\varepsilon(t) + \int_{-\infty}^t G'(t-\tau)\varepsilon(\tau)\mathrm{d}\tau, \tag{4.27}$$

$$\varepsilon(t) = J(0)\sigma(t) + \int_{-\infty}^t J'(t-\tau)\sigma(\tau)\mathrm{d}\tau \tag{4.28}$$

obtained by partial integration of (4.19) and (4.22), express a weighting of the strain (resp. stress) history and a decreasing dependence on past values necessitates decreasing weighting functions $|\dot{G}|$ and $|\dot{J}|$ in (4.27) and (4.28), which together with (4.21) and (4.26) leads to

$$\ddot{G}(t) \geq 0, \quad \ddot{J}(t) \leq 0, \quad t \geq 0. \tag{4.29}$$

Moreover, a distinction between solids and fluids influences the asymptotic behavior of relaxation and creep functions. A fluid in a constant state of deformation shows a stress relaxation to zero and, on the contrary, when subjected to a constant stress, a lasting increase in strain will occur such that

$$\lim_{t\to\infty} G(t) = 0, \quad \lim_{t\to\infty} J(t) = \infty.$$

A solid under constant strain will relax to a constant state of stress whereas a constant stress results in a finite long-term strain response, which can be expressed as

$$\lim_{t\to\infty} G(t) = G_\infty > 0, \quad \lim_{t\to\infty} J(t) = J_\infty < \infty.$$

The previous steps to identify properties of viscoelastic constitutive equations are mainly based on general physical principles, viz. the memory hypothesis, translation-invariance, causality, the fundamental laws of thermodynamics and the fading memory principle. Together with assumptions on linearity and continuity, one obtains a full description of viscoelastic material behavior by a non-negative, non-increasing, convex relaxation function G or, alternatively by a non-negative, non-decreasing, concave creep function J. Both functions are thereby connected through (4.23). A typical shape of these functions under the additional assumption of a solid material, which will be the case of interest in the further course, is shown in Figure 4.1. These graphs show another characteristic property of solid materials, namely an instantaneous elastic behavior which is evoked by $G(0) = G_0 < \infty$ and $J(0) = J_0 > 0$.

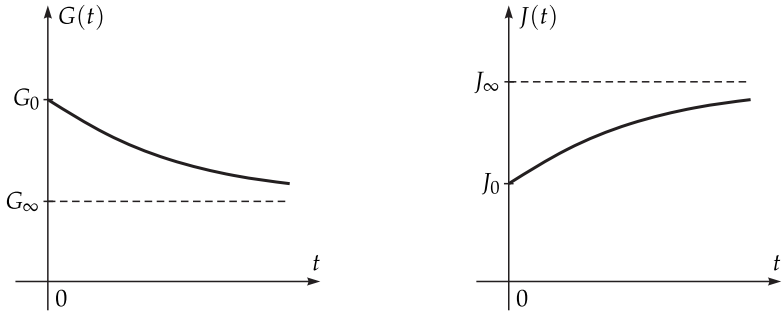

Figure 4.1: Typical shape of relaxation (left) and creep functions (right) for a viscoelastic solid.

Relaxation and retardation spectra

The most simple relaxation and creep functions that satisfy the above requirements are given by

$$G(t) = G_\infty + (G_0 - G_\infty)\mathrm{e}^{-\frac{t}{\tau_\sigma}}, \quad 0 < G_\infty < G_0 < \infty,\ \tau_\sigma > 0 \tag{4.30}$$

and

$$J(t) = J_0 + (J_\infty - J_0)\left(1 - \mathrm{e}^{-\frac{t}{\tau_\varepsilon}}\right), \quad 0 < J_0 < J_\infty < \infty,\ \tau_\varepsilon > 0, \tag{4.31}$$

where τ_σ and τ_ε are the characteristic *relaxation* and *retardation time* constants. As mentioned before, the correspondence of the parameters in (4.30) and (4.31) is given by (4.23) such that

$$J_0 = \frac{1}{G_0}, \quad J_\infty = \frac{1}{G_\infty}, \quad \tau_\varepsilon = \frac{G_0}{G_\infty}\tau_\sigma$$

must hold. The models (4.30) (or (4.31)) show a relaxation (or creep) behavior only in a quite narrow time range around τ_σ (or τ_ε), see the graphs with logarithmic time scale in Figure 4.2. However, the relaxation and creep behavior of

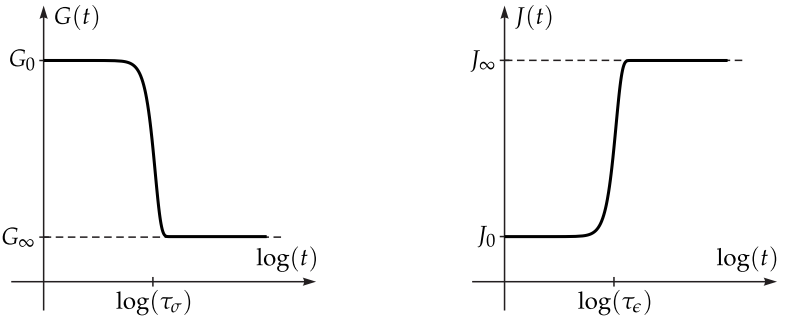

Figure 4.2: Sketched graphs of relaxation function (4.30) (left) and creep function (4.31) (right) using a logarithmic time scale.

real materials covers many decades in time, i.e., more than one characteristic time affects the constitutive law. The most general description of relaxation and creep even includes a continuous spectrum of characteristic time constants such that (4.30) and (4.31) are generalized as

$$G(t) = G_\infty + (G_0 - G_\infty) \int_0^\infty R_\sigma(\tau) \mathrm{e}^{-\frac{t}{\tau}} \mathrm{d}\tau, \tag{4.32}$$

$$J(t) = J_0 + (J_\infty - J_0) \int_0^\infty R_\varepsilon(\tau) \left(1 - \mathrm{e}^{-\frac{t}{\tau}}\right) \mathrm{d}\tau \tag{4.33}$$

with the *relaxation spectrum* R_σ and the *retardation spectrum* R_ε *in time*, that fulfill

$$\int_0^\infty R_\sigma(\tau)\mathrm{d}\tau = 1, \quad \int_0^\infty R_\varepsilon(\tau)\mathrm{d}\tau = 1,$$

see Gross (1953), Mainardi (2010, Chap. 2.5). The degree of generality of the representations (4.32) and (4.33) becomes obvious by introducing the relaxation (or retardation) frequency $\lambda = \frac{1}{\tau}$ together with the *relaxation spectrum* S_σ and the *retardation spectrum* S_ε *in frequency*, given by

$$S_\sigma(\lambda) := (G_0 - G_\infty) \frac{R_\sigma\left(\frac{1}{\lambda}\right)}{\lambda^2}, \quad S_\varepsilon(\lambda) := (J_\infty - J_0) \frac{R_\varepsilon\left(\frac{1}{\lambda}\right)}{\lambda^2}$$

such that (4.32) and (4.33) can be rewritten as

$$G(t) = G_\infty + \int_0^\infty S_\sigma(\lambda) \mathrm{e}^{-\lambda t} \mathrm{d}\lambda, \tag{4.34}$$

$$J(t) = J_0 + \int_0^\infty S_\varepsilon(\lambda) \left(1 - \mathrm{e}^{-\lambda t}\right) \mathrm{d}\lambda = J_\infty - \int_0^\infty S_\varepsilon(\lambda) \mathrm{e}^{-\lambda t} \mathrm{d}\lambda. \tag{4.35}$$

Hence, the relaxation and creep function are given as Laplace transforms (2.12) of relaxation and retardation spectrum and the spectra are in turn determined by the inverse Laplace transform of the relaxation function or the rate of the creep function, respectively.

Prony series, mechanical network models and the differential operator representation

The spectra defined above denote the starting point to consider specific viscoelastic constitutive laws. An explicitly given spectrum results in a relaxation or creep function with certain parameters that can be fitted to experimental relaxation or creep data. The choice of discrete spectra leads to a class of classical multiparameter models that consider a finite number of relaxation (or retardation) times or frequencies described by a *Prony series*. Particularly, a relaxation spectrum

$$S_\sigma(\lambda) = \sum_{i=1}^{m} G_i\, \delta(\lambda - \lambda_i), \quad \sum_{i=1}^{m} G_i = G_0 - G_\infty\,, \tag{4.36}$$

where δ represents the *Dirac distribution*, leads using (4.34) to a relaxation function

$$G(t) = G_\infty + \sum_{i=1}^{m} G_i \mathrm{e}^{-\lambda_i t}. \tag{4.37}$$

Analogously, a retardation spectrum

$$S_\varepsilon(\lambda) = \sum_{j=1}^{n} J_j\, \delta(\lambda - \bar{\lambda}_j), \quad \sum_{j=1}^{n} J_j = J_\infty - J_0$$

results together with (4.35) in a creep function

$$J(t) = J_0 + \sum_{j=1}^{n} J_j \left(1 - \mathrm{e}^{-\bar{\lambda}_j t}\right). \tag{4.38}$$

The case $m = n = 1$ in (4.37) and (4.38) directly yields (4.30) and (4.31).

The Prony series approach is linked to a mechanical interpretation of viscoelastic constitutive equations as networks consisting of springs and dashpots, see Mainardi (2010, Chap. 2.4). Thereby, a spring is considered as a perfectly elastic element that fulfills Hooke's law

$$\sigma(t) = E\varepsilon(t) \quad \Rightarrow \quad G(t) = E, \quad J(t) = \frac{1}{E}$$

with a constant elastic modulus $E > 0$ and a dashpot is meant to behave like a viscous Newtonian fluid such that

$$\sigma(t) = \eta\dot{\varepsilon}(t) \quad \Rightarrow \quad G(t) = \eta\, \delta(t), \quad J(t) = \frac{t}{\eta}$$

with a constant damper viscosity $\eta > 0$, see Figure 4.3(a). The most obvious networks result from a connection of spring and dashpot in series such that

$$\sigma(t) + \frac{\eta}{E}\dot{\sigma}(t) = \eta\dot{\varepsilon}(t),\ \sigma(0) = E\varepsilon(0) \quad \Rightarrow \quad G(t) = E\mathrm{e}^{-\frac{E}{\eta}t}, \quad J(t) = \frac{t}{\eta} + \frac{1}{E},$$

known as *Maxwell model* or a connection in parallel such that

$$\sigma(t) = \bar{E}\varepsilon(t) + \bar{\eta}\dot{\varepsilon}(t) \quad \Rightarrow \quad G(t) = \bar{E} + \bar{\eta}\,\delta(t), \quad J(t) = \frac{1}{\bar{E}}\left(1 - \mathrm{e}^{-\frac{\bar{E}}{\bar{\eta}}t}\right),$$

named *Kelvin(-Voigt) model*, see Figure 4.3(b). Furthermore, the connection of a Maxwell model in parallel to a spring leads to

$$\sigma(t) + \frac{\eta}{E_1}\dot{\sigma}(t) = E_0\varepsilon(t) + \frac{\eta}{E_1}(E_0 + E_1)\dot{\varepsilon}(t),\ \sigma(0) = (E_0 + E_1)\varepsilon(0)$$

$$\Rightarrow \quad G(t) = E_0 + E_1\mathrm{e}^{-\frac{E_1}{\eta}t}, \quad J(t) = \frac{1}{E_0 + E_1} + \frac{E_1}{E_0(E_0 + E_1)}\left(1 - \mathrm{e}^{-\frac{E_0E_1}{\eta(E_0+E_1)}t}\right),$$

which is equivalent to a Kelvin model connected in series to a spring such that

$$(\bar{E}_0 + \bar{E}_1)\sigma(t) + \bar{\eta}\dot{\sigma}(t) = \bar{E}_0\bar{E}_1\varepsilon(t) + \bar{E}_0\bar{\eta}\dot{\varepsilon}(t),\ \sigma(0) = \bar{E}_0\varepsilon(0)$$

$$\Rightarrow \quad G(t) = \frac{\bar{E}_0\bar{E}_1}{\bar{E}_0 + \bar{E}_1} + \frac{\bar{E}_0^2}{\bar{E}_0 + \bar{E}_1}\mathrm{e}^{-\frac{\bar{E}_0+\bar{E}_1}{\bar{\eta}}t}, \quad J(t) = \frac{1}{\bar{E}_0} + \frac{1}{\bar{E}_1}\left(1 - \mathrm{e}^{-\frac{\bar{E}_1}{\bar{\eta}}t}\right).$$

Both models (Figure 4.3(c)) are referred to as *Zener model* or *standard linear solid*, see Zener (1948), which represents the most simple mechanical model of a viscoelastic solid, as it is related to (4.30), (4.31). If more Kelvin elements in series or Maxwell elements in parallel are added (Figure 4.3(d)), the associated relaxation and creep functions are just of the form (4.37) and (4.38) with $m = n$.

Another description of viscoelastic constitutive laws that is also derived from the Prony series approach is the *differential operator representation*. It results from a Laplace transform (2.12) of (4.37) and (4.38) given by

$$\tilde{G}(s) := \mathcal{L}\{G(t)\}(s) = \frac{G_\infty}{s} + \sum_{i=1}^{m}\frac{G_i}{s + \lambda_i}, \tag{4.39}$$

$$\tilde{J}(s) := \mathcal{L}\{J(t)\}(s) = \frac{J_\infty}{s} - \sum_{j=1}^{n}\frac{J_j}{s + \bar{\lambda}_j}. \tag{4.40}$$

The terms in (4.39) and (4.40) represent partial fraction expansions of complex rational functions with simple poles and zeros in $(-\infty, 0]$. Some algebraic calculation leads to representations

$$\begin{aligned} s\tilde{G}(s) &= \frac{G_\infty + \sum_{i=1}^{m} a_i s^i}{1 + \sum_{i=1}^{m} b_i s^i} = \frac{\sum_{i=0}^{m-1}\bar{a}_i s^i + G_0 s^m}{\sum_{i=0}^{m-1}\bar{b}_i s^i + s^m}, \\ s\tilde{J}(s) &= \frac{1 + \sum_{j=1}^{n} c_j s^j}{1/J_\infty + \sum_{j=1}^{n} d_j s^j} = \frac{\sum_{j=0}^{n-1}\bar{c}_j s^j + s^n}{\sum_{j=0}^{n-1}\bar{d}_j s^j + s^n/J_0}. \end{aligned} \tag{4.41}$$

(a) Spring (left) and dashpot (right).

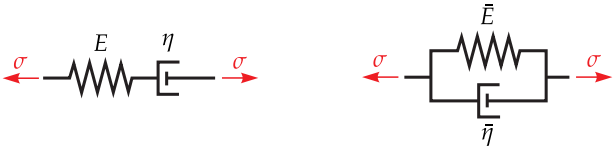

(b) Maxwell model (left) and Kelvin model (right).

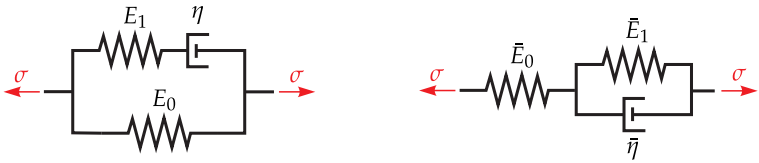

(c) Zener models.

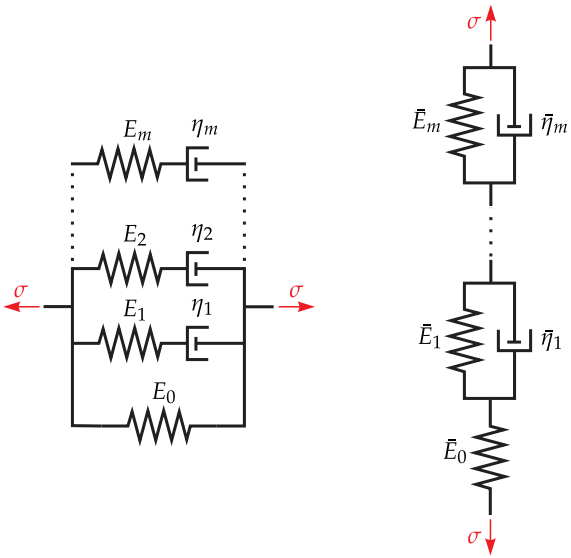

(d) Generalized Zener models.

Figure 4.3: Mechanical representation of constitutive laws.

If (4.37) and (4.38) represent the same constitutive equations, consider the Laplace transform of (4.23) using Proposition 2.9 c), viz.

$$\tilde{G}(s)\tilde{J}(s) = \frac{1}{s^2} \Leftrightarrow s\tilde{G}(s) = \frac{1}{s\tilde{J}(s)}\,, \tag{4.42}$$

which particularly yields by comparison of coefficients in (4.41)

$$\begin{aligned} m = n, \quad G_0 = \frac{1}{J_0}\,, \quad G_\infty = \frac{1}{J_\infty}\,, \\ a_i = d_i\,, \quad \bar{a}_i = \bar{d}_i\,, \quad b_i = c_i\,, \quad \bar{b}_i = \bar{c}_i\,. \end{aligned} \tag{4.43}$$

Furthermore, considering zero histories $\sigma(t) = 0$, $\varepsilon(t) = 0$ for $t < 0$, the Laplace transforms

$$\tilde{\sigma}(s) = \tilde{G}(s)s\tilde{\varepsilon}(s), \quad \tilde{\varepsilon}(s) = \tilde{J}(s)s\tilde{\sigma}(s)$$

of the constitutive equations (4.19) and (4.22) lead, together with (4.41) and (4.43), to

$$\left(1 + \sum_{i=1}^{m} b_i s^i\right)\tilde{\sigma}(s) = \left(G_\infty + \sum_{i=1}^{m} a_i s^i\right)\tilde{\varepsilon}(s).$$

This results by inverse Laplace transform in the differential operator representation

$$\sigma(t) + \sum_{i=1}^{m} b_i \mathrm{D}^i\sigma(t) = G_\infty\varepsilon(t) + \sum_{i=1}^{m} a_i \mathrm{D}^i\varepsilon(t) \tag{4.44}$$

under assumption of compatible initial conditions

$$\sum_{i=k}^{m} b_i \sigma^{(i-k)}(0) = \sum_{i=k}^{m} a_i \varepsilon^{(i-k)}(0), \quad k = 1, \ldots, m,$$

see Christensen (2013, Chap. 1.4).

The mechanical models in Figure 4.3 and the differential operator representation (4.44) are two alternative starting points for the formulation of viscoelastic constitutive equations. However, the derivations above emphasize that both approaches are derived from (4.37) (or (4.38)), which are obtained from discrete relaxation (or retardation) spectra and hence represent a special case. One major disadvantage of models that assume a finite number of relaxation (or retardation) times is the poor extrapolation of material behavior. The model parameters, including characteristic time constants obtained from relaxation and creep tests, can only fit the experimental curves in the measured time ranges and will predict a fast decay of creep and relaxation phenomena outside the measured time span. But many materials show a long-term viscoelastic behavior instead, which can only be described using continuous relaxation and retardation spectra. One possibility to formulate continuous spectra is related to fractional calculus and will

be given in Section 4.2 and the drawbacks of discrete spectra in material modeling are shown for real material data in Section 4.3. A collection of further candidate functions for spectra that have been used to identify real material behavior is listed by Gross (1953, Chap. XIII).

Complex modulus and complex compliance functions

Whereas relaxation and creep functions are quantities that represent viscoelastic material behavior under static deformation or loading conditions in the time domain, there are also observables that describe the dynamic properties in the frequency domain, named the *complex modulus* and the *complex compliance*. These quantities determine the response of a linear viscoelastic model to an oscillatory input. Particularly, the complex modulus E^* relates the stress $\hat{\sigma}(t)$ to an oscillatory strain $\hat{\varepsilon}(t) = \mathrm{e}^{\mathrm{i}\omega t}$. Together with (4.19) and the decomposition

$$G(t) = G_\infty + \hat{G}(t),$$

one obtains the representation

$$\begin{aligned} \hat{\sigma}(t) &= E^*(\mathrm{i}\omega)\hat{\varepsilon}(t), \\ E^*(\mathrm{i}\omega) &= G_\infty + \mathrm{i}\omega \int_0^\infty \hat{G}(s)\mathrm{e}^{-\mathrm{i}\omega s}\mathrm{d}s = G_\infty + \mathrm{i}\omega \mathcal{L}\left\{\hat{G}\right\}(\mathrm{i}\omega), \end{aligned} \tag{4.45}$$

in which E^* can be separated into real and imaginary part

$$\begin{aligned} E^*(\mathrm{i}\omega) &= E_1^*(\omega) + \mathrm{i}E_2^*(\omega), \\ E_1^*(\omega) = G_\infty + \omega \int_0^\infty \hat{G}(s)\sin(\omega s)\mathrm{d}s, &\quad E_2^*(\omega) = \omega \int_0^\infty \hat{G}(s)\cos(\omega s)\mathrm{d}s. \end{aligned} \tag{4.46}$$

The quantities E_1^* and E_2^* are sometimes referred to as *storage* and *loss modulus*, respectively, see Christensen (2013, Chap. 1.6) and Lakes (1999, Chap. 3). This nomenclature becomes clear by using (4.46) in (4.45) such that

$$\hat{\sigma}(t) = E_1^*(\omega)\hat{\varepsilon}(t) + \frac{E_2^*(\omega)}{\omega}\dot{\hat{\varepsilon}}(t).$$

An equivalent representation given by the imaginary part of (4.45), namely

$$\varepsilon(t) = \sin(\omega t) \quad \Rightarrow \quad \sigma(t) = E_1^*(\omega)\sin(\omega t) + E_2^*(\omega)\cos(\omega t),$$

illustrates that E_1^* is the component of the modulus in phase to the applied strain, whereas E_2^* represents the anti-phase part. Equation (4.46) allows the calculation of the complex modulus from the creep function such that dynamic properties can

be computed from static experimental data. Vice versa, the relaxation function can be obtained from dynamic data by Fourier inversion of (4.46), i.e.,

$$\hat{G}(t) = \frac{2}{\pi}\int_0^\infty \frac{E_1^*(\omega) - G_\infty}{\omega}\sin(\omega t)\,\mathrm{d}\omega = \frac{2}{\pi}\int_0^\infty \frac{E_2^*(\omega)}{\omega}\cos(\omega t)\,\mathrm{d}\omega. \tag{4.47}$$

The complex modulus can alternatively be given in terms of the relaxation spectrum. Substituting (4.34) in (4.46), interchanging integrals and using the Laplace transforms of sine and cosine, see Proposition 2.9, leads to

$$E_1^*(\omega) = G_\infty + \omega^2\int_0^\infty \frac{S_\sigma(\lambda)}{\lambda^2+\omega^2}\mathrm{d}\lambda, \tag{4.48}$$

$$E_2^*(\omega) = \omega\int_0^\infty \frac{S_\sigma(\lambda)\lambda}{\lambda^2+\omega^2}\mathrm{d}\lambda, \tag{4.49}$$

as given by Gross (1953, Chap. V.3). For the example of a discrete relaxation spectrum (4.36) in (4.48) and (4.49), one obtains

$$E_1^*(\omega) = G_\infty + \omega^2\sum_{i=1}^m \frac{G_i}{\lambda_i^2+\omega^2}\,, \quad E_2^*(\omega) = \omega\sum_{i=1}^m \frac{G_i\lambda_i}{\lambda_i^2+\omega^2}\,. \tag{4.50}$$

A sketch of the above storage and loss moduli for the case $m = 1$ is given in Figure 4.4. Particularly, the moduli in (4.50) show the predominantly elastic behavior of a viscoelastic solid for very small frequencies as

$$\lim_{\omega\to 0} E_1^*(\omega) = G_\infty > 0, \quad \lim_{\omega\to 0} E_2^*(\omega) = 0$$

and for extremely large frequencies because

$$\lim_{\omega\to\infty} E_1^*(\omega) = G_\infty + \sum_{i=1}^m G_i = G_0 > 0, \quad \lim_{\omega\to\infty} E_2^*(\omega) = 0.$$

Similar as in previous sections, the role of stress and strain can be swapped for an equivalent representation, i.e., one can consider the strain response $\hat{\varepsilon}$ to an oscillatory stress history $\hat{\sigma}(t) = \mathrm{e}^{\mathrm{i}\omega t}$, which is given by the *complex compliance* J^*. Equation (4.22) together with the decomposition

$$J(t) = J_\infty - \hat{J}(t)$$

leads to the representation

$$\begin{aligned} \hat{\varepsilon}(t) &= J^*(\mathrm{i}\omega)\hat{\sigma}(t), \\ J^*(\mathrm{i}\omega) &= J_\infty - \mathrm{i}\omega\int_0^\infty \hat{J}(s)\mathrm{e}^{-\mathrm{i}\omega s}\mathrm{d}s = J_\infty - \mathrm{i}\omega\mathcal{L}\left\{\hat{J}\right\}(\mathrm{i}\omega) \end{aligned} \tag{4.51}$$

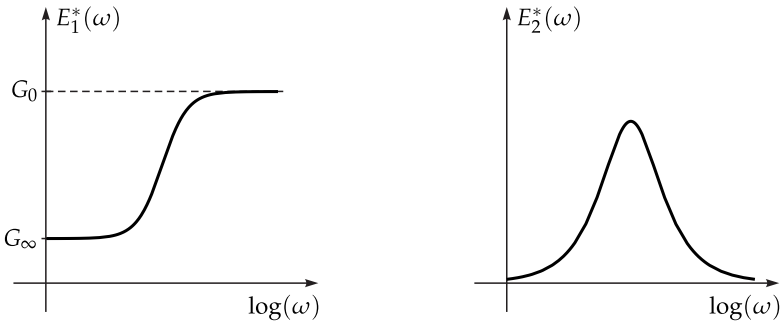

Figure 4.4: Frequency dependence of storage and loss modulus for a Zener model.

together with the decomposition

$$J^*(\mathrm{i}\omega) = J_1^*(\omega) - \mathrm{i}J_2^*(\omega),$$
$$J_1^*(\omega) = J_\infty - \omega\int_0^\infty \hat{J}(s)\sin(\omega s)\mathrm{d}s, \quad J_2^*(\omega) = \omega\int_0^\infty \hat{J}(s)\cos(\omega s)\mathrm{d}s.$$

A comparison of (4.45) and (4.51) reveals using (4.42) the correspondence

$$J^*(\mathrm{i}\omega) = \frac{1}{E^*(\mathrm{i}\omega)}$$

between complex modulus and complex compliance. Similar formulas as (4.47), (4.48) and (4.49) hold for J^* as well and are given by Gross (1953, Chap. VI).

4.2 Fractional linear viscoelasticity

A possible choice of a continuous relaxation spectrum is given by

$$S_\sigma(\lambda) := p\frac{\sin(\alpha\pi)}{\pi}\lambda^{\alpha-1} = p\mu_{1-\alpha}(\lambda), \quad p > 0,\ \alpha \in (0,1). \tag{4.52}$$

This spectrum is the starting point for the formulation of a class of viscoelastic constitutive laws, that are related to fractional calculus. Indeed, using (4.34) and (2.28), the associated relaxation function

$$G(t) = p\frac{t^{-\alpha}}{\Gamma(1-\alpha)} \tag{4.53}$$

can be identified, which leads in view of (4.19) and Definition 2.5 to the linear constitutive equation

$$\sigma(t) = p\,{}^{\mathrm{C}}\mathrm{D}^\alpha\varepsilon(t). \tag{4.54}$$

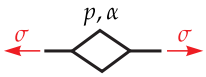

(a) Springpot.

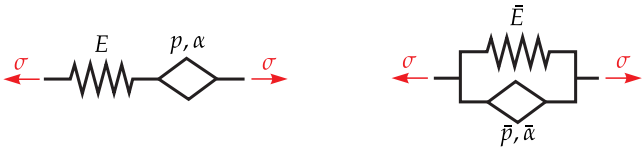

(b) Fractional Maxwell model (left) and fractional Kelvin model (right).

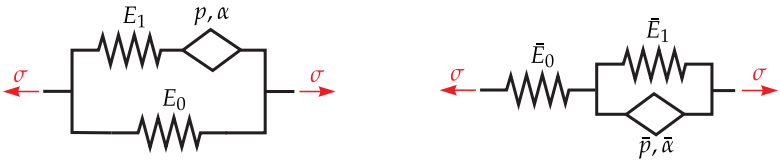

(c) Fractional Zener models.

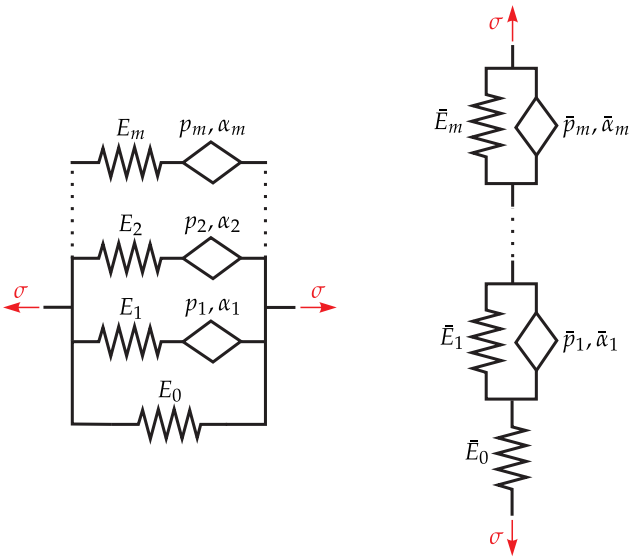

(d) Generalized fractional Zener models.

Figure 4.5: Mechanical representation of fractional constitutive laws.

Fractional calculus has been used by several authors in the 1930s and 1940s as an empirical method to describe viscoelastic material behavior, see the references in Mainardi (2010, Chap. 3). Particularly, Scott Blair (1947) introduced (4.54) to model intermediate material behavior interpolating between Hooke's and Newton's law. Later, Koeller (1984) related (4.54) to a new rheological element to be used in mechanical network models, besides the spring and the dashpot element. The fractional rheological element was named *springpot*[1] and depicted as a rhombus, see Figure 4.5(a). In view of (4.53), a springpot shows a long-term relaxation behavior. It fulfills the necessary conditions (4.18), (4.21) and (4.29) to represent a linear viscoelastic medium properly. However, a springpot by itself cannot describe solid behavior as

$$\lim_{t\to 0} G(t) = \infty, \quad \lim_{t\to\infty} G(t) = 0.$$

The most simple way to bound the initial value of the relaxation function is adding a spring in series to the springpot, which is known as *fractional Maxwell model* (Figure 4.5(b)) and given by the equation

$${}^{\mathrm{C}}\mathrm{D}^{\alpha}\varepsilon(t) = \frac{1}{E}\,{}^{\mathrm{C}}\mathrm{D}^{\alpha}\sigma(t) + \frac{1}{p}\sigma(t). \tag{4.55}$$

The associated relaxation function G can be obtained by assuming a unit-step strain $\varepsilon(t) = \Theta(t)$ and an elastic initial relaxation $G(0) = E$ (due to the spring with modulus E). This translates (4.55) into

$${}^{\mathrm{C}}\mathrm{D}_0^{\alpha} G(t) = -\frac{E}{p} G(t), \quad G(0) = E, \tag{4.56}$$

where (4.6) and the properties

$${}^{\mathrm{C}}\mathrm{D}^{\alpha}\Theta(t) = \int_{-\infty}^{t} \frac{(t-\tau)^{-\alpha}}{\Gamma(1-\alpha)}\delta(\tau)\mathrm{d}\tau = \frac{t^{-\alpha}}{\Gamma(1-\alpha)},$$

$${}^{\mathrm{C}}\mathrm{D}^{\alpha} G(t) = {}^{\mathrm{C}}\mathrm{D}^{\alpha}\{G(0)\Theta(t)\} + {}^{\mathrm{C}}\mathrm{D}_0^{\alpha}\{G(t) - G(0)\} = G(0)\frac{t^{-\alpha}}{\Gamma(1-\alpha)} + {}^{\mathrm{C}}\mathrm{D}_0^{\alpha} G(t)$$

are used. Thus, (4.56) is solved by a Mittag-Leffler function, see (2.14), as

$$G(t) = E\,\mathrm{E}_{\alpha}\left(-\frac{E}{p}t^{\alpha}\right).$$

For the Mittag-Leffler function, (4.18), (4.21) and (4.29) still hold according to Proposition 2.14. Furthermore, an additional spring in parallel to a fractional

[1] Originally, Koeller (1984) used the spelling *spring-pot*. The author prefers an unhyphenated notation.

Maxwell model (Figure 4.5(c)) leads to a non-zero asymptotic relaxation, i.e.,

$$G(t) = E_0 + E_1 \mathrm{E}_\alpha\left(-\frac{E_1}{p}t^\alpha\right). \tag{4.57}$$

The relaxation function (4.57) finally fulfills all properties of a constitutive law describing linear viscoelastic solids. The associated mechanical model is referred to as *fractional Zener model*. Omitting the mechanical interpretation, (4.57) can be reformulated with new parameters as

$$G(t) = G_\infty + (G_0 - G_\infty)\mathrm{E}_\alpha(-\gamma_\sigma t^\alpha), \quad 0 < G_\infty < G_0,\ \gamma_\sigma > 0,\ \alpha \in (0,1). \tag{4.58}$$

A fractional relaxation (4.58) also corresponds to a continuous relaxation spectrum. To see this, the Laplace transform of the Mittag-Leffler function in Proposition 2.12 is expedient. More precisely, the inverse transform

$$\mathrm{E}_\alpha(-\gamma t^\alpha) = \frac{1}{2\pi \mathrm{i}} \int_{\delta-\mathrm{i}\infty}^{\delta+\mathrm{i}\infty} \frac{s^{\alpha-1}}{s^\alpha + \gamma} \mathrm{e}^{st} \mathrm{d}s, \quad \delta > 0$$

can be obtained by an integral along a Bromwich contour in the complex plane and using the residue theorem[2]. The only non-vanishing contributions to this integral stem from the sides of the branch cut along the negative real axis. The result is given by

$$\mathrm{E}_\alpha(-\gamma t^\alpha) = -\frac{1}{\pi}\int_0^\infty \mathrm{Im}\left(\left.\frac{s^{\alpha-1}}{s^\alpha+\gamma}\right|_{s=\lambda \mathrm{e}^{\mathrm{i}\pi}}\right) \mathrm{e}^{-\lambda t}\mathrm{d}\lambda. \tag{4.59}$$

Using (4.59) together with (4.58) in (4.34) leads to the relaxation spectrum

$$S_\sigma(\lambda) = (G_0 - G_\infty)\frac{\gamma_\sigma \mu_{1-\alpha}(\lambda)}{\lambda^{2\alpha} + 2\gamma_\sigma \lambda^\alpha \cos(\alpha\pi) + \gamma_\sigma^2}, \tag{4.60}$$

which is shown in Figure 4.6 for various values of $\alpha \in (0,1)$. Particularly, the graphs lead to the proposition

$$\lim_{\alpha \to 1} S_\sigma(\lambda) = (G_0 - G_\infty)\delta(\lambda - \gamma_\sigma),$$

which represents the case $m = 1$ in (4.36).

The fractional Zener model can, of course, also be represented by a creep function. Hereto, consider a spring in parallel to a springpot leading to a *fractional Kelvin model* (Figure 4.5(b)) described by

$$\sigma(t) = \bar{E}\varepsilon(t) + p\,{}^{\mathrm{C}}\mathrm{D}^{\bar{\alpha}}\varepsilon(t). \tag{4.61}$$

[2]The details are omitted here. A more complicated example using this procedure is described in detail in Chapter 5.

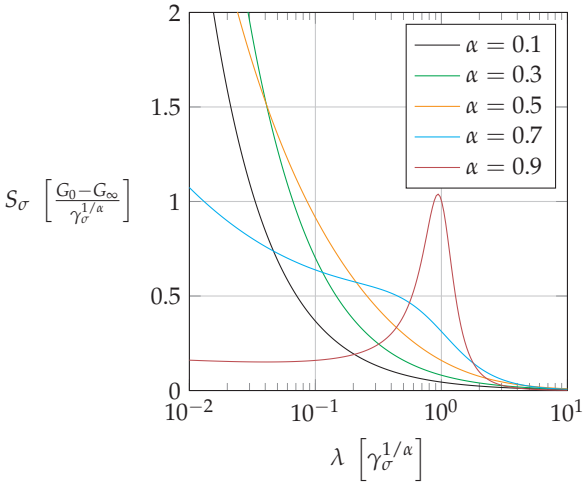

Figure 4.6: Relaxation spectrum $S_\sigma(\lambda)$ for different values of $\alpha \in (0,1)$.

A unit-step stress and the assumption of zero initial strain transform (4.61) into

$$ {}^{\mathrm{C}}\mathrm{D}_0^{\bar{\alpha}} J(t) = \frac{1}{\bar{p}} - \frac{\bar{E}}{\bar{p}} J(t), \quad J(0) = 0, $$

which is again solved by a Mittag-Leffler function as

$$ J(t) = \frac{1}{\bar{E}} \left(1 - \mathrm{E}_{\bar{\alpha}}\left(-\frac{\bar{E}}{\bar{p}} t^{\bar{\alpha}}\right)\right). $$

Adding another spring in series finally yields the creep representation of the fractional Zener model (Figure 4.5(c))

$$ J(t) = \frac{1}{\bar{E}_0} + \frac{1}{\bar{E}_1} \left(1 - \mathrm{E}_{\bar{\alpha}}\left(-\frac{\bar{E}_1}{\bar{p}} t^{\bar{\alpha}}\right)\right). \tag{4.62} $$

Alternatively, the creep function is in view of (4.58) and in analogy to (4.30) and (4.31) given as

$$ J(t) = J_0 + (J_\infty - J_0)\left(1 - \mathrm{E}_{\bar{\alpha}}\left(-\gamma_\varepsilon t^{\bar{\alpha}}\right)\right). \tag{4.63} $$

Thereby, the relation (4.42) leads to a correspondence of parameters in (4.58) and (4.63) given by

$$ J_0 = \frac{1}{G_0}, \quad J_\infty = \frac{1}{G_\infty}, \quad \gamma_\varepsilon = \frac{G_\infty}{G_0}\gamma_\sigma, \quad \bar{\alpha} = \alpha, $$

which yields in view of (4.57) and (4.62)

$$\bar{E}_0 = E_0 + E_1\,, \quad \bar{E}_1 = \frac{E_0}{E_1}(E_0 + E_1), \quad \bar{p} = \left(\frac{E_0 + E_1}{E_1}\right)^2 p, \quad \bar{\alpha} = \alpha. \tag{4.64}$$

A creep function as in (4.62) has been used for instance by Schmidt and Gaul (2002) to describe the material behavior of a polymer. Another application on creep of salt concrete is explicated in Section 4.3. Moreover, using (4.59) in (4.63) yields the retardation spectrum

$$S_\varepsilon(\lambda) = (J_\infty - J_0)\frac{\gamma_\varepsilon \mu_{1-\alpha}(\lambda)}{\lambda^{2\alpha} + 2\gamma_\varepsilon \lambda^\alpha \cos(\alpha\pi) + \gamma_\varepsilon^2}$$

similar to (4.60). A further generalization of fractional Zener models as in Figure 4.5(d) is analogously to (4.37) and (4.38) given by

$$G(t) = G_\infty + \sum_{i=1}^{m} G_i \mathrm{E}_{\alpha_i}\left(-\gamma_{\sigma,i} t^{\alpha_i}\right), \quad \sum_{i=1}^{m} G_i = G_0 - G_\infty\,,$$
$$J(t) = J_0 + \sum_{i=1}^{m} J_i \left(1 - \mathrm{E}_{\alpha_i}\left(-\gamma_{\sigma,i} t^{\alpha_i}\right)\right), \quad \sum_{i=1}^{m} J_i = J_\infty - J_0\,.$$

However, the applications in the following chapters are confined to simple fractional Zener models.

To conclude this section, the dynamic properties of fractional constitutive laws are studied. For the springpot, one obtains the storage and loss moduli by substituting (4.52) in (4.48) and (4.49) to obtain

$$E_1^*(\omega) = \omega^2 \int_0^\infty \frac{p\mu_{1-\alpha}(\lambda)}{\lambda^2 + \omega^2} = p\cos\left(\frac{\alpha\pi}{2}\right)\omega^\alpha, \tag{4.65}$$
$$E_2^*(\omega) = \omega \int_0^\infty \frac{p\mu_{1-\alpha}(\lambda)\lambda}{\lambda^2 + \omega^2} = p\sin\left(\frac{\alpha\pi}{2}\right)\omega^\alpha, \tag{4.66}$$

where the right-hand expressions result from Proposition 3.3. Accordingly, the storage and loss moduli of the springpot can be rediscovered in the reformulated infinite state representation (3.4). Particularly, the constitutive law (4.54) can be described by

$$\begin{aligned} \sigma(t) = p\,{}^{\mathrm{C}}\mathrm{D}^\alpha \varepsilon(t) &= E_1^*(\omega)\varepsilon(t) + \frac{E_2^*(\omega)}{\omega}\dot{\varepsilon}(t) \\ &\quad - p\int_0^\infty \mathrm{K}_\omega(\alpha,\lambda)(\omega^2 Z(\lambda,t) + \dot{z}(\lambda,t))\mathrm{d}\lambda, \\ \dot{Z}(\eta,t) &= \varepsilon(t) - \eta Z(\eta,t), \\ \dot{z}(\eta,t) &= \dot{\varepsilon}(t) - \eta z(\eta,t), \end{aligned} \tag{4.67}$$

where E_1^* and E_2^* are assumed to fulfill (4.65) and (4.66). The representation (4.67) will prove to be useful in Section 5.3. Alternatively, for the case of a fractional Zener model, the complex modulus is obtained by substituting (4.58) in (4.45) and using Proposition 2.12 such that

$$\begin{aligned} E^*(\mathrm{i}\omega) &= G_\infty + \mathrm{i}\omega(G_0 - G_\infty)\mathcal{L}\left\{\mathrm{E}_\alpha(-\gamma_\sigma t^\alpha)\right\}(\mathrm{i}\omega) \\ &= G_\infty + (G_0 - G_\infty)\frac{(\mathrm{i}\omega)^\alpha}{(\mathrm{i}\omega)^\alpha + \gamma_\sigma} \\ \Rightarrow \quad E_1^*(\omega) &= G_\infty + (G_0 - G_\infty)\frac{\omega^{2\alpha} + \gamma_\sigma\omega^\alpha\cos(\frac{\alpha\pi}{2})}{\omega^{2\alpha} + 2\gamma_\sigma\omega^\alpha\cos(\frac{\alpha\pi}{2}) + \gamma_\sigma^2}\,, \\ E_2^*(\omega) &= (G_0 - G_\infty)\frac{\gamma_\sigma\omega^\alpha\sin(\frac{\alpha\pi}{2})}{\omega^{2\alpha} + 2\gamma_\sigma\omega^\alpha\cos(\frac{\alpha\pi}{2}) + \gamma_\sigma^2}\,. \end{aligned} \tag{4.68}$$

The graphs of storage and loss moduli as in (4.68) are shown in Figure 4.7. As expected, the case $\alpha \to 1$ yields (4.50) with $m = 1$. The complex modulus in (4.68) and the associated relaxation spectrum (4.52) have initially been proposed by Cole and Cole (1941) to describe experimental results regarding dielectric relaxation. Augmented spectra with improved fitting properties are introduced by Havriliak and Negami (1966) and Hilfer (2002, 2019). Applications to viscoelastic material behavior are among others given by Nolle (1950); Caputo and Mainardi (1971); Bagley and Torvik (1983, 1985, 1986); Schmidt and Gaul (2002).

4.3 Identification of a fractional Zener model for salt concrete

As a part of the project "ProVerB", it is the aim to model and predict the viscoelastic behavior of the salt concrete M2, as introduced in Section 1.5. Therefore, experimental results from creep tests are considered for a parameter calibration of a fractional Zener model. The results are illustrated subsequently.

Test record and data

A test series is considered run at the Materials Testing Institute (MPA) of the University of Stuttgart starting in January 2019 and lasting for about two years. The experiments included creep and shrinkage tests for three specimens of the concrete M2 each. The cylinder-shaped concrete bodies were produced at the Materials Testing Institute in Brunswick (Germany) and the tests at MPA Stuttgart started at an age of the specimens of 56 days. Just before starting the tests, the compressive strength of M2 was determined to 25 MPa on average. The creep tests were driven at a constant compressive axial load of 8.3 MPa, which is about $\frac{1}{3}$ of the compressive strength and hence small enough such that no cracking occurred during the test. The shortening of the specimens in axial direction has

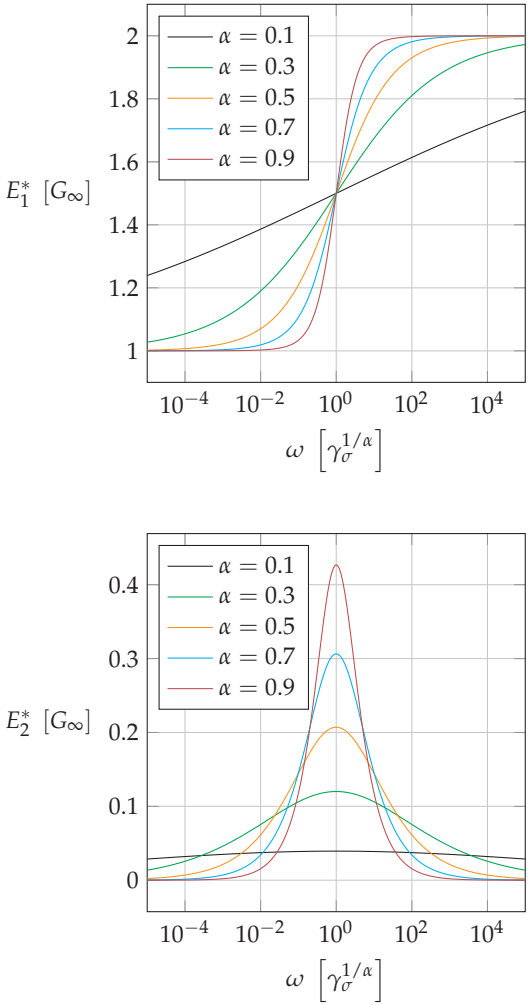

Figure 4.7: Storage modulus $E_1^*(\omega)$ (top) and loss modulus $E_2^*(\omega)$ (bottom) for the case $G_0 = 2G_\infty$ in (4.68) and different values of $\alpha \in (0, 1)$.

been measured with the help of three dial gauges, the lateral strain has been determined using two strain gauges[3], see Figure 4.8. The deformation has been measured in the central part of the specimens, where it is assumed that boundary effects have decayed and stress and strain states are homogeneous. In parallel to

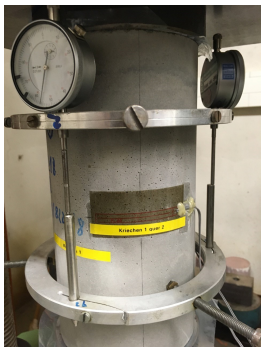

Figure 4.8: Experimental setup of creep tests. The dial gauges measure the axial strain in the central part of the cylindrical specimens. Strain gauges are used to measure the circumferential strain in the middle of the specimen.

the creep tests, the autogenic shrinkage of unloaded specimens has been determined by dial gauges, as shrinkage is not covered by the constitutive model and has to be subtracted from the measured data to obtain elastic and creep strain. The deformation data have been recorded in logarithmic time steps, which is important for the parameter identification. All details regarding the test series are summarized in Table 4.1.

The results of the measurements at MPA are depicted in Figure 4.9. For each of the three specimens, the average strains measured by the dial and strain gauges are given. The bottom right graph shows the averages of axial and lateral strain of the three specimens as well as the mean shrinkage together with error bars that represent an uncertainty of one empirical standard deviation.

Modeling, parametrization and parameter identification

It is assumed that the concrete M2 can be represented on the given time and length scale by an isotropic viscoelastic material, i.e., the constitutive law is fully described by (4.15) and (4.16) for certain creep functions in isotropic compression J_{h} and shear J_{d}. In the following, both creep functions are chosen to be of fractional

[3]The average axial and lateral strain data are used for the further analysis in order to compensate for slightly asymmetric strain of the specimens.

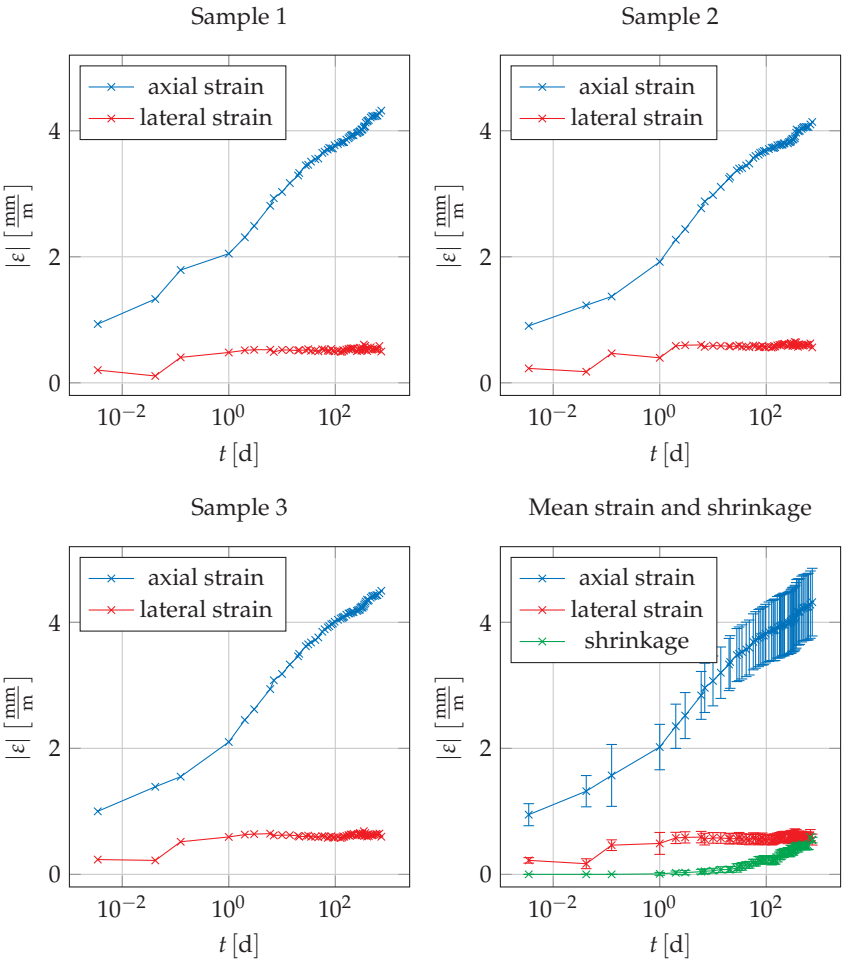

Figure 4.9: Measured absolute values of axial and lateral strain of all specimens at MPA, mean strains and shrinkage with error bars representing one empirical standard deviation.

test series	creep test (3 specs.), shrinkage test (3 specs.)
geometry	cylindrical, height $\approx$ 300 mm, diameter $\approx$ 150 mm
compressive strength	25 MPa at the age of 55 days
start	January 29, 2019 at the age of 56 days
compressive load	8.3 MPa
measured data	total axial and lateral strain, shrinkage
climate	$\theta = (20 \pm 2)°\mathrm{C}$, $RH = (65 \pm 5)\%$

Table 4.1: Details of the test series with concrete M2 at MPA Stuttgart.

Zener type (4.62) such that

$$J_{\mathrm{h}}(t) = \frac{1}{\bar{E}_{0,\mathrm{h}}} + \frac{1}{\bar{E}_{1,\mathrm{h}}}\left(1 - \mathrm{E}_{\bar{\alpha}_{\mathrm{h}}}\left(-\frac{\bar{E}_{1,\mathrm{h}}}{\bar{p}_{\mathrm{h}}} t^{\bar{\alpha}_{\mathrm{h}}}\right)\right), \tag{4.69}$$

$$J_{\mathrm{d}}(t) = \frac{1}{\bar{E}_{0,\mathrm{d}}} + \frac{1}{\bar{E}_{1,\mathrm{d}}}\left(1 - \mathrm{E}_{\bar{\alpha}_{\mathrm{d}}}\left(-\frac{\bar{E}_{1,\mathrm{d}}}{\bar{p}_{\mathrm{d}}} t^{\bar{\alpha}_{\mathrm{d}}}\right)\right). \tag{4.70}$$

Accordingly, the constitutive law is determined by the parameters $\bar{E}_{0,\mathrm{h}}$, $\bar{E}_{1,\mathrm{h}}$, $\bar{p}_{\mathrm{h}}$, $\bar{\alpha}_{\mathrm{h}}$, $\bar{E}_{0,\mathrm{d}}$, $\bar{E}_{1,\mathrm{d}}$, $\bar{p}_{\mathrm{d}}$ and $\bar{\alpha}_{\mathrm{d}}$.

To identify the parameters from the given creep tests, a constant load is assumed that is brought up instantaneously at the beginning of the test at $t = 0$. This results in the stress history in the form of a step function

$$\boldsymbol{\sigma}(t) = \boldsymbol{\sigma}_0 \Theta(t),$$

where $\boldsymbol{\sigma}_0$ is the initial stress with hydrostatic part $\sigma_{0,\mathrm{h}}$ and deviatoric part $\boldsymbol{\sigma}_{0,\mathrm{d}}$. For this case, one obtains, in view of (4.9) and using the constitutive laws (4.69) and (4.70), the response of the strain components

$$\begin{aligned} \varepsilon_{\mathrm{h}}(t) &= \sigma_{0,\mathrm{h}}\left(\frac{1}{\bar{E}_{0,\mathrm{h}}} + \frac{1}{\bar{E}_{1,\mathrm{h}}}\left(1 - \mathrm{E}_{\bar{\alpha}_{\mathrm{h}}}\left(-\frac{\bar{E}_{1,\mathrm{h}}}{\bar{p}_{\mathrm{h}}} t^{\bar{\alpha}_{\mathrm{h}}}\right)\right)\right), \ t \geq 0, \\ \boldsymbol{\varepsilon}_{\mathrm{d}}(t) &= \boldsymbol{\sigma}_{0,\mathrm{d}}\left(\frac{1}{\bar{E}_{0,\mathrm{d}}} + \frac{1}{\bar{E}_{1,\mathrm{d}}}\left(1 - \mathrm{E}_{\bar{\alpha}_{\mathrm{d}}}\left(-\frac{\bar{E}_{1,\mathrm{d}}}{\bar{p}_{\mathrm{d}}} t^{\bar{\alpha}_{\mathrm{d}}}\right)\right)\right), \ t \geq 0. \end{aligned} \tag{4.71}$$

For the specific compression test performed at MPA, one can consider stress and strain tensors expressed in the principal coordinate system I of the test cylinders

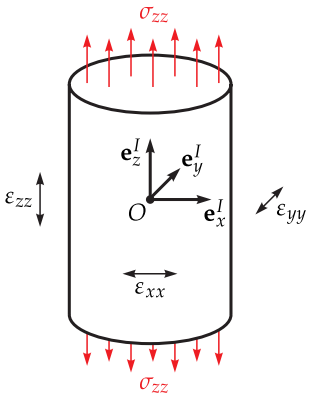

Figure 4.10: Model of a cylindrical specimen with stress and strain state expressed in the inertial coordinate system.

(Figure 4.10) as

$$ {}_I\boldsymbol{\sigma} = \begin{bmatrix} 0 & 0 & 0 \\ 0 & 0 & 0 \\ 0 & 0 & \sigma_{zz} \end{bmatrix}, \quad {}_I\boldsymbol{\varepsilon} = \begin{bmatrix} \varepsilon_{xx} & 0 & 0 \\ 0 & \varepsilon_{yy} & 0 \\ 0 & 0 & \varepsilon_{zz} \end{bmatrix}, \tag{4.72} $$

where $\sigma_{zz}, \varepsilon_{zz} < 0$ and $\varepsilon_{xx} = \varepsilon_{yy} > 0$. The assumptions in (4.72) are justified by the uniaxial loading in $\mathbf{e}_z^I$-direction, the axisymmetry and the purely axial stretch in principal directions of the specimens observed in the experiments, at least in the central area of the concrete bodies, where the measurements are taken. All of the magnitudes $\sigma_{zz}, \varepsilon_{xx} = \varepsilon_{yy}$ and ε_{zz} that occur in (4.72) are measured during the experiments. A connection between (4.71) and (4.72) can be derived using (4.11) and (4.12) as

$$ \begin{aligned} {}_I\sigma_{\mathrm{h}} &= \frac{1}{3}\sigma_{zz}, \quad {}_I\boldsymbol{\sigma}_{\mathrm{d}} = -\frac{1}{3}\sigma_{zz} \begin{bmatrix} 1 & 0 & 0 \\ 0 & 1 & 0 \\ 0 & 0 & -2 \end{bmatrix}, \\ {}_I\varepsilon_{\mathrm{h}} &= \frac{1}{3}(2\varepsilon_{xx} + \varepsilon_{zz}), \quad {}_I\boldsymbol{\varepsilon}_{\mathrm{d}} = \frac{1}{3}(\varepsilon_{xx} - \varepsilon_{zz}) \begin{bmatrix} 1 & 0 & 0 \\ 0 & 1 & 0 \\ 0 & 0 & -2 \end{bmatrix}. \end{aligned} \tag{4.73} $$

Particularly, using (4.73), the constitutive law for the deviatoric components reduces to a scalar equation with

$$ {}_I\sigma_{\mathrm{d}} = -\frac{1}{3}\sigma_{zz}, \quad {}_I\varepsilon_{\mathrm{d}} = \frac{1}{3}(\varepsilon_{xx} - \varepsilon_{zz}). $$

Finally, using (4.71) and (4.73) together with the measured data, the parameters in (4.69) and (4.70) can be identified.

To illustrate the influence of its parameters, consider the creep function (4.62) of the fractional Zener model in log-log plots and study the resulting S-shaped graphs. Clearly, the initial value of the creep function corresponding to the purely elastic component of the material response is given by $\bar{E}_0$ as

$$J(0) = \frac{1}{\bar{E}_0}\,.$$

The slope of the central part of the graph, i.e., the velocity of creep, is determined by the parameter $\bar{\alpha}$ (Figure 4.11). Changing the springpot coefficient $\bar{p}$ results in a shift of the graph along the time axis (Figure 4.12), whereas the parameter $\bar{E}_1$ determines the asymptotic behavior as

$$\lim_{t\to\infty} J(t) = \frac{1}{\bar{E}_0} + \frac{1}{\bar{E}_1}\,,$$

see Figure 4.13.

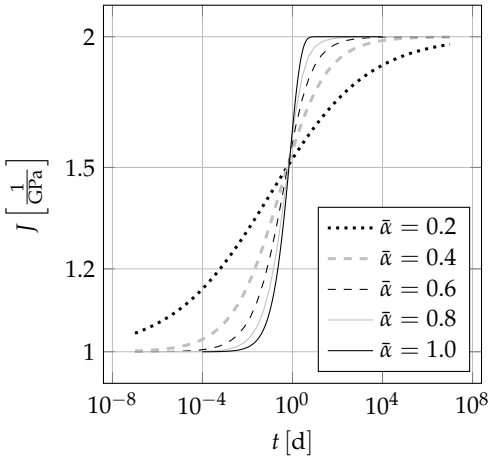

Figure 4.11: Creep function of a fractional Zener model for $\bar{E}_0 = \bar{E}_1 = 1\,\text{GPa}$, $\bar{p} = 1\,\text{GPa}\cdot\text{d}^{\bar{\alpha}}$ and various values of $\bar{\alpha} \in (0,1)$.

The parameter identification is finally obtained from a weighted nonlinear least-squares optimization applied to the mean experimental data. Therefore, the squared residuals of $(\varepsilon_{xx}(t_i),\, \varepsilon_{zz}(t_i))_{i=1,\dots,n}$, where t_i, $i = 1,\dots,n$ are the time instants of measurement, are weighted by the inverse empirical variances $\frac{1}{s^2}$. The

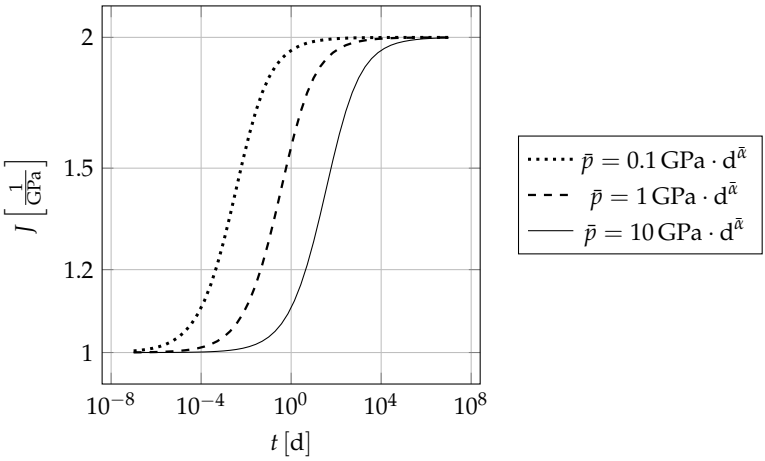

Figure 4.12: Creep function of a fractional Zener model for $\bar{E}_0 = \bar{E}_1 = 1\,\mathrm{GPa}$, $\bar{\alpha} = 0.5$ and various values of $\bar{p}$.

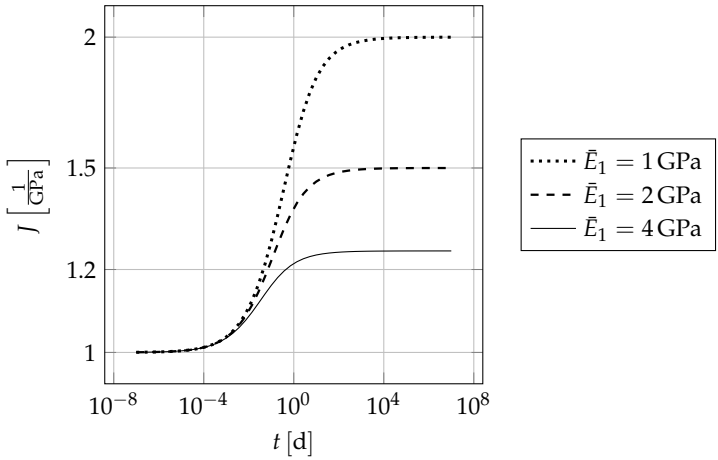

Figure 4.13: Creep function of a fractional Zener model for $\bar{E}_0 = 1\,\mathrm{GPa}$, $\bar{\alpha} = 0.5$, $\bar{p} = 1\,\mathrm{GPa}\cdot\mathrm{d}^{\bar{\alpha}}$ and various values of $\bar{E}_1$.

variances are obtained from the data, see Figure 4.9, as

$$s^2 = \left(0.1\,\frac{\text{mm}}{\text{m}}\right)^2 \text{ for } (\varepsilon_{xx}(t_i))_{i=1,\dots,n}\,,$$
$$s^2 = \left(0.5\,\frac{\text{mm}}{\text{m}}\right)^2 \text{ for } (\varepsilon_{zz}(t_i))_{i=1,\dots,n}\,.$$

Results and discussion

The least-squares calibration yields the optimal parameters

$$\bar{E}_{0,\text{h}} = 14.34\,\text{GPa}, \quad \bar{E}_{1,\text{h}} = 3.32\,\text{GPa}, \quad \bar{p}_\text{h} = 17.59\,\text{GPa}\,\text{d}^{\bar{\alpha}_\text{h}}, \quad \bar{\alpha}_\text{h} = 0.62,$$
$$\bar{E}_{0,\text{d}} = 8.00\,\text{GPa}, \quad \bar{E}_{1,\text{d}} = 2.04\,\text{GPa}, \quad \bar{p}_\text{d} = 4.08\,\text{GPa}\,\text{d}^{\bar{\alpha}_\text{d}}, \quad \bar{\alpha}_\text{d} = 0.42$$

and the resulting predicted curves for hydrostatic and deviatoric components together with experimental data are shown in Figure 4.14. The fitted curves pro-

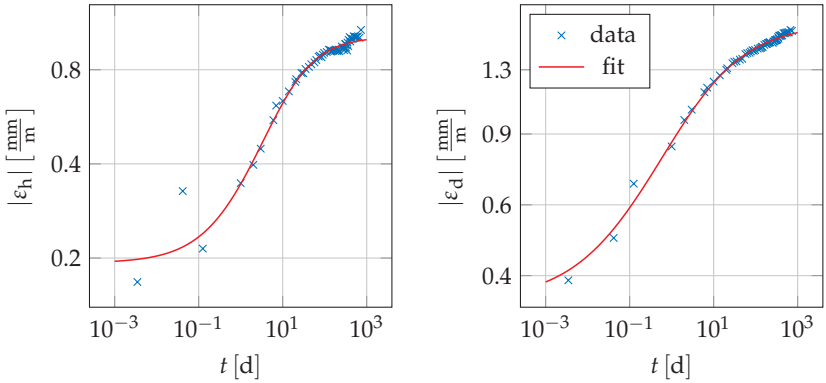

Figure 4.14: Results of the parameter identification using the method of weighted nonlinear least squares.

vide a good representation of the experimental results and it is shown that the slow creep process of the concrete M2 is well described by the fractional Zener model. Small deviations due to measurement errors just after the loading of the specimens are visible. The fitting of the deviatoric strain component is slightly better than for the hydrostatic part. A deeper analysis of the parameter identification (in terms of probability distributions) is given by Hinze et al. (2021). The article discusses the identifiability of the parameters by the given experimental setup and reveals comparably large parameter uncertainties.

To conclude this section, the advantages of fractional models in modeling viscoelastic material behavior are discussed by the example of the given con-

crete creep data. As mentioned earlier, if creep or relaxation data are well represented by a fractional model, an alternative modeling by spring-dashpot networks would require a large amount of parameters for a good fitting, which is inconvenient. Moreover, an extrapolation of the material behavior outside the measured time range is impossible with spring-dashpot models. Both effects occur due to the short time-range in which exponential functions grow. To illustrate these arguments, the creep data of M2 are used once again for a model calibration. This time, the results for three different constitutive models are compared. Consider a generalized Zener model with one or three Kelvin elements for hydrostatic and deviatoric stress and strain components (six or fourteen parameters) and, alternatively, as above a fractional Zener model for each component (eight parameters). For the parameter identification, only the data of the first ten days are considered. The results are shown in Figure 4.15. As conjectured above, the Zener model with one Kelvin element yields a limited curve fitting for the first ten days and a poor extrapolation, whereas the Zener model with three Kelvin elements leads to a good fit for small time ranges but a bad extrapolation, too. The fractional Zener model shows a good fit and a much better extrapolation (which is yet not as good as in Figure 4.14 because of the narrow time range for fitting) with comparatively few parameters.

4.4 Mechanical representation of springpots

Although mechanical network models consisting of springs and dashpots restrict viscoelastic constitutive laws to discrete spectra, they allow at least for a mechanical interpretation and provide simple representations of stored and dissipated energy. It will be shown hereafter that a springpot can be interpreted as a generalized Maxwell model with an infinite number of parallel Maxwell elements, see Hinze et al. (2018, 2020b) and similarly Schiessel and Blumen (1993); Papoulia et al. (2010). This derivation yields three new insights. First, it reveals the similarity and differences of fractional and mechanical network models, second, it provides a mechanical interpretation of the infinite state representation, and, third, it leads to a potential energy expression of a springpot, which will be used in Chapter 5.

For the generalized Maxwell model in Figure 4.16, consider the stress $\sigma(t)$ to result from a stress distribution $g(\lambda, t)\mathrm{d}\lambda$, $\lambda \in (0, \infty)$, allocated to the individual Maxwell elements such that

$$\sigma(t) = \int_0^\infty g(\lambda, t)\mathrm{d}\lambda. \tag{4.74}$$

The springs of the Maxwell elements are characterized by their strain $\varepsilon_{\mathrm{sp}}(\lambda, t)$ together with their distributed modulus $E(\lambda)\mathrm{d}\lambda$ and the dashpots by the strain

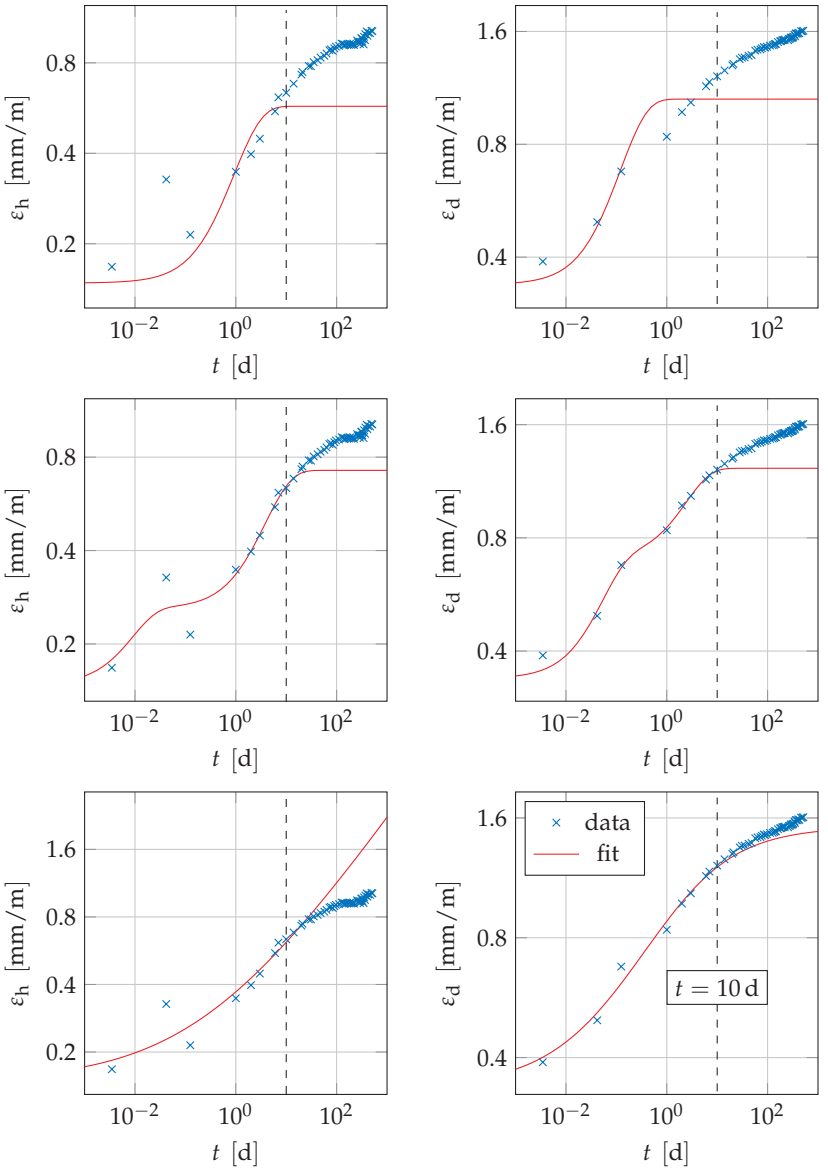

Figure 4.15: Fit of concrete creep data using a generalized Zener model with one (top) or three (middle) Kelvin elements and a fractional Zener model (bottom). Only the first ten days have been considered for fitting.

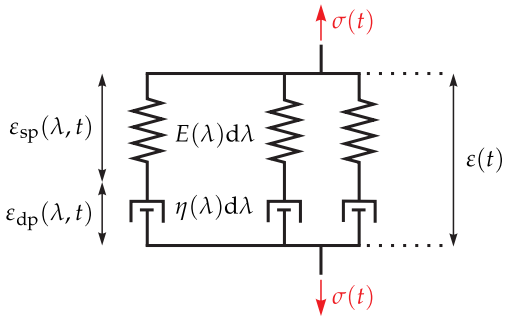

Figure 4.16: Schematic mechanical representation of a springpot.

$\varepsilon_{dp}(\lambda,t)$ together with the distributed viscosity $\eta(\lambda)d\lambda$ such that the entire strain $\varepsilon(t)$ of the network appears as

$$\varepsilon(t) = \varepsilon_{sp}(\lambda,t) + \varepsilon_{dp}(\lambda,t), \quad \lambda > 0. \tag{4.75}$$

The stress density is thereby related to the internal strains by the constitutive laws

$$g(\lambda,t)d\lambda = E(\lambda)d\lambda\,\varepsilon_{sp}(\lambda,t) = \eta(\lambda)d\lambda\,\dot{\varepsilon}_{dp}(\lambda,t). \tag{4.76}$$

Differentiation of (4.75) and substitution of (4.76) leads to

$$\frac{\dot{g}(\lambda,t)}{E(\lambda)} = \dot{\varepsilon}(t) - \frac{g(\lambda,t)}{\eta(\lambda)}. \tag{4.77}$$

Comparison of (4.74) and (4.77) to the infinite state representation of the springpot

$$\begin{aligned} \sigma(t) &= p\int_0^\infty \mu_{1-\alpha}(\lambda)z(\lambda,t)d\lambda, \\ \dot{z}(\lambda,t) &= \dot{\varepsilon}(t) - \lambda z(\lambda,t), \quad \lambda > 0, \end{aligned}$$

results in the identification

$$\begin{aligned} g(\lambda,t) &= p\mu_{1-\alpha}(\lambda)z(\lambda,t), \quad E(\lambda) = p\mu_{1-\alpha}(\lambda), \\ \eta(\lambda) &= \frac{p\mu_{1-\alpha}(\lambda)}{\lambda}, \quad \lambda = \frac{E(\lambda)}{\eta(\lambda)}. \end{aligned} \tag{4.78}$$

Furthermore, one obtains using (4.78) and (4.76) an interpretation of the infinite states $z(\lambda,t)$ of the springpot as the strain of the internal springs, since

$$z(\lambda,t) = \frac{g(\lambda,t)}{p\mu_{1-\alpha}(\lambda)} = \frac{g(\lambda,t)}{E(\lambda)} = \varepsilon_{sp}(\lambda,t). \tag{4.79}$$

As the potential energy E_{pot} of the generalized Maxwell element is given by the energy stored in its springs, i.e.,

$$E_{\text{pot}}(t) = \frac{1}{2}\int_0^\infty E(\lambda)\varepsilon_{\text{sp}}^2(\lambda,t)\mathrm{d}\lambda,$$

the potential energy of the springpot is in view of (4.78) and (4.79) given by

$$E_{\text{pot}}(t) = \frac{p}{2}\int_0^\infty \mu_{1-\alpha}(\lambda)z^2(\lambda,t)\mathrm{d}\lambda. \tag{4.80}$$

The above representation relates springpots and mechanical spring-dashpot networks. The crucial difference between both types of models is the infinite number of states for springpots leading to distributed stiffness ($E(\lambda)$) and viscosity ($\eta(\lambda)$) quantities, which is related to continuous relaxation and retardation spectra, whereas spring-dashpot networks only have a finite number of internal states (e.g. the strains of a finite number of springs) governed by discrete stiffness and viscosity parameters. The awareness of this difference reveals a great advantage of fractional constitutive models as discussed in Section 4.3.

The benefit of fractional viscoelastic models is accompanied by a more sophisticated analysis and associated computational methods. This fact demands for a generalization of many aspects in viscoelastic material description. Two of those are considered in the following chapters, namely the stability of mechanical systems with fractional damping (Chapter 5) and the (numerical) solution of boundary value problems for arbitrarily shaped viscoelastic bodies within the finite element method (Chapter 6). The methods developed by the author for both aspects are based on the (reformulated) infinite state representation of fractional derivatives.

CHAPTER 5

Stability and the direct method of Lyapunov

The following chapter is concerned with a generalization of the well-known direct method of Lyapunov (1892) for dynamical systems with fractional damping. The reader is guided by classical results for ordinary differential equations (ODEs) and known generalizations for functional differential equations (FDEs). It is shown that fractionally damped (mechanical) systems represent a special class of FDEs and certain Lyapunov functionals for different stability statements are presented.

5.1 Ordinary differential equations

Basic properties and stability

An *ordinary differential equation (ODE)* is given by

$$\dot{\mathbf{x}} = \mathbf{f}(t, \mathbf{x}), \tag{5.1}$$

where $\mathbf{f} : D \to \mathbb{R}^n$ is a continuous function defined on an open subset $D \subset \mathbb{R}^{n+1}$, $n \in \mathbb{N}$. The variable t is usually referred to as *time* and $\mathbf{x}$ denotes the *state* representing certain quantities of a physical system. Given an *initial value* $\mathbf{x}_0$ at time t_0 such that $(t_0, \mathbf{x}_0) \in D$, a function $\mathbf{x} : [0, T) \to \mathbb{R}^n$ is called a *solution* of (5.1) with initial value

$$\mathbf{x}(t_0) = \mathbf{x}_0\,, \tag{5.2}$$

if it fulfills (5.2) and (5.1) on a subset $[0, T) \times B \subset D$ for a neighborhood $B \subset \mathbb{R}^n$ of $\mathbf{x}_0$, $0 \leq t_0 < T$. In order to explicitly indicate the initial conditions of a solution, the notation $\mathbf{x}(t) = \mathbf{x}(t, t_0, \mathbf{x}_0)$ is sometimes used. An introduction to ODEs can be found e.g. in the books of Hirsch and Smale (1974); Burton (2005); Khalil (2002). Therein, classical results regarding existence, uniqueness and continuous dependence on initial conditions can be found, which are summarized in the following theorems.

Section 5.3 and Section 5.4 are based on Hinze et al. (2020a,b).

Theorem 5.1 (Existence and Uniqueness). *Let $\mathbf{f} : D \to \mathbb{R}^n$ be a continuous function that fulfills a local Lipschitz condition w.r.t. the second argument, i.e., for each compact subset $K \subset D$ there exists an $L > 0$ such that for all $(t, \mathbf{x})$, $(t, \mathbf{y}) \in K$*

$$\|\mathbf{f}(t, \mathbf{x}) - \mathbf{f}(t, \mathbf{y})\|_2 \leq L\|\mathbf{x} - \mathbf{y}\|_2 .$$

Then there exists one and only one solution of the initial value problem (5.1), (5.2) *at least for $t \in [t_0, t_0 + \delta]$ for some $\delta > 0$.*

Proof. One possible proof uses Picard's successive approximations of the equivalent integral equation

$$\mathbf{x}(t) = \mathbf{x}_0 + \int_{t_0}^{t} \mathbf{f}(\tau, \mathbf{x}(\tau))\mathrm{d}\tau$$

given by

$$\begin{aligned} \mathbf{x}_1(t) &= \mathbf{x}_0, \\ \mathbf{x}_{m+1}(t) &= \mathbf{x}_0 + \int_{t_0}^{t} \mathbf{f}(\tau, \mathbf{x}_m(\tau))\mathrm{d}\tau \quad m = 1, 2, \dots . \end{aligned} \tag{5.3}$$

The Lipschitz condition renders the mapping

$$\mathbf{T}(\mathbf{x}) := \mathbf{x}_0 + \int_{t_0}^{t} \mathbf{f}(\tau, \mathbf{x}(\tau))\mathrm{d}\tau$$

contractive for $t \geq t_0$ small enough, where $\mathbf{T}$ is defined on a space of continuous functions together with the uniform norm $\|\cdot\|_\infty$. Indeed, one obtains

$$\begin{aligned} \|\mathbf{T}(\mathbf{x}) - \mathbf{T}(\mathbf{y})\|_\infty &= \sup_{t \in [t_0, t_0+\delta]} \left\| \int_{t_0}^{t} \mathbf{f}(\tau, \mathbf{x}(\tau))\mathrm{d}\tau - \int_{t_0}^{t} \mathbf{f}(\tau, \mathbf{y}(\tau))\mathrm{d}\tau \right\|_2 \\ &\leq \sup_{t \in [t_0, t_0+\delta]} \int_{t_0}^{t} \|\mathbf{f}(\tau, \mathbf{x}(\tau)) - \mathbf{f}(\tau, \mathbf{y}(\tau))\|_2 \,\mathrm{d}\tau \\ &\leq \sup_{t \in [t_0, t_0+\delta]} L \int_{t_0}^{t} \|\mathbf{x}(\tau) - \mathbf{y}(\tau)\|_2 \,\mathrm{d}\tau \leq \delta L \|\mathbf{x} - \mathbf{y}\|_\infty \end{aligned}$$

such that the choice $\delta < \frac{1}{L}$ yields contractivity. According to Banach's fixed point theorem, the iteration (5.3) has a unique fixed point, which completes the proof. □

Remark 5.2. If it is additionally known that solutions of (5.1), (5.2) lie entirely in a compact set $K \ni (t_0, \mathbf{x}_0)$, then there exists a unique solution for all $t \geq t_0$, see Khalil (2002, Thm. 3.3).

Theorem 5.3 (Continuous dependence on initial conditions)**.** *Let* $\mathbf{f}$ *fulfill the conditions in Theorem 5.1 with a uniform Lipschitz constant* $L > 0$*. For two solutions* $\mathbf{x}(t, t_0, \mathbf{x}_0)$ *and* $\mathbf{y}(t, t_0, \mathbf{y}_0)$ *of the initial value problem, the inequality*

$$\|\mathbf{x}(t) - \mathbf{y}(t)\|_2 \leq \|\mathbf{x}_0 - \mathbf{y}_0\|_2 \, \mathrm{e}^{L(t-t_0)}$$

holds for $t \geq t_0$ *as long as the solutions exist.*

Proof. The Lipschitz condition and Gronwall's lemma yield the proof. □

The properties mentioned in the above theorems are essential for an ODE to represent a useful mathematical description of a deterministic physical system as identical initial conditions have to lead to a reproducible evolution of system states and arbitrarily small changes of the initial data should not result in an immediate large deviation of solutions. A question associated to a much stronger condition than continuous dependence on initial conditions is, whether solutions starting nearby will remain nearby for all future times. Such a property usually only holds for certain distinguished solutions and is denoted by the term *stability*. When there exist *stable* solutions, then the qualitative behavior of the system (5.1) is mainly determined by them, making stability an important attribute. For a definition of stability, consider a solution $\bar{\mathbf{x}}(t)$ of (5.1) existing in $[0, \infty)$ such that a neighborhood

$$[0, \infty) \times Q_H := \{(t, x) \,|\, t \geq 0, \, \|\mathbf{x} - \bar{\mathbf{x}}(t)\|_2 < H\}, \quad H > 0$$

of the solution is contained in D.

Definition 5.4 (Stability)**.** The solution $\bar{\mathbf{x}}(t)$ is called *stable*, if for all $\varepsilon > 0$ and all $t_0 \in [0, \infty)$ there exists a $\delta = \delta(\varepsilon, t_0) > 0$ such that for all $t \geq t_0$

$$\|\mathbf{x}_0 - \bar{\mathbf{x}}(t_0)\|_2 < \delta \quad \Rightarrow \quad \|\mathbf{x}(t, t_0, \mathbf{x}_0) - \bar{\mathbf{x}}(t)\|_2 < \varepsilon.$$

If $\bar{\mathbf{x}}(t)$ is not stable, it is called *unstable*.

When solutions do not only remain nearby $\bar{\mathbf{x}}(t)$ but approach it for $t \to \infty$, the following term is used.

Definition 5.5 (Asymptotic stability)**.** The solution $\bar{\mathbf{x}}(t)$ is called *(locally) asymptotically stable*, if it is stable and for all $t_0 \in [0, \infty)$ there is a $\gamma = \gamma(t_0) > 0$ such that for $\mathbf{x}_0$ with $\|\mathbf{x}_0 - \bar{\mathbf{x}}(t_0)\|_2 < \gamma$, the solution $\mathbf{x}(t, t_0, \mathbf{x}_0)$ exists for all $t \geq t_0$ and it holds that

$$\lim_{t \to \infty} \|\mathbf{x}(t, t_0, \mathbf{x}_0) - \bar{\mathbf{x}}(t)\|_2 = 0.$$

The set of all $\mathbf{x}_0 \in \mathbb{R}^n$ with the above property is called the *domain of attraction* (depending on t_0). When this domain is the entire $\mathbb{R}^n$, $\bar{\mathbf{x}}(t)$ is called *globally asymptotically stable*.

Remark 5.6. Equivalently, asymptotic stability can be characterized by the following statement: For all $t_0 \geq 0$, there exists $\gamma = \gamma(t_0) > 0$ and, for all $\varepsilon > 0$ and a given $\mathbf{x}_0$, there exists $T = T(\varepsilon, t_0, \mathbf{x}_0)$ such that

$$\|\mathbf{x}_0 - \bar{\mathbf{x}}(t_0)\|_2 < \gamma \quad \Rightarrow \quad \|\mathbf{x}(t, t_0, \mathbf{x}_0) - \bar{\mathbf{x}}(t)\|_2 < \varepsilon \text{ for all } t > t_0 + T. \tag{5.4}$$

In general, δ in Definition 5.4 and γ and T in (5.4) cannot be chosen independently of t_0 and $\mathbf{x}_0$. If this is the case though, stronger stability notions arise. If δ in Definition 5.4 is independent of t_0, $\bar{\mathbf{x}}(t)$ is called *uniformly stable*. If, additionally, γ and T in (5.4) are independent of t_0 and $\mathbf{x}_0$, then $\bar{\mathbf{x}}(t)$ is called *uniformly asymptotically stable*.

Especially interesting is the stability of constant solutions of (5.1), called *equilibria*, that fulfill $\bar{\mathbf{x}}(t) \equiv \mathbf{x}^*$ and hence $\mathbf{f}(t, \mathbf{x}^*) = \mathbf{0}$ for all $t \geq 0$. Particularly, the stability of a special solution $\bar{\mathbf{x}}(t)$ is related to the stability of the zero solution, often called *trivial equilibrium*, of a translated ODE. To see this, consider the translation

$$\mathbf{y}(t) := \mathbf{x}(t) - \bar{\mathbf{x}}(t)$$

in (5.1), leading to

$$\dot{\mathbf{y}} = \mathbf{f}(t, \mathbf{y} + \bar{\mathbf{x}}(t)) - \mathbf{f}(t, \bar{\mathbf{x}}(t)) =: \tilde{\mathbf{f}}(t, \mathbf{y}). \tag{5.5}$$

The definition of $\tilde{\mathbf{f}}$ in (5.5) directly yields $\tilde{\mathbf{f}}(t, \mathbf{0}) = \mathbf{0}$ for all $t \geq 0$ such that (5.5) has the zero solution as equilibrium which is (asymptotically) stable if and only if the solution $\bar{\mathbf{x}}(t)$ of (5.1) is (asymptotically) stable. Therefore, all conditions for stability given in the rest of this chapter are related to the trivial equilibrium. The formulation of stability criteria is the major aim in the following paragraphs and the conditions strongly depend on whether the function $\mathbf{f}$ in (5.1) is explicitly time-dependent. If this is the case, (5.1) is called *nonautonomous*, whereas the system

$$\dot{\mathbf{x}} = \mathbf{f}(\mathbf{x}) \tag{5.6}$$

is called *autonomous*. Particularly, if (5.6) has an equilibrium $\mathbf{x}^*$, the translated system (5.5) with $\mathbf{y} = \mathbf{x} - \mathbf{x}^*$ is still autonomous and has the trivial solution as equilibrium. The current part is concluded with a simple mechanical example.

Example 5.7. Consider a weakly damped harmonic oscillator (with mass $m > 0$, damping coefficient d, stiffness $k > \frac{d^2}{4m}$), see Figure 5.1, which is through Newton's law given by the equation of motion

$$m\ddot{q} + d\dot{q} + kq = 0, \tag{5.7}$$

where q is the position of the mass. Equation (5.7) is equivalent to the linear

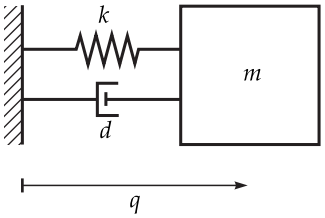

Figure 5.1: Damped harmonic oscillator.

autonomous ODE

$$\dot{\mathbf{x}} = \mathbf{A}\mathbf{x}, \quad \mathbf{A} = \begin{bmatrix} 0 & 1 \\ -\frac{k}{m} & -\frac{d}{m} \end{bmatrix}, \quad \mathbf{x} = \begin{bmatrix} q \\ \dot{q} \end{bmatrix} \tag{5.8}$$

whose solution is given by

$$\begin{aligned} \mathbf{x}(t, t_0, \mathbf{x}_0) &= \mathrm{e}^{\gamma(t-t_0)} \left(\cos(\omega(t-t_0)) + \mathbf{C}\sin(\omega(t-t_0))\right) \mathbf{x}_0\,, \\ \gamma = -\frac{d}{2m}\,, \quad \omega^2 &= \frac{k}{m} - \gamma^2 > 0, \quad \mathbf{C} = -\mathbf{C}^{-1} = \frac{1}{\omega}(\mathbf{A} - \gamma\mathbf{I}). \end{aligned} \tag{5.9}$$

As the trigonometric terms in (5.9) are bounded, it follows immediately from the asymptotic behavior of the exponential function that the trivial solution of (5.8) is stable for $\gamma \leq 0$ and even asymptotically stable for $\gamma < 0$.

The direct method of Lyapunov for nonautonomous systems

For a general (nonlinear) ODE (5.1), it is usually not possible to analytically determine solutions as in Example 5.7 and thereby obtain a stability statement. An approach that provides sufficient conditions for (asymptotic) stability for which it is not necessary to know the solutions in closed form has been introduced by Lyapunov (1892) and is known as the *direct method of Lyapunov*. It uses the properties of so-called *Lyapunov functions* to prove (uniform asymptotic) stability of the trivial equilibrium (i.e., assume $\mathbf{f}(t, \mathbf{0}) \equiv \mathbf{0}$) as given by the following theorem, see e.g. Burton (2005, Chap. 6); Hahn (1967, § 42); Khalil (2002, Chap. 4.5); Slotine and Li (1991, Chap. 4.2).

Theorem 5.8 (Direct method of Lyapunov)**.** *Let* $\mathbf{f} : D \to \mathbb{R}^n$ *in* (5.1) *be such that* $[0, \infty) \times Q_H \subset D$ *and* $\mathbf{f}(t, \mathbf{0}) = \mathbf{0}$ *for* $t \geq 0$*. Denote* $u_i : [0, \infty) \to [0, \infty)$*,* $i = 1, 2, 3$ *some scalar, continuous, strictly increasing functions such that* $u_i(0) = 0$ *and* $u_i(r) > 0$ *for* $r > 0$*. If there exists a continuously differentiable function* $V : [0, \infty) \times \bar{Q}_H \to \mathbb{R}$*,*

$V(t, \mathbf{0}) \equiv 0$ *such that*

$$u_1(\|\mathbf{x}\|_2) \leq V(t, \mathbf{x}) \leq u_2(\|\mathbf{x}\|_2), \tag{5.10}$$

$$\dot{V}(t, \mathbf{x}) = \frac{\partial V}{\partial t} + \frac{\partial V}{\partial \mathbf{x}} \cdot \mathbf{f}(t, \mathbf{x}) \leq 0 \tag{5.11}$$

for all $t \geq 0$, $\mathbf{x} \in Q_H$, *then the trivial solution of* (5.1) *is uniformly stable. If additionally*

$$\dot{V}(t, \mathbf{x}) \leq -u_3(\|\mathbf{x}\|_2) \tag{5.12}$$

holds for all $t \geq 0$, $\mathbf{x} \in Q_H$, *then the trivial solution of* (5.1) *is uniformly asymptotically stable. Moreover, if* $Q_H = \mathbb{R}^n$ *and*

$$u_1(r) \to \infty \text{ for } r \to \infty, \tag{5.13}$$

the trivial solution is globally uniformly asymptotically stable.

Remark 5.9.

a) The function V is called *Lyapunov function*. The left-hand inequality in (5.10) is defined as *positive definiteness* of V, the right-hand inequality makes V *decrescent*. The total time derivative of V can be expressed as in (5.11) using the dynamics (5.1). The inequality (5.11) reveals that V is nonincreasing along solutions of (5.1). If the stronger condition (5.12) holds, $\dot{V}$ is called *negative definite*. The statement (5.13) renders V *radially unbounded*.

b) The conditions in Theorem 5.8 reveal that the direct method of Lyapunov uses certain storage and comparison functions for a stability proof but no explicit information about solutions of (5.1).

c) If the function V can be chosen to be not explicitly time-dependent and fulfills $V(\mathbf{0}) = 0$, $V(\mathbf{x}) > 0$ for $\mathbf{x} \in Q_H \backslash \mathbf{0}$, then (5.10) is automatically fulfilled.

Proof. The left-hand relation in (5.10) together with (5.11) are sufficient for stability. To see this, given $\varepsilon \in (0, H]$ and $t_0 \geq 0$, choose $\delta > 0$ such that $\|\mathbf{x}_0\|_2 < \delta$ implies $V(t_0, \mathbf{x}_0) < u_1(\varepsilon)$. (This is possible as V is continuous and $V(t_0, \mathbf{0}) = 0$). This results for $\mathbf{x}(t) = \mathbf{x}(t, t_0, \mathbf{x}_0)$ in

$$u_1(\|\mathbf{x}(t)\|_2) \leq V(t, \mathbf{x}(t)) \leq V(t_0, \mathbf{x}_0) < u_1(\varepsilon)$$

and hence $\|\mathbf{x}(t)\|_2 < \varepsilon$.

For uniform stability and a given $\varepsilon \in (0, H]$, select $\delta > 0$ small enough such that $u_2(\delta) < u_1(\varepsilon)$. For $t_0 \geq 0$, $\|\mathbf{x}_0\|_2 < \delta$ and $\mathbf{x}(t) = \mathbf{x}(t, t_0, \mathbf{x}_0)$, $t \geq t_0$, one obtains

$$u_1(\|\mathbf{x}(t)\|_2) \leq V(t, \mathbf{x}(t)) \leq V(t_0, \mathbf{x}_0) \leq u_2(\|\mathbf{x}_0\|_2) < u_2(\delta) < u_1(\varepsilon)$$

or $\|\mathbf{x}(t)\|_2 < \varepsilon$.

To prove uniform asymptotic stability, let $\|\mathbf{x}_0\|_2 < \gamma$, with γ obtained from a uniform stability estimation, i.e., $u_2(\gamma) < u_1(\rho)$ for some $\rho > 0$. Let $\varepsilon \in (0, \gamma)$ and find a $\delta = \delta(\varepsilon)$ such that $u_2(\delta) < u_1(\varepsilon)$. Define

$$T := \frac{u_2(\gamma)}{u_3(\delta)}$$

and assume that $\|\mathbf{x}(t)\|_2 > \delta$ for all $t \in [t_0, t_0 + T]$. Then, one obtains

$$\begin{aligned} 0 < u_1(\delta) \leq V(t_0 + T, \mathbf{x}(t_0 + T)) &\leq V(t_0, \mathbf{x}_0) - \int_{t_0}^{t_0+T} u_3(\|\mathbf{x}(s)\|_2)\mathrm{d}s \\ &\leq V(t_0, \mathbf{x}_0) - u_3(\delta)T \\ &\leq u_2(\gamma) - u_3(\delta)T = 0, \end{aligned}$$

which is a contradiction. Hence, there must exist $t_* \in [t_0, t_0 + T]$ such that $\|\mathbf{x}(t_*)\|_2 \leq \delta$ and thus for all $t \geq t_*$

$$u_1(\|\mathbf{x}(t)\|_2) \leq V(t, \mathbf{x}(t)) \leq V(t_*, \mathbf{x}(t_*)) \leq u_2(\delta) < u_1(\varepsilon)$$

which finally results in $\|\mathbf{x}(t)\|_2 < \varepsilon$ for $t \geq t_0 + T \geq t_*$.

If u_1 is additionally radially unbounded, ρ can be found such that an inequality $u_2(\gamma) < u_1(\rho)$ used in the steps above can be fulfilled for any $\gamma > 0$ and γ can be made arbitrarily large leading to global uniform asymptotic stability. □

A problem regarding the direct method of Lyapunov is that there does not exist a general technique for construction of Lyapunov functions and finding such a function is difficult for many applications. Particularly, to prove asymptotic stability, the requirement (5.12) in Theorem 5.8 is often difficult to meet. There are large classes of systems though, for which weaker conditions are sufficient for asymptotic stability, as will be shown in the following.

LaSalle's invariance principle for autonomous systems

For autonomous ODEs (5.6) with $\mathbf{f}$ defined on a neighborhood $B \subset \mathbb{R}^n$, $Q_H \subset B$, fulfilling a Lipschitz condition and $\mathbf{f}(\mathbf{0}) = \mathbf{0}$, the assumptions in Theorem 5.8 can be weakened. To this end, the notion of *invariant sets* is introduced. Previously note that a solution of (5.6) with (5.2) does not explicitly depend on the initial time t_0 but on the time lapse $t - t_0$ passed. Hence, without loss of generality, choose $t_0 = 0$ and denote the solution $\mathbf{x}(t, \mathbf{x}_0)$ instead of $\mathbf{x}(t, 0, \mathbf{x}_0)$. This implies the relation

$$\mathbf{x}(t, t_0, \mathbf{x}_0) = \mathbf{x}(t - t_0, \mathbf{x}_0) \text{ for } t \geq t_0 \text{ and } \mathbf{x}_0 \in B.$$

Definition 5.10. Let $\mathbf{x}(t) = \mathbf{x}(t, \mathbf{x}_0)$ be a solution of (5.6) existing for $t \in \mathbb{R}$.

a) A point $\mathbf{p}$ is called *positive limit point* of $\mathbf{x}(t)$, if there exists a nonnegative sequence $\{t_n\}_{n\in\mathbb{N}}$ with $t_n \to \infty$ as $n \to \infty$ such that

$$\lim_{n\to\infty} \|\mathbf{x}(t_n) - \mathbf{p}\|_2 = 0.$$

b) The set $\Omega(\mathbf{x})$ of all positive limit points of $\mathbf{x}(t)$ is called *positive limit set*.

c) A set $Q \subset \mathbb{R}^n$ is called *(positively) invariant*, if $\mathbf{x}(t, \mathbf{x_0}) \in Q$ for all $\mathbf{x}_0 \in Q$ and all ($t \geq 0$ resp.) $t \in \mathbb{R}$.

The following theorem according to LaSalle (1968) uses certain properties of invariant sets to prove asymptotic stability.

Theorem 5.11 (Invariance principle)**.** *Let $V : \bar{Q}_H \to \mathbb{R}$ be a continuously differentiable function such that $\dot{V}(\mathbf{x}) \leq 0$ in $\bar{Q}_H$. Let*

$$E := \{\mathbf{x} \in \bar{Q}_H \mid \dot{V}(\mathbf{x}) = 0\}$$

and M be the largest invariant set in E. Then every bounded solution $\mathbf{x}(t)$ of (5.6) *starting and existing in Q_H for $t \geq 0$ approaches M for $t \to \infty$, i.e.,*

$$\lim_{t\to\infty} \operatorname{dist}(\mathbf{x}(t), M) = 0.$$

To prove the invariance principle, a fundamental property of limit sets formulated in the following proposition is needed. The proof (of the proposition) is given by Khalil (2002, App. C.3).

Proposition 5.12. *Let $\mathbf{x}(t)$ be a bounded solution of* (5.6) *belonging to Q_H. The positive limit set $\Omega(\mathbf{x})$ is a nonempty, compact, invariant set and $\mathbf{x}(t)$ approaches $\Omega(\mathbf{x})$, i.e.,*

$$\lim_{t\to\infty} \operatorname{dist}(\mathbf{x}(t), \Omega(\mathbf{x})) = 0.$$

Proof of Theorem 5.11. Let $\mathbf{x}(t)$ be a solution of (5.6) starting and existing in Q_H for $t \geq 0$. As $\dot{V}(\mathbf{x}) \leq 0$ in $\bar{Q}_H$, $V(\mathbf{x}(t))$ is a continuous, decreasing function of time, defined on a compact set $\bar{Q}_H$. It is bounded from below and therefore has a limit $V(\mathbf{x}(t)) \to c$ for $t \to \infty$. The positive limit set $\Omega(\mathbf{x})$ (which is nonempty according to Proposition 5.12) is in $\bar{Q}_H$ and for any $\mathbf{p} \in \Omega(\mathbf{x})$, there is a sequence t_n with $t_n \to \infty$ and $\mathbf{x}(t_n) \to \mathbf{p}$ as $n \to \infty$. As V is continuous,

$$V(\mathbf{p}) = \lim_{n\to\infty} V(\mathbf{x}(t_n)) = c,$$

i.e., $V(\mathbf{x}) = c$ in $\Omega(\mathbf{x})$. Since $\Omega(\mathbf{x})$ is invariant due to Proposition 5.12, $\dot{V}(\mathbf{x}) = 0$ in $\Omega(\mathbf{x})$ and hence $\Omega(\mathbf{x}) \subset M \subset E$. Finally, as $\mathbf{x}(t)$ approaches $\Omega(\mathbf{x})$ for $t \to \infty$, it has to approach M. □

A special case in Theorem 5.11 leads to a variation of Theorem 5.8 with weaker assumptions to prove asymptotic stability of the trivial equilibrium.

Corollary 5.13. *Let* $\mathbf{f}(\mathbf{0}) = \mathbf{0}$ *and* $V : \bar{Q}_H \to \mathbb{R}$ *be a continuously differentiable function such that*

$$V(\mathbf{0}) = 0 \text{ and } V(\mathbf{x}) > 0 \text{ for } \mathbf{x} \in \bar{Q}_H \backslash \mathbf{0},$$
$$\dot{V}(\mathbf{x}) \leq 0 \text{ for } \mathbf{x} \in \bar{Q}_H .$$

If $M = \{\mathbf{0}\}$ *is the largest invariant set in* E *(as defined in Theorem 5.11), then the trivial equilibrium is asymptotically stable. If* V *is defined on* $\mathbb{R}^n$ *and* $V(\mathbf{x}) \to \infty$ *for* $\|\mathbf{x}\|_2 \to \infty$*, then the trivial equilibrium is globally asymptotically stable.*

Proof. Stability of $\mathbf{x} \equiv \mathbf{0}$ follows from Theorem 5.8. Particularly, if $\mathbf{x}_0$ is sufficiently small, $\mathbf{x}(t)$ exists for $t \geq 0$, is bounded and approaches M according to Theorem 5.11. The global statement follows using the same argument as in the proof of Theorem 5.8. □

Example 5.14. Revisit the weakly damped harmonic oscillator from Example 5.7 and consider the Lyapunov function

$$V(\mathbf{x}) = \frac{1}{2}\left(k + \frac{d^2}{2m}\right) x_1^2 + \frac{d}{2} x_1 x_2 + \frac{m}{2} x_2^2 = \frac{k}{2} x_1^2 + \frac{m}{4} x_2^2 + \left(\frac{d}{2\sqrt{m}} x_1 + \frac{\sqrt{m}}{2} x_2\right)^2$$

being positive definite and radially unbounded. Its time-derivative along solutions fulfills

$$\begin{aligned}
\dot{V} &= \left(k + \frac{d^2}{2m}\right) x_1 \dot{x}_1 + \frac{d}{2}(\dot{x}_1 x_2 + x_1 \dot{x}_2) + m x_2 \dot{x}_2 \\
&= \left(k + \frac{d^2}{2m}\right) x_1 x_2 + \frac{d}{2}\left(x_2^2 + x_1\left(-\frac{k}{m} x_1 - \frac{d}{m} x_2\right)\right) - k x_1 x_2 - d x_2^2 \\
&= -\frac{k}{m} x_1^2 - \frac{d}{2} x_2^2 ,
\end{aligned}$$

i.e., $\dot{V}$ is negative definite for $d > 0$ such that all conditions in Theorem 5.8 are fulfilled and the trivial solution is globally asymptotically stable. The above Lyapunov function is derived from another, more natural Lyapunov function, namely the total mechanical energy of the system

$$V_{\text{mech}}(\mathbf{x}) = \frac{k}{2} x_1^2 + \frac{m}{2} x_2^2$$

with derivative

$$\dot{V}_{\text{mech}} = -d x_2^2 \leq 0.$$

Although $\dot{V}_{\text{mech}}$ is not negative definite, no other solution than the trivial equilibrium remains in the set $E = \{\mathbf{x} \in \mathbb{R}^2 \mid x_2 = 0\}$ and Corollary 5.13 yields global asymptotic stability.

The examples considered so far deal with linear autonomous systems

$$\dot{\mathbf{x}} = \mathbf{A}\mathbf{x}. \tag{5.14}$$

For ODEs of the form (5.14), there exists a methodology to find Lyapunov functions which can be generalized for certain nonlinear systems as shown below. Consider the general solution

$$\mathbf{x}(t, t_0, \mathbf{x}_0) = \exp(\mathbf{A}(t - t_0))\mathbf{x}_0$$

of (5.14), which can be expressed in terms of the eigenvalues λ_j, $j = 1, \dots, k$ with algebraic multiplicity μ_j and generalized eigenvectors $\mathbf{z}_j$, $j = 1, \dots, k$ of the matrix $\mathbf{A} \in \mathbb{R}^{n \times n}$ as

$$\mathbf{x}(t, t_0, \mathbf{x}_0) = \sum_{j=1}^{k} \mathrm{e}^{\lambda_j (t - t_0)} \sum_{m=0}^{\mu_j - 1} \frac{(t - t_0)^m}{m!} (\mathbf{A} - \lambda_j \mathbf{I})^m \mathbf{z}_j \tag{5.15}$$

such that

$$\mathbf{x}_0 = \sum_{j=1}^{k} \mathbf{z}_j, \quad \mathbf{z}_j \in \operatorname{Ker}(\mathbf{A} - \lambda_j \mathbf{I})^{\mu_j},$$

see Knobloch and Kappel (1974, Chap. II.8). A stability statement can be obtained directly from (5.15) using the properties of the exponential function, see Khalil (2002, Thm. 4.5)

Proposition 5.15. *The trivial equilibrium is stable if and only if all eigenvalues of* $\mathbf{A}$ *satisfy* $\operatorname{Re}(\lambda_j) \leq 0$ *and for every eigenvalue with* $\operatorname{Re}(\lambda_j) = 0$*, algebraic and geometric multiplicity coincide. The trivial equilibrium is globally asymptotically stable if and only if all eigenvalues of* $\mathbf{A}$ *satisfy* $\operatorname{Re}(\lambda_j) < 0$.

A matrix $\mathbf{A}$ for which $\operatorname{Re}(\lambda_j) < 0$ holds for all eigenvalues is called a *Hurwitz matrix*. For this case, a Lyapunov function can be constructed by solving a linear equation.

Proposition 5.16. *A matrix* $\mathbf{A}$ *is Hurwitz if and only if for any given positive definite symmetric matrix* $\mathbf{Q}$ *there exists a positive definite symmetric matrix* $\mathbf{P}$ *such that*

$$\mathbf{A}^{\mathrm{T}}\mathbf{P} + \mathbf{P}\mathbf{A} = -\mathbf{Q} \tag{5.16}$$

holds.

Proof. Consider only the sufficiency part of the proof by Khalil (2002, Thm. 4.6) as it shows the origin of the so-called *Lyapunov equation* (5.16). Let $\mathbf{P}$ positive definite and symmetric be given such that (5.16) is fulfilled for a positive definite symmetric matrix $\mathbf{Q}$. The Lyapunov function

$$V(\mathbf{x}) = \mathbf{x}^{\mathrm{T}}\mathbf{P}\mathbf{x} \geq \lambda_{\min}(\mathbf{P})\|\mathbf{x}\|_2^2$$

is positive definite and radially unbounded as the minimal eigenvalue $\lambda_{\min}(\mathbf{P})$ of $\mathbf{P}$ is positive due to the properties of $\mathbf{P}$. Furthermore, the time-derivative of V along solutions of (5.14) is given by

$$\dot{V} = \dot{\mathbf{x}}^{\mathrm{T}}\mathbf{P}\mathbf{x} + \mathbf{x}^{\mathrm{T}}\mathbf{P}\dot{\mathbf{x}} = \mathbf{x}^{\mathrm{T}}\left(\mathbf{A}^{\mathrm{T}}\mathbf{P} + \mathbf{P}\mathbf{A}\right)\mathbf{x} = -\mathbf{x}^{\mathrm{T}}\mathbf{Q}\mathbf{x} \leq -\lambda_{\min}(\mathbf{Q})\|\mathbf{x}\|_2^2$$

such that $\dot{V}$ is negative definite as $\lambda_{\min}(\mathbf{Q})$ is the minimal eigenvalue of $\mathbf{Q}$ which is positive. Accordingly, Theorem 5.8 yields global asymptotic stability of the trivial equilibrium and, by Proposition 5.15, $\mathbf{A}$ has to be a Hurwitz matrix. □

The idea of solving a Lyapunov equation (5.16) for a stability proof in linear systems does not lead to a computational advantage compared to an eigenvalue analysis according to Proposition 5.15. However, it leads to a stability statement even in the nonlinear case. To see this, consider (5.6) with $\mathbf{f}(\mathbf{0}) = \mathbf{0}$, $\mathbf{f}$ continuously differentiable and study the Taylor expansion

$$\mathbf{f}(\mathbf{x}) = \mathbf{A}\mathbf{x} + \mathbf{g}(\mathbf{x})$$

with the Jacobian matrix

$$\mathbf{A} = \left.\frac{\partial \mathbf{f}}{\partial \mathbf{x}}\right|_{\mathbf{x}=\mathbf{0}} \tag{5.17}$$

and the nonlinear part $\mathbf{g}$ of $\mathbf{f}$ which fulfills

$$\lim_{\|\mathbf{x}\|_2 \to 0} \frac{\|\mathbf{g}(\mathbf{x})\|_2}{\|\mathbf{x}\|_2} = 0,$$

which is equivalent to the statement that for all $\gamma > 0$, there exists $\delta > 0$ such that

$$\|\mathbf{x}\|_2 < \delta \quad \Rightarrow \quad \|\mathbf{g}(\mathbf{x})\|_2 < \gamma\|\mathbf{x}\|_2\,. \tag{5.18}$$

Proposition 5.17. *Let* $\mathbf{f}$ *in* (5.6) *be continuously differentiable and* $\mathbf{f}(\mathbf{0}) = \mathbf{0}$. *The trivial equilibrium is asymptotically stable if the Jacobian matrix* (5.17) *is a Hurwitz matrix.*

Proof. The proof is according to Khalil (2002, Thm. 4.7). As in the proof of Proposition 5.16, choose the Lyapunov function

$$V(\mathbf{x}) = \mathbf{x}^{\mathrm{T}}\mathbf{P}\mathbf{x}$$

with the solution $\mathbf{P}$ of (5.16). The derivative of V along solutions of (5.1) is given by

$$\begin{aligned}\dot{V} &= \dot{\mathbf{x}}^{\mathrm{T}}\mathbf{P}\mathbf{x} + \mathbf{x}^{\mathrm{T}}\mathbf{P}\dot{\mathbf{x}} = [\mathbf{A}\mathbf{x} + \mathbf{g}(\mathbf{x})]^{\mathrm{T}}\mathbf{P}\mathbf{x} + \mathbf{x}^{\mathrm{T}}\mathbf{P}[\mathbf{A}\mathbf{x} + \mathbf{g}(\mathbf{x})] \\ &= \mathbf{x}^{\mathrm{T}}(\mathbf{A}^{\mathrm{T}}\mathbf{P} + \mathbf{P}\mathbf{A})\mathbf{x} + 2\mathbf{x}^{\mathrm{T}}\mathbf{P}\mathbf{g}(\mathbf{x}) = -\mathbf{x}^{\mathrm{T}}\mathbf{Q}\mathbf{x} + 2\mathbf{x}^{\mathrm{T}}\mathbf{P}\mathbf{g}(\mathbf{x})\end{aligned}$$

To estimate the last term, use the Cauchy-Schwarz inequality, the spectral norm

$$\|\mathbf{P}\|_2 := \sup_{\mathbf{x}\neq\mathbf{0}} \frac{\|\mathbf{P}\mathbf{x}\|_2}{\|\mathbf{x}\|_2} = \lambda_{\max}(\mathbf{P})$$

and choose

$$\gamma < \frac{\lambda_{\min}(\mathbf{Q})}{2\lambda_{\max}(\mathbf{P})}$$

in (5.18) to obtain for $\|\mathbf{x}\|_2 < \delta$

$$\begin{aligned}2\mathbf{x}^{\mathrm{T}}\mathbf{P}\mathbf{g}(\mathbf{x}) &\leq 2\,|\mathbf{x}^{\mathrm{T}}\mathbf{P}\mathbf{g}(\mathbf{x})| \\ &\leq 2\|\mathbf{x}\|_2\|\mathbf{P}\mathbf{g}(\mathbf{x})\|_2 \leq 2\|\mathbf{x}\|_2\lambda_{\max}(\mathbf{P})\|\mathbf{g}(\mathbf{x})\|_2 < 2\gamma\lambda_{\max}(\mathbf{P})\|\mathbf{x}\|_2^2\end{aligned}$$

and hence

$$\dot{V} < -\left(\lambda_{\min}(\mathbf{Q}) - 2\gamma\lambda_{\max}(\mathbf{P})\right)\|\mathbf{x}\|_2^2 < 0 \text{ for } \|\mathbf{x}\|_2 < \delta,\ \mathbf{x} \neq \mathbf{0}$$

such that Theorem 5.8 yields (at least local) asymptotic stability of the trivial equilibrium. □

In view of Theorem 5.11, the matrix $\mathbf{Q}$ can even be chosen positive semidefinite to prove global asymptotic stability of the trivial solution, if it is additionally guaranteed that $\{\mathbf{0}\}$ is the largest invariant set in $\{\mathbf{x} \in \mathbb{R}^n \mid \dot{V}(\mathbf{x}) = 0\}$. Further, note that Proposition 5.17 yields a stability statement by an eigenvalue analysis of the Jacobian matrix (if it is a Hurwitz matrix) and no explicit Lyapunov function is required. Proposition 5.17 is known a the *indirect method of Lyapunov*.

Example 5.18. Revisit the Lyapunov function for the weakly damped oscillator in Example 5.14. It has the form

$$V(\mathbf{x}) = \mathbf{x}^{\mathrm{T}}\mathbf{P}\mathbf{x},$$

where

$$\mathbf{P} = \frac{1}{2}\begin{bmatrix} k + \frac{d^2}{2m} & \frac{d}{2} \\ \frac{d}{2} & m \end{bmatrix}$$

is the solution of (5.16) for

$$\mathbf{Q} = \begin{bmatrix} \frac{k}{m} & 0 \\ 0 & \frac{d}{2} \end{bmatrix}.$$

Consider now the oscillator with a cubic spring such that the equation of motion

$$m\ddot{q} + d\dot{q} + k_1 q + k_3 q^3 = 0 \tag{5.19}$$

holds, see Figure 5.2 with mass $m > 0$, damping coefficient $d > 0$, stiffness coefficients $k_1 > 0$, $k_3 < 0$ and position q. The system (5.19) (transformed in first-order

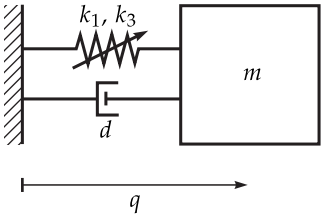

Figure 5.2: Damped nonlinear oscillator with a cubic spring.

form) has three equilibria

$$\mathbf{x}_1^* = \mathbf{0}, \quad \mathbf{x}_{2/3}^* = \begin{pmatrix} \pm\sqrt{\frac{k_1}{-k_3}} \\ 0 \end{pmatrix}.$$

As the linearization of (5.19) at $\mathbf{x}_1^*$ coincides with (5.7), the asymptotic stability result from Example 5.7 and Example 5.14 leads in view of Proposition 5.17 to local asymptotic stability of the trivial equilibrium $\mathbf{x}_1^*$ of (5.19). Nevertheless, another Lyapunov function will be studied here, which again represents the total mechanical energy of the system, viz.

$$V_{\text{mech}}(\mathbf{x}) = \frac{k_1}{2}x_1^2 + \frac{k_3}{4}x_1^4 + \frac{m}{2}x_2^2,$$

which has positive values and is strictly increasing for

$$x_1^2 < \frac{k_1}{-k_3}, \quad \mathbf{x} \neq 0$$

and it holds that

$$V_{\text{mech}}\left(\pm\sqrt{\frac{k_1}{-k_3}}, 0\right) = \frac{k_1^2}{-4k_3}.$$

Accordingly, as

$$\dot{V}_{\text{mech}} = -dx_2^2 \leq 0,$$

the set

$$Q = \left\{ \mathbf{x} \in \mathbb{R}^2 \mid x_1^2 < \frac{k_1}{-k_3},\ V_{\text{mech}}(\mathbf{x}) \leq \frac{k_1^2}{-4k_3} \right\}$$

is bounded, positively invariant and hence, a solution starting in Q approaches the largest invariant set in $E = \{\mathbf{x} \in \mathbb{R}^2 \mid x_2 = 0\}$ from Theorem 5.11, which is $\{\mathbf{0}\}$ as in Example 5.14. This shows another potential of the direct method of Lyapunov, as the set Q represents a conservative estimate of the domain of attraction of the trivial equilibrium, see Figure 5.3.

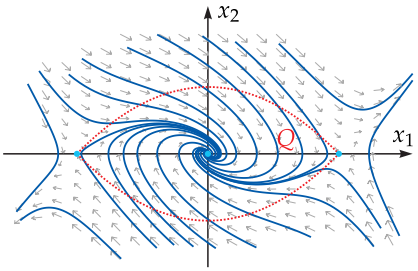

Figure 5.3: Phase portrait with solutions (blue) of (5.19) and a Lyapunov estimate Q of the domain of attraction of the trivial equilibrium (red).

Generalized invariance principle for asymptotically autonomous systems

For the general nonautonomous case, the terms *positive limit point* and *positive limit set* in Definition 5.10 are still well-defined and the positive limit set $\Omega(\mathbf{x})$ of a bounded solution $\mathbf{x}(t)$ is nonempty and compact, whereas the invariance property is lost. This leads to a much weaker assertion according to LaSalle (1968) than the invariance principle in Theorem 5.11.

Theorem 5.19. *Let $V : [0,\infty) \times \bar{Q}_H \to \mathbb{R}$ be a continuously differentiable function such that $V(t,\mathbf{x})$ is bounded from below for all $t \geq 0$ and all $\mathbf{x} \in \bar{Q}_H$ and let there exist a continuous, nonnegative function $W : \bar{Q}_H \to \mathbb{R}$ such that*

$$\dot{V}(t,\mathbf{x}) \leq -W(\mathbf{x}) \text{ for all } t \geq 0,\ \mathbf{x} \in Q_H\,.$$

If, additionally, $\mathbf{f}(t,\mathbf{x})$ is bounded for all $t \geq 0$ and all $\mathbf{x} \in \bar{Q}_H$, then every bounded solution $\mathbf{x}(t)$ of (5.1) *starting and existing in Q_H for $t \geq 0$ approaches the set*

$$E := \{\mathbf{x} \in \bar{Q}_H \mid W(\mathbf{x}) = 0\},$$

i.e., $\Omega(\mathbf{x}) \subset E$.

The following example by Haddock (1997) shows that, in contrast to the autonomous case, solutions do not in general approach the largest invariant set in E.

Example 5.20. Consider the system

$$\begin{aligned}\dot{x}_1 &= x_2\,,\\ \dot{x}_2 &= -x_1 - \left(2+\mathrm{e}^t\right) x_2\,.\end{aligned}$$

For the Lyapunov function

$$V(\mathbf{x}) = \frac{1}{2}x_1^2 + \frac{1}{2}x_2^2$$

one obtains

$$\dot{V}(t,\mathbf{x}) = -\left(2+\mathrm{e}^t\right) x_2^2 \leq -2x_2^2 = -W(\mathbf{x})$$

such that $E = \{\mathbf{x} \in \mathbb{R}^2 \mid x_2 = 0\}$ and the largest set that remains identically in E is $\{\mathbf{0}\}$. However, one solution of the system is given by

$$\mathbf{x}(t) = \left[1+\mathrm{e}^{-t}, -\mathrm{e}^{-t}\right]^{\mathrm{T}}\,,$$

which approaches E but not $\{\mathbf{0}\}$.

If additional assumptions on the time evolution of the function $\mathbf{f}$ in (5.1) are made, an invariance property of the positive limit set can be regained. The most simple situation where this is possible occurs for *asymptotically autonomous* systems as introduced by Markus (1956) and elaborated e.g. by Artstein (1977) and Yoshizawa (1963). The basic idea is that the function $\mathbf{f} = \mathbf{f}(t,\mathbf{x})$ in (5.1) converges in some sense for $t \to \infty$ to a function $\mathbf{f}^*(\mathbf{x})$ independent of time, leading to an autonomous system

$$\dot{\mathbf{x}} = \mathbf{f}^*(\mathbf{x}), \tag{5.20}$$

which is called *limiting equation*. Subsequently, the main result regarding asymptotically autonomous systems is given. It is formulated according to Yoshizawa (1963, Thm. 3) but the convergence of $\mathbf{f}$ to $\mathbf{f}^*$ in the sense of Markus (1956) is used. Generalizations can be found e.g. in the books of LaSalle and Artstein (1976, App. A) and Rouche et al. (1977, Chap. VIII).

Theorem 5.21. *Let* $\mathbf{f}$ *in* (5.1) *and* $\mathbf{f}^*$ *in* (5.20) *be continuous and for each compact set* $K \subset \mathbb{R}^n$ *where* $\mathbf{f}$ *is defined and for each* $\varepsilon > 0$*, there is a* $T(K,\varepsilon) > t_0$ *such that*

$$\|\mathbf{f}(t,\mathbf{x}) - \mathbf{f}^*(\mathbf{x})\|_2 < \varepsilon \;\text{ for all }\; \mathbf{x} \in K,\; t > T.$$

For every bounded solution $\mathbf{x}(t,t_0,\mathbf{x}_0)$ *of* (5.1) *belonging to* Q_H*, the positive limit set* $\Omega(\mathbf{x})$ *is an invariant set of* (5.20)*.*

Corollary 5.22. *Assume the conditions in Theorem 5.19 and Theorem 5.21. Every bounded solution* $\mathbf{x}(t)$ *of* (5.1) *starting and existing in* Q_H *for* $t \geq 0$ *approaches the largest invariant set of* (5.20) *in* E*.*

5.2 Functional differential equations

Basic properties and stability

A natural generalization of ODEs is obtained, when the function $\mathbf{f}$ in (5.1) is in its second argument not defined on a subset of $\mathbb{R}^n$ but on a certain function space. To be more precise, one can consider so-called *retarded functional differential equations (FDEs)*

$$\dot{\mathbf{x}} = \mathbf{f}(t, \mathbf{x}_t), \tag{5.21}$$

where $\mathbf{f} : [0, T) \times B \to \mathbb{R}^n$ for a neighborhood $B \subset X$ is defined on a space X of $\mathbb{R}^n$-valued functions defined on $[-a, 0]$ for some $a \in (0, \infty]$[1] and

$$\mathbf{x}_t(s) := \mathbf{x}(t + s), \quad s \in [-a, 0].$$

As opposed to an ODE for which the initial data are given by an initial point x_0 and initial time $t_0 \in [0, T)$, the initial data of an FDE are determined by an *initial function* $\boldsymbol{\varphi} \in X$ such that

$$\mathbf{x}_{t_0}(s) = \boldsymbol{\varphi}(s), \quad s \in [-a, 0]. \tag{5.22}$$

Accordingly, a *solution* $\mathbf{x}(t) = \mathbf{x}(t, t_0, \boldsymbol{\varphi})$ with initial function $\boldsymbol{\varphi} \in X$ is a continuous function defined on the interval $[-a, T)$ such that $\mathbf{x}_t \in B$ for $t \in [t_0, T)$, (5.22) holds and $\mathbf{x}(t)$ satisfies (5.21) for $t \in [t_0, T)$. The broad class of FDEs includes particularly ODEs (5.1) ($a = 0$), *differential difference equations*

$$\dot{\mathbf{x}}(t) = \mathbf{g}(t, \mathbf{x}(t), \mathbf{x}(t - a)),$$

and *integro-differential equations*

$$\dot{\mathbf{x}} = \int_{-a}^{0} \mathbf{h}(t, \mathbf{x}_t(s))\mathrm{d}s.$$

For the case $a \in (0, \infty)$, the setting described so far does not require special properties of the function space X to obtain quite general existence and uniqueness results, which can be found in the work of Driver (1962); Hale (1977); Burton (2005); Kolmanovskii and Nosov (1986). The situation becomes a little more delicate, when an *FDE with infinite delay*, i.e., the case $a \to \infty$, is considered. In that case, which is of major interest for subsequent applications, some special requirements on X have to be fulfilled, see Hale and Kato (1978); Kappel and Schappacher (1980); Sawano (1982). For the purposes of this thesis, the Banach space

$$X := BU((-\infty, 0]; \mathbb{R}^n)$$

[1] For the special case $a \to \infty$, the interval $[-a, 0]$ is thought of as $(-\infty, 0]$.

of bounded uniformly continuous functions mapping $(-\infty, 0]$ to $\mathbb{R}^n$ is chosen together with the uniform norm $\|\cdot\|_\infty$ defined by

$$\|\boldsymbol{\varphi}\|_\infty = \sup_{s\le 0} \|\boldsymbol{\varphi}(s)\|_2\,, \quad \boldsymbol{\varphi} \in X.$$

The crucial property of the space X is thereby that the mapping

$$t \mapsto \mathbf{x}_t \text{ is continuous on } [t_0, T) \text{ if } \mathbf{x}(t, t_0, \boldsymbol{\varphi}) \text{ is continuous on } [t_0, T). \tag{5.23}$$

This property is, for example, not fulfilled for the space of bounded continuous functions $CB((-\infty, 0]; \mathbb{R}^n)$, see the example $\varphi(s) = \sin(s^2)$, $s \le 0$ in Sawano (1982) and Kappel and Schappacher (1980, Rem. 2.3). If the continuity property (5.23) is fulfilled, one obtains the following assertions regarding existence, uniqueness and continuous dependence on initial conditions.

Theorem 5.23. *Let $\mathbf{f} : [0, T) \times B \to \mathbb{R}^n$ be a continuous function that fulfills a Lipschitz condition, i.e., assume that there exists a constant $L > 0$ such that*

$$\|\mathbf{f}(t, \boldsymbol{\varphi}) - \mathbf{f}(t, \boldsymbol{\psi})\|_2 \le L\|\boldsymbol{\varphi} - \boldsymbol{\psi}\|_\infty \text{ for } t \in [0, T),\ \boldsymbol{\varphi}, \boldsymbol{\psi} \in B \subset X.$$

Then there exists one and only one solution of (5.21) *with* (5.22) *and there exists a continuous function $l(t)$ such that*

$$\|\mathbf{x}_t(t_0, \boldsymbol{\varphi}) - \mathbf{x}_t(t_0, \boldsymbol{\psi})\|_\infty \le l(t - t_0)\|\boldsymbol{\varphi} - \boldsymbol{\psi}\|_\infty\,, \quad t \ge t_0\,.$$

Proof. The proof by Hale and Kato (1978, Thms. 2.1, 2.2) considers the equivalent integral relation

$$\begin{aligned} \mathbf{x}_{t_0} &= \boldsymbol{\varphi}, \\ \mathbf{x}(t) &= \boldsymbol{\varphi}(0) + \int_{t_0}^{t} \mathbf{f}(s, \mathbf{x}_s)\mathrm{d}s, \quad t \ge t_0 \end{aligned} \tag{5.24}$$

for the existence part. The property (5.23) ensures that the integral term in (5.24) maps into the space of continuous functions. Additionally, the Lipschitz condition yields a contractive mapping such that a generalized fixed point theorem and Gronwall's lemma conclude the proof. □

Further, (5.23) guarantees the following compactness property of bounded orbits of $\mathbf{f}$ in (5.21), which will be used to formulate a generalized invariance principle later. For the proof, see Hale (1969); Hale and Kato (1978).

Proposition 5.24. *Let $\mathbf{f}$ in* (5.21) *map bounded sets in its second argument into bounded sets. Every orbit $\{\mathbf{x}_t \mid t \ge 0\}$ in the space X generated by a solution $\mathbf{x}$ of* (5.21) *with $\mathbf{x}(t)$ bounded on $[0, \infty)$ belongs to a compact subset of X.*

Similar as for ODEs, a generalized definition of stability of solutions of FDEs can be given. As in the ODE case, stability of a solution is related to the stability of the trivial equilibrium of a translated FDE (i.e., $\mathbf{f}(t, \mathbf{0}) = \mathbf{0}$ for all $t \geq 0$). Hence, stability is defined only for the trivial equilibrium and the set B on which $\mathbf{f}$ is defined, is assumed to contain

$$Q_H := \{\boldsymbol{\varphi} \in X \mid \|\boldsymbol{\varphi}\|_\infty < H\}, \quad H > 0.$$

Further, let $\mathbf{f}$ be defined in its first argument for all $t \geq 0$.

Definition 5.25. The trivial solution of (5.21) is called

a) *stable*, if for all $\varepsilon > 0$ and all $t_0 \geq 0$ there exists $\delta = \delta(\varepsilon, t_0) > 0$ such that for all $t \geq t_0$

$$\boldsymbol{\varphi} \in Q_\delta \quad \Rightarrow \quad \|\mathbf{x}(t, t_0, \boldsymbol{\varphi})\|_2 < \varepsilon.$$

b) *asymptotically stable*, if it is stable and for all $t_0 \geq 0$ there exists $\gamma = \gamma(t_0) > 0$ such that for $\boldsymbol{\varphi} \in Q_\gamma$, the solution $\mathbf{x}(t, t_0, \boldsymbol{\varphi})$ exists for all $t \geq t_0$ and it holds

$$\lim_{t \to \infty} \|\mathbf{x}(t, t_0, \boldsymbol{\varphi})\|_2 = 0.$$

Generalizations of the terms *uniform (asymptotic) stability* can be given similar as in Remark 5.6.

Generalized Lyapunov methods

A generalization of the direct method of Lyapunov for FDEs is based on the works of Razumikhin (1956) using Lyapunov functions and Krasovskii (1956) using Lyapunov functionals for a stability proof. The latter method is used to obtain the subsequent results. The following assertion for FDEs with infinite delay, which is the analogue to Theorem 5.8, can be found in the books of Burton (1985, Thm. 4.4.1) and Kolmanovskii and Nosov (1986, Chap. 2, Thm. 5.4).

Theorem 5.26 (Direct method of Lyapunov for FDEs)**.** *Let* $\mathbf{f} : D \to \mathbb{R}^n$ *in* (5.21) *be such that* $[0, \infty) \times Q_H \subset D$ *and* $\mathbf{f}(t, \mathbf{0}) = \mathbf{0}$ *for* $t \geq 0$. *Denote* $u_i : [0, \infty) \to [0, \infty)$, $i = 1, 2, 3$ *some scalar, continuous, strictly increasing functions such that* $u_i(0) = 0$ *and* $u_i(r) > 0$ *for* $r > 0$. *If there exists a continuous functional* $V : [0, \infty) \times \bar{Q}_H \to \mathbb{R}$, $V(t, \mathbf{0}) \equiv 0$ *such that*

$$V(t, \boldsymbol{\varphi}) \geq u_1(\|\boldsymbol{\varphi}(0)\|_2), \tag{5.25}$$

$$V(t, \boldsymbol{\varphi}) \leq u_2(\|\boldsymbol{\varphi}\|_\infty), \tag{5.26}$$

$$\dot{V}(t, \mathbf{x}_t) = \frac{\partial V}{\partial t} + \frac{\partial V}{\partial \boldsymbol{\varphi}} \cdot \mathbf{f}(t, \mathbf{x}_t) \leq 0,$$

for all $t \geq 0$, $\boldsymbol{\varphi} \in Q_H$, then the trivial solution of (5.21) *is uniformly stable. If, additionally, there is an $l > 0$ such that $\|\mathbf{f}(t, \boldsymbol{\varphi})\|_2 \leq l$ for $t \geq t_0$, $\boldsymbol{\varphi} \in Q_H$ and*

$$\dot{V}(t, \mathbf{x}_t) \leq -u_3(\|\mathbf{x}(t, t_0, \boldsymbol{\varphi})\|_2) \tag{5.27}$$

holds for all $t \geq t_0$, $\mathbf{x}_t \in Q_H$, then the trivial solution of (5.21) *is asymptotically stable. Moreover, if $Q_H = X$ and*

$$u_1(r) \to \infty \text{ for } r \to \infty, \tag{5.28}$$

the trivial solution is globally asymptotically stable.

The functional V in Theorem 5.26 is called *Lyapunov functional*. If the properties in (5.25), (5.26) and (5.28) are fulfilled, the Lyapunov functional is, similar as for ODEs, called *positive definite*, *decrescent* or *radially unbounded*, respectively.

Aside from the general method, weaker conditions on Lyapunov functionals can be given for *autonomous FDEs*

$$\dot{\mathbf{x}} = \mathbf{f}(\mathbf{x}_t). \tag{5.29}$$

Hereto, the notion of *limit sets* and *invariant sets* have to be recast.

Definition 5.27. Let $\mathbf{x}(t) = \mathbf{x}(t, \boldsymbol{\varphi})$ be a solution of (5.29) existing for $t \in \mathbb{R}$.

a) A function $\boldsymbol{\psi} \in X$ is called *positive limit function* of $\mathbf{x}(t)$, if there exists a nonnegative sequence $\{t_n\}_{n \in \mathbb{N}}$ with $t_n \to \infty$ as $n \to \infty$ such that

$$\lim_{n \to \infty} \|\mathbf{x}_{t_n} - \boldsymbol{\psi}\|_\infty = 0.$$

b) The set $\Omega(\mathbf{x})$ of all positive limit functions of $\mathbf{x}(t)$ is called *positive limit set*.

c) A set $Q \subset X$ is called *(positively) invariant*, if $\mathbf{x}_t(\boldsymbol{\varphi}) \in Q$ for all $\boldsymbol{\varphi} \in Q$ and all ($t \geq 0$ resp.) $t \in \mathbb{R}$.

The counterpart of Proposition 5.12 can be formulated as follows, see Hale and Kato (1978, Thm. 3.2).

Proposition 5.28. *Let $\mathbf{x}$ be a solution of* (5.29) *and assume $\{\mathbf{x}_t \mid t \geq 0\}$ belongs to a compact subset of Q_H, then $\Omega(\mathbf{x})$ is nonempty, compact, invariant and*

$$\operatorname{dist}(\mathbf{x}_t, \Omega(\mathbf{x})) \to 0 \ \text{ as } \ t \to \infty.$$

The result of Proposition 5.24 and Proposition 5.28 is an invariance principle for FDEs.

Theorem 5.29 (Invariance principle). *Let $V : Q_H \to \mathbb{R}$ be a continuous functional such that $\dot{V}(\mathbf{x}_t) \leq 0$ in Q_H. Let*

$$E := \{\boldsymbol{\varphi} \in Q_H \mid \dot{V}(\boldsymbol{\varphi}) = 0\}$$

and M be the largest invariant set in E. Then every bounded solution $\mathbf{x}(t)$ of (5.29) starting and existing in Q_H for $t \geq 0$ approaches M for $t \to \infty$, i.e.,

$$\lim_{t\to\infty} \operatorname{dist}(\mathbf{x}_t, M) = 0.$$

Proof. Proposition 5.24 ensures that V is defined on a compact set. The further argumentation is the same as for Theorem 5.11. □

Corollary 5.30. *Let $\mathbf{f} : B \supset Q_H \to \mathbb{R}^n$ mapping bounded sets into bounded sets be such that $\mathbf{f}(\mathbf{0}) = \mathbf{0}$ and denote $u : [0,\infty) \to [0,\infty)$ some scalar, continuous, strictly increasing function such that $u(0) = 0$ and $u(r) > 0$ for $r > 0$. Let there exist a continuous functional $V : Q_H \to \mathbb{R}$ such that*

$$V(\mathbf{0}) = \mathbf{0} \text{ and } V(\boldsymbol{\varphi}) \geq u(\|\boldsymbol{\varphi}(0)\|_2) \text{ for all } \boldsymbol{\varphi} \in Q_H\,, \tag{5.30}$$

$$\dot{V}(\mathbf{x}_t) \leq 0 \text{ for all } t \geq 0,\ \mathbf{x}_t \in Q_H\,. \tag{5.31}$$

If $M = \{\mathbf{0}\}$ is the largest invariant set in E, then the trivial equilibrium is asymptotically stable. If V is defined on X and $u(r) \to \infty$ for $r \to \infty$, then the trivial equilibrium is globally asymptotically stable.

Finally, one more generalization for FDEs, viz. an invariance result for asymptotically autonomous systems with limiting equation

$$\dot{\mathbf{x}} = \mathbf{f}^*(\mathbf{x}_t) \tag{5.32}$$

is stated, being a special case of a theorem by Andreev (2009, Thm. 65).

Theorem 5.31. *Let $V : [0,\infty) \times Q_H \to \mathbb{R}$ be a continuous functional and denote $u : [0,\infty) \to [0,\infty)$ some scalar, continuous, strictly increasing function such that $u(0) = 0$ and $u(r) > 0$ for $r > 0$ and*

$$V(t,\mathbf{0}) = \mathbf{0}, \quad V(t,\boldsymbol{\varphi}) \geq u(\|\boldsymbol{\varphi}(0)\|_2) \text{ for } t \geq 0,\ \varphi \in Q_H\,.$$

Further, let there exist a continuous, nonnegative functional $W : Q_H \to [0,\infty)$ such that

$$\dot{V}(t,\boldsymbol{\varphi}) \leq -W(\boldsymbol{\varphi}) \leq 0 \text{ for } t \geq 0,\ \varphi \in Q_H$$

and let $\mathbf{f}^*$ with $\mathbf{f}^*(\mathbf{0}) = \mathbf{0}$ in (5.32) be the limiting equation of $\mathbf{f}$ in (5.21), i.e., for each compact set $K \subset X$, where $\mathbf{f}$ is defined and for each $\varepsilon > 0$ there is a $T(K,\varepsilon) > t_0$ such that

$$\|\mathbf{f}(t,\boldsymbol{\varphi}) - \mathbf{f}^*(\boldsymbol{\varphi})\|_2 < \varepsilon \text{ for all } \boldsymbol{\varphi} \in K,\ t > T.$$

If no other solution of the limiting equation (5.32) *than the trivial solution remains in the set*

$$E := \{\boldsymbol{\varphi} \in Q_H \mid W(\boldsymbol{\varphi}) = 0\},$$

then the trivial solution of (5.21) *is asymptotically stable.*

5.3 Fractionally damped mechanical systems

The considerations in Section 4.2 reveal that damping mechanisms of mechanical systems described by fractional derivatives are of interest from a modeling perspective. The present section deals with stability problems for certain systems of such type using Lyapunov theory for FDEs. Particularly, consider a finite-dimensional mechanical system with fractional damping described by the equations of motion

$$\mathbf{M}(t,\mathbf{q})\ddot{\mathbf{q}} - \mathbf{h}\left(t,\mathbf{q},{}^{\mathrm{C}}\mathrm{D}^{\alpha}\mathbf{q},\dot{\mathbf{q}}\right) = \mathbf{0}, \tag{5.33}$$

with generalized coordinates $\mathbf{q} \in \mathbb{R}^f$, $f := \frac{n}{2} \in \mathbb{N}$, a nonsingular symmetric mass matrix $\mathbf{M}(t,\mathbf{q})$ and a vector $\mathbf{h}\left(t,\mathbf{q},{}^{\mathrm{C}}\mathrm{D}^{\alpha}\mathbf{q},\dot{\mathbf{q}}\right)$ including (non-)potential, gyroscopic and external forces as well as forces of springpots ($\alpha \in (0,1)$). In view of Section 2.2, (5.33) represents an FODE of the form (2.25), when (5.33) is premultiplied by the inverse of $\mathbf{M}(t,\mathbf{q})$ and given in first-order form

$$\begin{aligned} \dot{\mathbf{q}} &= \mathbf{v}, \\ \dot{\mathbf{v}} &= (\mathbf{M}(t,\mathbf{q}))^{-1}\mathbf{h}\left(t,\mathbf{q},{}^{\mathrm{C}}\mathrm{D}^{\alpha}\mathbf{q},\mathbf{v}\right). \end{aligned} \tag{5.34}$$

Therein, a reparametrization of the fractional derivative (2.10) leads to the expression

$${}^{\mathrm{C}}\mathrm{D}^{\alpha}\mathbf{q}(t) = \int_{-\infty}^{0} \frac{(-s)^{-\alpha}}{\Gamma(1-\alpha)}\mathbf{q}'(t+s)\mathrm{d}s = \int_{-\infty}^{0} \frac{(-s)^{-\alpha}}{\Gamma(1-\alpha)}\mathbf{v}_t(s)\mathrm{d}s \tag{5.35}$$

such that (5.34) can be reformulated as an FDE (5.21) with infinite delay

$$\begin{aligned} \dot{\mathbf{q}} &= \mathbf{v}, \\ \dot{\mathbf{v}} &= \tilde{\mathbf{h}}\left(t,\mathbf{q},\mathbf{v}_t\right). \end{aligned} \tag{5.36}$$

Subsequently, Lyapunov functionals for several examples of (5.33) are examined to obtain stability results. It turns out that already the linear case requires a relatively complex construction of such functionals. The starting point to search for appropriate functionals is the total mechanical energy.

Section 5.3 is based on Hinze et al. (2020a,b).

Single degree-of-freedom oscillator

Consider a single degree-of-freedom, fractionally damped oscillator (Figure 5.4) that fulfills the equation of motion

$$m\ddot{q}(t) + d\dot{q}(t) + c\,{}^{\mathrm{C}}\mathrm{D}^{\alpha}q(t) + kq(t) = 0, \quad t \geq 0 \tag{5.37}$$

with mass $m > 0$, elongation q, damping coefficient $d \geq 0$, stiffness $k > 0$, spring-pot coefficient $c > 0$ and differentiation order $\alpha \in (0,1)$ and a given continuously-differentiable initial function φ such that $\varphi, \varphi' \in BU((-\infty, 0]; \mathbb{R})$ and

$$q(s) = \varphi(s), \quad s \leq 0.$$

In view of (5.35) and (5.36), (5.37) results in an FDE

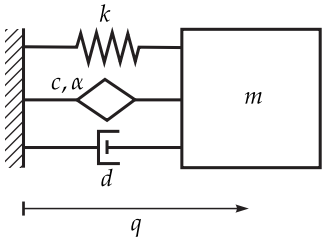

Figure 5.4: Single degree-of-freedom oscillator with viscous and fractional damping.

$$\begin{aligned} \dot{q}(t) =& v(t), \\ \dot{v}(t) =& -\frac{k}{m}q(t) - \frac{d}{m}v(t) - \frac{c}{m}\int_{-\infty}^{0} \frac{(-s)^{-\alpha}}{\Gamma(1-\alpha)} v_t(s)\mathrm{d}s. \end{aligned} \tag{5.38}$$

Using the infinite state representation in (2.29) or, equivalently, inserting (2.28) and

$$z(\eta, t) = \int_{-\infty}^{t} \mathrm{e}^{-\eta(t-\tau)} v(\tau)\mathrm{d}\tau = \int_{-\infty}^{0} \mathrm{e}^{\eta s} v_t(s)\mathrm{d}s \tag{5.39}$$

in the last term of (5.38), it can be reformulated equivalently as

$$\begin{aligned} \dot{q}(t) =& v(t), \\ \dot{v}(t) =& -\frac{k}{m}q(t) - \frac{d}{m}v(t) - \frac{c}{m}\int_{0}^{\infty} \mu_{1-\alpha}(\lambda) z(\lambda, t)\mathrm{d}\lambda, \\ \dot{z}(\eta, t) =& v(t) - \eta z(\eta, t), \quad \eta > 0. \end{aligned} \tag{5.40}$$

As all the Lyapunov functionals used for the following stability proofs are formulated with the help of the infinite states z and Z from (2.29) and (2.26), the

formulation (5.40) is preferred. Nevertheless, it is useful to keep in mind that (5.37) can be interpreted as an FDE (5.38).

In the following, asymptotic stability of the trivial equilibrium of (5.38) for several cases using Theorem 5.26 and Corollary 5.30 is proven. Hence, to be sure that the right-hand side of (5.40) is bounded for bounded inputs, the improper integral is estimated by splitting the interval of integration for λ in two parts which yields

$$\begin{aligned}\left|\int_1^\infty \mu_{1-\alpha}(\lambda)\int_{-\infty}^0 \mathrm{e}^{\lambda s} v_t(s)\mathrm{d}s\,\mathrm{d}\lambda\right| &\le \int_1^\infty \mu_{1-\alpha}(\lambda)\int_{-\infty}^0 \mathrm{e}^{\lambda s}\mathrm{d}s\,\mathrm{d}\lambda\|v_t\|_\infty \\ &= \frac{\sin(\alpha\pi)}{\pi}\int_1^\infty \lambda^{\alpha-2}\mathrm{d}\lambda\|v_t\|_\infty = \frac{\sin(\alpha\pi)}{(1-\alpha)\pi}\|v_t\|_\infty\end{aligned} \tag{5.41}$$

and

$$\begin{aligned}\left|\int_0^1 \mu_{1-\alpha}(\lambda)\int_{-\infty}^0 \mathrm{e}^{\lambda s} q_t'(s)\mathrm{d}s\,\mathrm{d}\lambda\right| &\le \int_0^1 \mu_{1-\alpha}(\lambda)\left|q(t)-\lambda\int_{-\infty}^0 \mathrm{e}^{\lambda s} q_t(s)\mathrm{d}s\right|\mathrm{d}\lambda \\ &\le \int_0^1 \mu_{1-\alpha}(\lambda)\left(\|q_t\|_\infty + \lambda\int_{-\infty}^0 \mathrm{e}^{\lambda s}\mathrm{d}s\|q_t\|_\infty\right)\mathrm{d}\lambda \\ &= 2\int_0^1 \mu_{1-\alpha}(\lambda)\mathrm{d}\lambda\|q_t\|_\infty = 2\frac{\sin(\alpha\pi)}{\alpha\pi}\|q_t\|_\infty .\end{aligned} \tag{5.42}$$

Further, as a first example, consider the case $d = 0$ in (5.37), i.e., viscous damping is absent and all dissipation is due to the springpot $c > 0$, and use the total mechanical energy

$$V_1(q_t, v_t) = \frac{k}{2}q_t^2(0) + \frac{m}{2}v_t^2(0) + \frac{c}{2}\int_0^\infty \mu_{1-\alpha}(\lambda)z^2(\lambda,t)\mathrm{d}\lambda,$$

as a Lyapunov functional, which contains the potential energy term (4.80) of the springpot. Asymptotic stability of the trivial solution is proven with the help of Corollary 5.30. It is obvious that inequality (5.30) holds for V_1. Furthermore, as

$$\begin{aligned}\dot V_1 &= kq_t(0)q_t'(0) + mv_t(0)v_t'(0) + c\int_0^\infty \mu_{1-\alpha}(\lambda)z(\lambda,t)\dot z(\lambda,t)\mathrm{d}\lambda \\ &= v_t(0)\left(mq_t''(0) + kq_t(0) + c\int_0^\infty \mu_{1-\alpha}(\lambda)z(\lambda,t)\,\mathrm{d}\lambda\right) \\ &\quad - c\int_0^\infty \mu_{1-\alpha}(\lambda)\,\lambda\,z^2(\lambda,t)\,\mathrm{d}\lambda \\ &= -c\int_0^\infty \mu_{1-\alpha}(\lambda)\,\lambda\,z^2(\lambda,t)\,\mathrm{d}\lambda \le 0,\end{aligned} \tag{5.43}$$

inequality (5.31) is fulfilled such that the trivial solution is stable. Moreover, examine the largest invariant set in $E = \{\boldsymbol{\varphi} \in X \mid \dot V_1 = 0\}$. From (5.43), one can conclude in E

$$z(\eta,\cdot) = 0 \text{ for almost all } \eta \ge 0$$

and substitution in the z-dynamics of (5.40) results in

$$\dot{q} = v = 0,$$

which together with (5.37) implies that $\{\mathbf{0}\}$ is the largest invariant set in E. Finally, all conditions of Corollary 5.30 are fulfilled and the trivial solution is globally asymptotically stable. Note that $\dot{V}_1$ in (5.43) can be interpreted as internal power losses of the springpot, see Hinze et al. (2018); Papoulia et al. (2010); Schiessel and Blumen (1993) or, for an analogue electrical system Hartley et al. (2015); Trigeassou and Maamri (2019).

Second, consider the case $d > 0$ in (5.37), i.e., dissipation due to the viscous damper as well as the springpot. Using the energy functional V_1 again leads to a nonpositive rate of V_1

$$\dot{V}_1 = -dv^2(t) - c\int_0^\infty \mu_{1-\alpha}(\lambda)\,\lambda\, z^2(\lambda,t)\,\mathrm{d}\lambda \leq 0,$$

which proves asymptotic stability of the equilibrium using the invariance argument as for the case without viscous damping. Alternatively, study an augmented candidate Lyapunov functional inspired from Example 5.14, which contains the potential energy term (4.80) to prove asymptotic stability with the help of Theorem 5.26. Therefore, the functional includes an additional term using the infinite states from (2.26). It has the form

$$\begin{aligned} V_2(q_t, v_t) = {} & \frac{k}{2}q_t^2(0) + \frac{m}{2}v_t^2(0) + \frac{d^2}{4m}q_t^2(0) + \frac{d}{2}q_t(0)v_t(0) \\ & + \frac{c}{2}\int_0^\infty \mu_{1-\alpha}(\lambda) z^2(\lambda,t)\mathrm{d}\lambda + \frac{cd}{4m}\int_0^\infty \mu_{1-\alpha}(\lambda)\,\lambda\, Z^2(\lambda,t)\mathrm{d}\lambda. \end{aligned} \tag{5.44}$$

Check the assumptions in Theorem 5.26. For (5.25), one can estimate

$$\begin{aligned} V_2(q_t, v_t) &\geq \frac{k}{2}q_t^2(0) + \frac{m}{2}v_t^2(0) + \frac{d^2}{4m}q_t^2(0) + \frac{d}{2}q_t(0)v_t(0) \\ &= \frac{k}{2}q_t^2(0) + \frac{m}{4}v_t^2(0) + \left(\frac{d}{2\sqrt{m}}q_t(0) + \frac{\sqrt{m}}{2}v_t(0)\right)^2 \\ &\geq \frac{k}{2}q_t^2(0) + \frac{m}{4}v_t^2(0) \end{aligned}$$

such that (5.25) and (5.28) are fulfilled. Moreover, computing the rate of V_2 along solution curves yields

$$\begin{aligned} \dot{V}_2 = {} & kq_t(0)q_t'(0) + mv_t(0)v_t'(0) + \frac{d}{2}q_t'(0)v_t(0) + \frac{d}{2}q_t(0)v_t'(0) + \frac{d^2}{2m}q_t(0)q_t'(0) \\ & + c\int_0^\infty \mu_{1-\alpha}(\lambda) z(\lambda,t)\dot{z}(\lambda,t)\mathrm{d}\lambda + \frac{cd}{2m}\int_0^\infty \mu_{1-\alpha}(\lambda)\,\lambda\, Z(\lambda,t)\dot{Z}(\lambda,t)\mathrm{d}\lambda, \end{aligned}$$

$$
\begin{aligned}
\dot{V}_2 &= -dv_t^2(0) - cv_t(0)\int_0^\infty \mu_{1-\alpha}(\lambda)z(\lambda,t)\mathrm{d}\lambda + \frac{d}{2}v_t^2(0) \\
&\quad + \frac{d}{2}q_t(0)\left[-\frac{k}{m}q_t(0) - \frac{d}{m}v_t(0) - \frac{c}{m}\int_0^\infty \mu_{1-\alpha}(\lambda)z(\lambda,t)\mathrm{d}\lambda\right] \\
&\quad + \frac{d^2}{2m}q_t(0)v_t(0) + c\int_0^\infty \mu_{1-\alpha}(\lambda)z(\lambda,t)\left(v_t(0) - \lambda\, z(\lambda,t)\right)\mathrm{d}\lambda \\
&\quad + \frac{cd}{2m}\int_0^\infty \mu_{1-\alpha}(\lambda)\left(q_t(0) - z(\lambda,t)\right)z(\lambda,t)\mathrm{d}\lambda \\
&= -\frac{kd}{2m}q_t^2(0) - \frac{d}{2}v_t^2(0) - c\int_0^\infty \mu_{1-\alpha}(\lambda)\left(\lambda + \frac{d}{2m}\right)z^2(\lambda,t)\mathrm{d}\lambda \\
&\leq -\frac{kd}{2m}q^2(t) - \frac{d}{2}v^2(t),
\end{aligned}
$$

which proves (5.27) and hence, Theorem 5.26 leads to global asymptotic stability of the trivial equilibrium without using an invariance argumentation. The particular structure of the functional V_2 in (5.44) is revisited for a stability proof in Section 5.4.

Single degree-of-freedom oscillator with viscous anti-damping

For the case $d < 0$, whose physical interpretation is explained and motivated in an example at the end of the present section, the trivial equilibrium of (5.37) is expected to remain stable only for certain values of d. This will be examined by a spectral analysis (as the system is linear) using the method of Laplace transforms in the following. Moreover, it turns out that the reformulated infinite state representation of fractional derivatives yields a Lyapunov functional to prove asymptotic stability. Finally, the quality of both results will be compared.

Spectral analysis

The asymptotic behavior of solutions of linear autonomous ODEs is determined by the eigenvalues of the system matrix, see Proposition 5.15. A similar assertion is valid for (5.40), which will be shown by studying the Laplace transform of (5.40) and using the residue theorem. Therefore, using Proposition 2.9, consider the Laplace transform of (2.29)

$$
\begin{aligned}
\mathcal{L}\left\{{}^{\mathrm{C}}\mathrm{D}^\alpha q(t)\right\}(s) &= \int_0^\infty \mu_{1-\alpha}(\lambda)\mathcal{L}\left\{z(\lambda,t)\right\}(s)\mathrm{d}\lambda, \\
s\mathcal{L}\left\{z(\eta,t)\right\}(s) - z(\eta,0) &= s\mathcal{L}\left\{q(t)\right\}(s) - q(0) - \eta\mathcal{L}\left\{z(\eta,t)\right\}(s).
\end{aligned}
\tag{5.45}
$$

Substituting the second equation of (5.45) in the first results in

$$
\mathcal{L}\left\{{}^{\mathrm{C}}\mathrm{D}^\alpha q(t)\right\}(s) = \int_0^\infty \mu_{1-\alpha}\frac{s\mathcal{L}\left\{q(t)\right\}(s) - q(0) + z(\lambda,0)}{\lambda + s}\mathrm{d}\lambda,
$$

which can, using Proposition 3.1 and in view of (2.13), be written as

$$\begin{aligned}\mathcal{L}\left\{{}^{\mathrm{C}}\mathrm{D}^{\alpha}q(t)\right\}(s) &= s^{\alpha}\mathcal{L}\left\{q(t)\right\}(s) - s^{\alpha-1}q(0) + \int_0^{\infty}\mu_{1-\alpha}(\lambda)\frac{z(\lambda,0)}{\lambda+s}\mathrm{d}\lambda \\ &= \mathcal{L}\left\{{}^{\mathrm{C}}\mathrm{D}_0^{\alpha}q(t)\right\}(s) + \int_0^{\infty}\mu_{1-\alpha}(\lambda)\frac{z(\lambda,0)}{\lambda+s}\mathrm{d}\lambda.\end{aligned} \tag{5.46}$$

Accordingly, the Laplace transform of (5.37) is given by

$$\begin{aligned}&m\left(s^2\mathcal{L}\left\{q(t)\right\}(s) - sq(0) - \dot{q}(0)\right) + d\left(s\mathcal{L}\left\{q(t)\right\}(s) - q(0)\right) \\ &\quad + c\left(s^{\alpha}\mathcal{L}\left\{q(t)\right\}(s) - s^{\alpha-1}q(0) + \int_0^{\infty}\mu_{1-\alpha}(\lambda)\frac{z(\lambda,0)}{\lambda+s}\mathrm{d}\lambda\right) + k\mathcal{L}\left\{q(t)\right\}(s) = 0\end{aligned}$$

and can be solved for

$$\begin{aligned}\mathcal{L}\left\{q(t)\right\}(s) = &\frac{m(sq(0)+\dot{q}(0))}{ms^2+ds+cs^{\alpha}+k} + c\frac{s^{\alpha-1}q(0) - \int_0^{\infty}\mu_{1-\alpha}(\lambda)\frac{z(\lambda,t)}{\lambda+s}\mathrm{d}\lambda}{ms^2+ds+cs^{\alpha}+k} \\ &+ \frac{dq(0)}{ms^2+ds+cs^{\alpha}+k}.\end{aligned} \tag{5.47}$$

The inverse Laplace transform can be obtained by integrating along a Hankel contour and using the residue theorem, similar as described by Kempfle et al. (2002); Liu and Duan (2015); Naber (2010). The entire derivation is accomplished later to see that, similar to the classical case, stability of the equilibrium depends on the real part of the poles of (5.47), i.e., the equation

$$ms^2 + ds + cs^{\alpha} + k = 0 \tag{5.48}$$

has to be studied. Let $s = r\mathrm{e}^{\mathrm{i}\theta}$ and compute the real and imaginary part of (5.48) as

$$\begin{aligned}mr^2\cos(2\theta) + dr\cos(\theta) + cr^{\alpha}\cos(\alpha\theta) + k = 0, \\ mr^2\sin(2\theta) + dr\sin(\theta) + cr^{\alpha}\sin(\alpha\theta) = 0.\end{aligned} \tag{5.49}$$

It is the aim to derive conditions from (5.49) such that the roots of (5.48) are located in the left-half complex plane. Therefore, consider the critical case for stability $\theta = \pm\frac{\pi}{2}$ (i.e., s is on the imaginary axis) first, which turns (5.49) into

$$\begin{aligned}-mr^2 + cr^{\alpha}\cos\left(\frac{\alpha\pi}{2}\right) + k = 0, \\ dr + cr^{\alpha}\sin\left(\frac{\alpha\pi}{2}\right) = 0.\end{aligned} \tag{5.50}$$

For fixed m, c, k and α, the first equation of (5.50) has a unique solution $r = \omega > 0$, which may be inserted in the second equation to compute a critical $d < 0$ for stability

$$d_{\mathrm{crit}} = -c\sin\left(\frac{\alpha\pi}{2}\right)\omega^{\alpha-1}.$$

By numerical solution of (5.50), one obtains the critical negative damping parameter d_{crit} depending on the value of $\alpha \in (0,1)$ and the parameters m, c, k, see Figure 5.5. The value $|d_{\text{crit}}|$ is a measure for the damping capability of the springpot. As expected, it holds that $d_{\text{crit}} \to 0$ for $\alpha \to 0$, as in this case the springpot degenerates to a spring, which stores energy and $d_{\text{crit}} \to -c$ for $\alpha \to 1$, as the springpot becomes a dashpot. The dependency of d_{crit} on α for $\alpha \in (0,1)$ may change drastically for different parameters m and k.

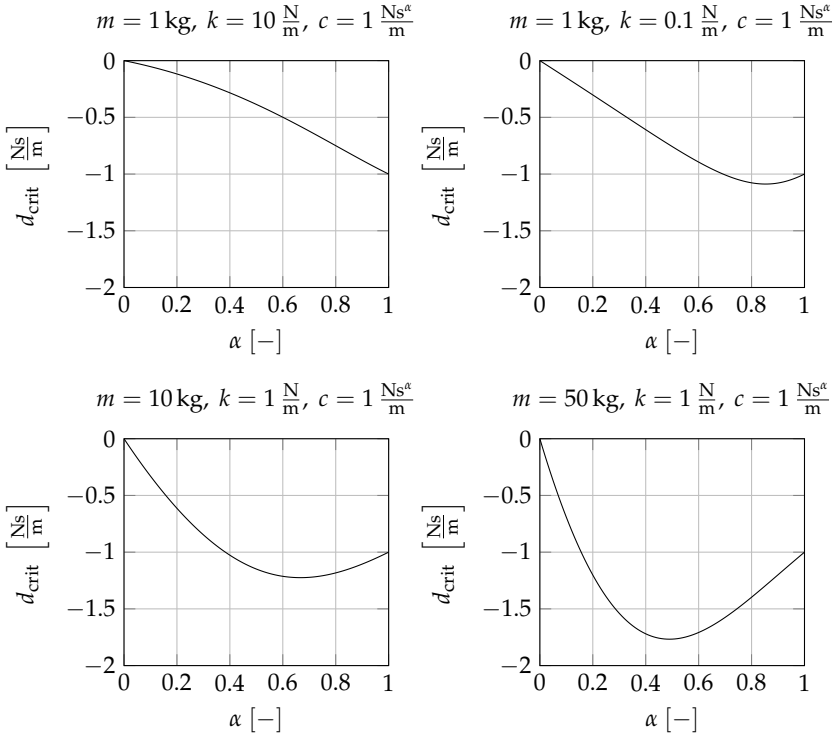

Figure 5.5: Critical negative damping parameter depending on $\alpha \in (0,1)$ for different parameters.

From the critical case for stability, the following inequality conditions on r can be derived such that a solution $s = re^{i\theta}$ of (5.48) is located in the left-half complex plane. More specifically, the following proposition is proven.

Proposition 5.32. *Let the inequalities*

$$-mr^2 + cr^\alpha \cos\left(\frac{\alpha\pi}{2}\right) + k \leq 0, \tag{5.51}$$

$$dr + cr^\alpha \sin\left(\frac{\alpha\pi}{2}\right) > 0 \tag{5.52}$$

have a non-empty solution set for $r > 0$. Then there exists a pair of complex conjugate roots $s = re^{i\theta}$, $\bar{s} = re^{-i\theta}$ of (5.48) such that $\frac{\pi}{2} < \theta < \frac{\pi}{2-\alpha}$. Furthermore, there exists no solution outside the sectors $\left\{\theta \in \left(\frac{\pi}{2}, \pi\right)\right\}$ and $\left\{\theta \in \left(-\pi, -\frac{\pi}{2}\right)\right\}$.

Remark 5.33. To depict the solution set of inequalities (5.51) and (5.52), consider Figure 5.6 below, where $\omega < \bar{\omega}$ has to hold.

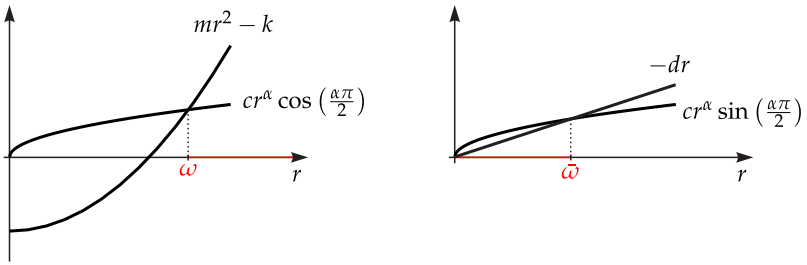

Figure 5.6: Representation of the solution set of inequalities (5.51) and (5.52).

Proof of Proposition 5.32. From (5.49), one can see that for each root $s = re^{i\theta}$ of (5.48), its complex conjugate $\bar{s} = re^{-i\theta}$ is another root. Therefore, consider only $\theta \in [0, \pi]$. The following cases are examined.

- **Case 1:** $\theta = 0$
  In this case, (5.48) degenerates to one equation

  $$mr^2 + dr + cr^\alpha + k = 0. \tag{5.53}$$

  Using (5.51) and (5.52), it can be estimated

  $$mr^2 + dr + cr^\alpha + k > cr^\alpha \left(1 + \cos\left(\frac{\alpha\pi}{2}\right) - \sin\left(\frac{\alpha\pi}{2}\right)\right) + 2k.$$

  As the function

  $$h(\alpha) := 1 + \cos\left(\frac{\alpha\pi}{2}\right) - \sin\left(\frac{\alpha\pi}{2}\right)$$

fulfills

$$h(0) = 2, \quad h(1) = 0,$$
$$h'(\alpha) = -\frac{\pi}{2}\left(\sin\left(\frac{\alpha\pi}{2}\right) + \cos\left(\frac{\alpha\pi}{2}\right)\right) < 0 \text{ for all } \alpha \in (0,1),$$

one obtains

$$mr^2 + dr + cr^\alpha + k > 0$$

and there exists no solution of (5.53).

- **Case 2:** $\theta = \pi$
  The second equation of (5.49) in this case reads as

$$cr^\alpha \sin(\alpha\pi) = 0,$$

which has no solution for $\alpha \in (0,1)$ except $r = 0$, which does not solve the first equation of (5.49)

$$mr^2 - dr + cr^\alpha \cos(\alpha\pi) + k = 0.$$

- **Case 3:** $0 < \theta < \frac{\pi}{2}$
  Multiplying the first equation of (5.49) by $\cos(\theta)$ and the second by $\sin(\theta)$ sums up as

$$mr^2\cos(\theta) + dr + cr^\alpha \cos((1-\alpha)\theta) + k\cos(\theta) = 0. \tag{5.54}$$

The left-hand side of (5.54) may be estimated with (5.51) and (5.52) as

$$\begin{aligned} &mr^2\cos(\theta) + dr + cr^\alpha\cos((1-\alpha)\theta) + k\cos(\theta) \\ &\quad > cr^\alpha\left(\cos(\theta)\cos\left(\frac{\alpha\pi}{2}\right) + \cos((1-\alpha)\theta) - \sin\left(\frac{\alpha\pi}{2}\right)\right) + 2k\cos(\theta) > 0, \end{aligned}$$

because

$$\cos(\theta)\cos\left(\frac{\alpha\pi}{2}\right) > 0$$

and

$$\cos((1-\alpha)\theta) - \sin\left(\frac{\alpha\pi}{2}\right) = \cos((1-\alpha)\theta) - \cos\left((1-\alpha)\frac{\pi}{2}\right) > 0.$$

Hence, there is no solution of (5.48) for $\theta \in \left(0, \frac{\pi}{2}\right)$ and $\alpha \in (0,1)$.

- **Case 4:** $\frac{\pi}{2} < \theta < \pi$
  Multiplying the second equation of (5.49) by $\cos(\alpha\theta)$ and subtracting the first equation multiplied by $\sin(\alpha\theta)$ leads to

$$mr^2\sin((2-\alpha)\theta) + dr\sin((1-\alpha)\theta) - k\sin(\alpha\theta) = 0,$$

which may be solved for $r > 0$ as

$$r(\theta) = -\frac{d}{2m}\frac{\sin((1-\alpha)\theta)}{\sin((2-\alpha)\theta)} + \sqrt{\left(\frac{d}{2m}\frac{\sin((1-\alpha)\theta)}{\sin((2-\alpha)\theta)}\right)^2 + \frac{k}{m}\frac{\sin(\alpha\theta)}{\sin((2-\alpha)\theta)}}. \tag{5.55}$$

Furthermore, multiplying the first equation of (5.49) by $\sin(2\theta)$ and subtracting the second equation multiplied by $\cos(2\theta)$ leads to

$$dr\sin(\theta) + cr^{\alpha}\sin((2-\alpha)\theta) + k\sin(2\theta) = 0. \tag{5.56}$$

As the first and the last term on the left-hand side of (5.56) are negative for $\theta \in \left(\frac{\pi}{2}, \pi\right)$, the second term has to be positive to solve the equation, i.e.,

$$\sin((2-\alpha)\theta) > 0 \quad \Rightarrow \quad \frac{\pi}{2} < \theta < \frac{\pi}{2-\alpha}.$$

Further, consider the left-hand side of (5.56) as a function of θ

$$g(\theta) := dr(\theta)\sin(\theta) + cr^{\alpha}(\theta)\sin((2-\alpha)\theta) + k\sin(2\theta), \quad \theta \in \left(\frac{\pi}{2}, \frac{\pi}{2-\alpha}\right)$$

with $r(\theta)$ given by (5.55). The function g is continuous for $\theta \in \left(\frac{\pi}{2}, \frac{\pi}{2-\alpha}\right)$ and it holds that

$$g\left(\frac{\pi}{2}\right) = dr + cr^{\alpha}\sin\left((2-\alpha)\frac{\pi}{2}\right) = dr + cr^{\alpha}\sin\left(\frac{\alpha\pi}{2}\right) > 0$$

as follows from (5.52). Furthermore, it can be seen from (5.55) that there exists a constant $C > 0$ such that

$$\lim_{\theta \to \frac{\pi}{2-\alpha}} r(\theta) = \lim_{\theta \to \frac{\pi}{2-\alpha}} \frac{C}{\sin((2-\alpha)\theta)} = \infty$$

so that

$$\lim_{\theta \to \frac{\pi}{2-\alpha}} g(\theta) = \lim_{\theta \to \frac{\pi}{2-\alpha}} \left[d\frac{C}{\sin((2-\alpha)\theta)}\sin\left(\frac{\pi}{2-\alpha}\right) + c\left(\frac{C}{\sin((2-\alpha)\theta)}\right)^{\alpha}\sin((2-\alpha)\theta) + k\sin\left(\frac{2\pi}{2-\alpha}\right)\right] = -\infty.$$

Therefore, there is at least one root of g, i.e., one pair of complex conjugate solutions of (5.48) such that $\theta \in \left(\frac{\pi}{2}, \frac{\pi}{2-\alpha}\right)$. □

The above proposition provides conditions for solutions of the characteristic equation (5.48) to be in the left-half complex plane. This will be used subsequently

to prove asymptotic stability of the trivial solution by inverse Laplace transform using fundamental ideas of complex analysis. Therefore, reformulate (5.47) as

$$\begin{aligned}\mathcal{L}\{q(t)\}(s) = &\frac{ms+d+cs^{\alpha-1}}{ms^2+ds+cs^\alpha+k}q_0 + \frac{m}{ms^2+ds+cs^\alpha+k}v_0 \\ &- \frac{c}{ms^2+ds+cs^\alpha+k}\int_0^\infty \mu_{1-\alpha}(\lambda)\frac{z(\lambda,0)}{\lambda+s}\mathrm{d}\lambda.\end{aligned} \tag{5.57}$$

Similar as Liu and Duan (2015), consider the function

$$\Xi(s) := \frac{ms+d+cs^{\alpha-1}}{ms^2+ds+cs^\alpha+k}$$

and compute the inverse Laplace transform $\xi(t)$ of $\Xi(s) = \mathcal{L}\{\xi(t)\}(s)$. As

$$\xi(0) = \lim_{s\to\infty} s\Xi(s) = 1,$$

one obtains

$$\mathcal{L}\{\dot\xi(t)\}(s) = s\Xi(s) - \xi(0) = \frac{ms^2+ds+cs^\alpha}{ms^2+ds+cs^\alpha+k} - 1 = -\frac{k}{ms^2+ds+cs^\alpha+k},$$

which together with (5.57) leads to the solution

$$q(t) = q_0\xi(t) - \frac{m}{k}v_0\dot\xi(t) + \frac{c}{k}\int_0^\infty \mu_{1-\alpha}(\lambda)z(\lambda,0)\int_0^t \mathrm{e}^{-\lambda(t-\tau)}\xi'(\tau)\mathrm{d}\tau\mathrm{d}\lambda \tag{5.58}$$

of (5.37). Accordingly, the asymptotic behavior of q can be examined from ξ and $\dot\xi$. Therefore, determine the inverse Laplace transform

$$\xi(t) = \frac{1}{2\pi\mathrm{i}}\int_{\delta-\mathrm{i}\infty}^{\delta+\mathrm{i}\infty}\Xi(s)\mathrm{e}^{st}\mathrm{d}s, \quad \delta > 0$$

with the help of the residue theorem, see Knopp (1945, §33)

$$\frac{1}{2\pi\mathrm{i}}\int_\Sigma \Xi(s)\mathrm{e}^{st}\mathrm{d}s = \sum_j \mathrm{Res}\left(\Xi(s)\mathrm{e}^{st}, s_j\right),$$

where s_j are the roots of (5.48) and the closed curve Σ (Figure 5.7) is split up in six parts such that

$$\xi(t) = \sum_j \mathrm{Res}\left(\Xi(s)\mathrm{e}^{st}, s_j\right) - \frac{1}{2\pi\mathrm{i}}\lim_{\substack{R\to\infty\\ \varepsilon\to 0}}\int_{\mathrm{II}-\mathrm{VI}}\Xi(s)\mathrm{e}^{st}\mathrm{d}s.$$

First, compute the residues for a pair of complex conjugate roots s_1, $s_2 = \bar s_1$ of (5.48). As $s_{1/2}$ are simple poles of Ξ, one obtains the residue by derivation of the denominator as

$$\begin{aligned}&\mathrm{Res}\left(\Xi(s)\mathrm{e}^{st}, s_1\right) + \mathrm{Res}\left(\Xi(s)\mathrm{e}^{st}, s_2\right) \\ &\quad = \frac{ms_1+d+cs_1^{\alpha-1}}{2ms_1+d+c\alpha s_1^{\alpha-1}}\mathrm{e}^{s_1t} + \frac{ms_2+d+cs_2^{\alpha-1}}{2ms_2+d+c\alpha s_2^{\alpha-1}}\mathrm{e}^{s_2t}.\end{aligned}$$

As the two addends are conjugate, one obtains with $s_1 = a + \mathrm{i}b = r\mathrm{e}^{\mathrm{i}\theta}$

$$\begin{aligned}\operatorname{Res}\left(\Xi(s)\mathrm{e}^{st}, s_1\right) + \operatorname{Res}\left(\Xi(s)\mathrm{e}^{st}, s_2\right) &= 2\mathrm{Re}\left(\frac{ms_1 + d + cs_1^{\alpha-1}}{2ms_1 + d + c\alpha s_1^{\alpha-1}}\mathrm{e}^{s_1 t}\right)\\ &= 2\mathrm{e}^{at}\cos(bt)\frac{f_1(r,\theta)}{f_3(r,\theta)} + 2\mathrm{e}^{at}\sin(bt)\frac{f_2(r,\theta)}{f_3(r,\theta)}\end{aligned}$$

with

$$\begin{aligned}f_1(r,\theta) &= 2m^2r^2 + d^2 + 3mrd\cos(\theta) + (1+\alpha)cdr^{\alpha-1}\cos((1-\alpha)\theta)\\ &\quad + (2+\alpha)mcr^{\alpha}\cos((2-\alpha)\theta) + c^2\alpha r^{2(\alpha-1)},\\ f_2(r,\theta) &= (2-\alpha)mcr^{\alpha}\sin((2-\alpha)\theta) + mdr\sin(\theta) + (1-\alpha)cdr^{\alpha-1}\sin((1-\alpha)\theta),\\ f_3(r,\theta) &= 4m^2r^2 + d^2 + 4mdr\cos(\theta) + 2cd\alpha r^{\alpha-1}\cos((1-\alpha)\theta)\\ &\quad + 4mc\alpha r^{\alpha}\cos((2-\alpha)\theta) + c^2\alpha^2 r^{2(\alpha-1)}.\end{aligned}$$

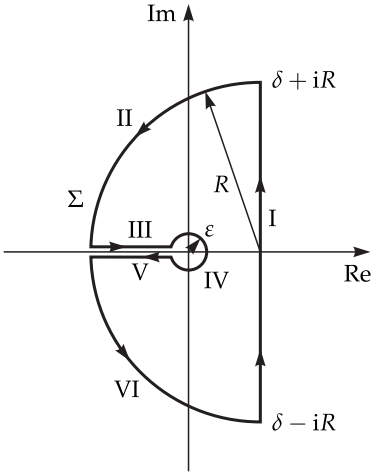

Figure 5.7: Curve Σ used for integration to apply the residue theorem.

Continue by considering the contribution of the integral along the paths II − VI to the value of ξ. There is no contribution of II, because

$$\begin{aligned}\left|\frac{1}{2\pi\mathrm{i}}\int_{\mathrm{II}}\Xi(s)\mathrm{e}^{st}\mathrm{d}s\right| &= \left|\frac{1}{2\pi\mathrm{i}}\int_{\frac{\pi}{2}}^{\pi}\Xi\left(\delta + R\mathrm{e}^{\mathrm{i}\varphi}\right)\mathrm{e}^{\delta t}\mathrm{e}^{R\cos(\varphi)t}\mathrm{e}^{\mathrm{i}R\sin(\varphi)t}\mathrm{i}R\mathrm{e}^{\mathrm{i}\varphi}\mathrm{d}\varphi\right|\\ &\leq \frac{1}{2\pi}C_1(t)\mathrm{e}^{-C_2Rt}R\cdot\frac{\pi}{2}R \underset{R\to\infty}{\longrightarrow} 0\end{aligned}$$

with $C_1, C_2 > 0$ as $\Xi(s) \to 0$ for $s \to \infty$ and $\cos(\varphi) < 0$ for $\varphi \in (\frac{\pi}{2}, \pi)$. The same argumentation holds for path VI. For path IV, one obtains

$$\frac{1}{2\pi \mathrm{i}} \int_{\mathrm{IV}} \Xi(s) \mathrm{e}^{st} \mathrm{d}s = -\frac{1}{2\pi \mathrm{i}} \int_{-\pi}^{\pi} \Xi\left(\varepsilon \mathrm{e}^{\mathrm{i}\varphi}\right) \mathrm{e}^{\varepsilon t(\cos(\varphi)+\mathrm{i}\sin(\varphi))} \mathrm{i}\varepsilon \mathrm{e}^{\mathrm{i}\varphi} \mathrm{d}\varphi \underset{\varepsilon \to 0}{\longrightarrow} 0,$$

as $s\Xi(s) \to 0$ for $s \to 0$. Finally, paths III and V yield a contribution

$$\begin{aligned} \frac{1}{2\pi \mathrm{i}} \int_{\mathrm{III,V}} \Xi(s) \mathrm{e}^{st} \mathrm{d}s &= \frac{1}{2\pi \mathrm{i}} \int_0^{\infty} \left(\Xi\left(\lambda \mathrm{e}^{\mathrm{i}\pi}\right) - \Xi\left(\lambda \mathrm{e}^{-\mathrm{i}\pi}\right)\right) \mathrm{e}^{-\lambda t} \mathrm{d}\lambda \\ &= \frac{1}{\pi} \int_0^{\infty} \mathrm{Im}\left(\Xi\left(\lambda \mathrm{e}^{\mathrm{i}\pi}\right)\right) \mathrm{e}^{-\lambda t} \mathrm{d}\lambda \end{aligned}$$

with

$$\begin{aligned} \frac{1}{\pi} \mathrm{Im}\left(\Xi\left(\lambda \mathrm{e}^{\mathrm{i}\pi}\right)\right) &= -\frac{1}{\pi} \frac{kc\lambda^{\alpha-1} \sin(\alpha\pi)}{(m\lambda^2 - d\lambda + k)^2 + 2c\lambda^{\alpha} \cos(\alpha\pi)(m\lambda^2 - d\lambda + k) + c^2\lambda^{2\alpha}} \\ &= -\frac{\mu_{1-\alpha}(\lambda) kc}{(m\lambda^2 - d\lambda + k)^2 + 2c\lambda^{\alpha} \cos(\alpha\pi)(m\lambda^2 - d\lambda + k) + c^2\lambda^{2\alpha}}. \end{aligned}$$

This leads to the inverse Laplace transform of Ξ

$$\begin{aligned} \xi(t) = &\sum_{j \text{ odd}} \left(2\mathrm{e}^{a_j t} \cos(b_j t) \frac{f_1(r_j, \theta_j)}{f_3(r_j, \theta_j)} + 2\mathrm{e}^{a_j t} \sin(b_j t) \frac{f_2(r_j, \theta_j)}{f_3(r_j, \theta_j)}\right) \\ &+ \int_0^{\infty} \mu_{1-\alpha}(\lambda) H(\lambda) \mathrm{e}^{-\lambda t} \mathrm{d}\lambda \end{aligned} \tag{5.59}$$

for roots $s_{j/j+1} = a_j \pm \mathrm{i}b_j = r_j \mathrm{e}^{\pm \mathrm{i}\theta_j}$ of (5.48), where

$$H(\lambda) = \frac{kc}{(m\lambda^2 - d\lambda + k)^2 + 2c\lambda^{\alpha} \cos(\alpha\pi)(m\lambda^2 - d\lambda + k) + c^2\lambda^{2\alpha}}.$$

The asymptotic behavior of ξ is determined by the exponential functions in the first addends of (5.59), which decay, as $a_j < 0$ for all j, if the inequalities (5.51) and (5.52) have a non-empty solution set. Furthermore, the asymptotic behavior of the last term in (5.59) may be estimated as follows. It holds that

$$\begin{aligned} &(m\lambda^2 - d\lambda + k)^2 + 2c\lambda^{\alpha} \cos(\alpha\pi)(m\lambda^2 - d\lambda + k) + c^2\lambda^{2\alpha} \\ &\quad > (m\lambda^2 - d\lambda + k - c\lambda^{\alpha})^2 \geq 0. \end{aligned}$$

Hence, H is continuous and bounded in $[0, \infty)$ and by the mean value theorem, there exists $C_3 > 0$ such that

$$\int_0^{\infty} \mu_{1-\alpha}(\lambda) H(\lambda) \mathrm{e}^{-\lambda t} \mathrm{d}\lambda = C_3 \int_0^{\infty} \mu_{1-\alpha}(\lambda) \mathrm{e}^{-\lambda t} \mathrm{d}\lambda = C_3 \frac{t^{-\alpha}}{\Gamma(1-\alpha)},$$

which leads to algebraic decay of order α for the last term in (5.59) for $t \to \infty$. For $\dot{\xi}$, one obtains the expression

$$\dot{\xi}(t) = \sum_{j \text{ odd}} 2\frac{e^{a_j t}}{f_3(r_j,\theta_j)}\Big((a_j f_1(r_j,\theta_j) + b_j f_2(r_j,\theta_j))\cos(b_j t) + (a_j f_2(r_j,\theta_j) - b_j f_1(r_j,\theta_j))\sin(b_j t)\Big) - \int_0^\infty \mu_{1-\alpha}(\lambda)H(\lambda)\lambda e^{-\lambda t}d\lambda,$$

where the first terms again describe an exponentially decaying oscillation and the last term fulfills

$$-\int_0^\infty \mu_{1-\alpha}(\lambda)H(\lambda)\lambda e^{-\lambda t}d\lambda = -\alpha C_3 \frac{t^{-\alpha-1}}{\Gamma(1-\alpha)},$$

which again implies algebraic decay, this time of order $1+\alpha$ for $t \to \infty$. To conclude asymptotic stability of the trivial solution of (5.37) from the asymptotic behavior of ξ, the last term in (5.58) still has to be considered. Therefore, recall from (5.39) that the initial infinite state $z(\eta,0)$ has the form

$$z(\eta,0) = \int_{-\infty}^0 e^{\eta\tau} q'(\tau)d\tau,$$

which may be estimated as

$$|z(\eta,0)| = \left|\int_{-\infty}^0 e^{\eta\tau}q'(\tau)d\tau\right| = \left|[e^{\eta\tau}q(\tau)]_{-\infty}^0 - \eta\int_{-\infty}^0 e^{\eta\tau}q(\tau)d\tau\right| \le \|q\|_\infty + \eta\int_{-\infty}^0 e^{\eta\tau}d\tau\|q\|_\infty = 2\|q\|_\infty,$$

which is bounded if $q \in BU((-\infty,0];\mathbb{R})$. Furthermore, consider the reformulation

$$\int_0^t e^{-\lambda(t-\tau)}\xi'(\tau)d\tau = \frac{d}{dt}\int_0^t e^{-\lambda(t-\tau)}\xi(\tau)d\tau - \xi(0)e^{-\lambda t} \tag{5.60}$$

of the inner integral in the last term of (5.58). The last term in (5.60) results in a term

$$\left|\int_0^\infty \mu_{1-\alpha}(\lambda)z(\lambda,0)e^{-\lambda t}d\lambda\right| \le 2\|q\|_\infty \frac{t^{-\alpha}}{\Gamma(1-\alpha)}$$

in (5.58). Substitution of the exponential terms of ξ in the last term of (5.58) using (5.60) leads to the estimation

$$\begin{aligned}
&\left|\int_0^\infty \mu_{1-\alpha}(\lambda) z(\lambda,0) \frac{\mathrm{d}}{\mathrm{d}t} \int_0^t \mathrm{e}^{-\lambda(t-\tau)} \mathrm{e}^{s_j\tau} \mathrm{d}\tau \mathrm{d}\lambda\right| \\
&\quad \le 2\|q\|_\infty \left|\int_0^\infty \mu_{1-\alpha}(\lambda) \frac{1}{\lambda+s_j}\left(s_j \mathrm{e}^{s_j t} + \lambda \mathrm{e}^{-\lambda t}\right) \mathrm{d}\lambda\right| \\
&\quad \le 2\|q\|_\infty \left(\left|s_j \int_0^\infty \frac{\mu_{1-\alpha}(\lambda)}{\lambda+s_j} \mathrm{d}\lambda\right| \mathrm{e}^{\mathrm{Re}(s_j)t} + \int_0^\infty \mu_{1-\alpha}(\lambda) \mathrm{e}^{-\lambda t} \mathrm{d}\lambda\right) \\
&\quad = 2\|q\|_\infty \left(\left|s_j^\alpha\right| \mathrm{e}^{\mathrm{Re}(s_j)t} + \frac{t^{-\alpha}}{\Gamma(1-\alpha)}\right)
\end{aligned}$$

with roots s_j of (5.48). For the algebraic decay part in ξ one obtains, again using the mean value theorem, a constant $C_4 > 0$ and the term

$$\begin{aligned}
&\left|\int_0^\infty \mu_{1-\alpha}(\lambda) z(\lambda,0) \frac{\mathrm{d}}{\mathrm{d}t} \int_0^t \mathrm{e}^{-\lambda(t-\tau)} \int_0^\infty \mu_{1-\alpha}(\eta) H(\eta) \mathrm{e}^{-\eta\tau} \mathrm{d}\eta \mathrm{d}\tau \mathrm{d}\lambda\right| \\
&\quad \le C_4 \left|\frac{\mathrm{d}}{\mathrm{d}t} \int_0^\infty \mu_{1-\alpha}(\lambda) \int_0^t \mathrm{e}^{-\lambda(t-\tau)} \frac{\tau^{-\alpha}}{\Gamma(1-\alpha)} \mathrm{d}\tau \mathrm{d}\lambda\right| \\
&\quad = C_4 \left|\frac{\mathrm{d}}{\mathrm{d}t}\, {}^{\mathrm{C}}\mathrm{D}_0^\alpha \left(\frac{t^{1-\alpha}}{\Gamma(2-\alpha)}\right)\right| = C_4 |1-2\alpha| \frac{t^{-2\alpha}}{\Gamma(2-2\alpha)}\,.
\end{aligned}$$

in the last term of (5.58). In summary, sufficient conditions (5.51) and (5.52) for global asymptotic stability of the equilibrium of (5.37) have been obtained, which can be formulated in the following assertion.

Proposition 5.34. *Let $m, k, c > 0$, $\alpha \in (0,1)$ and let $r = \omega > 0$ be the solution of*

$$-mr^2 + cr^\alpha \cos\left(\frac{\alpha\pi}{2}\right) + k = 0. \tag{5.61}$$

Let $d \in \mathbb{R}$ be such that the inequality

$$d\omega + c\omega^\alpha \sin\left(\frac{\alpha\pi}{2}\right) > 0$$

holds. Then the trivial solution of (5.37) *is globally asymptotically stable.*

Remark 5.35. It is even possible to obtain a purely exponential solution of (5.37) without algebraic decay. Choose the initial function $q(\tau) = \mathrm{e}^{s_j\tau}$ for $\tau \in (-\infty, 0]$ (which is not in $BU((-\infty,0];\mathbb{R})$) for a root s_j of (5.48). This leads to initial conditions

$$q'(\tau) = s_j \mathrm{e}^{s_j\tau}, \quad z(\eta,0) = \int_{-\infty}^0 \mathrm{e}^{\eta\tau} s_j \mathrm{e}^{s_j\tau} \mathrm{d}\tau = \frac{s_j}{\eta + s_j}\,.$$

Using this function in the Laplace transform (5.57) leads to

$$\begin{aligned}\mathcal{L}\{q(t)\}(s) &= \frac{ms+d+cs^{\alpha-1}}{ms^2+ds+cs^\alpha+k} + \frac{ms_j}{ms^2+ds+cs^\alpha+k} \\ &\quad - \frac{cs_j}{ms^2+ds+cs^\alpha+k}\int_0^\infty \frac{\mu_{1-\alpha}(\lambda)}{(\lambda+s)(\lambda+s_j)}\mathrm{d}\lambda \\ &= \frac{ms+d+cs^{\alpha-1}+ms_j}{ms^2+ds+cs^\alpha+k} - cs_j\frac{\int_0^\infty \frac{\mu_{1-\alpha}(\lambda)}{\lambda+s_j}\mathrm{d}\lambda - \int_0^\infty \frac{\mu_{1-\alpha}(\lambda)}{\lambda+s}\mathrm{d}\lambda}{(s-s_j)(ms^2+ds+cs^\alpha+k)} \\ &= \frac{\left(ms+d+cs^{\alpha-1}+ms_j\right)(s-s_j)}{(s-s_j)(ms^2+ds+cs^\alpha+k)} - cs_j\frac{s_j^{\alpha-1}-s^{\alpha-1}}{(s-s_j)(ms^2+ds+cs^\alpha+k)} \\ &= \frac{1}{s-s_j}\,.\end{aligned}$$

Hence, the solution is

$$q(t) = \mathrm{e}^{s_j t} \text{ for all } t,$$

which shows that the integral term in (5.46) should in general not be omitted.

Lyapunov functional

For an alternative proof of Proposition 5.34 with the help of the direct method of Lyapunov, the energy functional is not usable any more, as anti-damping can lead to an increasing energy in some time intervals, see Trigeassou et al. (2016b). Therefore, a different Lyapunov functional has to be introduced, which is motivated by the reformulated infinite state representation (3.4) of the fractional derivative

$$\begin{aligned}{}^{\mathrm{C}}\mathrm{D}^\alpha q(t) &= \sin\left(\frac{\alpha\pi}{2}\right)\omega^{\alpha-1}\dot{q}(t) - \int_0^\infty \mathrm{K}(\alpha,\lambda)\dot{z}(\lambda,t)\mathrm{d}\lambda \\ &\quad + \cos\left(\frac{\alpha\pi}{2}\right)\omega^\alpha q(t) - \omega^2\int_0^\infty \mathrm{K}(\alpha,\lambda)Z(\lambda,t)\mathrm{d}\lambda,\end{aligned}$$

in which ω is assumed to be the solution of (5.61) and $\mathrm{K}(\alpha,\cdot) := \mathrm{K}_\omega(\alpha,\cdot)$. This leads to a reformulation of the equation of motion (5.37) as

$$\begin{aligned}m\ddot{q}(t) = &-\left(k + c\cos\left(\frac{\alpha\pi}{2}\right)\omega^\alpha\right)q(t) - \left(d + c\sin\left(\frac{\alpha\pi}{2}\right)\omega^{\alpha-1}\right)\dot{q}(t) \\ &+ c\omega^2\int_0^\infty \mathrm{K}(\alpha,\lambda)Z(\lambda,t)\mathrm{d}\lambda + c\int_0^\infty \mathrm{K}(\alpha,\lambda)\dot{z}(\lambda,t)\mathrm{d}\lambda,\end{aligned} \tag{5.62}$$

which contains modified stiffness and damping parameters

$$\tilde{k} := k + c\cos\left(\frac{\alpha\pi}{2}\right)\omega^\alpha, \quad \tilde{d} := d + c\sin\left(\frac{\alpha\pi}{2}\right)\omega^{\alpha-1}. \tag{5.63}$$

Obviously, the parameter $\tilde{k}$ is positive, while $\tilde{d}$ becomes nonpositive for $d \leq d_{\text{crit}}$. A coordinate transformation to modified positions

$$\begin{aligned} \tilde{q}(t) &= q(t) - \frac{c}{\tilde{k}}\omega^2 \int_0^\infty \mathrm{K}(\alpha,\lambda) Z(\lambda,t)\mathrm{d}\lambda \\ &= \frac{k}{\tilde{k}} q(t) + \frac{c}{\tilde{k}}\omega^2 \int_0^\infty \frac{\mathrm{K}(\alpha,\lambda)}{\lambda} z(\lambda,t)\mathrm{d}\lambda \end{aligned} \tag{5.64}$$

and modified velocities

$$\tilde{v}(t) = \dot{q}(t) - \frac{c}{m}\int_0^\infty \mathrm{K}(\alpha,\lambda) z(\lambda,t)\mathrm{d}\lambda \tag{5.65}$$

transforms (5.62) to a reformulated system

$$\begin{aligned} \dot{\tilde{q}}(t) &= \tilde{v}(t), \\ \dot{\tilde{v}}(t) &= -\frac{\tilde{k}}{m}\tilde{q}(t) - \frac{\tilde{d}}{m}\tilde{v}(t) - \frac{\tilde{d}c}{m^2}\int_0^\infty \mathrm{K}(\alpha,\lambda) z(\lambda,t)\mathrm{d}\lambda \\ \dot{z}(\eta,t) &= \tilde{v}(t) + \frac{c}{m}\int_0^\infty \mathrm{K}(\alpha,\lambda) z(\lambda,t)\mathrm{d}\lambda - \eta z(\eta,t), \quad \eta > 0 \end{aligned} \tag{5.66}$$

in first-order form. Note that the first equation in (5.66) holds because $m\omega^2 = \tilde{k}$, as ω is the solution of (5.61). At this point, the Lyapunov proof of asymptotic stability can be accomplished, see Hinze et al. (2020a).

Proof of Proposition 5.34. Again, prove that all conditions in Corollary 5.30 are fulfilled. Consider the candidate Lyapunov functional

$$V_3(q_t, v_t) = \frac{\tilde{k}}{2}\tilde{q}_t^2(0) + \frac{m}{2}\tilde{v}_t^2(0) + \frac{\tilde{d}c}{2m}\int_0^\infty \mathrm{K}(\alpha,\lambda) z^2(\lambda,t)\mathrm{d}\lambda \tag{5.67}$$

and prove inequality (5.30) for V_3 w.r.t. the functions q_t and v_t. Hereto, consider the split of the integral term in (5.67)

$$\int_0^\infty \mathrm{K}(\alpha,\lambda) z^2(\lambda,t)\mathrm{d}\lambda = \int_0^1 \mathrm{K}(\alpha,\lambda) z^2(\lambda,t)\mathrm{d}\lambda + \int_1^\infty \mathrm{K}(\alpha,\lambda) z^2(\lambda,t)\mathrm{d}\lambda$$

and use the mean value theorem for the first term and the inequality $\lambda \geq 1$ in the second term to find a constant $\tilde{C} \in (0,1]$ such that

$$\int_0^\infty \mathrm{K}(\alpha,\lambda) z^2(\lambda,t)\mathrm{d}\lambda \geq \tilde{C}\int_0^\infty \frac{\mathrm{K}(\alpha,\lambda)}{\lambda} z^2(\lambda,t)\mathrm{d}\lambda.$$

Moreover, use Hölder's inequality and Proposition 3.3 to obtain

$$\begin{aligned} \left(\int_0^\infty \frac{\mathrm{K}(\alpha,\lambda)}{\lambda} z(\lambda,t)\mathrm{d}\lambda\right)^2 &\leq \int_0^\infty \frac{\mathrm{K}(\alpha,\lambda)}{\lambda}\mathrm{d}\lambda \cdot \int_0^\infty \frac{\mathrm{K}(\alpha,\lambda)}{\lambda} z^2(\lambda,t)\mathrm{d}\lambda \\ &= \cos\left(\frac{\alpha\pi}{2}\right)\omega^{\alpha-2}\int_0^\infty \frac{\mathrm{K}(\alpha,\lambda)}{\lambda} z^2(\lambda,t)\mathrm{d}\lambda \end{aligned} \tag{5.68}$$

and

$$\begin{aligned}\left(\int_0^\infty \mathrm{K}(\alpha,\lambda)z(\lambda,t)\mathrm{d}\lambda\right)^2 &\leq \int_0^\infty \mathrm{K}(\alpha,\lambda)\mathrm{d}\lambda \cdot \int_0^\infty \mathrm{K}(\alpha,\lambda)z^2(\lambda,t)\mathrm{d}\lambda \\ &= \sin\left(\frac{\alpha\pi}{2}\right)\omega^{\alpha-1}\int_0^\infty \mathrm{K}(\alpha,\lambda)z^2(\lambda,t)\mathrm{d}\lambda.\end{aligned} \tag{5.69}$$

By splitting the third term in (5.67) in two equal parts, estimating the first with (5.68) and the second with (5.69), (5.67) can be estimated as

$$\begin{aligned}V_3(q_t,v_t) \geq \frac{\tilde{k}}{2}\tilde{q}_t^2(0) &+ \frac{\tilde{d}c\tilde{C}}{4m\cos\left(\frac{\alpha\pi}{2}\right)\omega^{\alpha-2}}\left(\int_0^\infty \frac{\mathrm{K}(\alpha,\lambda)}{\lambda}z(\lambda,t)\mathrm{d}\lambda\right)^2 \\ &+ \frac{m}{2}\tilde{v}_t^2(0) + \frac{\tilde{d}c}{4m\sin\left(\frac{\alpha\pi}{2}\right)\omega^{\alpha-1}}\left(\int_0^\infty \mathrm{K}(\alpha,\lambda)z(\lambda,t)\mathrm{d}\lambda\right)^2.\end{aligned} \tag{5.70}$$

Finally, applying the general relation

$$(a+b)^2+\gamma b^2 = \frac{\gamma}{1+\gamma}a^2 + \left(\frac{a}{\sqrt{1+\gamma}}+\sqrt{1+\gamma}b\right)^2$$

for $a,b,\gamma\in\mathbb{R},\ \gamma>0$ on the first two and the last two terms of (5.70) using (5.64) and (5.65), one obtains inequality (5.30) for V_3. Furthermore, the rate of V_3 can be computed as

$$\dot{V}_3 = \tilde{k}\tilde{q}_t(0)\tilde{q}_t'(0) + m\tilde{v}_t'(0)\tilde{v}_t(0) + \frac{\tilde{d}c}{m}\int_0^\infty \mathrm{K}(\alpha,\lambda)z(\lambda,t)\dot{z}(\lambda,t)\mathrm{d}\lambda.$$

Inserting the dynamics from (5.66) yields

$$\begin{aligned}\dot{V}_3 &= \tilde{v}(t)\left(-\tilde{d}\tilde{v}(t) - \frac{\tilde{d}c}{m}\int_0^\infty \mathrm{K}(\alpha,\lambda)z(\lambda,t)\mathrm{d}\lambda\right) + \tilde{v}(t)\frac{\tilde{d}c}{m}\int_0^\infty \mathrm{K}(\alpha,\lambda)z(\lambda,t)\mathrm{d}\lambda \\ &\quad + \frac{\tilde{d}c^2}{m^2}\left(\int_0^\infty \mathrm{K}(\alpha,\lambda)z(\lambda,t)\mathrm{d}\lambda\right)^2 - \frac{\tilde{d}c}{m}\int_0^\infty \mathrm{K}(\alpha,\lambda)\,\lambda\, z^2(\lambda,t)\mathrm{d}\lambda \\ &= -\tilde{d}\tilde{v}^2(t) + \frac{\tilde{d}c^2}{m^2}\left(\int_0^\infty \mathrm{K}(\alpha,\lambda)z(\lambda,t)\mathrm{d}\lambda\right)^2 - \frac{\tilde{d}c}{m}\int_0^\infty \mathrm{K}(\alpha,\lambda)\,\lambda\, z^2(\lambda,t)\mathrm{d}\lambda.\end{aligned}$$

Again, Hölder's inequality and Proposition 3.3 lead to

$$\begin{aligned}\left(\int_0^\infty \mathrm{K}(\alpha,\lambda)z(\lambda,t)\mathrm{d}\lambda\right)^2 &\leq \int_0^\infty \frac{\mathrm{K}(\alpha,\lambda)}{\lambda}\mathrm{d}\lambda \cdot \int_0^\infty \mathrm{K}(\alpha,\lambda)\,\lambda\, z^2(\lambda,t)\mathrm{d}\lambda \\ &= \cos\left(\frac{\alpha\pi}{2}\right)\omega^{\alpha-2}\int_0^\infty \mathrm{K}(\alpha,\lambda)\,\lambda\, z^2(\lambda,t)\mathrm{d}\lambda\end{aligned} \tag{5.71}$$

and finally results in

$$\dot{V}_3 \leq -\tilde{d}\tilde{v}^2(t) - \frac{\tilde{d}c}{m}\left(1-\tfrac{c}{m}\cos\left(\tfrac{\alpha\pi}{2}\right)\omega^{\alpha-2}\right)\int_0^\infty \mathrm{K}(\alpha,\lambda)\,\lambda\, z^2(\lambda,t)\mathrm{d}\lambda,$$

where, due to (5.61)

$$m\omega^2 - c\cos\left(\frac{\alpha\pi}{2}\right)\omega^\alpha = k > 0 \quad \Rightarrow \quad 1 - \frac{c}{m}\cos\left(\frac{\alpha\pi}{2}\right)\omega^{\alpha-2} > 0.$$

Hence, (5.31) holds for $d > d_{\text{crit}}$ and, using the same arguments as for the case $d > 0$, one can conclude that $\{\mathbf{0}\}$ is the largest invariant set in $\{\boldsymbol{\varphi} \in X \mid \dot{V}_3(\boldsymbol{\varphi}) = 0\}$ such that all conditions of Corollary 5.30 are fulfilled. This leads to the proof of global asymptotic stability of the trivial equilibrium. □

Finally, a Lyapunov functional V_3 could be found such that $\dot{V}_3 \leq 0$, which has the form of an energy functional w.r.t. the new coordinates $\tilde{q}_t$ and $\tilde{v}_t$. Hinze et al. (2020b) used Theorem 5.26 for the stability proof by introducing the more elaborate Lyapunov functional

$$\begin{aligned} V_4(q_t, v_t) = {} & \frac{\tilde{k}}{2}\tilde{q}_t^2(0) + \frac{m}{2}\tilde{v}_t^2(0) + \frac{\tilde{d}^2}{4m}\tilde{q}_t^2(0) + \frac{\tilde{d}}{2}\tilde{q}_t(0)\tilde{v}_t(0) \\ & + \frac{\tilde{d}c}{2m}\int_0^\infty \mathrm{K}(\alpha,\lambda) z^2(\lambda,t)\mathrm{d}\lambda + \frac{\tilde{d}^2 c}{4m^2}\int_0^\infty \mathrm{K}(\alpha,\lambda)\lambda Z^2(\lambda,t)\mathrm{d}\lambda \\ & - \frac{\tilde{d}^2 c}{4m^2}\frac{c}{\tilde{k}}\omega^2\left(\int_0^\infty \mathrm{K}(\alpha,\lambda) Z(\lambda,t)\mathrm{d}\lambda\right)^2, \end{aligned}$$

which fulfills (5.27) for $d > d_{\text{crit}}$, see Hinze et al. (2020b) for the details. However, the invariance principle renders the use of V_4 redundant for the proof. In summary, the Lyapunov proofs in this section lead to the following conclusions.

Remark 5.36.

a) The energy of a springpot (4.80) and the infinite states $z(\eta,\cdot)$ in (2.29) and $Z(\eta,\cdot)$ in (2.26), $\eta > 0$ are valuable expressions for the formulation of Lyapunov functionals for fractionally damped systems.

b) The conditions for asymptotic stability in Proposition 5.34 are equivalent to the necessary and sufficient conditions obtained by the spectral analysis. Furthermore, it is possible to obtain the same conditions using the energy balance principle as it was done by Trigeassou et al. (2016a,b) for an electrical system. As such, the choice of the functional V_3 is optimal to estimate the critical negative damping parameter. Moreover, the direct method of Lyapunov has advantages over a spectral analysis or the energy balance principle, as it can lead to global stability results in the nonlinear case, avoids the cumbersome computation of eigenvalues and may even give results in the non-hyperbolic case where an eigenvalue analysis fails.

c) The reformulated infinite state representation (3.4) does not only lead to a numerical scheme for the solution of FODEs but also yields a Lyapunov functional for a stability proof. Moreover, it extracts the stiffness and viscous

damping behavior of a springpot through the parameters $\tilde{k}$ and $\tilde{d}$ in (5.63) leading to an improved mechanical interpretation of fractional damping.

Fractionally damped stick-slip oscillator

The following example describes a mechanical system for which effective negative viscous damping occurs in the linearization of the equation of motion around an equilibrium. Sufficient conditions for local asymptotic stability of the equilibrium using Proposition 5.34 are examined. As opposed to the classical single degree-of-freedom stick-slip oscillator, see Galvanetto et al. (1995); Ibrahim (1994); Leine and Nijmeijer (2004), the dashpot is replaced here by a springpot element. Consider a mass m suspended by a spring with spring coefficient k, and a spring-

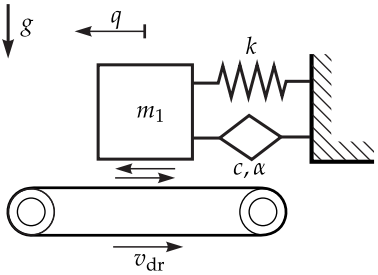

Figure 5.8: Fractionally damped oscillator with dry friction.

pot with coefficient c and differentiation order $\alpha \in (0,1)$, which is sliding on a conveyor belt as in Figure 5.8. By q, denote the displacement of the mass. The belt moves in the contact area with a constant velocity $v_{\mathrm{dr}} > 0$ in positive q-direction and friction between the mass and the belt is assumed, which leads to a friction force F_{T} such that the equation of motion reads as

$$m\ddot{q}(t) = F_{\mathrm{T}} - c\,{}^{\mathrm{C}}\mathrm{D}^{\alpha}q(t) - kq(t). \tag{5.72}$$

A set-valued Coulomb friction law may be considered, which correctly describes stiction, see Leine and Nijmeijer (2004). However, here, the focus is on the local behavior in the vicinity of the equilibrium residing in the slip phase. For the friction force F_{T} in the slip phase, consider the force law

$$F_{\mathrm{T}} = -\mu(v_{\mathrm{rel}})F_{\mathrm{N}}\,\mathrm{sign}(v_{\mathrm{rel}}), \quad v_{\mathrm{rel}} \neq 0,$$

where

$$v_{\mathrm{rel}}(t) = \dot{q}(t) - v_{\mathrm{dr}}$$

is the relative velocity between mass and belt,

$$F_{\mathrm{N}} = mg$$

is the constant normal force acting on the mass and $\mu : \mathbb{R} \to \mathbb{R}$, $\mu(v_{\mathrm{rel}}) = \mu(-v_{\mathrm{rel}})$ is the friction coefficient depending on the relative velocity, where the function μ decreases (at least) for small magnitudes of v_{rel}, i.e.,

$$\mu'(v_{\mathrm{rel}}) < 0 \ \text{ for } \ v_{\mathrm{rel}} > 0, \quad |v_{\mathrm{rel}}| \ll 1$$

and, correspondingly,

$$\mu'(v_{\mathrm{rel}}) > 0 \ \text{ for } \ v_{\mathrm{rel}} < 0, \quad |v_{\mathrm{rel}}| \ll 1,$$

which is known as the *Stribeck effect*. Consider the equilibrium q^* of (5.72) in slip

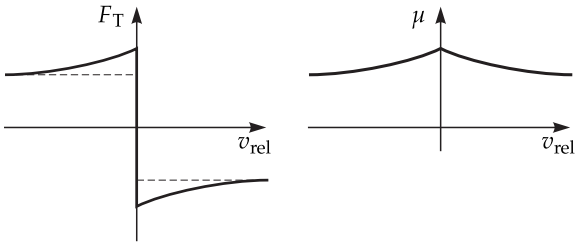

Figure 5.9: Graphs of a set-valued force law describing the Stribeck effect and the related friction coefficient μ, see Leine and Nijmeijer (2004).

(i.e., $v_{\mathrm{rel}} = -v_{\mathrm{dr}}$)

$$\begin{aligned} 0 &= F_{\mathrm{T}} - kq^*, \\ -F_{\mathrm{T}} &= \mu(-v_{\mathrm{dr}}) F_{\mathrm{N}} \operatorname{sign}(-v_{\mathrm{dr}}) = -\mu(-v_{\mathrm{dr}}) mg, \end{aligned}$$

which implies

$$q^* = \frac{\mu(-v_{\mathrm{dr}})mg}{k}. \tag{5.73}$$

By introducing a new coordinate

$$\bar{q} = q - q^*,$$

the FDE (5.72) can be reformulated in terms of $\bar{q}$ as

$$m\ddot{\bar{q}}(t) + c\,{}^{\mathrm{C}}\mathrm{D}^{\alpha}\bar{q}(t) + k(\bar{q}(t) + q^*) = -\mu(\dot{\bar{q}}(t) - v_{\mathrm{dr}})mg \operatorname{sign}(\dot{\bar{q}}(t) - v_{\mathrm{dr}}). \tag{5.74}$$

Linearizing the right-hand side of (5.74) near the equilibrium leads to

$$m\ddot{\bar{q}}(t) + c\,{}^{\mathrm{C}}\mathrm{D}^{\alpha}\bar{q}(t) + k(\bar{q}(t) + q^*) = \mu(-v_{\mathrm{dr}})mg + \mu'(-v_{\mathrm{dr}})mg\dot{\bar{q}}(t) + \mathcal{O}\left(\dot{\bar{q}}^2\right),$$

which together with (5.73) leads to the linearized equation

$$m\ddot{\bar{q}}(t) - \mu'(-v_{\mathrm{dr}})mg\dot{\bar{q}}(t) + c\,{}^{\mathrm{C}}\mathrm{D}^{\alpha}\bar{q}(t) + k\bar{q}(t) = 0,$$

where $\mu'(-v_{\mathrm{dr}}) > 0$. Hence, using Proposition 5.34, one obtains the condition

$$c\omega^{\alpha-1}\sin\left(\frac{\alpha\pi}{2}\right) > \mu'(-v_{\mathrm{dr}})mg$$

for local asymptotic stability of the slip equilibrium q^*, where again ω is the solution of (5.61).

Linear finite-dimensional mechanical systems

The proposed Lyapunov approach for the one-dimensional case can be extended to a general linear mechanical system

$$\mathbf{M}\ddot{\mathbf{q}} + (\mathbf{D} + \mathbf{G})\dot{\mathbf{q}} + \mathbf{K}\mathbf{q} - \mathbf{W}\nu = \mathbf{0}, \quad -\nu = c\,{}^{\mathrm{C}}\mathrm{D}^{\alpha}g \tag{5.75}$$

with generalized coordinates $\mathbf{q} \in \mathbb{R}^f$, mass matrix $\mathbf{M}$, damping matrix $\mathbf{D}$, gyroscopic matrix $\mathbf{G}$, stiffness matrix $\mathbf{K}$, springpot coefficient $c > 0$ and differentiation order α, where $\mathbf{M} = \mathbf{M}^{\mathrm{T}}$, $\mathbf{D} = \mathbf{D}^{\mathrm{T}}$ and $\mathbf{K} = \mathbf{K}^{\mathrm{T}}$ are constant symmetric positive definite matrices and $\mathbf{G} = -\mathbf{G}^{\mathrm{T}}$ is a constant skew-symmetric matrix in $\mathbb{R}^{f\times f}$. Furthermore, consider a generalized force $\mathbf{W}\nu$ with constant generalized force direction $\mathbf{W} \in \mathbb{R}^{f\times 1}$ and a force law ν of a springpot with elongation g that fulfills the linear geometric relation

$$g = \mathbf{W}^{\mathrm{T}}\mathbf{q}.$$

To prove stability of the trivial equilibrium, proceed as in the one-dimensional case using infinite states (2.29) and the energy Lyapunov functional

$$V_5(\mathbf{q}_t, \mathbf{q}'_t) = \frac{1}{2}\mathbf{q}_t(0)^{\mathrm{T}}\mathbf{K}\mathbf{q}_t(0) + \frac{1}{2}\mathbf{q}'_t(0)^{\mathrm{T}}\mathbf{M}\mathbf{q}'_t(0) + \frac{c}{2}\int_0^{\infty}\mu_{1-\alpha}(\lambda)z^2(\lambda,t)\mathrm{d}\lambda,$$

which fulfills (5.30) as $\mathbf{K}$, $\mathbf{M}$ are positive definite and (5.31) as

$$\dot{V}_5 = -\dot{\mathbf{q}}^{\mathrm{T}}\mathbf{D}\dot{\mathbf{q}} - c\int_0^{\infty}\mu_{1-\alpha}(\lambda)\,\lambda\,z^2(\lambda,\cdot)\mathrm{d}\lambda \le 0.$$

As $\mathbf{D}$ is positive definite and $c > 0$, again $\{\mathbf{0}\}$ is the largest invariant set in $\{\boldsymbol{\varphi} \in X \mid \dot{V}_5(\boldsymbol{\varphi}) = 0\}$ and asymptotic stability of the trivial equilibrium can be concluded using Corollary 5.30 as before.

Moreover, the case of anti-damping can be generalized for finite dimensions. Therefore, let $\mathbf{M}$ and $\mathbf{K}$ be symmetric and positive definite as before, whereas $\mathbf{G} = \mathbf{0}$ and $\mathbf{D}$ is symmetric but has one (possibly) nonpositive eigenvalue

$$d > -c \sin\left(\frac{\alpha\pi}{2}\right) \omega^{\alpha-1}$$

with normalized eigenvector $\mathbf{W}$, $\mathbf{W}^{\mathrm{T}}\mathbf{W} = 1$, where ω solves the generalized eigenvalue problem

$$\left(\mathbf{K}\mathbf{M}^{-1} + c\cos\left(\frac{\alpha\pi}{2}\right)\mathbf{W}^{\mathrm{T}}\mathbf{M}^{-1}\mathbf{W}r^{\alpha} - r^2\right)\mathbf{W} = \mathbf{0} \tag{5.76}$$

such that $\mathbf{W}$ is an eigendirection of $\mathbf{K}$ (with eigenvalue k) and $\mathbf{M}$ (with eigenvalue m) as well, i.e., ω is the solution of (5.61) as in the one-dimensional case. This means particularly that the force direction of anti-damping and of the springpot have to be collinear. Using the reformulated infinite state representation (3.4) of the fractional derivative and the infinite states (2.29), (5.75) can be reformulated as

$$\mathbf{0} = \mathbf{M}\ddot{\mathbf{q}} + \tilde{\mathbf{D}}\dot{\mathbf{q}} + \tilde{\mathbf{K}}\mathbf{q} - c\mathbf{W}\int_0^{\infty} \mathrm{K}(\alpha,\lambda)\dot{z}(\lambda,\cdot)\mathrm{d}\lambda - c\omega^2\mathbf{W}\int_0^{\infty} \mathrm{K}(\alpha,\lambda)Z(\lambda,\cdot)\mathrm{d}\lambda$$

with new stiffness and damping matrices

$$\tilde{\mathbf{K}} := \mathbf{K} + c\cos\left(\frac{\alpha\pi}{2}\right)\omega^{\alpha}\mathbf{W}\mathbf{W}^{\mathrm{T}},$$
$$\tilde{\mathbf{D}} := \mathbf{D} + c\sin\left(\frac{\alpha\pi}{2}\right)\omega^{\alpha-1}\mathbf{W}\mathbf{W}^{\mathrm{T}},$$

which both are symmetric and positive definite. Again, a coordinate transformation

$$\tilde{\mathbf{q}} = \mathbf{q} - c\mathbf{M}^{-1}\mathbf{W}\int_0^{\infty} \mathrm{K}(\alpha,\lambda)Z(\lambda,\cdot)\mathrm{d}\lambda$$

results, using (5.76) in the modified equations of motion

$$\mathbf{0} = \mathbf{M}\ddot{\tilde{\mathbf{q}}} + \tilde{\mathbf{D}}\dot{\tilde{\mathbf{q}}} + \tilde{\mathbf{K}}\tilde{\mathbf{q}} + c\tilde{\mathbf{D}}\mathbf{M}^{-1}\mathbf{W}\int_0^{\infty} \mathrm{K}(\alpha,\lambda)z(\lambda,\cdot)\mathrm{d}\lambda. \tag{5.77}$$

The assumptions above directly yield

$$\tilde{\mathbf{D}}\mathbf{M}^{-1}\mathbf{W} = \left(d + c\sin\left(\frac{\alpha\pi}{2}\right)\omega^{\alpha-1}\right)m^{-1}\mathbf{W} =: \frac{\tilde{d}}{m}\mathbf{W},$$

which leads to the Lyapunov functional

$$V_6(\mathbf{q}_t, \mathbf{q}_t') = \frac{1}{2}\tilde{\mathbf{q}}_t(0)^{\mathrm{T}}\tilde{\mathbf{K}}\tilde{\mathbf{q}}_t(0) + \frac{1}{2}\tilde{\mathbf{q}}_t'(0)^{\mathrm{T}}\mathbf{M}\tilde{\mathbf{q}}_t'(0) + \frac{c\tilde{d}}{2m}\int_0^{\infty} \mathrm{K}(\alpha,\lambda)z^2(\lambda,t)\mathrm{d}\lambda.$$

Similar as for V_3, (5.30) can be shown for V_6 as $\tilde{\mathbf{K}}$, $\mathbf{M}$ are positive definite and its time derivative can be estimated by inserting the dynamics (5.77) and using (5.71) and (5.76) as

$$\begin{aligned}
\dot{V}_6 &= -\dot{\tilde{\mathbf{q}}}^{\mathrm{T}}\tilde{\mathbf{D}}\dot{\tilde{\mathbf{q}}} + \frac{c\tilde{d}}{m} c\mathbf{W}^{\mathrm{T}}\mathbf{M}^{-1}\mathbf{W}\left(\int_0^\infty \mathrm{K}(\alpha,\lambda) z(\lambda,\cdot)\mathrm{d}\lambda\right)^2 \\
&\quad - \frac{c\tilde{d}}{m}\int_0^\infty \mathrm{K}(\alpha,\lambda)\,\lambda\, z^2(\lambda,\cdot)\mathrm{d}\lambda \\
&\leq -\dot{\tilde{\mathbf{q}}}^{\mathrm{T}}\tilde{\mathbf{D}}\dot{\tilde{\mathbf{q}}} - \frac{c\tilde{d}}{m}\left(1 - \tfrac{c}{m}\cos\left(\tfrac{\alpha\pi}{2}\right)\omega^{\alpha-2}\right)\int_0^\infty \mathrm{K}(\alpha,\lambda)\,\lambda\, z^2(\lambda,\cdot)\mathrm{d}\lambda \\
&= -\dot{\tilde{\mathbf{q}}}^{\mathrm{T}}\tilde{\mathbf{D}}\dot{\tilde{\mathbf{q}}} - \frac{c\tilde{d}k}{m^2\omega^2}\int_0^\infty \mathrm{K}(\alpha,\lambda)\,\lambda\, z^2(\lambda,\cdot)\mathrm{d}\lambda \leq 0
\end{aligned}$$

such that (5.31) holds and $\{\mathbf{0}\}$ is the largest invariant set in $\{\boldsymbol{\varphi} \in X \mid \dot{V}_6(\boldsymbol{\varphi}) = 0\}$. Corollary 5.30 yields asymptotic stability as usual. A further generalization for several springpot elements is straightforward.

5.4 Controlled systems with fractional damping

In the following section, the Lyapunov approach derived for fractionally damped mechanical systems is applied to a more general tracking control problem with fractional and nonlinear damping. The basic ideas for the construction of Lyapunov functionals are similar to those presented so far.

Classical formulation of a Lur'e system and convergence

The following paragraph summarizes well known results regarding the stability of Lur'e systems, see e.g. Khalil (2002) for a more in-depth exposition. Moreover, it is meant as an introduction to certain controlled dynamical systems and the notion of convergence, see Pavlov et al. (2006), before these concepts are generalized for the fractionally damped case in subsequent sections. A *Lur'e system*, in the classical sense, is the connection of a linear system and an output dependent nonlinearity of the form

$$\begin{aligned}
\dot{\mathbf{x}} &= \mathbf{A}\mathbf{x} + \mathbf{B}w + \mathbf{D}\Lambda, \\
y &= \mathbf{C}\mathbf{x}, \\
-\Lambda &= \varphi(y),
\end{aligned} \tag{5.78}$$

where $\mathbf{x} \in \mathbb{R}^n$ is the system state, $w \in \mathbb{R}$ the (single) input and $y \in \mathbb{R}$ the (single) output of the system. Furthermore, the system matrices $\mathbf{A}$, $\mathbf{B}$, $\mathbf{C}$, $\mathbf{D}$ are considered

Section 5.4 is based on Hinze et al. (2020a).

to be constant and the pair $(\mathbf{A}, \mathbf{B})$ is controllable, $(\mathbf{A}, \mathbf{C})$ is observable. The nonlinearity $\varphi = \varphi(y)$ is a continuous function of the output y with $\varphi(0) = 0$. The uniform asymptotic stability of the origin of (5.78) (in the absence of the input w) for a certain class of nonlinearities φ is called *absolute stability*, named after Lur'e who originally formulated the problem, see Khalil (2002, Chap. 7). A related task considered by Yakubovich (1964) is the formulation of conditions on (5.78) such that for a class of inputs $w(t)$ asymptotic stability of all solutions is guaranteed. This leads to the more general notion of *convergent systems* as defined by Pavlov et al. (2006).

Definition 5.37 (Convergence)**.** A nonlinear system

$$\dot{\mathbf{x}} = \mathbf{f}(\mathbf{x}, w)$$

is called *(uniformly) convergent* for a class of piecewise continuous and bounded inputs $\mathcal{N}$, if there exists a solution $\bar{\mathbf{x}}_w(t)$ that is defined and bounded for all $t \in \mathbb{R}$ and globally (uniformly) asymptotically stable for every input $w \in \mathcal{N}$.

Hence, for a (uniformly) convergent system, the solution $\bar{\mathbf{x}}_w(t)$ is the unique *steady-state solution*. For a uniformly convergent system, it is known that a constant input $w(t)$ leads to a constant steady-state solution and a periodic input $w(t)$ with period time T results in a periodic steady-sate solution with the same period time T, see Pavlov et al. (2006). A specific task using known results on convergence is to solve the tracking problem for (5.78), i.e., to design a control law $w(t)$ such that a desired solution $\mathbf{x}_\mathrm{d}(t)$ is globally asymptotically stable for a certain class of nonlinearities φ. Particularly, consider monotonically nondecreasing functions φ with $\varphi(0) = 0$ such that

$$(y_1 - y_2)(\varphi(y_1) - \varphi(y_2)) \geq 0 \text{ for all } y_1, y_2 \in \mathbb{R}. \tag{5.79}$$

For this case it can be shown, see Pavlov et al. (2006, Sec. 5.4), that the tracking problem can be solved using a combination of linear tracking error-feedback and feedforward control in the form

$$w = \mathbf{K}(\mathbf{x} - \mathbf{x}_\mathrm{d}) + w_\mathrm{ff}\,, \tag{5.80}$$

where $\mathbf{K} \in \mathbb{R}^{1\times n}$ is the feedback gain matrix and w_ff the feedforward control. Together with (5.78), the closed-loop dynamics are given by

$$\begin{aligned} \dot{\mathbf{x}} &= \mathbf{A}_\mathrm{cl}\mathbf{x} + \mathbf{B}(w_\mathrm{ff} - \mathbf{K}\mathbf{x}_\mathrm{d}) + \mathbf{D}\Lambda, \\ y &= \mathbf{C}\mathbf{x}, \\ -\Lambda &= \varphi(y), \end{aligned} \tag{5.81}$$

where

$$\mathbf{A}_\mathrm{cl} = \mathbf{A} + \mathbf{B}\mathbf{K}. \tag{5.82}$$

The feedforward $w_{\mathrm{ff}}(t)$ in (5.80) is chosen such that $\mathbf{x}_{\mathrm{d}}(t)$ is a solution of (5.81) and the control gain $\mathbf{K}$ is designed such that all solutions of (5.81) approach $\mathbf{x}_{\mathrm{d}}(t)$, i.e., (5.81) is a convergent system. To give sufficient conditions for convergence of (5.81), consider the *incremental Lyapunov function* of two solutions $\mathbf{x}_1$ and $\mathbf{x}_2$ as

$$V_7(\mathbf{x}_1 - \mathbf{x}_2) = \frac{1}{2}(\mathbf{x}_1 - \mathbf{x}_2)^{\mathrm{T}}\mathbf{P}(\mathbf{x}_1 - \mathbf{x}_2), \tag{5.83}$$

where $\mathbf{P}$ is symmetric and positive definite. The application of Theorem 5.8 leads to the following absolute stability result of Yakubovich (1964) (see also Pavlov et al. (2004) for a historic review).

Theorem 5.38. *Consider the system* (5.81) *with* (5.79), (5.82), *where* w_{ff} *is chosen such that* $\mathbf{x}_{\mathrm{d}}$ *is a bounded continuous solution of* (5.81). *If there exists a symmetric, positive definite matrix* $\mathbf{P}$ *and a feedback gain* $\mathbf{K}$ *such that the relations*

$$\mathbf{A}_{\mathrm{cl}}^{\mathrm{T}}\mathbf{P} + \mathbf{P}\mathbf{A}_{\mathrm{cl}} < 0, \tag{5.84}$$

$$\mathbf{D}^{\mathrm{T}}\mathbf{P} = \mathbf{C} \tag{5.85}$$

hold, then all solutions of (5.81) *asymptotically approach* $\mathbf{x}_{\mathrm{d}}(t)$.

Proof. The Lyapunov function (5.83) is a positive definite and radially unbounded function of the error between two solutions

$$\mathbf{e} := \mathbf{x}_1 - \mathbf{x}_2\,,$$

i.e., (5.83) can be reformulated as

$$V_7(\mathbf{e}) = \frac{1}{2}\mathbf{e}^{\mathrm{T}}\mathbf{P}\mathbf{e}.$$

The associated error dynamics can be derived from (5.81) as

$$\dot{\mathbf{e}} = \mathbf{A}_{\mathrm{cl}}\mathbf{e} - \mathbf{D}(\varphi(\mathbf{C}\mathbf{x}_1(t)) - \varphi(\mathbf{C}\mathbf{x}_1(t) - \mathbf{C}\mathbf{e})),$$

which represents a nonautonomous ODE. The time-derivative of V_7 along solutions yields

$$\begin{aligned}
\dot{V}_7 &= \dot{\mathbf{e}}^{\mathrm{T}}\mathbf{P}\mathbf{e} = \left(\mathbf{A}_{\mathrm{cl}}\mathbf{e} - \mathbf{D}(\varphi(\mathbf{C}\mathbf{x}_1(t)) - \varphi(\mathbf{C}\mathbf{x}_1(t) - \mathbf{C}\mathbf{e}))\right)^{\mathrm{T}}\mathbf{P}\mathbf{e} \\
&= \frac{1}{2}\mathbf{e}^{\mathrm{T}}\left(\mathbf{A}_{\mathrm{cl}}^{\mathrm{T}}\mathbf{P} + \mathbf{P}\mathbf{A}_{\mathrm{cl}}\right)\mathbf{e} - (\varphi(\mathbf{C}\mathbf{x}_1(t)) - \varphi(\mathbf{C}\mathbf{x}_1(t) - \mathbf{C}\mathbf{e}))\mathbf{D}^{\mathrm{T}}\mathbf{P}\mathbf{e} \\
&= \frac{1}{2}\mathbf{e}^{\mathrm{T}}\left(\mathbf{A}_{\mathrm{cl}}^{\mathrm{T}}\mathbf{P} + \mathbf{P}\mathbf{A}_{\mathrm{cl}}\right)\mathbf{e} - (\varphi(\mathbf{C}\mathbf{x}_1(t)) - \varphi(\mathbf{C}\mathbf{x}_1(t) - \mathbf{C}\mathbf{e}))\mathbf{C}\mathbf{e},
\end{aligned}$$

where (5.85) is applied in the last line. The monotonicity condition (5.79) and (5.84) reveal that $\dot{V}_7$ is negative definite and hence, according to Theorem 5.8, the tracking error dynamics is globally asymptotically stable and particularly, the bounded solution $\mathbf{x}_{\mathrm{d}}$ of (5.81) is asymptotically approached by all solutions of (5.81). □

Generalization for the case of fractional damping

The above results will be generalized for a class of fractionally damped nonlinear systems of the form

$$\begin{aligned} \dot{\mathbf{x}} &= \mathbf{A}\mathbf{x} + \mathbf{B}w + \mathbf{D}\Lambda + \mathbf{F}\nu, \\ y &= \mathbf{C}\mathbf{x}, \\ -\Lambda &= \varphi(y), \\ -\nu &= c\,{}^{\mathrm{C}}\mathrm{D}^{\alpha} g, \quad g = \mathbf{E}_0\mathbf{x}, \quad \dot{g} = \mathbf{E}_1\mathbf{x}, \end{aligned} \tag{5.86}$$

where again $\mathbf{x} \in \mathbb{R}^n$ is the system state, $w \in \mathbb{R}$ the (single) input, $y \in \mathbb{R}$ and $g \in \mathbb{R}$ the outputs of the linear system and $\mathbf{A}$, $\mathbf{B}$, $\mathbf{C}$, $\mathbf{D}$, $\mathbf{E}_0$, $\mathbf{E}_1$, $\mathbf{F}$ are constant matrices that fulfill

$$\mathbf{E}_1 = \mathbf{E}_0\mathbf{A}, \quad \mathbf{E}_0\mathbf{B} = \mathbf{E}_0\mathbf{D} = \mathbf{E}_0\mathbf{F} = 0.$$

Furthermore, ${}^{\mathrm{C}}\mathrm{D}^{\alpha} g$ is the fractional derivative of the elongation g of a springpot and $\varphi = \varphi(y)$ is a nonlinear function of the output y that fulfills (5.79). Again, consider the problem of tracking a desired solution $\mathbf{x}_{\mathrm{d}}(t)$ of (5.86) using a control law of the form (5.80), which leads to the closed-loop dynamics

$$\begin{aligned} \dot{\mathbf{x}} &= \mathbf{A}_{\mathrm{cl}}\mathbf{x} + \mathbf{B}(w_{\mathrm{ff}} - \mathbf{K}\mathbf{x}_{\mathrm{d}}) + \mathbf{D}\Lambda + \mathbf{F}\nu, \\ y &= \mathbf{C}\mathbf{x}, \\ -\Lambda &= \varphi(y), \\ -\nu &= c\,{}^{\mathrm{C}}\mathrm{D}^{\alpha} g, \quad g = \mathbf{E}_0\mathbf{x}, \quad \dot{g} = \mathbf{E}_1\mathbf{x} \end{aligned} \tag{5.87}$$

with $\mathbf{A}_{\mathrm{cl}}$ as in (5.82). As before, the feedforward $w_{\mathrm{ff}}(t)$ in (5.80) is chosen such that $\mathbf{x}_{\mathrm{d}}(t)$ is a solution of (5.87) and the control gain $\mathbf{K}$ is designed to render (5.87) convergent. Sufficient conditions for that will be given with the help of a Lyapunov functional inspired from (5.83) and adapted to the fractional derivative terms in (5.87). Hereto, consider the infinite states

$$\begin{aligned} \dot{z}(\eta, t) &= \dot{g}(t) - \eta z(\eta, t), \quad \eta \geq 0, \\ z(\eta, 0) &= \int_{-\infty}^{0} \mathrm{e}^{\eta\tau} g'(\tau)\mathrm{d}\tau, \quad \eta \geq 0 \end{aligned}$$

of a springpot as in (2.29) such that

$${}^{\mathrm{C}}\mathrm{D}^{\alpha} g(t) = \int_0^{\infty} \mu_{1-\alpha}(\lambda) z(\lambda, t)\mathrm{d}\lambda$$

and the second kind of infinite states

$$\begin{aligned} \dot{Z}(\eta, t) &= z(\eta, t) = g(t) - \eta Z(\eta, t), \quad \eta \geq 0, \\ Z(\eta, 0) &= \int_{-\infty}^{0} \mathrm{e}^{\eta\tau} g(\tau)\mathrm{d}\tau, \quad \eta \geq 0 \end{aligned}$$

as in (2.26). This leads together with (5.87) to the reformulated system

$$\begin{aligned}
\dot{\mathbf{x}} &= \mathbf{A}_{\mathrm{cl}}\mathbf{x} + \mathbf{B}(w_{\mathrm{ff}} - \mathbf{K}\mathbf{x}_{\mathrm{d}}) + \mathbf{D}\Lambda - c\mathbf{F}\int_0^\infty \mu_{1-\alpha}(\lambda) z(\lambda,\cdot)\mathrm{d}\lambda,\\
\dot{Z}(\eta,\cdot) &= z(\eta,\cdot) = \mathbf{E}_0\mathbf{x} - \eta Z(\eta,\cdot),\\
\dot{z}(\eta,\cdot) &= \mathbf{E}_1\mathbf{x} - \eta z(\eta,\cdot),\\
y &= \mathbf{C}\mathbf{x},\\
-\Lambda &= \varphi(y).
\end{aligned} \tag{5.88}$$

To give sufficient conditions for convergence of (5.88), consider the incremental Lyapunov functional of two solutions $\mathbf{x}_1$ and $\mathbf{x}_2$ as

$$\begin{aligned}
V_8(\mathbf{x}_{1,t} - \mathbf{x}_{2,t}) = \frac{1}{2}&(\mathbf{x}_{1,t}(0) - \mathbf{x}_{2,t}(0))^{\mathrm{T}}\mathbf{P}(\mathbf{x}_{1,t}(0) - \mathbf{x}_{2,t}(0))\\
&+ \frac{\delta_0}{2}\int_0^\infty \mu_{1-\alpha}(\lambda)\,\lambda\,(Z_1(\lambda,t) - Z_2(\lambda,t))^2\mathrm{d}\lambda\\
&+ \frac{\delta_1}{2}\int_0^\infty \mu_{1-\alpha}(\lambda)(z_1(\lambda,t) - z_2(\lambda,t))^2\mathrm{d}\lambda,
\end{aligned} \tag{5.89}$$

where $\mathbf{P}$ is symmetric, positive definite and $\delta_0 \geq 0$, $\delta_1 > 0$. Similar as for the classical case, the functional (5.89) can be reformulated in terms of the error between two solutions, which now includes the infinite states, namely

$$\begin{aligned}
\mathbf{e} &= \mathbf{x}_1 - \mathbf{x}_2,\\
e_Z(\eta,\cdot) &= Z_1(\eta,\cdot) - Z_2(\eta,\cdot),\\
e_z(\eta,\cdot) &= z_1(\eta,\cdot) - z_2(\eta,\cdot).
\end{aligned}$$

Thus, V_8 is given by

$$\begin{aligned}
V_8(\mathbf{e}_t) = \frac{1}{2}&\mathbf{e}_t(0)^{\mathrm{T}}\mathbf{P}\mathbf{e}_t(0) + \frac{\delta_0}{2}\int_0^\infty \mu_{1-\alpha}(\lambda)\,\lambda\, e_Z^2(\lambda,t)\mathrm{d}\lambda\\
&+ \frac{\delta_1}{2}\int_0^\infty \mu_{1-\alpha}(\lambda) e_z^2(\lambda,t)\mathrm{d}\lambda,
\end{aligned}$$

which represents a Lyapunov functional for the nonautonomous error dynamics derived from (5.88) as

$$\begin{aligned}
\dot{\mathbf{e}} &= \mathbf{A}_{\mathrm{cl}}\mathbf{e} - \mathbf{D}(\varphi(\mathbf{C}\mathbf{x}_1(t)) - \varphi(\mathbf{C}\mathbf{x}_1(t) - \mathbf{C}\mathbf{e})) - c\mathbf{F}\int_0^\infty \mu_{1-\alpha}(\lambda) e_z(\lambda,\cdot)\mathrm{d}\lambda,\\
\dot{e}_Z(\eta,\cdot) &= e_z(\eta,\cdot) = \mathbf{E}_0\mathbf{e} - \eta e_Z(\eta,\cdot),\\
\dot{e}_z(\eta,\cdot) &= \mathbf{E}_1\mathbf{e} - \eta e_z(\eta,\cdot).
\end{aligned} \tag{5.90}$$

The time-derivative of V_8 along solutions of (5.90) results in

$$\begin{aligned}
\dot{V}_8 &= \dot{\mathbf{e}}^{\mathrm{T}}\mathbf{P}\mathbf{e} + \delta_0 \int_0^\infty \mu_{1-\alpha}(\lambda)\, \lambda\, e_Z(\lambda,\cdot)\dot{e}_Z(\lambda,\cdot)\,\mathrm{d}\lambda \\
&\quad + \delta_1 \int_0^\infty \mu_{1-\alpha}(\lambda)\dot{e}_z(\lambda,\cdot)e_z(\lambda,\cdot)\,\mathrm{d}\lambda, \\
&= \left(\mathbf{A}_{\mathrm{cl}}\mathbf{e} - \mathbf{D}(\varphi(\mathbf{C}\mathbf{x}_1(t)) - \varphi(\mathbf{C}\mathbf{x}_1(t) - \mathbf{C}\mathbf{e})) - c\mathbf{F}\int_0^\infty \mu_{1-\alpha}(\lambda)e_z(\lambda,\cdot)\mathrm{d}\lambda\right)^{\mathrm{T}}\mathbf{P}\mathbf{e} \\
&\quad + \delta_0 \int_0^\infty \mu_{1-\alpha}(\lambda)(\mathbf{E}_0\mathbf{e} - e_z(\lambda,\cdot))e_z(\lambda,\cdot)\mathrm{d}\lambda \\
&\quad + \delta_1 \int_0^\infty \mu_{1-\alpha}(\lambda)(\mathbf{E}_1\mathbf{e} - \lambda\, e_z(\lambda,\cdot))e_z(\lambda,\cdot)\mathrm{d}\lambda \qquad (5.91) \\
&= \frac{1}{2}\mathbf{e}^{\mathrm{T}}(\mathbf{A}_{\mathrm{cl}}^{\mathrm{T}}\mathbf{P} + \mathbf{P}\mathbf{A}_{\mathrm{cl}})\mathbf{e} - (\varphi(\mathbf{C}\mathbf{x}_1(t)) - \varphi(\mathbf{C}\mathbf{x}_1(t) - \mathbf{C}\mathbf{e}))\mathbf{D}^{\mathrm{T}}\mathbf{P}\mathbf{e} \\
&\quad + \int_0^\infty \mu_{1-\alpha}(\lambda)e_z(\lambda,\cdot)\,\mathrm{d}\lambda\,(\delta_0\mathbf{E}_0 + \delta_1\mathbf{E}_1 - c\mathbf{F}^{\mathrm{T}}\mathbf{P})\,\mathbf{e} \\
&\quad - \int_0^\infty \mu_{1-\alpha}(\lambda)(\delta_0 + \delta_1\lambda)e_z^2(\lambda,\cdot)\,\mathrm{d}\lambda.
\end{aligned}$$

From the terms in (5.91), conditions for convergence of (5.88) can be extracted, which are formulated in the following theorem.

Theorem 5.39. *Consider the system* (5.88) *with* (5.79) *and* (5.82), *where* $w_{\mathrm{ff}}(t)$ *is chosen such that* $\mathbf{x}_{\mathrm{d}}(t)$ *is a bounded continuous solution of* (5.88). *If there exists a symmetric, positive definite matrix* $\mathbf{P}$, *coefficients* $\delta_0 \geq 0$, $\delta_1 > 0$ *and a feedback gain* $\mathbf{K}$ *such that the relations*

$$\mathbf{A}_{\mathrm{cl}}^{\mathrm{T}}\mathbf{P} + \mathbf{P}\mathbf{A}_{\mathrm{cl}} \leq 0, \qquad (5.92)$$

$$\mathbf{D}^{\mathrm{T}}\mathbf{P} = \mathbf{C}, \qquad (5.93)$$

$$\delta_0\mathbf{E}_0 + \delta_1\mathbf{E}_1 = c\mathbf{F}^{\mathrm{T}}\mathbf{P}, \qquad (5.94)$$

$$\ker(\mathbf{E}_1) \cap \ker(\mathbf{E}_1\mathbf{A}_{\mathrm{cl}}) \cap \ker(\mathbf{A}_{\mathrm{cl}}^{\mathrm{T}}\mathbf{P} + \mathbf{P}\mathbf{A}_{\mathrm{cl}}) = \{\mathbf{0}\} \qquad (5.95)$$

hold, then all solutions of (5.88) *asymptotically approach* $\mathbf{x}_{\mathrm{d}}(t)$.

The condition (5.92) is weaker than the classical Lyapunov inequality (5.84) in Theorem 5.38. Hence, for the theorem to hold, the generalized invariance principle in Theorem 5.31 is applied to prove asymptotic stability.

Proof of Theorem 5.39. Initially, it has to be guaranteed that the right-hand side of (5.90) is bounded for bounded inputs. The proof results from (5.41) and (5.42) as for the single degree-of freedom oscillator. The second step is to determine the limiting equation (5.32) of (5.90). Therefore, consider the Lyapunov functional V_8,

being bounded from below and defined on a compact set in X, which contains $\{\mathbf{e}_t \mid t \geq 0\}$ such that the limit

$$\lim_{t\to\infty} V_8(\mathbf{e}_t) = a \geq 0 \tag{5.96}$$

exists. Further, consider the time derivative (5.91) of V_8, which in view of (5.93) and (5.94) fulfills

$$\begin{aligned}\dot{V}_8 = \frac{1}{2}\mathbf{e}^{\mathrm{T}}(\mathbf{A}_{\mathrm{cl}}^{\mathrm{T}}\mathbf{P} + \mathbf{P}\mathbf{A}_{\mathrm{cl}})\mathbf{e} - (\varphi(\mathbf{C}\mathbf{x}_1) - \varphi(\mathbf{C}\mathbf{x}_1 - \mathbf{C}\mathbf{e}))\mathbf{C}\mathbf{e} \\ - \int_0^\infty \mu_{1-\alpha}(\lambda)(\delta_0 + \delta_1\lambda)e_z^2(\lambda,\cdot)\,\mathrm{d}\lambda.\end{aligned} \tag{5.97}$$

A further estimation of (5.97) yields

$$\dot{V}_8 \leq -(\varphi(\mathbf{C}\mathbf{x}_1(t)) - \varphi(\mathbf{C}\mathbf{x}_1(t) - \mathbf{C}\mathbf{e}))\mathbf{C}\mathbf{e}.$$

Assume that

$$\varphi(\mathbf{C}\mathbf{x}_1(t)) - \varphi(\mathbf{C}\mathbf{x}_1(t) - \mathbf{C}\mathbf{e}) \tag{5.98}$$

would not vanish for $t \to \infty$. Then, $\dot{V}_8$ would have a negative limit, which contradicts (5.96). Accordingly, the term (5.98) has to vanish for $t \to \infty$, which leads to the limiting equation of (5.90)

$$\begin{aligned}\dot{\mathbf{e}} = \mathbf{f}^*(\mathbf{e}_t) = \mathbf{A}_{\mathrm{cl}}\mathbf{e}_t(0) - c\mathbf{F}\int_0^\infty \mu_{1-\alpha}(\lambda)e_z(\lambda,\cdot)\mathrm{d}\lambda, \\ \dot{e}_Z(\eta,\cdot) = e_z(\eta,\cdot) = \mathbf{E}_0\mathbf{e} - \eta e_Z(\eta,\cdot), \\ \dot{e}_z(\eta,\cdot) = \mathbf{E}_1\mathbf{e} - \eta e_z(\eta,\cdot).\end{aligned} \tag{5.99}$$

Hence, Theorem 5.31 can be applied. Therefore, consider another estimation of (5.97), viz.

$$\dot{V}_8 \leq \frac{1}{2}\mathbf{e}_t(0)^{\mathrm{T}}(\mathbf{A}_{\mathrm{cl}}^{\mathrm{T}}\mathbf{P} + \mathbf{P}\mathbf{A}_{\mathrm{cl}})\mathbf{e}_t(0) - \int_0^\infty \mu_{1-\alpha}(\lambda)(\delta_0 + \delta_1\lambda)e_z^2(\lambda,\cdot)\,\mathrm{d}\lambda =: W(\mathbf{e}_t) \tag{5.100}$$

and examine the largest invariant set w.r.t. (5.99) in $E := \{\boldsymbol{\varphi} \in X \mid W(\boldsymbol{\varphi}) = 0\}$. The integral term in (5.100) yields

$$e_z(\eta, t) = 0 \text{ for almost all } \eta \geq 0,\ t \geq 0,\ \mathbf{e}_t \in E \tag{5.101}$$

and substitution of (5.101) in the e_z-dynamics of (5.99) leads to

$$\mathbf{E}_1\mathbf{e} = 0 \text{ for } \mathbf{e}_t \in E,\ t \geq 0. \tag{5.102}$$

Moreover, using (5.102) in the $\mathbf{e}$-dynamics of (5.99) results in

$$\mathbf{E}_1\dot{\mathbf{e}} = 0 = \mathbf{E}_1\mathbf{A}_{\mathrm{cl}}\mathbf{e} \text{ for } \mathbf{e}_t \in E,\ t \geq 0.$$

Considering the first term in (5.100) and using condition (5.95), one obtains that $\{\mathbf{0}\}$ is the largest invariant set in E. From Theorem 5.31, one can conclude that all solutions of (5.88) converge to each other. As $\mathbf{x}_{\mathrm{d}}$ is a bounded solution of (5.88), all solutions asymptotically approach $\mathbf{x}_{\mathrm{d}}$. □

Tracking control of a motor-load archetype system

Consider a typical motor-load configuration where the nonlinear damping Λ and the actuation w are non-collocated (Figure 5.10), inspired from the example by Leine and van de Wouw (2008, Sec. 8.4.2). Herein, the translational motion of two interconnected masses, representing motor and load, is considered being mechanically equivalent to its rotational counterpart. The aim in this tracking problem is to track the (translational resp. rotational) *velocity* of the load and not its position. Following Leine and van de Wouw (2008), consider two masses m_1 and m_2 with coordinates q_1 and q_2 which are linked by a spring (stiffness k). The first mass is actuated by a control force w and on the second mass acts a nonlinear damping force $-\Lambda = \varphi(\dot{q}_2)$ that fulfills (5.79). The results by Leine and van de Wouw (2008) are generalized by replacing the dashpot between the two masses by a springpot (coefficient $c > 0$, differentiation order $\alpha \in (0,1)$). Using the law of linear momentum, one obtains a system of the form (5.86), where

$$\begin{gathered}\mathbf{A} = \begin{bmatrix} 0 & -1 & 1 \\ \frac{k}{m_1} & 0 & 0 \\ -\frac{k}{m_2} & 0 & 0 \end{bmatrix}, \ \mathbf{B} = \begin{bmatrix} 0 \\ \frac{1}{m_1} \\ 0 \end{bmatrix}, \ \mathbf{D} = \begin{bmatrix} 0 \\ 0 \\ -\frac{1}{m_2} \end{bmatrix}, \\ \mathbf{F} = \begin{bmatrix} 0 \\ -\frac{1}{m_1} \\ \frac{1}{m_2} \end{bmatrix}, \ \mathbf{C}^{\mathrm{T}} = \begin{bmatrix} 0 \\ 0 \\ -1 \end{bmatrix}, \ \mathbf{E}_0^{\mathrm{T}} = \begin{bmatrix} 1 \\ 0 \\ 0 \end{bmatrix}\end{gathered} \tag{5.103}$$

and $\mathbf{x} = \begin{bmatrix} q_2 - q_1 & \dot{q}_1 & \dot{q}_2 \end{bmatrix}^{\mathrm{T}}$. Note that this state vector does not contain the absolute positions q_1 and q_2 as velocity tracking is the aim of this control strategy. Initially, a stationary solution with desired velocity v_{d} (for both masses) shall be

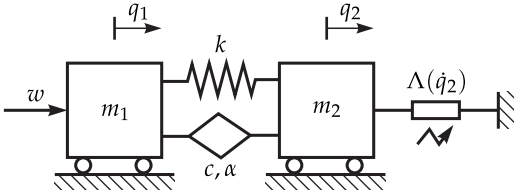

Figure 5.10: Typical motor-load configuration with non-collocated nonlinear damping and actuation.

tracked. Therefore, introduce a control law (5.80) and reformulate the system as in (5.88). Related to the desired solution of constant velocity is an equilibrium of (5.87)

$$\mathbf{x}_{\mathrm{d}} = \begin{bmatrix} -\frac{1}{k}\varphi(v_{\mathrm{d}}) & v_{\mathrm{d}} & v_{\mathrm{d}} \end{bmatrix}^{\mathrm{T}}$$

when a feedforward control

$$w_{\mathrm{ff}} = \varphi(v_{\mathrm{d}})$$

is used. When choosing

$$\mathbf{P} = \begin{bmatrix} 2k & -\sqrt{km_1} & 0 \\ -\sqrt{km_1} & m_1 & 0 \\ 0 & 0 & m_2 \end{bmatrix}, \quad \delta_0 = c\sqrt{\frac{k}{m_1}}, \quad \delta_1 = c$$

together with the feedback gain

$$\mathbf{K} = \begin{bmatrix} -k & -2\sqrt{km_1} & \sqrt{km_1} \end{bmatrix}, \tag{5.104}$$

all conditions in Theorem 5.39 are fulfilled. In particular,

$$\mathbf{A}_{\mathrm{cl}}^{\mathrm{T}}\mathbf{P} + \mathbf{P}\mathbf{A}_{\mathrm{cl}} = -2\sqrt{km_1}\begin{bmatrix} 0 & 0 & 0 \\ 0 & 1 & 0 \\ 0 & 0 & 0 \end{bmatrix} \leq 0,$$

$$\ker(\mathbf{E}_1) = \left\langle \begin{bmatrix} 1 \\ 0 \\ 0 \end{bmatrix}, \begin{bmatrix} 0 \\ 1 \\ 1 \end{bmatrix} \right\rangle,$$

$$\ker(\mathbf{E}_1\mathbf{A}_{\mathrm{cl}}) = \left\langle \begin{bmatrix} 0 \\ 1 \\ 2 \end{bmatrix}, \begin{bmatrix} -m_2 \\ 0 \\ \sqrt{km_1} \end{bmatrix} \right\rangle,$$

$$\ker(\mathbf{A}_{\mathrm{cl}}^{\mathrm{T}}\mathbf{P} + \mathbf{P}\mathbf{A}_{\mathrm{cl}}) = \left\langle \begin{bmatrix} 1 \\ 0 \\ 0 \end{bmatrix}, \begin{bmatrix} 0 \\ 0 \\ 1 \end{bmatrix} \right\rangle.$$

The control law given above is implemented in order to simulate the solutions of the closed loop system (5.88) with (5.103), parameters

$$m_1 = m_2 = 1\,\mathrm{kg}, \quad k = 100\,\frac{\mathrm{N}}{\mathrm{m}}, \quad c = 1\,\frac{\mathrm{Ns}^{\alpha}}{\mathrm{m}}, \quad \alpha = 0.5, \tag{5.105}$$

desired velocity $v_{\mathrm{d}} = 1\,\frac{\mathrm{m}}{\mathrm{s}}$ and a nonlinearity

$$\varphi(y) = b\tanh\left(\frac{y}{v_{\mathrm{d}}}\right), \quad b = 1\,\mathrm{N},$$

that models regularized Coulomb friction for the second mass. The reformulated infinite state scheme from Chapter 3 is used and tracking is depicted in Figure 5.11 for the initial conditions

$$\mathbf{x}(0) = \begin{bmatrix} 0 & 5 & 5 \end{bmatrix}^{\mathrm{T}}, \quad Z(\eta, 0) = 0, \quad z(\eta, 0) = 0, \quad \eta \geq 0. \tag{5.106}$$

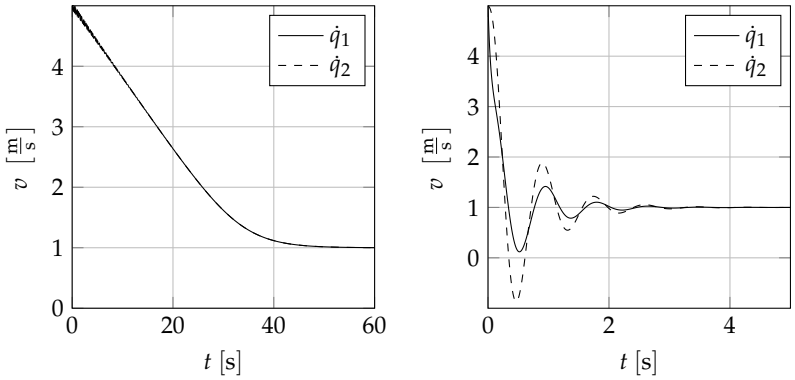

Figure 5.11: Tracking of $v_\text{d} = 1\,\frac{\text{m}}{\text{s}}$ for both masses with feedforward (left) or feedback and feedforward control (right).

It can be observed that, even without feedback control, tracking is achieved (although much slower), as the nonlinearity contributes to the attractivity of $\mathbf{x}_\text{d}$.

In a second step, it will be shown that the feedback gain (5.104) can be used to stabilize any bounded time-varying desired solution $\mathbf{x}_\text{d}$. However, for a non-constant desired solution the determination of the associated feedforward w_ff becomes cumbersome and generally has to be computed numerically. Here, an example with solution in closed form is provided. Consider the nonlinear damping

$$\varphi(y) = dy^3, \quad d > 0$$

and a desired oscillating velocity of the second mass

$$\dot{q}_{2,\text{d}}(t) = A\Omega\cos(\Omega t). \tag{5.107}$$

Using the harmonic balance method, the associated desired trajectory $\mathbf{x}_\text{d}$ with components

$$\begin{aligned}
x_{\text{d},1}(t) &= P_\text{s}\sin(\Omega t) + P_\text{c}\cos(\Omega t) + R_\text{s}\sin(3\Omega t) + R_\text{c}\cos(3\Omega t),\\
x_{\text{d},2}(t) &= (A - P_\text{s})\Omega\cos(\Omega t) + P_\text{c}\Omega\sin(\Omega t) - 3R_\text{s}\Omega\cos(3\Omega t) + 3R_\text{c}\Omega\sin(3\Omega t),\\
x_{\text{d},3}(t) &= A\Omega\cos(\Omega t)
\end{aligned}$$

is obtained together with the feedforward

$$\begin{aligned}
w_\text{ff}(t) = (m_1(P_\text{s} - A) - m_2 A)\Omega^2\sin(\Omega t) + \left(m_1 P_\text{c} + \frac{3}{4}dA^3\Omega\right)\Omega^2\cos(\Omega t)\\
+ 9m_1 R_\text{s}\Omega^2\sin(3\Omega t) + \left(9m_1 R_\text{c} + \frac{1}{4}dA^3\Omega\right)\Omega^2\cos(3\Omega t)
\end{aligned}$$

with coefficients

$$
\begin{aligned}
P_\mathrm{s} &= \left(m_2 \left(k + c\cos\left(\frac{\alpha\pi}{2}\right)\Omega^\alpha \right) - \frac{3}{4} d A^2 \Omega c \sin\left(\frac{\alpha\pi}{2}\right)\Omega^\alpha \right) A\Omega^2 / L_1 \,, \\
P_\mathrm{c} &= -\left(\frac{3}{4} d A^2 \Omega \left(k + c\cos\left(\frac{\alpha\pi}{2}\right)\Omega^\alpha \right) + m_2 c \sin\left(\frac{\alpha\pi}{2}\right)\Omega^\alpha \right) A\Omega^2 / L_1 \,, \\
L_1 &= \left(k + c\cos\left(\frac{\alpha\pi}{2}\right)\Omega^\alpha \right)^2 + \left(c\sin\left(\frac{\alpha\pi}{2}\right)\Omega^\alpha \right)^2 , \\
R_\mathrm{s} &= -\frac{1}{4} d A^3 \Omega^3 c \sin\left(\frac{\alpha\pi}{2}\right)(3\Omega)^\alpha / L_3 \,, \\
R_\mathrm{c} &= -\frac{1}{4} d A^3 \Omega^3 \left(k + c\cos\left(\frac{\alpha\pi}{2}\right)(3\Omega)^\alpha \right) / L_3 \,, \\
L_3 &= \left(k + c\cos\left(\frac{\alpha\pi}{2}\right)(3\Omega)^\alpha \right)^2 + \left(c\sin\left(\frac{\alpha\pi}{2}\right)(3\Omega)^\alpha \right)^2 .
\end{aligned}
$$

Using parameters as in (5.105) together with

$$
d = 0.2\,\frac{\mathrm{Ns}^3}{\mathrm{m}^3}\,, \quad A = 1\,\mathrm{m}, \quad \Omega = 1\,\frac{1}{\mathrm{s}}
$$

and initial conditions (5.106), tracking is achieved (with and without feedback) as shown in Figure 5.12. The addition of feedback greatly ameliorates the tracking speed.

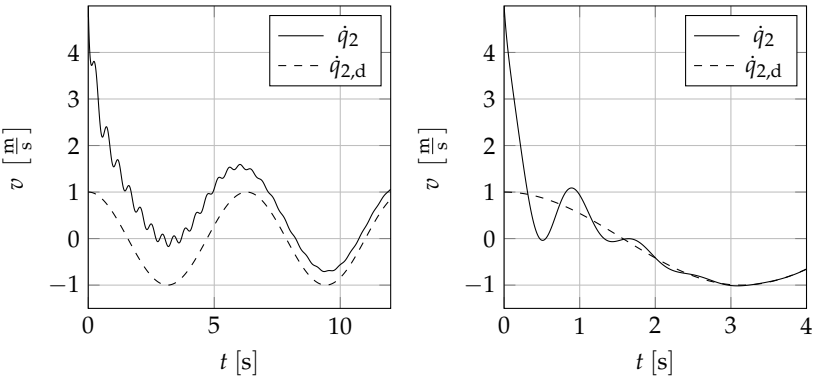

Figure 5.12: Tracking of $\dot{q}_{2,\mathrm{d}}$ from (5.107) with feedforward (left) or feedback and feedforward control (right).

CHAPTER 6

Finite element method

The following chapter introduces a method which incorporates a fractional Zener model (for hydrostatic and deviatoric components) of a three-dimensional continuum (assuming small deformations) in the finite element method. The algorithm uses the reformulated infinite state representation and the associated numerical scheme introduced in Chapter 3.

6.1 Formulation of the fractional Zener model for a 3D continuum

Initially, consider once again a (one-dimensional) fractional Zener model (Figure 6.1) as introduced in Section 4.2. As an alternative to the relaxation function

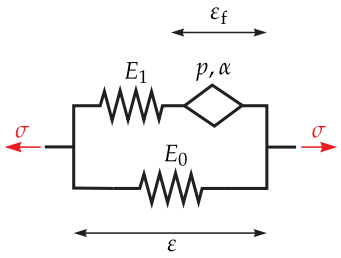

Figure 6.1: Fractional Zener model.

(4.57), the model is described by the equations

$$\begin{aligned} \sigma(x,t) &= (E_0 + E_1)\varepsilon(x,t) - E_1\varepsilon_f(x,t), \\ p\,{}^{C}\mathrm{D}^{\alpha}\varepsilon_f(x,t) &= E_1(\varepsilon(x,t) - \varepsilon_f(x,t)), \end{aligned} \tag{6.1}$$

where the internal variable ε_f denotes the strain of the springpot in Figure 6.1. This representation is according to the state variables approach for classical vis-

coelastic constitutive laws introduced by Creus (1986, Chap. VII) and Marques and Creus (2012, Chaps. 3 and 9) or the internal variable model by Simo and Hughes (1998, Chap. 10). In the formulation (6.1), the position dependence of stress and strain is explicitly taken into consideration. Thus, the model parameters are assumed to be independent of the position variable x, i.e., a homogeneous material is considered. Further, plugging the reformulated infinite state representation (3.4) of the fractional derivative of ε_{f} in (6.1) yields

$$\begin{aligned}
\sigma(x,t) &= (E_0+E_1)\varepsilon(x,t) - E_1\varepsilon_{\mathrm{f}}(x,t),\\
p\sin\left(\frac{\alpha\pi}{2}\right)\omega^{\alpha-1}\dot{\varepsilon}_{\mathrm{f}}(x,t) - p\int_0^\infty \mathrm{K}(\alpha,\lambda)\dot{z}(\lambda,x,t)\mathrm{d}\lambda &\\
= E_1\varepsilon(x,t) - \left(E_1 + p\cos\left(\frac{\alpha\pi}{2}\right)\omega^{\alpha}\right)\varepsilon_{\mathrm{f}}(x,t) &\\
+ p\omega^2\int_0^\infty \mathrm{K}(\alpha,\lambda)Z(\lambda,x,t)\mathrm{d}\lambda, &\\
\dot{Z}(\eta,x,t) = \varepsilon_{\mathrm{f}}(x,t) - \eta Z(\eta,x,t), &\\
\dot{z}(\eta,x,t) = \dot{\varepsilon}_{\mathrm{f}}(x,t) - \eta z(\eta,x,t). &
\end{aligned} \tag{6.2}$$

Similar as in Section 4.3, for the three-dimensional isotropic case, assume a fractional Zener model (6.2) for hydrostatic and deviatoric components each. To formulate the associated relations, use the Cauchy stress tensor

$$\tilde{\boldsymbol{\sigma}} = \left[\sigma_{xx}\ \sigma_{yy}\ \sigma_{zz}\ \sigma_{xy}\ \sigma_{yz}\ \sigma_{zx}\right]^{\mathrm{T}} \tag{6.3}$$

and the linear strain tensor

$$\tilde{\boldsymbol{\varepsilon}} = \left[\varepsilon_{xx}\ \varepsilon_{yy}\ \varepsilon_{zz}\ \gamma_{xy}\ \gamma_{yz}\ \gamma_{zx}\right]^{\mathrm{T}} \tag{6.4}$$

in *Voigt notation*. The separation in hydrostatic and deviatoric parts is, equivalent to (4.11) and (4.12), given by

$$\begin{aligned}
\tilde{\boldsymbol{\sigma}} &= \tilde{\boldsymbol{\sigma}}_{\mathrm{h}} + \tilde{\boldsymbol{\sigma}}_{\mathrm{d}} = \mathbf{T}_{\mathrm{h}}\tilde{\boldsymbol{\sigma}} + \mathbf{T}_{\mathrm{d}}\tilde{\boldsymbol{\sigma}},\\
\tilde{\boldsymbol{\varepsilon}} &= \tilde{\boldsymbol{\varepsilon}}_{\mathrm{h}} + \tilde{\boldsymbol{\varepsilon}}_{\mathrm{d}} = \mathbf{T}_{\mathrm{h}}\tilde{\boldsymbol{\varepsilon}} + \mathbf{T}_{\mathrm{d}}\tilde{\boldsymbol{\varepsilon}}
\end{aligned} \tag{6.5}$$

with

$$\mathbf{T}_{\mathrm{h}} = \begin{bmatrix}
\frac{1}{3} & \frac{1}{3} & \frac{1}{3} & 0 & 0 & 0\\
\frac{1}{3} & \frac{1}{3} & \frac{1}{3} & 0 & 0 & 0\\
\frac{1}{3} & \frac{1}{3} & \frac{1}{3} & 0 & 0 & 0\\
0 & 0 & 0 & 0 & 0 & 0\\
0 & 0 & 0 & 0 & 0 & 0\\
0 & 0 & 0 & 0 & 0 & 0
\end{bmatrix}, \quad
\mathbf{T}_{\mathrm{d}} = \begin{bmatrix}
\frac{2}{3} & -\frac{1}{3} & -\frac{1}{3} & 0 & 0 & 0\\
-\frac{1}{3} & \frac{2}{3} & -\frac{1}{3} & 0 & 0 & 0\\
-\frac{1}{3} & -\frac{1}{3} & \frac{2}{3} & 0 & 0 & 0\\
0 & 0 & 0 & 1 & 0 & 0\\
0 & 0 & 0 & 0 & 1 & 0\\
0 & 0 & 0 & 0 & 0 & 1
\end{bmatrix},$$

similar as introduced by Schmidt and Gaul (2002). Finally, adding up the hydrostatic and deviatoric versions of (6.2) results using (6.5) in the constitutive law

$$\begin{aligned}
\tilde{\boldsymbol{\sigma}}(\mathbf{x},t) &= \left((E_{0,\mathrm{h}}+E_{1,\mathrm{h}})\mathbf{T}_\mathrm{h}+(E_{0,\mathrm{d}}+E_{1,\mathrm{d}})\mathbf{T}_\mathrm{d}\right)\tilde{\boldsymbol{\varepsilon}}(\mathbf{x},t)\\
&\quad-\left(E_{1,\mathrm{h}}\mathbf{T}_\mathrm{h}+E_{1,\mathrm{d}}\mathbf{T}_\mathrm{d}\right)\tilde{\boldsymbol{\varepsilon}}_\mathrm{f}(\mathbf{x},t),\\
&\Big(p_\mathrm{h}\sin\Big(\frac{\alpha_\mathrm{h}\pi}{2}\Big)\omega_\mathrm{h}^{\alpha_\mathrm{h}-1}\mathbf{T}_\mathrm{h}+p_\mathrm{d}\sin\Big(\frac{\alpha_\mathrm{d}\pi}{2}\Big)\omega_\mathrm{d}^{\alpha_\mathrm{d}-1}\mathbf{T}_\mathrm{d}\Big)\dot{\tilde{\boldsymbol{\varepsilon}}}_\mathrm{f}(\mathbf{x},t)\\
&\quad-\int_0^\infty\left(p_\mathrm{h}\mathrm{K}(\alpha_\mathrm{h},\lambda)\mathbf{T}_\mathrm{h}+p_\mathrm{d}\mathrm{K}(\alpha_\mathrm{d},\lambda)\mathbf{T}_\mathrm{d}\right)\dot{\tilde{\mathbf{z}}}(\lambda,\mathbf{x},t)\mathrm{d}\lambda\\
&=(E_{1,\mathrm{h}}\mathbf{T}_\mathrm{h}+E_{1,\mathrm{d}}\mathbf{T}_\mathrm{d})\tilde{\boldsymbol{\varepsilon}}(\mathbf{x},t)-\Big(\Big(E_{1,\mathrm{h}}+p_\mathrm{h}\cos\Big(\frac{\alpha_\mathrm{h}\pi}{2}\Big)\omega_\mathrm{h}^{\alpha_\mathrm{h}}\Big)\mathbf{T}_\mathrm{h}\\
&\quad+\Big(E_{1,\mathrm{d}}+p_\mathrm{d}\cos\Big(\frac{\alpha_\mathrm{d}\pi}{2}\Big)\omega_\mathrm{d}^{\alpha_\mathrm{d}}\Big)\mathbf{T}_\mathrm{d}\Big)\tilde{\boldsymbol{\varepsilon}}_\mathrm{f}(\mathbf{x},t)\\
&\quad+\int_0^\infty\Big(p_\mathrm{h}\omega_\mathrm{h}^2\mathrm{K}(\alpha_\mathrm{h},\lambda)\mathbf{T}_\mathrm{h}+p_\mathrm{d}\omega_\mathrm{d}^2\mathrm{K}(\alpha_\mathrm{d},\lambda)\mathbf{T}_\mathrm{d}\Big)\tilde{\mathbf{Z}}(\lambda,\mathbf{x},t)\mathrm{d}\lambda,\\
\dot{\tilde{\mathbf{Z}}}(\eta,\mathbf{x},t)&=\tilde{\boldsymbol{\varepsilon}}_\mathrm{f}(\mathbf{x},t)-\eta\tilde{\mathbf{Z}}(\eta,\mathbf{x},t),\\
\dot{\tilde{\mathbf{z}}}(\eta,\mathbf{x},t)&=\dot{\tilde{\boldsymbol{\varepsilon}}}_\mathrm{f}(\mathbf{x},t)-\eta\tilde{\mathbf{z}}(\eta,\mathbf{x},t).
\end{aligned}\tag{6.6}$$

6.2 FEM formulation

The equilibrium equations for a deformable body represented by a spatial domain $\Omega\subset\mathbb{R}^3$ can be formulated in terms of the displacement field $\mathbf{u}=\mathbf{u}(\mathbf{x},t)$ being kinematically related to the linear strain $\boldsymbol{\varepsilon}$. In case of a Cartesian coordinate system, the strain-displacement relation is given by

$$\begin{aligned}
&\varepsilon_{xx}=\frac{\partial u_x}{\partial x}(\mathbf{x},t),\ \varepsilon_{yy}=\frac{\partial u_y}{\partial y}(\mathbf{x},t),\ \varepsilon_{zz}=\frac{\partial u_z}{\partial z}(\mathbf{x},t),\ \gamma_{xy}=\frac{\partial u_x}{\partial y}(\mathbf{x},t)+\frac{\partial u_y}{\partial x}(\mathbf{x},t),\\
&\gamma_{yz}=\frac{\partial u_y}{\partial z}(\mathbf{x},t)+\frac{\partial u_z}{\partial y}(\mathbf{x},t),\ \gamma_{zx}=\frac{\partial u_z}{\partial x}(\mathbf{x},t)+\frac{\partial u_x}{\partial z}(\mathbf{x},t).
\end{aligned}\tag{6.7}$$

The principle of virtual work

$$0=\delta W_\mathrm{dyn}+\delta W_\mathrm{int}+\delta W_\mathrm{ext}$$

including the virtual work of inertia δW_dyn, of internal forces δW_int and of external forces δW_ext yields the equation

$$\begin{aligned}
0=&-\int_\Omega\delta\mathbf{u}^\mathrm{T}(\mathbf{x},t)\rho(\mathbf{x})\ddot{\mathbf{u}}(\mathbf{x},t)\mathrm{d}V-\int_\Omega\delta\tilde{\boldsymbol{\varepsilon}}^\mathrm{T}(\mathbf{x},t)\tilde{\boldsymbol{\sigma}}(\mathbf{x},t)\mathrm{d}V\\
&+\int_\Omega\delta\mathbf{u}^\mathrm{T}(\mathbf{x},t)\mathbf{b}(\mathbf{x},t)\mathrm{d}V+\int_{\partial\Omega}\delta\mathbf{u}^\mathrm{T}(\mathbf{x},t)\mathbf{t}(\mathbf{x},t)\mathrm{d}A,
\end{aligned}\tag{6.8}$$

which is valid for all smooth virtual displacement fields $\delta\mathbf{u}$. Thereby, ρ is the (volumetric) mass density in Ω, $\mathbf{b}$ is the volume density of external forces in Ω and $\mathbf{t}$ is

the surface density of external forces on the boundary $\partial\Omega$. For the displacement field $\mathbf{u}$, consider a finite element discretization

$$\mathbf{u}(\mathbf{x},t) = \mathbf{H}(\mathbf{x})\mathbf{v}(t), \tag{6.9}$$

where the matrix $\mathbf{H}$ contains the chosen shape functions and $\mathbf{v}$ the associated nodal displacements. Furthermore, the linear strain field is discretized as

$$\tilde{\boldsymbol{\varepsilon}}(\mathbf{x},t) = \mathbf{B}(\mathbf{x})\mathbf{v}(t), \tag{6.10}$$

where the matrix $\mathbf{B}$ contains certain spatial derivatives of the shape functions used in $\mathbf{H}$ according to a strain-displacement relation such as (6.7). Assume similar relations for the internal variables $\tilde{\boldsymbol{\varepsilon}}_\mathrm{f}$, $\tilde{\mathbf{Z}}$ and $\tilde{\mathbf{z}}$ in the form

$$\tilde{\boldsymbol{\varepsilon}}_\mathrm{f}(\mathbf{x},t) = \mathbf{B}(\mathbf{x})\mathbf{v}_\mathrm{f}(t),\ \tilde{\mathbf{Z}}(\eta,\mathbf{x},t) = \mathbf{B}(\mathbf{x})\boldsymbol{Z}(\eta,t),\ \tilde{\mathbf{z}}(\eta,\mathbf{x},t) = \mathbf{B}(\mathbf{x})z(\eta,t) \tag{6.11}$$

with generalized internal nodal displacement variables $\mathbf{v}_\mathrm{f}$, $\boldsymbol{Z}$ and z. Using (6.9) and (6.10) in the principle of virtual work (6.8) results in

$$\begin{aligned} 0 = \delta\mathbf{v}^\mathrm{T}(t)\Bigg[&- \int_\Omega \rho(\mathbf{x})\mathbf{H}^\mathrm{T}(\mathbf{x})\mathbf{H}(\mathbf{x})\mathrm{d}V\,\ddot{\mathbf{v}}(t) - \int_\Omega \mathbf{B}^\mathrm{T}(\mathbf{x})\tilde{\boldsymbol{\sigma}}(\mathbf{x},t)\mathrm{d}V \\ &+ \int_\Omega \mathbf{H}^\mathrm{T}(\mathbf{x})\mathbf{b}(\mathbf{x},t)\mathrm{d}V + \int_{\partial\Omega} \mathbf{H}^\mathrm{T}(\mathbf{x})\mathbf{t}(\mathbf{x},t)\mathrm{d}A\Bigg] \ \text{ for all } \ \delta\mathbf{v}. \end{aligned} \tag{6.12}$$

Hence, inserting the constitutive law (6.6) in (6.12) leads to the equations of motion

$$\mathbf{M}\ddot{\mathbf{v}}(t) + \mathbf{K}\mathbf{v}(t) - \mathbf{C}\mathbf{v}_\mathrm{f}(t) = \mathbf{f}(t), \tag{6.13}$$

where

$$\begin{aligned} \mathbf{M} &= \int_\Omega \rho(\mathbf{x})\mathbf{H}^\mathrm{T}(\mathbf{x})\mathbf{H}(\mathbf{x})\mathrm{d}V, \\ \mathbf{K} &= (E_{0,\mathrm{h}} + E_{1,\mathrm{h}})\mathbf{Q}_\mathrm{h} + (E_{0,\mathrm{d}} + E_{1,\mathrm{d}})\mathbf{Q}_\mathrm{d}\,, \\ \mathbf{C} &= E_{1,\mathrm{h}}\mathbf{Q}_\mathrm{h} + E_{1,\mathrm{d}}\mathbf{Q}_\mathrm{d}\,, \\ \mathbf{f}(t) &= \int_\Omega \mathbf{H}^\mathrm{T}(\mathbf{x})\mathbf{b}(\mathbf{x},t)\mathrm{d}V + \int_{\partial\Omega} \mathbf{H}^\mathrm{T}(\mathbf{x})\mathbf{t}(\mathbf{x},t)\mathrm{d}A \end{aligned} \tag{6.14}$$

and the generalized system matrices

$$\mathbf{Q}_\mathrm{h} := \int_\Omega \mathbf{B}^\mathrm{T}(\mathbf{x})\mathbf{T}_\mathrm{h}\mathbf{B}(\mathbf{x})\mathrm{d}V, \quad \mathbf{Q}_\mathrm{d} := \int_\Omega \mathbf{B}^\mathrm{T}(\mathbf{x})\mathbf{T}_\mathrm{d}\mathbf{B}(\mathbf{x})\mathrm{d}V \tag{6.15}$$

have been introduced. Furthermore, multiplying the differential equations in (6.6) by $\mathbf{B}^{\mathrm{T}}$, using (6.11) and integration leads to

$$\begin{aligned}
&\left(p_{\mathrm{h}} \sin\left(\frac{\alpha_{\mathrm{h}}\pi}{2}\right) \omega_{\mathrm{h}}^{\alpha_{\mathrm{h}}-1}\mathbf{Q}_{\mathrm{h}} + p_{\mathrm{d}} \sin\left(\frac{\alpha_{\mathrm{d}}\pi}{2}\right) \omega_{\mathrm{d}}^{\alpha_{\mathrm{d}}-1}\mathbf{Q}_{\mathrm{d}}\right)\dot{\mathbf{v}}_{\mathrm{f}}(t) \\
&\quad - \int_0^\infty \left(p_{\mathrm{h}}\mathrm{K}(\alpha_{\mathrm{h}},\lambda)\mathbf{Q}_{\mathrm{h}} + p_{\mathrm{d}}\mathrm{K}(\alpha_{\mathrm{d}},\lambda)\mathbf{Q}_{\mathrm{d}}\right)\dot{\boldsymbol{z}}(\lambda,t)\mathrm{d}\lambda \\
&\qquad = (E_{1,\mathrm{h}}\mathbf{Q}_{\mathrm{h}} + E_{1,\mathrm{d}}\mathbf{Q}_{\mathrm{d}})\mathbf{v}(t) - \Bigg(\left(E_{1,\mathrm{h}} + p_{\mathrm{h}}\cos\left(\frac{\alpha_{\mathrm{h}}\pi}{2}\right)\omega_{\mathrm{h}}^{\alpha_{\mathrm{h}}}\right)\mathbf{Q}_{\mathrm{h}} \\
&\qquad\quad + \left(E_{1,\mathrm{d}} + p_{\mathrm{d}}\cos\left(\frac{\alpha_{\mathrm{d}}\pi}{2}\right)\omega_{\mathrm{d}}^{\alpha_{\mathrm{d}}}\right)\mathbf{Q}_{\mathrm{d}}\Bigg)\mathbf{v}_{\mathrm{f}}(t) \\
&\qquad\quad + \int_0^\infty \left(p_{\mathrm{h}}\omega_{\mathrm{h}}^2\mathrm{K}(\alpha_{\mathrm{h}},\lambda)\mathbf{Q}_{\mathrm{h}} + p_{\mathrm{d}}\omega_{\mathrm{d}}^2\mathrm{K}(\alpha_{\mathrm{d}},\lambda)\mathbf{Q}_{\mathrm{d}}\right)\boldsymbol{Z}(\lambda,t)\mathrm{d}\lambda, \\
&\dot{\boldsymbol{Z}}(\eta,t) = \mathbf{v}_{\mathrm{f}}(t) - \eta\boldsymbol{Z}(\eta,t), \\
&\dot{\boldsymbol{z}}(\eta,t) = \dot{\mathbf{v}}_{\mathrm{f}}(t) - \eta\boldsymbol{z}(\eta,t).
\end{aligned} \tag{6.16}$$

The equations of motion (6.13) together with (6.16) represent a reformulated system of FODEs, which can be solved numerically, given certain initial and boundary conditions. The states of the system include the nodal displacements $\mathbf{v}$ as well as internal states $\mathbf{v}_{\mathrm{f}}$ and infinite states $\boldsymbol{Z}$, $\boldsymbol{z}$.

6.3 Numerical implementation

As (6.13) and (6.16) result from an FODE, the reformulated infinite state scheme can be used to solve associated initial and and boundary value problems. Therefore, the equations (6.16) are approximated using (3.11) as

$$\begin{aligned}
&\left(p_{\mathrm{h}} \sin\left(\frac{\alpha_{\mathrm{h}}\pi}{2}\right) \omega_{\mathrm{h}}^{\alpha_{\mathrm{h}}-1}\mathbf{Q}_{\mathrm{h}} + p_{\mathrm{d}} \sin\left(\frac{\alpha_{\mathrm{d}}\pi}{2}\right) \omega_{\mathrm{d}}^{\alpha_{\mathrm{d}}-1}\mathbf{Q}_{\mathrm{d}}\right)\dot{\mathbf{v}}_{\mathrm{f}}(t) \\
&\quad - \sum_{k=0}^{K-1}\sum_{j=1}^{J} \left(p_{\mathrm{h}}\mathrm{K}(\alpha_{\mathrm{h}},\eta_{k,j})\mathbf{Q}_{\mathrm{h}} + p_{\mathrm{d}}\mathrm{K}(\alpha_{\mathrm{d}},\eta_{k,j})\mathbf{Q}_{\mathrm{d}}\right)\dot{\boldsymbol{z}}_{k,j}(t)w_{k,j} \\
&\qquad = (E_{1,\mathrm{h}}\mathbf{Q}_{\mathrm{h}} + E_{1,\mathrm{d}}\mathbf{Q}_{\mathrm{d}})\mathbf{v}(t) - \Bigg(\left(E_{1,\mathrm{h}} + p_{\mathrm{h}}\cos\left(\frac{\alpha_{\mathrm{h}}\pi}{2}\right)\omega_{\mathrm{h}}^{\alpha_{\mathrm{h}}}\right)\mathbf{Q}_{\mathrm{h}} \\
&\qquad\quad + \left(E_{1,\mathrm{d}} + p_{\mathrm{d}}\cos\left(\frac{\alpha_{\mathrm{d}}\pi}{2}\right)\omega_{\mathrm{d}}^{\alpha_{\mathrm{d}}}\right)\mathbf{Q}_{\mathrm{d}}\Bigg)\mathbf{v}_{\mathrm{f}}(t) \\
&\qquad\quad + \sum_{k=0}^{K-1}\sum_{j=1}^{J} \left(p_{\mathrm{h}}\omega_{\mathrm{h}}^2\mathrm{K}(\alpha_{\mathrm{h}},\eta_{k,j})\mathbf{Q}_{\mathrm{h}} + p_{\mathrm{d}}\omega_{\mathrm{d}}^2\mathrm{K}(\alpha_{\mathrm{d}},\eta_{k,j})\mathbf{Q}_{\mathrm{d}}\right)\boldsymbol{Z}_{k,j}(t)w_{k,j}\,, \\
&\dot{\boldsymbol{Z}}_{k,j}(t) = \mathbf{v}_{\mathrm{f}}(t) - \eta_{k,j}\boldsymbol{Z}_{k,j}(t), \\
&\dot{\boldsymbol{z}}_{k,j}(t) = \dot{\mathbf{v}}_{\mathrm{f}}(t) - \eta_{k,j}\boldsymbol{z}_{k,j}(t).
\end{aligned} \tag{6.17}$$

The integration of (6.13) and (6.17) can be performed as described in Chapter 3. The following examples provide basic insight in the application of the method.

Example 6.1. Consider the one-dimensional example of a two-node rod element of length l and cross sectional area A that is fixed at one end and loaded by a constant force F at initial time $t = 0$ at the other end, see Figure 6.2. For this simple case, the quantities of stress (6.3) and strain (6.4) become scalar and the finite element scheme can be derived directly from (6.2). For the FEM discretization,

Figure 6.2: Fractional viscoelastic rod (left) described as a two-node one-dimensional finite element (right).

consider linear shape functions such that

$$\mathbf{H}(x) = \begin{bmatrix} 1 - \frac{x}{l} & \frac{x}{l} \end{bmatrix}, \ \mathbf{B}(x) = \begin{bmatrix} -\frac{1}{l} & \frac{1}{l} \end{bmatrix}, \ \mathbf{v}(t) = \begin{bmatrix} v_1(t) & v_2(t) \end{bmatrix}^{\mathrm{T}}, \tag{6.18}$$

where v_1 and v_2 represent the displacement of left and right node, respectively. Neglecting inertia effects, (6.13) and (6.16) can be formulated for the given case as

$$\begin{aligned} &(E_0+E_1)A \int_0^l \mathbf{B}^{\mathrm{T}}(x)\mathbf{B}(x)\mathrm{d}x\, \mathbf{v}(t) - E_1 A \int_0^l \mathbf{B}^{\mathrm{T}}(x)\mathbf{B}(x)\mathrm{d}x\, \mathbf{v}_{\mathrm{f}}(t) = [f_1 \ \ F\Theta(t)]^{\mathrm{T}}, \\ &p \sin\left(\frac{\alpha\pi}{2}\right) \omega^{\alpha-1} \dot{\mathbf{v}}_{\mathrm{f}}(t) - p \int_0^\infty \mathrm{K}(\alpha,\lambda)\dot{\boldsymbol{z}}(\lambda,t)\mathrm{d}\lambda \\ &\quad = E_1 \mathbf{v}(t) - \left(E_1 + p\cos\left(\frac{\alpha\pi}{2}\right)\omega^{\alpha}\right)\mathbf{v}_{\mathrm{f}}(t) + p\omega^2 \int_0^\infty \mathrm{K}(\alpha,\lambda)\boldsymbol{Z}(\lambda,t)\mathrm{d}\lambda, \\ &\dot{\boldsymbol{Z}}(\eta,t) = \mathbf{v}_{\mathrm{f}}(t) - \eta \boldsymbol{Z}(\eta,t), \\ &\dot{\boldsymbol{z}}(\eta,t) = \dot{\mathbf{v}}_{\mathrm{f}}(t) - \eta \boldsymbol{z}(\eta,t). \end{aligned} \tag{6.19}$$

The numerical solution of (6.19) is carried out using RISS with quadrature parameters as in Section 3.4. As boundary conditions, consider the clamped left-hand side, i.e., $v_1 = 0$ and the force F acting on the right-hand side of the rod. Further, the rod is assumed fully relaxed initially such that all system states fulfill zero initial conditions.

The numerical solution can be evaluated by the closed form solution resulting from the creep function of the fractional Zener model. In view of the spatially constant unit-step stress field

$$\sigma(x,t) = \frac{F}{A}\Theta(t), \quad x \in (0,l)$$

and the creep function J from (4.62) together with (4.64), one obtains

$$\begin{aligned} v_2(t) = u(x=l,t) = \varepsilon(l,t)l &= \frac{F}{A} l J(t) \\ &= \frac{F}{A}\frac{l}{E_0+E_1}\left(1 + \frac{E_1}{E_0}\left(1 - \mathrm{E}_\alpha\left(-\frac{E_0E_1}{p(E_0+E_1)}t^\alpha\right)\right)\right), \ t \geq 0. \end{aligned}$$

The relative error Δ over time t between numerical and closed form solution for various values of α is shown in Figure 6.3. Therein, the Mittag-Leffler function has been computed as proposed by Garrappa (2014).

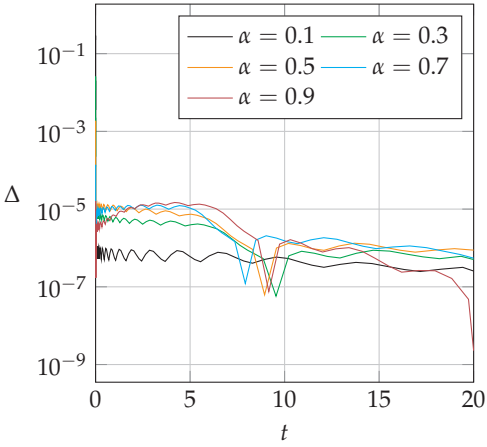

Figure 6.3: Relative error of the numerical solution of (6.19) using (6.18).

Example 6.2. As a second benchmark problem, a quadratic plate is modeled as a two-dimensional finite element under plane strain conditions (Figure 6.4). Accordingly, consider a reduced strain state

$$\tilde{\boldsymbol{\varepsilon}} = \left[\varepsilon_{xx}\ \varepsilon_{yy}\ \gamma_{xy}\right]^{\mathrm{T}},$$

resulting in a reduced stress state

$$\tilde{\boldsymbol{\sigma}} = \left[\sigma_{xx}\ \sigma_{yy}\ \sigma_{xy}\right]^{\mathrm{T}}. \tag{6.20}$$

Thereby, the stress σ_{zz} in normal direction does not vanish but may be expressed depending on the plane stress variables in (6.20). A finite element discretization can be given by

$$\begin{aligned}
\mathbf{H}(x,y) &= \begin{bmatrix} h_1 & 0 & h_2 & 0 & h_3 & 0 & h_4 & 0 \\ 0 & h_1 & 0 & h_2 & 0 & h_3 & 0 & h_4 \end{bmatrix}(x,y), \\
\mathbf{B}(x,y) &= \begin{bmatrix} \frac{\partial}{\partial x} & 0 & \frac{\partial}{\partial y} \\ 0 & \frac{\partial}{\partial y} & \frac{\partial}{\partial x} \end{bmatrix}^{\mathrm{T}} \mathbf{H}(x,y), \\
\mathbf{v}(t) &= \left[v_{1x}\ v_{1y}\ v_{2x}\ v_{2y}\ v_{3x}\ v_{3y}\ v_{4x}\ v_{4y}\right]^{\mathrm{T}}
\end{aligned} \tag{6.21}$$

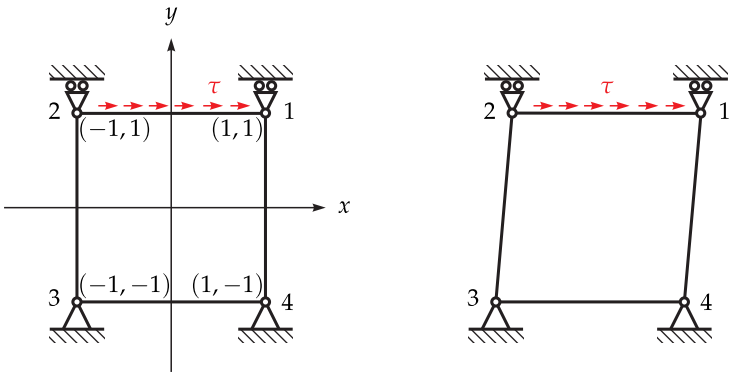

Figure 6.4: Fractional viscoelastic plate element in undeformed (left) and deformed configuration (right).

with displacements $v_{1x}, \ldots, v_{4y}$ in axial directions of the reference frame for the four nodes and bilinear shape functions

$$h_1(x,y) = \frac{1}{4}(1+x)(1+y), \quad h_2(x,y) = \frac{1}{4}(1-x)(1+y),$$
$$h_3(x,y) = \frac{1}{4}(1-x)(1-y), \quad h_4(x,y) = \frac{1}{4}(1+x)(1-y).$$

Further, in order to obtain a closed form solution of the problem, consider boundary conditions such that a purely deviatoric deformation occurs. In particular, nodes 3 and 4 on the bottom are clamped, nodes 1 and 2 are fixed in y-direction and there is a constant distributed shear loading τ in x-direction on the face between nodes 1 and 2 applied as a step function at time $t = 0$. This leads to an external force vector

$$\mathbf{f} = \left[f_{1x}\ f_{1y}\ f_{2x}\ f_{2y}\ f_{3x}\ f_{3y}\ f_{4x}\ f_{4y}\right]^{\mathrm{T}},$$

where, according to (6.14),

$$f_{1x}(t) = \int_{-1}^{1} h_1(x,1)\tau\Theta(t)\mathrm{d}x = \tau\Theta(t), \quad f_{2x}(t) = \int_{-1}^{1} h_2(x,1)\tau\Theta(t)\mathrm{d}x = \tau\Theta(t).$$

Again, neglecting inertia, (6.13) and (6.16) can be formulated as

$$\begin{aligned}
&(E_{0,\mathrm{d}} + E_{1,\mathrm{d}})\mathbf{Q}_\mathrm{d}\mathbf{v}(t) - E_{1,\mathrm{d}}\mathbf{Q}_\mathrm{d}\mathbf{v}_\mathrm{f}(t) = \mathbf{f}(t),\\
&p_\mathrm{d}\sin\left(\frac{\alpha_\mathrm{d}\pi}{2}\right)\omega_\mathrm{d}^{\alpha_\mathrm{d}-1}\dot{\mathbf{v}}_\mathrm{f}(t) - p_\mathrm{d}\int_0^\infty \mathrm{K}(\alpha_\mathrm{d},\lambda)\dot{\boldsymbol{z}}(\lambda,t)\mathrm{d}\lambda\\
&\qquad = E_{1,\mathrm{d}}\mathbf{v}(t) - \left(E_{1,\mathrm{d}} + p_\mathrm{d}\cos\left(\frac{\alpha_\mathrm{d}\pi}{2}\right)\omega_\mathrm{d}^{\alpha_\mathrm{d}}\right)\mathbf{v}_\mathrm{f}(t)\\
&\qquad\quad + p_\mathrm{d}\omega_\mathrm{d}^2\int_0^\infty \mathrm{K}(\alpha_\mathrm{d},\lambda)\boldsymbol{Z}(\lambda,t)\mathrm{d}\lambda,\\
&\dot{\boldsymbol{Z}}(\eta,t) = \mathbf{v}_\mathrm{f}(t) - \eta\boldsymbol{Z}(\eta,t),\\
&\dot{\boldsymbol{z}}(\eta,t) = \dot{\mathbf{v}}_\mathrm{f}(t) - \eta\boldsymbol{z}(\eta,t),
\end{aligned} \tag{6.22}$$

where $\mathbf{Q}_\mathrm{d}$ is computed as in (6.15) with a reduced matrix

$$\mathbf{T}_\mathrm{d} = \begin{bmatrix} \frac{2}{3} & -\frac{1}{3} & 0\\ -\frac{1}{3} & \frac{2}{3} & 0\\ 0 & 0 & 1 \end{bmatrix}.$$

Note that the parameters of the hydrostatic part of the constitutive law may be neglected due to the purely deviatoric deformation. Inserting the displacement boundary conditions $v_{1y} = v_{2y} = v_{3x} = v_{3y} = v_{4x} = v_{4y} = 0$, one can solve (6.22) for v_{1x} and v_{2x}.

Moreover, a closed form solution can be obtained from the spatially constant stress boundary condition

$$\sigma_{xy}(x,1,t) = \tau\Theta(t), \quad x \in (-1,1)$$

and a deviatoric creep function J_d similar as in (4.62) with (4.64). The resulting nodal displacement is given by

$$\begin{aligned}
v_{1x}(t) &= v_{2x}(t) = 2\gamma_{xy}(x,1,t) = 2\tau J_\mathrm{d}(t)\\
&= \frac{2\tau}{E_{0,\mathrm{d}} + E_{1,\mathrm{d}}}\left(1 + \frac{E_{1,\mathrm{d}}}{E_{0,\mathrm{d}}}\left(1 - \mathrm{E}_{\alpha_\mathrm{d}}\left(-\frac{E_{0,\mathrm{d}}E_{1,\mathrm{d}}}{p_\mathrm{d}(E_{0,\mathrm{d}} + E_{1,\mathrm{d}})}t^{\alpha_\mathrm{d}}\right)\right)\right),\ t \geq 0.
\end{aligned}$$

The relative error Δ over time t between the numerical and the closed form solution is depicted in Figure 6.5.

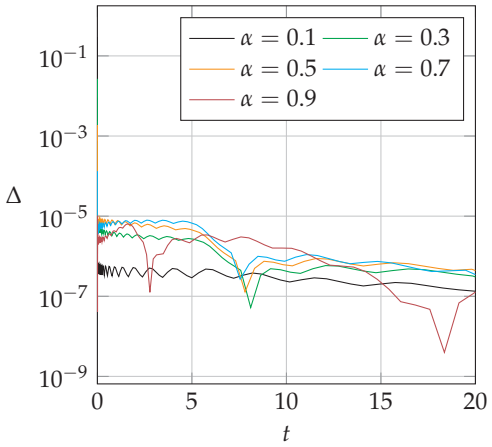

Figure 6.5: Relative error of the numerical solution of (6.22) using (6.21).

Chapter 7

Conclusions and outlook

This thesis presents a formulation of fractional calculus based on the (reformulated) infinite state representation with applications in numerical analysis, viscoelasticity, Lyapunov stability theory and the finite element method, thereby meeting the objective to strengthen the mathematical foundation, nonlinear analysis and numerical simulation of fractional dynamical systems. The two main results are given by a generalization of the direct method of Lyapunov for fractionally damped mechanical and controlled dynamical systems and, by the reformulated infinite state scheme (RISS), which is incorporated in a finite element formulation for fractional constitutive laws. A summary of the particular contributions of this thesis and an outlook on possible future research are given in the following.

Formulation of fractional calculus on unbounded intervals

The fractional-order operators used in the preceding chapters consider the entire history of the functions to which they are applied. This choice corresponds to the application in fractional viscoelasticity, where all past stress or strain values influence the current mechanical state of the material. This infinite-memory approach is consistently pursued throughout the thesis and particularly formulated in terms of the infinite state representation as the initial data of infinite states. The benefit and interpretation of this formulation in viscoelasticity and stability theory are presented. Especially, in stability theory of fractionally damped systems, the approach renders the fractional damping term an autonomous contribution to the functional differential equation, which allows for the use of a generalized invariance principle in order to obtain a stability statement. This advantage is accompanied by the necessity of a careful choice of the state space of functions. The associated theoretical subtleties of functional differential equations with infinite delays are preprocessed for the applied context of fractional damping. Generally, the provided infinite-memory approach is intended for applied problems. A

more formal strategy would study fractional calculus on unbounded intervals for various spaces of (generalized) functions as given by Kleiner and Hilfer (2021).

Development of the RISS scheme for fractional-order problems

The numerical solution of fractional-order problems is tackled in this thesis by exploiting the reformulated infinite state representation, being an original contribution of this thesis. The resulting scheme RISS, proposed here and by Hinze et al. (2019), is motivated by the mechanical stiffness and damping capabilities of springpots. The method is introduced in Chapter 3 and an error analysis as well as several benchmark problems are given. There are thus a lot of further investigations needed to evaluate the scheme. This includes an analysis of the combined error of the infinite state quadrature and the chosen time-stepping scheme and a more detailed comparison to other recent infinite state schemes, see Birk and Song (2010); Li (2010); Jiang et al. (2017); Baffet (2019); Zhang et al. (2020). Furthermore, the influence of the parameter ω in (3.11) on the performance of the method has to be examined and the question arises, whether an optimization with respect to ω is possible, similar as proposed in the scheme by Zhang et al. (2020). Finally, the method still has to be tested in the context of high-dimensional problems, which is related to the contribution discussed hereafter.

Implementation of fractional constitutive laws in FEM

The achievements in Chapter 6 provide an implementation of the fractional Zener model in the finite element method. The theoretical and motivational basis for fractional constitutive models is given in Chapter 4. Therein, it is particularly shown, how the infinite state representation of fractional constitutive laws can be interpreted in terms of viscoelasticity theory and a mechanical interpretation of a springpot as the continuous generalization of spring-dashpot models is given. Moreover, as an example for a viscoelastic material, the creep behavior of salt concrete is studied. It is shown that the deformation of the concrete under a constant load is well represented by a fractional Zener model over several time decades.

In contrast to most of the existing schemes, the method in Chapter 6 is not based on a Grünwald-Letnikov formulation but uses an infinite state scheme, namely RISS. Accordingly, the history of stress and strain magnitudes do not have to be stored and used in every computational step but are implicitly given in terms of the internal infinite states. The scheme, although given for a fractional Zener model, can be generalized for any other fractional constitutive law. So far, the method has been applied to simple problems for one- and two-dimensional finite elements. An application to more complex problems and different element types and loading conditions are necessary in the future to evaluate the method.

Development of a Lyapunov stability framework for fractionally damped systems

The stability of finite-dimensional systems with additional fractional damping is discussed in great detail in Chapter 5 and a generalized direct method of Lyapunov is introduced in the context of FDEs with infinite delay. The used Lyapunov functionals are deduced from the potential energy of springpots and a class of augmented Lyapunov functionals is obtained in terms of the reformulated infinite state representation. The latter functionals are especially useful for a stability proof in the case of anti-damping, which can be induced by certain non-monotone friction laws (Stribeck effect). The method is established for a single degree-of-freedom oscillator and generalized for linear multidimensional mechanical systems and the solution of a tracking problem for a class of nonlinear dynamical systems with fractional damping. Particularly, the stability proof for the tracking problem employs an invariance principle for asymptotically autonomous FDEs and a more detailed and elaborate explanation than given by Hinze et al. (2020a) is presented.

Further investigations of the proposed formalism are necessary to tackle related more general stability and control problems. One possible way could be the introduction of set-valued Coulomb friction laws in combination with fractional damping. Therefore, a generalized Lyapunov theory for FDE control systems with set-valued inputs is required. Another interesting question is, whether the method is still applicable for non-monotone friction laws in the general finite-dimensional case. As shown in Section 5.4, the method is not only accessible for mechanical but also for general fractional-order control problems with different applications.

Each of the individual merits of the thesis, as discussed above, contributes to the overall objective to provide a mathematically sound and practically tangible framework for fractional damping in mechanical systems. However, in retrospect, one also sees how the individual contributions are linked to each other. Interestingly, the development of Lyapunov stability techniques has led to insights that helped to come to an improved numerical scheme. Also, it becomes apparent, how stability results are beneficial for control purposes. Furthermore, the infinite state representation reveals the embedding of fractional-order differential equations in the context of more general functional differential equations.

As a last remark, the reader is invited to ponder over the applicability of the results, which have been developed for the study of viscoelasticity, to other application fields of fractional calculus.

Bibliography

K. Adolfsson and M. Enelund. Fractional derivative viscoelasticity at large deformations. *Nonlinear Dynamics*, 33(3):301–321, 2003.

R. Agarwal, D. O'Regan, and S. Hristova. Stability of Caputo fractional differential equations by Lyapunov functions. *Applications of Mathematics*, 60(6):653–676, 2015.

A. S. Andreev. The Lyapunov functionals method in stability problems for functional differential equations. *Automation and Remote Control*, 70(9):1438–1486, 2009.

Z. Artstein. The limiting equations of nonautonomous ordinary differential equations. *Journal of Differential Equations*, 25:184–202, 1977.

D. Baffet. A Gauss-Jacobi kernel compression scheme for fractional differential equations. *Journal of Scientific Computing*, 79(1):227–248, 2019.

R. L. Bagley and R. A. Calico. Fractional order state equations for the control of viscoelastically damped structures. *Journal of Guidance, Control, and Dynamics*, 14(2):304–311, 1991.

R. L. Bagley and P. J. Torvik. Fractional calculus - A different approach to the analysis of viscoelastically damped structures. *AIAA Journal*, 21(5):741–748, 1983.

R. L. Bagley and P. J. Torvik. Fractional calculus in the transient analysis of viscoelastically damped structures. *AIAA Journal*, 23(6):918 – 925, 1985.

R. L. Bagley and P. J. Torvik. On the fractional calculus model of viscoelastic behavior. *Journal of Rheology*, 30(1):133–155, 1986.

C. Birk and C. Song. An improved non-classical method for the solution of fractional differential equations. *Computational Mechanics*, 46:721–734, 2010.

T. A. Burton. *Stability and Periodic Solutions of Ordinary and Functional Differential Equations*, volume 178 of *Mathematics in Science and Engineering*. Academic Press, Orlando, 1985.

T. A. Burton. *Volterra Integral and Differential Equations*, volume 202 of *Mathematics in Science and Engineering*. Elsevier, Amsterdam, 2005.

T. A. Burton. Fractional differential equations and Lyapunov functionals. *Nonlinear Analysis: Theory, Methods & Applications*, 74(16):5648–5662, 2011.

M. Caputo and F. Mainardi. Linear models of dissipation in anelastic solids. *Rivista del Nuovo Cimento*, 1(2):161–198, 1971.

C. Celauro, C. Fecarotti, A. Pirrotta, and A. C. Collop. Experimental validation of a fractional model for creep/recovery testing of asphalt mixtures. *Construction and Building Materials*, 36:458–466, 2012.

A. Chatterjee. Statistical origins of fractional derivatives in viscoelasticity. *Journal of Sound and Vibration*, 284(3):1239 – 1245, 2005.

R. M. Christensen. *Theory of Viscoelasticity*. Dover Publications, Mineola (NY), 2. edition, 2013.

K. S. Cole and R. H. Cole. Dispersion and absorption in dielectrics - I. Alternating current characteristics. *Journal of Chemical Physics*, 9:341–351, 1941.

G. J. Creus. *Viscoelasticity - Basic Theory and Applications to Concrete Structures*, volume 16 of *Lecture Notes in Engineering*. Springer, Berlin, 1986.

P. J. Davis and P. Rabinowitz. *Methods of Numerical Integration*. Computer Science and Applied Mathematics. Academic Press, New York, 2. edition, 1984.

M. di Paola and M. F. Granata. Fractional model of concrete hereditary viscoelastic behaviour. *Archive of Applied Mechanics*, 87(2):335–348, 2016.

K. Diethelm. An investigation of some nonclassical methods for the numerical approximation of Caputo-type fractional derivatives. *Numerical Algorithms*, 47(4):361–390, 2008.

K. Diethelm. *The Analysis of Fractional Differential Equations: An Application-Oriented Exposition Using Differential Operators of Caputo Type*, volume 2004 of *Lecture Notes in Mathematics*. Springer, Berlin, 2010.

K. Diethelm and N. J. Ford. Multi-order fractional differential equations and their numerical solution. *Applied Mathematics and Computation*, 154(3):621 – 640, 2004.

K. Diethelm, N. J. Ford, and A. D. Freed. A predictor-corrector approach for the numerical solution of fractional differential equations. *Nonlinear Dynamics*, 29(1):3–22, 2002.

K. Diethelm, N. J. Ford, and A. D. Freed. Detailed error analysis for a fractional Adams method. *Numerical Algorithms*, 36(1):31–52, 2004.

K. Diethelm, R. Garrappa, and M. Stynes. Good (and not so good) practices in computational methods for fractional calculus. *Mathematics*, 8(3):324, 2020.

G. Doetsch and W. Nader. *Introduction to the Theory and Application of the Laplace Transformation*. Springer, Berlin Heidelberg, 1974.

R. D. Driver. Existence and stability of solutions of a delay-differential system. *Archive for Rational Mechanics and Analysis*, 10:401–426, 1962.

M. A. Duarte-Mermoud, N. Aguila-Camacho, J. A. Gallegos, and R. Castro-Linares. Using general quadratic Lyapunov functions to prove Lyapunov uniform stability for fractional order systems. *Communications in Nonlinear Science and Numerical Simulations*, 22:650–659, 2015.

M. Enelund and B. L. Josefson. Time-domain finite element analysis of viscoelastic structures with fractional derivatives constitutive relations. *AIAA Journal*, 35(10):1630–1637, 1997.

M. Enelund, L. Mähler, K. Runesson, and B. L. Josefson. Formulation and integration of the standard linear viscoelastic solid with fractional order rate laws. *International Journal of Solids and Structures*, 36(16):2417–2442, 1999.

A. Erdélyi, editor. *Higher Transcendental Functions*, volume 1. McGraw-Hill Book Co., New York, 1953.

A. Fenander. Modal synthesis when modeling damping by use of fractional derivatives. *AIAA Journal*, 34(5):1051–1058, 1996.

U. Galvanetto, S. R. Bishop, and L. Briseghella. Mechanical stick–slip vibrations. *International Journal of Bifurcation and Chaos*, 5(3):637–651, 1995.

R. Garrappa. Predictor-corrector PECE method for fractional differential equations. *MATLAB Central File Exchange*, 2012. File ID: 32918.

R. Garrappa. The Mittag-Leffler Function. *MATLAB Central File Exchange*, 2014. File ID: 48154.

R. Garrappa. Numerical evaluation of two and three parameter Mittag-Leffler functions. *SIAM Journal on Numerical Analysis*, 53(3):1350–1369, 2015.

A. Gemant. A method of analyzing experimental results obtained from elasto-viscous bodies. *Physics*, 7:311–317, 1936.

A. Gerasimov. A generalization of linear laws of deformation and its application to problems of internal friction. *Prikladnaya Matematika i Mekhanika*, 12(3):251–260, 1948.

R. Gorenflo, J. Loutchko, and Y. Luchko. Computation of the Mittag-Leffler function $E_{\alpha,\beta}(z)$ and its derivative. *Fractional Calculus and Applied Analysis*, 5(4):491–518, 2002.

R. Gorenflo, A. A. Kilbas, F. Mainardi, and S. V. Rogosin. *Mittag-Leffler Functions, Related Topics and Applications*. Springer, Berlin Heidelberg, 2014.

B. Gross. *Mathematical Structure of the Theories of Viscoelasticity*, volume 1190 of *Actualités scientifiques et industrielles*. Hermann, Paris, 1953.

M. E. Gurtin. *An Introduction to Continuum Mechanics*. Academic Press, Boston, 1981.

M. E. Gurtin and E. Sternberg. On the linear theory of viscoelasticity. *Archive for Rational Mechanics and Analysis*, 11:291–356, 1962.

J. R. Haddock. The "evolution" of invariance principles à la Liapunov's direct method. In S. Sivasundaram and A. A. Martynyuk, editors, *Advances in Nonlinear Dynamics*, volume 5 of *Stability and Control: Theory, Methods and Applications*, chapter 29, pages 261–272. Gordon and Breach, Amsterdam, 1997.

W. Hahn. *Stability of Motion*, volume 138 of *Die Grundlehren der mathematischen Wissenschaften in Einzeldarstellungen*. Springer, Berlin Heidelberg New York, 1967.

J. K. Hale. Dynamical systems and stability. *Journal of Mathematical Analysis and Applications*, 26:39–59, 1969.

J. K. Hale. *Theory of Functional Differential Equations*, volume 3 of *Applied Mathematical Sciences*. Springer, New York Heidelberg Berlin, 2. edition, 1977.

J. K. Hale and J. Kato. Phase space for retarded equations with infinite delay. *Funkcialaj Ekvacioj*, 21:11–41, 1978.

T. T. Hartley, C. F. Lorenzo, J.-C. Trigeassou, and N. Maamri. Equivalence of history-function based and infinite-dimensional-state initializations for fractional-order operators. *Journal of Computational and Nonlinear Dynamics*, 8(4):041014, 2013.

T. T. Hartley, J.-C. Trigeassou, C. F. Lorenzo, and N. Maamri. Energy storage and loss in fractional-order systems. *Journal of Computational and Nonlinear Dynamics*, 10(6):061006, 2015.

S. Havriliak and S. Negami. A complex plane analysis of α-dispersions in some polymer systems. *Journal of Polymer Science Part C: Polymer Symposia*, 14(1):99–117, 1966.

R. Hilfer, editor. *Applications of Fractional Calculus in Physics*. World Scientific, Singapore, 2000.

R. Hilfer. Experimental evidence for fractional time evolution in glass forming materials. *Chemical Physics*, 284(1-2):399–408, 2002.

R. Hilfer. Excess wing physics and nearly constant loss in glasses. *Journal of Statistical Mechanics: Theory and Experiment*, 2019(10):104007, 2019.

R. Hilfer and H. J. Seybold. Computation of the generalized Mittag-Leffler function and its inverse in the complex plane. *Integral Transforms and Special Functions*, 17(9):637–652, 2006.

M. Hinze, A. Schmidt, and R. I. Leine. Mechanical representation and stability of dynamical systems containing fractional springpot elements. *Proceedings of the IDETC Quebec, Canada*, 2018.

M. Hinze, A. Schmidt, and R. I. Leine. Numerical solution of fractional-order ordinary differential equations using the reformulated infinite state representation. *Fractional Calculus and Applied Analysis*, 22(5):1321–1350, 2019.

M. Hinze, A. Schmidt, and R. I. Leine. The direct method of Lyapunov for nolinear dynamical systems with fractional damping. *Nonlinear Dynamics*, 102(4):2017–2037, 2020a.

M. Hinze, A. Schmidt, and R. I. Leine. Lyapunov stability of a fractionally damped oscillator with linear (anti-)damping. *International Journal of Nonlinear Science and Numerical Simulation*, 21(5):425–442, 2020b.

M. Hinze, S. Xiao, A. Schmidt, and W. Nowak. Experimental evaluation and uncertainty quantification for a fractional viscoelastic model of salt concrete. *Mechanics of Time-Dependent Materials*, 2021. Manuscript submitted for publication.

M. W. Hirsch and S. Smale. *Differential Equations, Dynamical Systems, and Linear Algebra*, volume 60 of *Pure and Applied Mathematics*. Academic Press, New York London, 1974.

R. A. Ibrahim. Friction-induced vibration, chatter, squeal, and chaos; Part I: Mechanics of contact and friction. *ASME Applied Mechanics Reviews*, 47(7):209–226, 1994.

S. Jiang, J. Zhang, Q. Zhang, and Z. Zhang. Fast evaluation of the Caputo fractional derivative and its applications to fractional diffusion equations. *Communications in Computational Physics*, 21(3):650 – 678, 2017.

F. Kappel and W. Schappacher. Some considerations to the fundamental theory of infinite delay equations. *Journal of Differential Equations*, 37:141–183, 1980.

S. Kempfle and I. Schäfer. Fractional differential equations and initial conditions. *Fractional Calculus and Applied Analysis*, 3(4):387–400, 2000.

S. Kempfle, I. Schäfer, and H. Beyer. Fractional calculus via functional calculus: Theory and applications. *Nonlinear Dynamics*, 29:99–127, 2002.

H. K. Khalil. *Nonlinear Systems*. Prentice Hall, Upper Saddle River (NJ), 3. edition, 2002.

T. Kleiner and R. Hilfer. Convolution operators on weighted spaces of continuous functions and supremal convolution. *Annali di Matematica Pura ed Applicata*, 199(4):1547–1569, 2019a.

T. Kleiner and R. Hilfer. Weyl integrals on weighted spaces. *Fractional Calculus and Applied Analysis*, 22(5):1225–1248, 2019b.

T. Kleiner and R. Hilfer. Fractional glassy relaxation and convolution modules of distributions. *Analysis and Mathematical Physics*, 2021. in-press.

H. W. Knobloch and F. Kappel. *Gewöhnliche Differentialgleichungen*. Teubner, Stuttgart, 1974.

K. Knopp. *Theory of Functions*, volume 1: Elements of the General Theory of Analytic Functions. Dover, New York, 1. edition, 1945.

R. C. Koeller. Applications of fractional calculus to the theory of viscoelasticity. *Journal of Applied Mechanics*, 51(2):299–307, 1984.

V. B. Kolmanovskii and V. R. Nosov. *Stability of Functional Differential Equations*, volume 180 of *Mathematics in Science and Engineering*. Academic Press, London, 1986.

H. König and J. Meixner. Lineare Systeme und lineare Transformationen. *Mathematische Nachrichten*, 19:265–322, 1958.

N. N. Krasovskii. Asymptotic stability of systems with aftereffect. *Prikladnaya Matematika i Mekhanika*, 20(4):513–518, 1956.

R. S. Lakes. *Viscoelastic Solids*. CRC Mechanical Engineering Series. CRC Press, Boca Raton, 1999.

V. Lakshmikantham, S. Leela, and J. V. Devi. *Theory of Fractional Dynamic Systems*. Cambridge Scientific Publishers, Cottenham, 2009.

J. P. LaSalle. Stability theory for ordinary differential equations. *Journal of Differential Equations*, 4:57–65, 1968.

J. P. LaSalle and Z. Artstein. *The Stability of Dynamical Systems*. Regional Conference Series in Applied Mathematics; 25. Society for Industrial and Applied Mathematics, Philadelphia, 1976.

R. I. Leine and H. Nijmeijer. *Dynamics and Bifurcations of Non-Smooth Mechanical Systems*, volume 18 of *Lecture Notes in Applied and Computational Mechanics*. Springer, Berlin Heidelberg New York, 2004.

R. I. Leine and N. van de Wouw. *Stability and Convergence of Mechanical Systems with Unilateral Constraints*, volume 36 of *Lecture Notes in Applied and Computational Mechanics*. Springer, Berlin Heidelberg New York, 2008.

J.-R. Li. A fast time stepping method for evaluating fractional integrals. *SIAM Journal on Scientific Computing*, 31(6):4696–4714, 2010.

Y. Li, Y. Q. Chen, and I. Podlubny. Stability of fractional-order nonlinear dynamic systems: Lyapunov direct method and generalized Mittag–Leffler stability. *Computers & Mathematics with Applications*, 59(5):1810–1821, 2010.

A. Lion. Thermomechanically consistent formulations of the standard linear solid using fractional derivatives. *Archives of Mechanics*, 53(3):253–273, 2001.

L.-L. Liu and J.-S. Duan. A detailed analysis for the fundamental solution of fractional vibration equation. *Open Mathematics*, 13(1):826 – 838, 2015.

C. F. Lorenzo and T. T. Hartley. Initialization of fractional-order operators and fractional differential equations. *Journal of Computational and Nonlinear Dynamics*, 3(2):021101, 2008.

C. Lubich. Discretized fractional calculus. *SIAM Journal on Mathematical Analysis*, 17(3): 704–719, 1986.

A. M. Lyapunov. The general problem of the stability of motion. *Mathematical Society of Kharkov*, 55:531–773, 1892. Russian.

F. Mainardi. *Fractional Calculus and Waves in Linear Viscoelasticity*. Imperial College Press, London, 2010.

L. Markus. Asymptotically autonomous differential systems. In S. Lefschetz, editor, *Contribution to Nonlinear Oscillations*, volume 3, pages 17–29. Princeton University Press, Princeton (NJ), 1956.

S. P. C. Marques and G. J. Creus. *Computational Viscoelasticity*. SpringerBriefs in Computational Mechanics. Springer, Heidelberg, 2012.

D. Matignon. Stability results for fractional differential equations with applications to control processing. In *Computational Engineering in Systems Applications, IMACS, IEEE-SMC, Lille, France*, pages 963–968, 1996.

D. Matignon. Stability properties for generalized fractional differential systems. *ESAIM Proceedings*, 5:145–158, 1998.

K. S. Miller and B. Ross. *An Introduction to the Fractional Calculus and Fractional Differential Equations*. Wiley, New York, 1993.

C. A. Monje, Y. Chen, B. M. Vinagre, D. Xue, and V. Feliu. *Fractional-Order Systems and Controls: Fundamentals and Applications*. Advances in Industrial Control. Springer, London, 2010.

G. Montseny. Diffusive representation of pseudo-differential time-operators. *ESAIM Proceedings*, 5:159–175, 1998.

M. Naber. Linear fractionally damped oscillator. *International Journal of Differential Equations*, 2010:1–12, 2010.

A. W. Nolle. Dynamic mechanical properties of rubberlike materials. *Journal of Polymer Science*, 5(1):1–54, 1950.

K. Oldham and J. Spanier. *The Fractional Calculus: Theory and Applications of Differentiation and Integration to Arbitrary Order*. Academic Press, New York London, 1974.

A. Oustaloup. *La Dérivation Non Entière: Théorie, Synthèse et Applications*. Hermès, Paris, 1995.

J. Padovan. Computational algorithms for FE formulations involving fractional operators. *Computational Mechanics*, 2(4):271–287, 1987.

K. D. Papoulia, V. P. Panoskaltsis, N. V. Kurup, and I. Korovajchuk. Rheological representation of fractional order viscoelastic material models. *Rheologica Acta*, 49(4):381–400, 2010.

A. Pavlov, A. Pogromsky, N. van de Wouw, and H. Nijmeijer. Convergent dynamics, a tribute to Boris Pavlovich Demidovich. *Systems and Control Letters*, 52:257–261, 2004.

A. Pavlov, N. van de Wouw, and H. Nijmeijer. *Uniform Output Regulation of Nonlinear Systems: A Convergent Dynamics Approach*. Systems and Control: Foundations & Applications. Birkhäuser, Boston Basel Berlin, 2006.

I. Podlubny. *Fractional Differential Equations. An Introduction to Fractional Derivatives, Fractional Differential Equations, to Methods of their Solution and some of their Applications*, volume 198 of *Mathematics in Science and Engineering*. Academic Press, San Diego, 1999.

H. Pollard. The completely monotonic character of the Mittag-Leffler function $E_\alpha(-x)$. *Bulletin of the American Mathematical Society*, 54(12):1115–1116, 1948.

Y. N. Rabotnov. Equilibrium of an elastic medium with after effect. *Prikladnaya Matematika i Mekhanika*, 12(1):81–91, 1948.

B. S. Razumikhin. On the stability of systems with delay. *Prikladnaya Matematika i Mekhanika*, 20(4):500–512, 1956.

F. Riesz and B. Sz.-Nagy. *Functional Analysis*. F. Ungar Publishing, New York, 1955.

N. Rouche, P. Habets, and M. Laloy. *Stability Theory by Liapunov's Direct Method*, volume 22 of *Applied Mathematical Sciences*. Springer, New York, 1977.

W. Rudin. *Real and Complex Analysis*. McGraw-Hill, New York, 3. edition, 1986.

J. Sabatier, M. Moze, and C. Farges. LMI stability conditions for fractional order systems. *Computers & Mathematics with Applications*, 59(5):1594–1609, 2010.

S. G. Samko, A. A. Kilbas, and O. I. Marichev. *Fractional Integrals and Derivatives: Theory and Applications*. Gordon and Breach, Yverdon, 1993.

K. Sawano. Some considerations on the fundamental theorems of functional differential equations with infinite delay. *Funkcialaj Ekvacioj*, 25:97–104, 1982.

H. Schiessel and A. Blumen. Hierarchical analogues to fractional relaxation equations. *Journal of Physics A: Mathematical and General*, 26(19):5057–5069, 1993.

A. Schmidt and L. Gaul. Finite element formulation of viscoelastic constitutive equations using fractional time derivatives. *Nonlinear Dynamics*, 29(1):37–55, 2002.

A. Schmidt and L. Gaul. On a critique of a numerical scheme for the calculation of fractionally damped dynamical systems. *Mechanics Research Communications*, 33(1):99 – 107, 2006.

G. W. Scott Blair. The role of psychophysics in rheology. *Journal of Colloid Science*, 2(1):21–32, 1947.

H. Seybold and R. Hilfer. Numerical algorithm for calculating the generalized Mittag-Leffler function. *SIAM Journal on Numerical Analysis*, 47(1):69–88, 2009.

L. Shampine and M. Reichelt. The MATLAB ODE suite. *SIAM Journal on Scientific Computing*, 18(1):1–22, 1997.

J. C. Simo and T. J. R. Hughes. *Computational Inelasticity*. Interdisciplinary Applied Mathematics. Springer, New York, 1998.

S. J. Singh and A. Chatterjee. Galerkin projections and finite elements for fractional order derivatives. *Nonlinear Dynamics*, 45(1):183–206, 2006.

J.-J. E. Slotine and W. Li. *Applied Nonlinear Control*. Prentice-Hall, Englewood Cliffs (NJ), 1991.

G. F. J. Temple. *Cartesian tensors: An Introduction*. Methuen's Monographs on Physical Subjects. Methuen, London, 1960.

J.-C. Trigeassou and N. Maamri. *Analysis, Modeling and Stability of Fractional Order Differential Systems 2: The Infinite State Approach*. Wiley, Hoboken (NJ), 2019.

J.-C. Trigeassou, N. Maamri, and A. Oustaloup. Initialization of Riemann-Liouville and Caputo fractional derivatives. In *ASME 2011 International Design Engineering Technical Conferences and Computers and Information in Engineering Conference*, pages 219–226, 2011a.

J.-C. Trigeassou, N. Maamri, J. Sabatier, and A. Oustaloup. A Lyapunov approach to the stability of fractional differential equations. *Signal Processing*, 91(3):437–445, 2011b.

J.-C. Trigeassou, N. Maamri, J. Sabatier, and A. Oustaloup. State variables and transients of fractional order differential systems. *Computers & Mathematics with Applications*, 64(10): 3117–3140, 2012a.

J.-C. Trigeassou, N. Maamri, J. Sabatier, and A. Oustaloup. Transients of fractional-order integrator and derivatives. *Signal, Image and Video Processing*, 6(3):359–372, 2012b.

J.-C. Trigeassou, N. Maamri, and A. Oustaloup. Lyapunov stability of commensurate fractional order systems: A physical interpretation. *Journal of Computational and Nonlinear Dynamics*, 11(5):051007, 2016a.

J.-C. Trigeassou, N. Maamri, and A. Oustaloup. Lyapunov stability of noncommensurate fractional order systems: An energy balance approach. *Journal of Computational and Nonlinear Dynamics*, 11(4):041007, 2016b.

C. Truesdell, editor. *Mechanics of Solids II: Linear Theories of Elasticity and Thermoelasticity*. Springer, Berlin Heidelberg, 1973.

V. Volterra. *Theory of Functional and of Integral and Integro-Differential Equations*. Dover Publications, New York, 1959.

Y. Wei, P. W. Tse, B. Du, and Y. Wang. An innovative fixed-pole numerical approximation for fractional order systems. *ISA Transactions*, 62:94 – 102, 2016.

D. Xue. *Fractional-order Control Systems - Fundamentals and Numerical Implementations*. Fractional Calculus in Applied Sciences and Engineering. De Gruyter, Berlin, 2017.

D. Xue and L. Bai. Benchmark problems for Caputo fractional-order ordinary differential equations. *Fractional Calculus and Applied Analysis*, 20(5):1305 – 1312, 2017.

V. A. Yakubovich. The matrix-inequality method in the theory of the stability of nonlinear control systems. I. The absolute stability of forced vibrations. *Automation and Remote Control*, 25(7):905–917, 1964.

T. Yoshizawa. Asymptotic behavior of solutions of a system of differential equations. *Contributions to Differential Equations*, 1(3):371–388, 1963.

L. Yuan and O. P. Agrawal. A numerical scheme for dynamic systems containing fractional derivatives. *Journal of Vibration and Acoustics*, 124:321–324, 2002.

C. Zener. *Elasticity and Anelasticity of Metals*. University of Chicago Press, Chicago, 1948.

W. Zhang, A. Capilnasiu, G. Sommer, G. A. Holzapfel, and D. A. Nordsletten. An efficient and accurate method for modeling nonlinear fractional viscoelastic biomaterials. *Computer Methods in Applied Mechanics and Engineering*, 362:112834, 2020.

C. Zopf, S. E. Hoque, and M. Kaliske. Comparison of approaches to model viscoelasticity based on fractional time derivatives. *Computational Materials Science*, 98:287–296, 2015.